Electroorganic Chemistry as a Green Synthesis Methodology

A Thesis Submitted to
Cardiff University

for the Degree of
Doctor of Philosophy

presented by
Jakob Friedemann Seitz

Cardiff, September 2022

Acknowledgements

First of all, I would like to thank Professor Thomas Wirth for giving me the opportunity to work in his group and for his support. I would also like to thank my mentor Professor Rebecca Melen and my internal examiner Dr Louis Morrill, for the discussions and suggestions during our meetings.

Thanks to all the members of the Wirth group I had the pleasure to meet. I am especially grateful for all the coffee breaks and the hikes a could enjoy with you, but also for every helping hand, every piece of advice and every joke to brighten a log day in the laboratory.

I would also like to thank all my former housemates in Cardiff.

A special thanks goes to Beth, Tuhin and Leo for proof reading my thesis.

Ein herzlicher Dank geht auch an meine Familie an meine Eltern, Großeltern und meine Schwester.

Abstract

In recent years, the field of green chemistry has grown in importance as chemical processes are also evaluated on their environmental impact and the sustainability. This demand for green synthetic methodologies has been addressed with a variety of enabling technologies, such as mechanochemistry, photochemistry or electrochemistry. In this work, the focus will be on contributions of electroorganic synthesis towards green chemistry.

In the first part of this work, the development of chiral electrodes for asymmetric electrocatalysis was investigated. Two types of electrodes were prepared. The first electrode type was prepared according to the concept of organically doped metals. The chiral catalyst, a cinchona alkaloid, was entrapped in metal, which was then used as heterogeneous catalyst to press coin electrodes. Alternatively, the catalyst was coated onto a graphite electrode. These electrodes were tested for the electrocatalytic hydrogenation of ketones. The second electrode was prepared by coating an electrode with a chiral polymer, poly-L-valine. This electrode was tested for the asymmetric electrochemical oxidation of sulfides to sulfoxides. A chiral electrode could not be produced with these two concepts and further efforts would be required to confirm the methodologies.

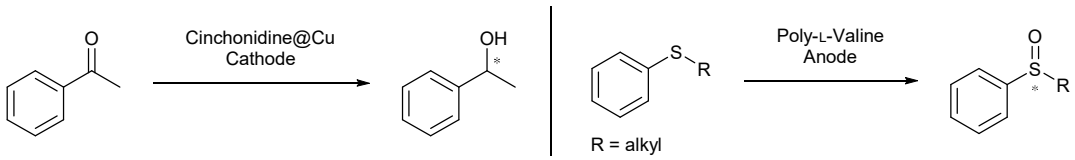

The reduction of molecular oxygen at the cathode can provide superoxide ions as reactive intermediates. The use of electrogenerated superoxide for the electrochemical oxychlorination of alkenes was tested in the second part of this work. The aim was to implement this type of reaction in continuous flow in order to investigate the biphasic gas-liquid interactions in a flow electrochemical reactor. However, this work focuses on the search for a homogeneous reaction solution for the batch electrochemical oxychlorination of styrene as a first step towards a flow procedure.

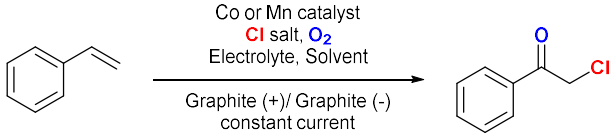

Finally, the electrochemical generation of elemental bromine was utilised for a variety of transformations. Depending on the concentration of bromide ions and the choice of cosolvent, alkenes could be converted to the corresponding dibromides, bromohydrins

or bromohydrin ethers. Alkenes containing internal nucleophiles would react to give bromo-cyclised products. The use of electrogenerated bromine provides a versatile synthetic procedure that can help to address some of the 12 principles of green chemistry.[1]

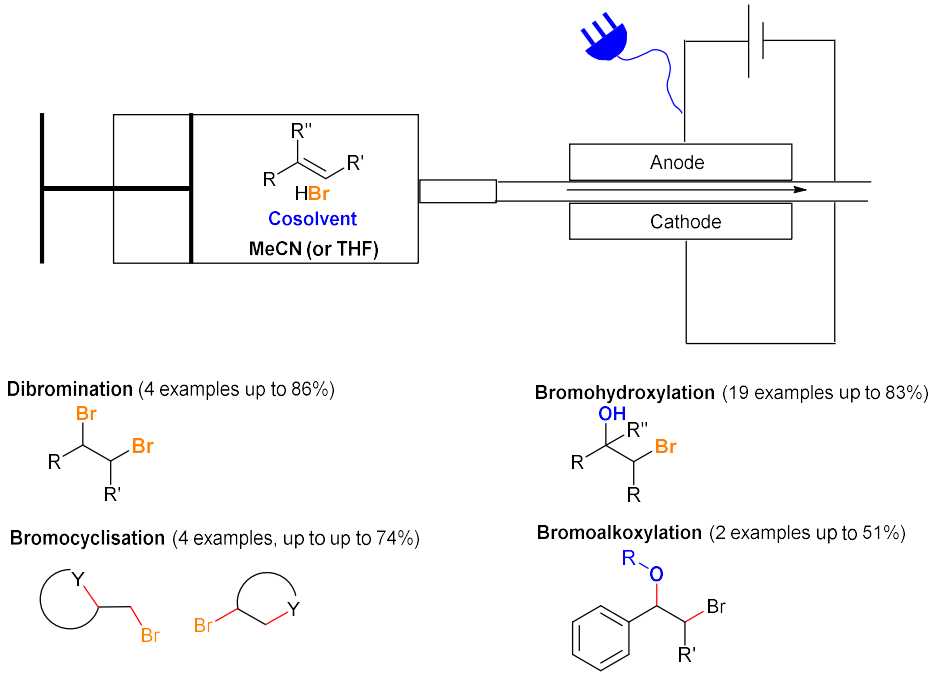

Publications

(1) J. Seitz, T. Wirth, *Organic & Biomolecular Chemistry* **2021**, *19*, 6892-6896: “Electrochemical bromofunctionalization of alkenes in a flow reactor”

List of Abbreviations

°C	Degree Celsius
δ	Chemical shift
2D-HPLC	Two-dimensional high performance liquid chromatography
A	Ampere
A	Area
Ac	Acetyl
ADPy	1-Aminopropyl-1'-methyl-4,4'-dipyridinium iodide
AOx	Amino acid oxidase
aq	aqueous
BPR	Backpressure regulator
bpy	2,2′-bipyridine
Bu	Butyl
C	Coulomb
calcd.	calculated
CI	Chemical ionisation
CD	Cinchonidine
S-CMF	S-chiral multi-farene
CN	Cinchonine
CIMP	Chiral imprinted mesoporous platinum
DMF	*N,N*-Dimethylformamide
DMSO	Dimethyl sulfoxide
DSA	Dimensionally stable anode
dr	diastereomeric ratio
E	Potential
E°	Standard potential
ECH	Electrocatalytic hydrogenation
ee	enantiomeric excess
EI	Electron ionisation
eq.	equivalent
Et	Ethyl
EtOAc	Ethyl acetate
EtOH	Ethanol
EWG	Electron withdrawing group
F	Faraday
FEP	Fluorinated ethylene propylene
g	gram

GC	Glassy carbon
h	hour
HFIP	1,1,1,3,3,3-hexafluoroisopropan-2-ol
HOPG	Highly ordered pyrolytic graphite
HPLC	High performance liquid chromatography
HRMS	High resolution mass spectrometry
Hz	Hertz
I	Current
IPA	Isopropanol
IR	Infrared
j	Current density
J	Coupling constant
L	liter
m	meter
M	molarity
MALDI	Matrix-assisted laser desorption/ionization
MeCN	Acetonitrile
Med	Mediator
MeOH	Methanol
min	minute
MP	Melting point
MWCNT	Multi-walled carbon nanotubes
m/z	mass over charge ratio
NBS	*N*-Bromosuccinimide
NCA	N-carboxy anhydride
NIS	*N*-Iodosuccinimide
NMI	1-Methyl-1*H*-imidazole
NMR	Nuclear magnetic resonance
Ox	Oxidised species
Ph	Phenyl
phen	1,10-phenanthroline
ppm	parts per million
PSSA	Poly(4-styrene sulfonic acid)
PTFE	Polytetrafluoroethylene
PVA	Poly(vinyl alcohol)
PVBA	Poly(vinylbenzyltrimethyl-ammonium hydroxide)
PYD	Pyridine derivative

Q	Charge
QD	Quinidine
QN	Quinine
R	Resistance
Red	Reduced species
RHE	Reversible hydrogen electrode
r.t.	Room temperature
RVC	Reticulated vitreous carbon
s	second
SCE	Saturated Calomel electrode
SDS	Sodium dodecylsulfate
SHE	Standard hydrogen electrode
Sub	Substrate
*t*Bu	tert-Butyl
TEMPO	(2,2,6,6-Tetramethylpiperidin-1-yl)oxyl
TFA	2,2,2-Trifluoroaceticacid
TFE	2,2,2-trifluoroethanol
THF	Tetrahydrofuran
TPP	*meso*-Tetraphenylporphyrin
t_R	Residence time
Ts	Toluenesulfonyl
U	Voltage
UV/Vis	Ultraviolet/Visible
V	Volt
Val	Valine
vbpy	4-methyl-4'-vinyl-2,2'-bipyridine
v/v	volume to volume ratio
wt%	weight percent
w/v	weight to volume ratio
XPS	X-ray photoelectron spectroscopy
XRD	X-ray diffraction

Table of Contents

Chapter 1: Introduction

1.1 Organic Electrochemistry

1.1.1 Introduction

In recent years, organic electrochemistry has seen a renaissance. As an enabling technology, organic electrochemistry offers reactivities that are not obtained in conventional organic synthesis. Furthermore, the use of the electron as a redox reagent allows to avoid toxic oxidants and reductants and the production of waste. Recently, more and more sustainable and environmentally benign electrochemical methodologies have been developed that contribute to the field of green chemistry. The renewed interest in organic electrochemistry has led to an increased development of commercially available electrochemical equipment, which helps the accessibility of the field and the adaptation of electrochemical methods by more synthetic chemists.[1,2]

Pioneering experiments in organic electrochemistry have been conducted in the 1830s by *Faraday* with the electrolysis of acetic acid.[3] In 1849, *Kolbe* investigated the oxidative decarboxylation of carboxylic acids **1** to form radicals that subsequently undergo a dimerization (Scheme 1.1).[4] In the beginning of the 20th century, voltammetric techniques that required control over the potential were developed, which led to the investigation of potential controlled synthesis.[5–10] In the middle of the 20th century, organic electrochemistry started to attract economic interest with *Simons* electrochemical production of fluorocarbons **4** and the Monsanto adiponitrile **6** process (Scheme 1.1).[11–15] In 1975, *Miller* and co-workers introduced the first chiral electrode, which served as a starting point for further investigations into modified electrodes for asymmetric synthesis and the development of chiral sensors.[16,17] A widely investigated electrochemical reaction is the *Shono oxidation*, through which alkyl amides **7** can be functionalised in α-position (Scheme 1.1).[18,19] In the 1980s, *Steckhan* developed the concept of indirect electrolysis.[20] With a renewed interest in organic electrochemistry, valuable contributions to the synthetic chemistry toolbox continue. Important recent advances have been made in electrochemical fluorination, electrochemical C-H activation, electrochemical cross-couplings of arenes or the electrochemical formation of heterocycles.[21,22] Electrochemistry was also explored as a synthetic tool for total synthesis and late stage functionalisations.[23,24]

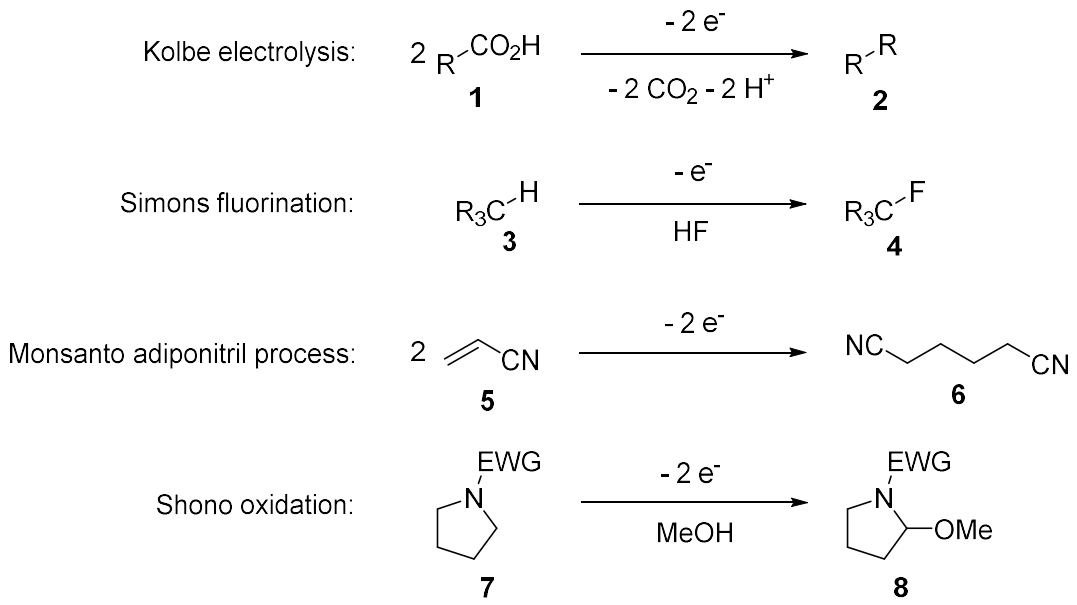

Scheme 1.1: Selection of important organic electrochemical processes from the 19th and 20th century.

1.1.2 Setup of Electrochemical cells

Electrochemical Cell

The setup of an electrochemical cell (Figure 1.1A) requires a reaction vessel with the solvent containing the substrate and a supporting electrolyte to ensure a sufficient conductivity. Two electrodes, the anode and the cathode, which are immersed in the solution, are connected to a power supply. Oxidations occur at the anode as electrons are pulled to the power supply and reductions at the cathode as electrons are pushed from the power supply to the cathode. The electrode at which the investigated electrochemical reaction is taking place is also called working electrode. The other electrode is then referred to as the counter electrode or auxiliary electrode. A reference electrode can be used for an exact measurement of the potential and is placed near the working electrode (Figure 1.1B). Reference electrodes are required for potentiostatic experiments or when performing electroanalytic experiments such as cyclic voltammetry. [25,26]

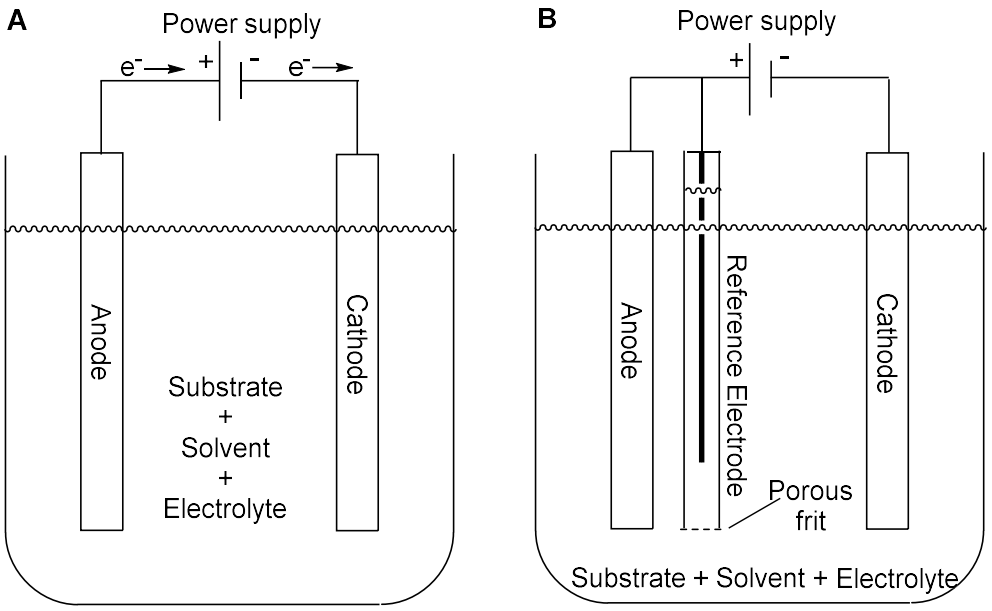

Figure 1.1: Setup of a simple electrochemical cell (undivided) (A) and an electrochemical cell equipped with a reference electrode (B).

If the counter reaction is interfering with the product formation or if the product is consumed at the counter electrode, a divided cell can be used (Figure 1.2) in contrast to the undivided cell shown above (Figure 1.1). The anodic and cathodic chamber are then separated by a membrane or porous glass frit that still allows for a charge transfer (Figure1.2A). A commonly used commercially available divided cell is the H-cell (Figure 1.2B). Generally, a bridge containing a porous frit connects the anodic and the cathodic compartment.[25]

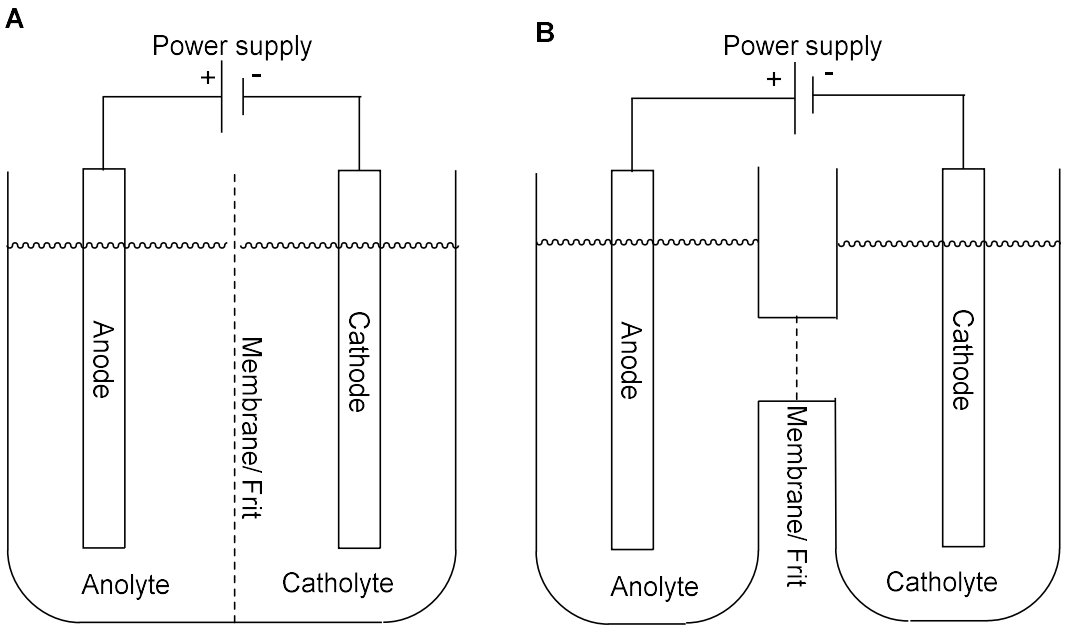

Figure 1.2: Divided electrochemical cell with anodic and cathodic compartments (A). Schematic representation of a H-type cell (B).

Electrodes

The reactivity or selectivity of an electrochemical process is influenced by the choice of electrode material. Commonly used electrode materials are for example graphite, glassy carbon, platinum or stainless steel. Examples for electrodes with a high surface area are reticulated vitreous carbon (RVC) and nickel foam electrodes. Ideal electrodes should be stable under the reaction conditions. However, certain reaction setups require the use of sacrificial electrodes to provide a counter reaction or metal ions to stabilise the product (Figure 1.3). Magnesium and zinc are examples for electrode materials, which are used as sacrificial anodes. The electrodes are consumed while releasing metal ions into the solution. [25–27]

Common reference electrodes used in aqueous systems are the standard hydrogen electrode (SHE), the saturated calomel electrode (SCE) and the Ag/AgCl electrode. Usually, a porous frit separates the reference electrode from the reaction mixture. To minimise the junction potential, the solvent and electrolyte used in the reference electrode and the experiment should be the same. Since many organic electrochemical experiments are conducted in non-aqueous solvents, non-aqueous Ag/Ag^+ reference electrodes are commonly used. This type of electrode can be made by placing a silver wire in an organic solvent such as acetonitrile containing $AgNO_3$ as silver salt.[28]

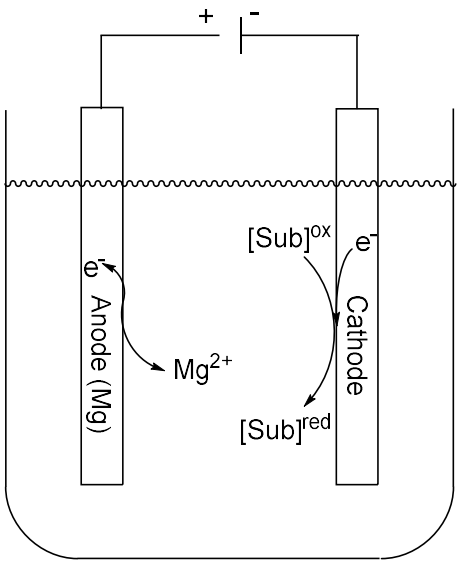

Figure 1.3: Schematic representation of an electrochemical cell with sacrificial magnesium anode (Sub = Substrate).

Solvent and electrolyte

The conductivity of a solvent is an important parameter in electrochemistry. Therefore, polar solvent with a good solubility of supporting electrolytes are preferred. In contrast to chemical reactions, the solvent has to offer a sufficient potential window and facilitate the counter reaction. Commonly used aprotic solvents are MeCN, DMF, DMSO, DMA and CH_2Cl_2. Alcohols such as MeOH and EtOH are commonly used as protic solvents. Fluorinated alcohols such as 1,1,3,3-hexafluoroisopropan-2-ol (HFIP) and 2,2,2-trifluoroethanol (TFE) are often used to stabilise radical intermediates.[29]

Common electrolytes consist of tetraalkylammonium, lithium or sodium as cations and perchlorate, tetrafluoroborate, hexafluorophosphate or halogens as anions. Solvents and electrolytes are chosen in order to obtain a large potential window for the electrochemical reaction, which is limited by the electrochemical decomposition of the solvent or electrolyte. The potential at which a desired reaction occurs (oxidation potential) should lie within this window.[25,26,28]

1.1.3 Galvanostatic vs. Potentiostatic Electrolysis

Electrochemical reactions can be conducted with a constant current (galvanostatic electrolysis) or a constant potential (potentiostatic electrolysis). The driving force behind the movement of electrons is the potential difference or voltage (*U*). The rate of the movement of electrons is described as current (*I*). Current and voltage are linked via the resistance (*R*) (Equation 1).[25,26]

$$U = R \times I$$

Equation 1: *U*: Potential in volt [V]; *R*: Resistance in ohm [Ω]; *I*: Current in ampere [A].

The number of electrons that are transferred is referred to as charge (*Q*), which is determined by the current per time interval (*t*) (Equation 2). In a galvanostatic experiment, where the stoichiometry of electrons is known, the required charge can be calculated with the number of electrons per substrate molecule (*z*), the number of moles (*n*) and the Faraday constant (*F*) (Equation 3). The equivalents of electrons that were used in an electrochemical reaction are commonly given in $F \cdot mol^{-1}$ where one Faraday (F) is equivalent to one mole of electrons. Often, an excess of charge is used due to a loss of energy.

$$Q = I \times t$$

Equation 2: *Q*: charge in Coulomb [C = A·s]; *I*: Current in ampere [A]; *t*: time in seconds [s].

$$Q = z \times n \times F$$

Equation 3: *Q*: charge in Coulomb [C = A·s]; *z*: Number of electrons per substrate molecule; *n*: number of moles [mol]; *F*: Faraday's constant [96485 $A \cdot s \cdot mol^{-1}$].

The current density (*j*) is a parameter that is important for the reproducibility of galvanostatic electrolysis procedures. The current density (*j*) can be calculated as the current (*I*) per area (*A*) (Equation 4).[26]

$$j = \frac{I}{A}$$

Equation 4: *j*: Current density [$A \cdot m^2$]; *I*: Electric current [A]; *A*: Surface area [m^2].

A potentiostatic electrolysis is usually conducted with a reference electrode for an accurate determination of the potential. The current will vary to obtain the constant potential. The transferred charge can still be calculated when the current is integrated as a function of the time. The potential (*E*) at which an electrochemical reaction occurs is usually higher than the standard potential (*E*°). The deviation from the standard potential can be calculated with the Nernst equation (Equation 6) for an electrochemical reaction in equilibrium (Equation 5).[25,28]

$$Ox + ze^- \rightleftharpoons Red$$

Equation 5: *Ox*: Oxidised species; *Red*: Reduced species

$$E = E° + \frac{RT}{zF} ln \frac{c(Ox)}{c(Red)}$$

Equation 6: E: Measured potential; $E°$: Standard reduction potential; R: Gas constant; T: temperature; F: Faraday's constant; z: Number of electrons per substrate molecule; $c(Ox)$: concentration of the oxidised species; $c(Red)$: concentration of the reduced species.

1.1.4 Indirect electrolysis – Electrocatalysts and Redox Mediators

The transfer of electrons from the electrode to the substrate can either proceed at the electrode surface as a direct electrolysis (Figure 1.4A) or in an indirect electrolysis where a redox reagent acts as an electron shuttle between the electrode and the substrate (Figure 1.4B).[30,31] Indirect electrolysis employs redox catalysts such as metal salts, halogens, transition metal catalysts or organic molecules. These are also referred to as mediators. Compared to direct electrolysis, the use of redox mediators can increase the efficiency of the electron transfer and improve the selectivity of a reaction. Chiral electrocatalysts have also been investigated to conduct asymmetric electrocatalysis.[17,32–34] Redox mediators transfer electrons while electrocatalysts transfer electrons and chemical information.[2] There are three ways to implement indirect electrolysis. Redox mediators can be used "ex-cell". In this case, the redox agent is generated *via* electrolysis and isolated before being used in a chemical reactor. For the "in-cell" use of a mediator, the electrochemical and the chemical step occur in the same reactor. After the chemical reaction, the redox reagent is regenerated at the electrode, which allows for a catalytic use of the mediator. Thirdly, indirect electrolysis can be realised by fixating the redox active agent on the electrode.[35,36] In this scenario, both the regeneration of the redox agent and the chemical step are heterogeneous processes at the electrode surface.[20,25]

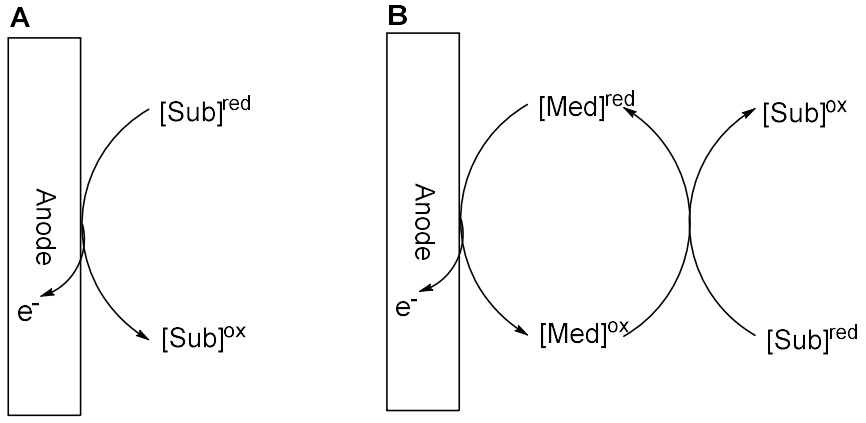

Figure 1.4: Direct electrolysis (A) and indirect electrolysis (B).

1.2 Flow Electrochemistry

In contrast to the flasks commonly used in batch chemistry, flow chemistry utilises channels and tubing to perform reactions in continuous flow. This gives several

advantages over batch chemistry and even allows to explore new reactivities in some cases, which would not be possible otherwise. Beneficial features of flow chemistry are the high mass and heat transfer rates. Hazardous reactants or intermediates can be generated *in situ* and can be contained within the reactor. Small internal volumes enable a better control over hazardous and exothermic reactions. The use of a continuous flow setup can also simplify the scale up process of a reaction. Furthermore, flow chemistry can be combined with other enabling technologies, such as photochemistry, microwave irradiation, bio-catalysis or electrochemistry. Multistep syntheses can be conducted in one continuous stream by connecting several reactors.[37–40]

An experiment in a flow chemistry setup starts with a pump that facilitates the flow of the reaction mixture. The reaction mixture is passed through tubing onto a reactor and is subsequently collected. There are several types of reactors such as a coil, a chip or a packed-bed (column) reactor. A column of a packed-bed reactor can be filled with reagents, catalysts or scavengers. The pressure within the channel can be controlled with a backpressure regulator (BPR). The reaction mixture can be analysed in flow with inline or online methods. Important parameters are the flow rate, the volume of the reactor, the residence time, which is also the reaction time, and the temperature of the reactor. As in batch chemistry, the concentration of reagents is also an important factor as well as the pressure. The mixing efficiency is an additional parameter to consider. This can be influenced by the flow rate, channel dimensions or channel geometry.[40]

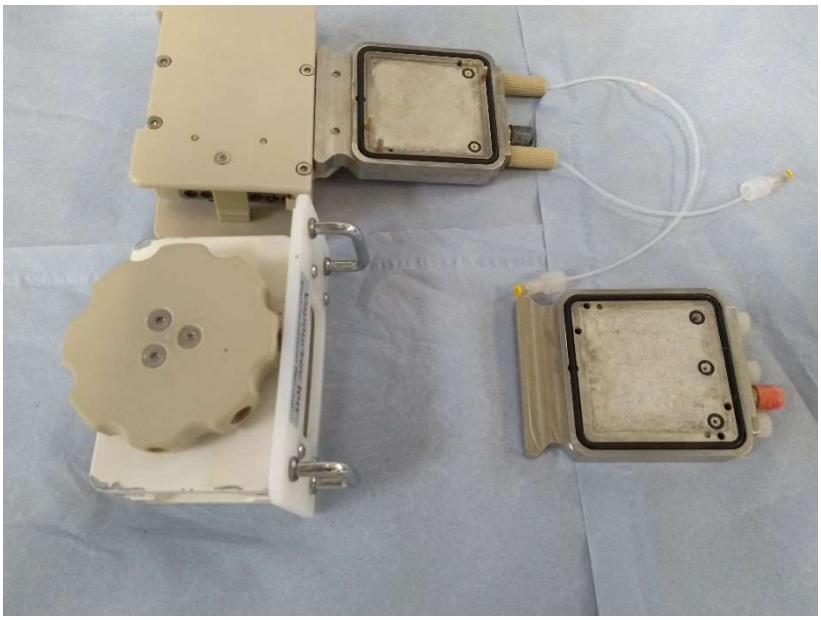

Figure 1.5: Ion electrochemical reactor with tubing from Vapourtec.[41]

In recent years, flow electrochemical methods have been gaining in popularity due to a renewed interest in organic electrochemistry. Commercial electrochemical reactors are available (Figure 1.5),[41] but home built systems are also reported.[42,43] A flow electrochemical reactor consists of two parallelly assembled electrodes (Figure 1.6), anode and cathode, which are separated by a nonconducting spacer. The flow path is cut into the spacer to leave a channel. The spacer thickness dictates the inter-electrode distance, which is usually not more than 1 mm. The reaction mixture is then passed through the channel and a current is applied to drive the reaction. The electrolysis in a flow electrochemical reactor is conducted with a constant current, but there are some examples that utilise a constant potential.[44] An example for an in-line reference electrode was provided by Stahl and co-workers.[45]

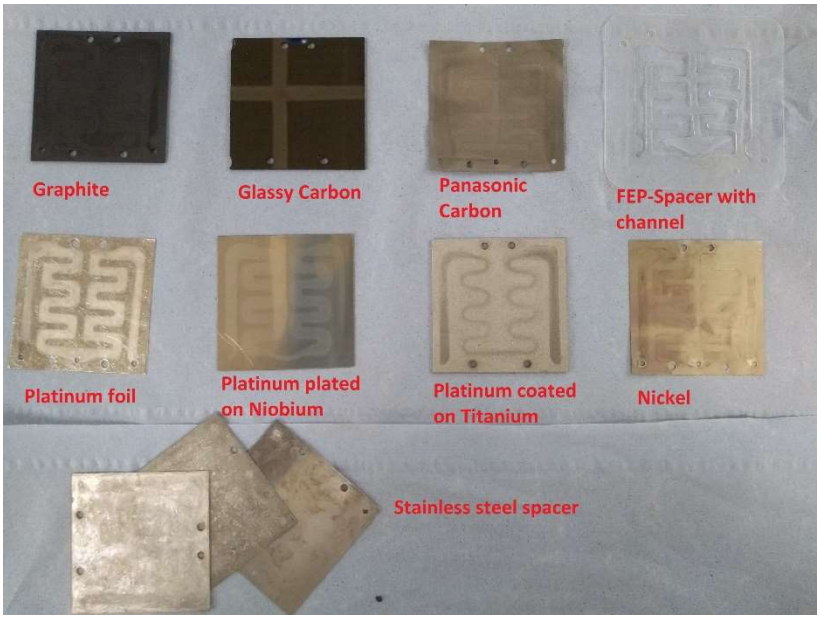

Figure 1.6: Electrodes and spacer with channel used in the flow electrochemical reactor.

The combination of electrochemistry and flow chemistry provides several advantages over batch electrochemistry. General benefits of flow chemistry apply here as well, such as the higher mass transfer rate and the uncomplicated scale up process. However, flow electrochemistry provides some improvements specific to electrochemistry. The higher electrode surface area to reactor volume ratio has a positive effect on the speed of the electrochemical reaction. A smaller inter-electrode distance decreases the resistance and allows the use of higher currents and lower amounts of supporting electrolyte or even supporting electrolyte-free conditions.[46–49] The automation of the flow electrochemical reaction can enhance the optimisation

process and mitigate the experimentalists risk of exposure to hazardous substances.[50,51]

1.3 Green Chemistry

As in other areas of society and economy, the environmental impact and the sustainability of processes are also considered in chemistry with a growing interest in green chemistry. The concept of green chemistry has been applied to produce inorganic, organic and coordination compounds or nanomaterials in a sustainable way. The corresponding processes are aiming to reduce the impact on the environment by increasing the sustainability with higher energy efficiency and decreased toxicity and waste production. Enabling technologies such as ball milling, microwave irradiation, photochemistry or bio-catalysis have been employed as green methodologies. These procedures possess distinctive advantages such as a higher energy efficiency, mild reaction conditions and the use of less toxic solvents or reagents compared to conventional chemical methods.[44,52]

The focus of this work will be on organic electrochemistry as a green synthesis methodology. Hereinafter, the contributions of electrochemistry to the fulfilment of the 12 principles of green chemistry are discussed:[53,54]

1) A major advantage of electrochemistry is the potential of **preventing waste** as the electron can be seen as a green reagent. The reduction or oxidation at the electrode surface can help to cut chemical oxidants and reductants out of the equation or implement strategies to recycle them at the electrodes.

2) A high **atom economy** can be achieved by the electrochemical activation and interconversion of functional groups. Chemical oxidants and reductants, which usually end up as waste after the reaction, can be avoided. The use of supporting electrolytes to ensure conductivity can be a drawback regarding atom economy. However, this problem can be addressed with flow electrochemical methods where the small inter-electrode distance can help to reduce or avoid additional supporting electrolytes.

3) **Less hazardous synthetic procedures** can be implemented by substituting toxic and hazardous oxidants and reductants for electricity.

4) Non-corrosive electrode materials are commonly favoured in organic electrochemistry. **Non-toxic** electrode materials have also been identified to replace

toxic electrode materials such as mercury, which had been used in cathodic reductions of organic molecules for its high hydrogen overpotential.

5) Environmentally benign and **safe solvents** such as water or alcohol water mixtures can be used for some electrochemical processes. Furthermore, ionic liquids have been used for their conductivity and low volatility.

6) Since compounds can be activated electrochemically at certain potentials, high temperatures and pressures can be avoided and **energy can be used more efficiently**. Mediator systems allow to conduct reactions at lower electrochemical potentials to bring down the energy consumption. By using both the anodic and the cathodic reaction to obtain value added products, the concept of paired electrolysis can further increase the energy efficiency of electrochemical processes.

7) **Renewable** sources of electricity and the use of chemicals from a renewable feedstock help to address another principle of green chemistry with electrochemistry.

8) The selective activation of functional groups at specific electrochemical potentials allows to reduce the number of reaction steps and to **avoid derivatisation**.

9) **Catalytic cycles** can be driven by the electrochemical oxidation or reduction of catalysts. Mediators can also be used for electrochemical reactions at lower potentials and thereby reduce the occurrence of side products.

10) Electrochemical processes have been investigated for the **degradation of toxic organic compounds.**

11) **Real-time analysis** of reactions can be realised with electrochemical sensing to avoid the formation of side products. Flow electrochemical reactions can be monitored by online analysis.

12) The *in situ* generation of hazardous reactants and intermediates can contribute to the **prevention of accidents**.

These benefits of electrochemistry can provide a substantial contribution to sustainable and environmentally friendly synthetic methodologies in the toolbox of green chemistry.

1.4 References

(1) Zhu, C.; Ang, N. W. J.; Meyer, T. H.; Qiu, Y.; Ackermann, L. Organic Electrochemistry: Molecular Syntheses with Potential. *ACS Cent. Sci.* **2021**, *7*, 415–431. https://doi.org/10.1021/acscentsci.0c01532.

(2) Novaes, L. F. T.; Liu, J.; Shen, Y.; Lu, L.; Meinhardt, J. M.; Lin, S. Electrocatalysis as an Enabling Technology for Organic Synthesis. *Chem. Soc. Rev.* **2021**, *50*, 7941–8002. https://doi.org/10.1039/d1cs00223f.

(3) Faraday, M. VI. Experimental Researches in Electricity.-Seventh Series. *Phil. Trans. R. Soc.* **1834**, *124*, 77–122. https://doi.org/10.1098/rstl.1834.0008.

(4) Kolbe, H. Untersuchungen Über Die Elektrolyse Organischer Verbindungen. *Justus Liebigs Ann. Chem.* **1849**, *69*, 257–294. https://doi.org/10.1002/jlac.18490690302.

(5) Heyrovský, J. XXIX. Electrolysis with a Dropping Mercury Cathode. Part I. Deposition of Alkali and Alkaline Earth Metals. *Lond. Edinb. Dublin philos. mag.* **1923**, *45*, 303–315. https://doi.org/10.1080/14786442308634117.

(6) Hickling, A. Studies in Electrode Polarisation. Part IV.-The Automatic Control of the Potential of a Working Electrode. *Trans. Faraday Soc.* **1942**, *38*, 27–33. https://doi.org/10.1039/TF9423800027.

(7) Lingane, J. J.; Gardner Swain, C.; Fields Vol, M.; James Lingane, B. J.; Fields, M.; Glasstone, S.; Hickling, A.; Kolthoñ, M.; Lingane, J. J. Polarographically Controlled Syntheses, with Particular Reference to Organic Chemistry. *J. Am. Chem. Soc.* **1943**, *65*, 1348–1353. https://doi.org/10.1021/ja01247a024.

(8) Heinze, J. Cyclic Voltammetry-"Electrochemical Spectroscopy". *Angew. Chem. Int. Ed.* **1984**, *23*, 831–918. https://doi.org/10.1002/anie.198408313.

(9) Bard, A. J.; Zoski, C. G. Voltammetry Retrospective. *Anal. Chem.* **2000**, *72*, 346–352. https://doi.org/10.1021/ac002791t.

(10) Randles, J. E. A Cathode Ray Polarograph. Part II.—The Current-Voltage Curves. *Trans. Faraday Soc.* **1948**, *44*, 327–338. https://doi.org/10.1039/TF9484400327.

(11) Simons, J. H. Production of Fluorocarbons: I. The Generalized Procedure and Its Use with Nitrogen Compounds. *J. Electrochem. Soc.* **1949**, *95*, 47–67. https://doi.org/10.1149/1.2776733.

(12) Baizer, M. M. Electrolytic Reductive Coupling: I . Acrylonitrile. *J. Electrochem. Soc.* **1964**, *111*, 215. https://doi.org/10.1149/1.2426086.

(13) Baizer, M. M. Recent Developments in Organic Synthesis by Electrolysis. *Tetrahedron* **1984**, *40*, 935–969. https://doi.org/10.1016/S0040-4020(01)91232-3.

(14) Cardoso, D. S. P.; Šljukić, B.; Santos, D. M. F.; Sequeira, C. A. C. Organic Electrosynthesis: From Laboratorial Practice to Industrial Applications. *Org. Process Res. Dev.* **2017**, 1213–1226. https://doi.org/10.1021/acs.oprd.7b00004.

(15) Leech, M. C.; Garcia, A. D.; Petti, A.; Dobbs, A. P.; Lam, K. Organic Electrosynthesis: From Academia to Industry. *React. Chem. Eng.* **2020**, *5*, 977–990. https://doi.org/10.1039/d0re00064g.

(16) Watkins, F. B.; Behling, J. R.; Kariv, E.; Miller, L. L. A Chiral Electrode. *J. Am. Chem. Soc.* **1975**, *97*, 3549–3550. https://doi.org/10.1021/ja00845a061.

(17) Arnaboldi, S.; Magni, M.; Mussini, P. R. Enantioselective Selectors for Chiral Electrochemistry and Electroanalysis: Stereogenic Elements and Enantioselection Performance. *Curr. Opin. Electrochem.* **2018**, *8*, 60–72. https://doi.org/10.1016/j.coelec.2018.01.002.

(18) Shono, T.; Hamaguchi, H.; Matsumura, Y. Electroorganic Chemistry. XX.1 Anodic Oxidation of Carbamates. *J. Am. Chem. Soc.* **1972**, *97*, 4264–4268. https://doi.org/10.1021/ja00848a020.

(19) Shono, T. Electroorganic Chemistry in Organic Synthesis. *Tetrahedron* **1984**, *40*, 811–850. https://doi.org/10.1016/S0040-4020(01)88790-1.

(20) Steckhan, E. Indirect Electroorganic Syntheses- A Modern Chapter of Organic Electrochemistry. *Angew. Chem. Int. Ed. Engl.* **1986**, *25*, 683–701. https://doi.org/10.1002/anie.198606831.

(21) Wiebe, A.; Gieshoff, T.; Möhle, S.; Rodrigo, E.; Zirbes, M.; Waldvogel, S. R. Electrifying Organic Synthesis. *Angewandte Chemie - International Edition* **2018**, *57* (20), 5594–5619. https://doi.org/10.1002/anie.201711060.

(22) Yan, M.; Kawamata, Y.; Baran, P. S. Synthetic Organic Electrochemical Methods since 2000: On the Verge of a Renaissance. *Chem Rev* **2017**, *117*, 13230–13319. https://doi.org/10.1021/acs.chemrev.7b00397.

(23) Rosen, B. R.; Werner, E. W.; O'Brien, A. G.; Baran, P. S. Total Synthesis of Dixiamycin B by Electrochemical Oxidation. *J. Am. Chem. Soc.* **2014**, *136*, 5571–5574. https://doi.org/10.1021/ja5013323.

(24) Tan, Z.; Liu, Y.; Helmy, R.; Rivera, N. R.; Hesk, D.; Tyagarajan, S.; Yang, L.; Su, J. Electrochemical Bromination of Late Stage Intermediates and Drug Molecules. *Tetrahedron Lett.* **2017**, *58*, 3014–3018. https://doi.org/10.1016/j.tetlet.2017.06.019.

(25) Schotten, C.; Nicholls, T. P.; Bourne, R. A.; Kapur, N.; Nguyen, B. N.; Willans, C. E. Making Electrochemistry Easily Accessible to the Synthetic Chemist. *Green Chem.* **2020**, *22*, 3358–3375. https://doi.org/10.1039/d0gc01247e.

(26) Kingston, C.; Palkowitz, M. D.; Takahira, Y.; Vantourout, J. C.; Peters, B. K.; Kawamata, Y.; Baran, P. S. A Survival Guide for the "Electro-Curious." *Acc. Chem. Res.* **2020**, *53*, 72–83. https://doi.org/10.1021/acs.accounts.9b00539.

(27) Heard, D. M.; Lennox, A. J. J. Electrode Materials in Modern Organic Electrochemistry. *Angew. Chem. Int. Ed.* **2020**, *59*, 18866–18884. https://doi.org/10.1002/anie.202005745.

(28) Elgrishi, N.; Rountree, K. J.; McCarthy, B. D.; Rountree, E. S.; Eisenhart, T. T.; Dempsey, J. L. A Practical Beginner's Guide to Cyclic Voltammetry. *J. Chem. Educ.* **2018**, *95*, 197–206. https://doi.org/10.1021/acs.jchemed.7b00361.

(29) Röckl, J. L.; Dörr, M.; Waldvogel, S. R. Electrosynthesis 2.0 in 1,1,1,3,3,3-Hexafluoroisopropanol/Amine Mixtures. *ChemElectroChem* **2020**, *7*, 3686–3694. https://doi.org/10.1002/celc.202000761.

(30) Chakraborty, P.; Mandal, R.; Garg, N.; Sundararaju, B. Recent Advances in Transition Metal-Catalyzed Asymmetric Electrocatalysis. *Coord. Chem. Rev.* **2021**, 214065. https://doi.org/10.1016/j.ccr.2021.214065.

(31) Francke, R.; Little, R. D. Redox Catalysis in Organic Electrosynthesis: Basic Principles and Recent Developments. *Chem Soc Rev* **2014**, *43*, 2492–2521. https://doi.org/10.1039/c3cs60464k.

(32) Lin, Q.; Li, L.; Luo, S. Asymmetric Electrochemical Catalysis. *Chem. Eur. J.* **2019**, *25*, 10033–10044. https://doi.org/10.1002/chem.201901284.

(33) Ghosh, M.; Shinde, V. S.; Rueping, M. A Review of Asymmetric Synthetic Organic Electrochemistry and Electrocatalysis: Concepts, Applications, Recent Developments and Future Directions. *Beilstein J. Org. Chem.* **2019**, *15*, 2710–2746. https://doi.org/10.3762/bjoc.15.264.

(34) Park, D. il; Jung, S.; Yoon, H. J.; Jin, K. Directing Electrochemical Asymmetric Synthesis at Heterogeneous Interfaces: Past, Present, and Challenges. *Electrochim. Acta*. **2021**, 139271. https://doi.org/10.1016/j.electacta.2021.139271.

(35) Deronzier, A.; Moutet, J.-C. Polymers of Platinum Metals Complexes Immobilised on Electrodes. *Platinum Metals Rev.* **1998**, *42*, 60–68.

(36) Osa, T.; Kashiwagi, Y.; Mukai, K.; Ohsawa, A.; Bobbitt, J. M. A Preparative Nitroxyl-Radical Coated, Graphite Felt Electrode for the Oxidation of Alcohols. *Chem Lett* **1990**, 75–78.

(37) Plutschack, M. B.; Pieber, B.; Gilmore, K.; Seeberger, P. H. The Hitchhiker's Guide to Flow Chemistry. *Chem. Rev.* **2017**, *117*, 11796–11893. https://doi.org/10.1021/acs.chemrev.7b00183.

(38) Wegner, J.; Ceylan, S.; Kirschning, A. Flow Chemistry - A Key Enabling Technology for (Multistep) Organic Synthesis. *Adv. Synth. Catal.* **2012**, *354*, 17–57. https://doi.org/10.1002/adsc.201100584.

(39) Ley, S. v. On Being Green: Can Flow Chemistry Help? *Chem. Rec.* **2012**, *12*, 378–390. https://doi.org/10.1002/tcr.201100041.

(40) Hone, C. A.; Kappe, C. O. Towards the Standardization of Flow Chemistry Protocols for Organic Reactions. *Chemistry–Methods* **2021**, *1*, 454–467. https://doi.org/10.1002/cmtd.202100059.

(41) Vapourtec Ltd. *Ion electrochemical reactor*. https://www.vapourtec.com/products/flow-reactors/ion-electrochemical-reactor-features/, (accessed September 2022).

(42) Folgueiras-Amador, A. A.; Philipps, K.; Guilbaud, S.; Poelakker, J.; Wirth, T. An Easy-to-Machine Electrochemical Flow Microreactor Efficient Synthesis of

Isoindolinone and Flow Functionalization. *Angew. Chem. Int. Ed.* **2017**, *56*, 15446–15450. https://doi.org/10.1002/anie.201709717.

(43) van Melis, C. G. W.; Penny, M. R.; Garcia, A. D.; Petti, A.; Dobbs, A. P.; Hilton, S. T.; Lam, K. Supporting-Electrolyte-Free Electrochemical Methoxymethylation of Alcohols Using a 3D-Printed Electrosynthesis Continuous Flow Cell System. *ChemElectroChem* **2019**, *6*, 4144–4148. https://doi.org/10.1002/celc.201900815.

(44) Laudadio, G.; Straathof, N. J. W.; Lanting, M. D.; Knoops, B.; Hessel, V.; Noël, T. An Environmentally Benign and Selective Electrochemical Oxidation of Sulfides and Thiols in a Continuous-Flow Microreactor. *Green Chem.* **2017**, *19*, 4061–4066. https://doi.org/10.1039/c7gc01973d.

(45) Zhong, X.; Hoque, M. A.; Graaf, M. D.; Harper, K. C.; Wang, F.; Genders, J. D.; Stahl, S. S. Scalable Flow Electrochemical Alcohol Oxidation: Maintaining High Stereochemical Fidelity in the Synthesis of Levetiracetam. *Org. Process Res. Dev.* **2021**, *25*, 2601–2607. https://doi.org/10.1021/acs.oprd.1c00036.

(46) Brown, R. C. D. The Longer Route Can Be Better: Electrosynthesis in Extended Path Flow Cells. *Chem. Rec.* **2021**, *21*, 2472–2487. https://doi.org/10.1002/tcr.202100163.

(47) Maljuric, S.; Jud, W.; Kappe, C. O.; Cantillo, D. Translating Batch Electrochemistry to Single-Pass Continuous Flow Conditions: An Organic Chemist's Guide. *J. Flow Chem.* **2020**, *10*, 181–190. https://doi.org/10.1007/s41981-019-00050-z.

(48) Folgueiras-Amador, A. A.; Wirth, T. Perspectives in Flow Electrochemistry. *J. Flow Chem.* **2017**, *7*, 94–95. https://doi.org/10.1556/1846.2017.00020.

(49) Pletcher, D.; Green, R. A.; Brown, R. C. D. Flow Electrolysis Cells for the Synthetic Organic Chemistry Laboratory. *Chem. Rev.* **2018**, *118*, 4573–4591. https://doi.org/10.1021/acs.chemrev.7b00360.

(50) Winterson, B.; Rennigholtz, T.; Wirth, T.; Flow Electrochemistry: A Safe Tool for Fluorine Chemistry. *Chem. Sci.* **2021**, *12*, 9053–9059. https://doi.org/10.1039/d1sc02123k.

(51) Amri, N.; Wirth, T. Automated Electrochemical Selenenylations. *Synthesis* **2020**, *52*, 1751–1761. https://doi.org/10.1055/s-0039-1690868.

(52) Kharissova, O. v.; Kharisov, B. I.; González, C. M. O.; Méndez, Y. P.; López, I. Greener Synthesis of Chemical Compounds and Materials. *R. Soc. Open Sci.* **2019**, *6*, 191378. https://doi.org/10.1098/rsos.191378.

(53) Frontana-Uribe, B. A.; Little, R. D.; Ibanez, J. G.; Palma, A.; Vasquez-Medrano, R. Organic Electrosynthesis: A Promising Green Methodology in Organic Chemistry. *Green Chem.* **2010**, *12*, 2099–2119. https://doi.org/10.1039/c0gc00382d.

(54) Schäfer, H. J. Contributions of Organic Electrosynthesis to Green Chemistry. *C. R. Chimie* **2011**, *14*, 745–765. https://doi.org/10.1016/j.crci.2011.01.002.

Chapter 2: Development of Chiral Electrodes for Organic Electrochemistry

2.1 Introduction

2.1.1 Chiral Electrodes for Electrosynthesis

Chiral electrodes are an interesting and promising approach in asymmetric electrochemical synthesis. The selectivity is either induced by immobilised chiral mediators or imprinted chiral information. Chiral electrodes can significantly improve the recovery and reusability of catalysts or mediators. Finetuning of the electrode material for a specific reactivity and stereoselectivity is another advantage of this concept. Several different preparation methods for chiral electrodes have been developed in the past decades, such as: covalent linking of chiral molecules to the electrode surface and the coating of electrodes with chiral polymers. Chiral molecules have also been immobilised in clay film electrodes by ion exchange and by entrapment in metal. Another recent approach focuses on the imprinting of chiral information in metal.

Covalently modified electrode surfaces

The first example of a chiral electrode was reported by Miller and co-workers (1975) (Scheme 2.1A).[1] The electrode was manufactured by linking (*S*)-phenylalanine methyl ester covalently to an oxidised graphite surface. This chiral electrode gave 9.7% *ee* and 94% yield for the electroreduction of ethyl phenyl glyoxylate **9a** to the corresponding alcohol **10a**.

The same modification method was used to anchor (*S*)-phenylalanine methyl ester on the edge surface of highly ordered pyrolytic graphite (HOPG). The presence of the (*S*)-phenylalanine methyl ester on the electrode was confirmed by X-ray photoelectron spectroscopy (XPS). This electrode was then used in the electrochemical reduction of 4-acetylpyridine **11** to the corresponding alcohol **12** (2% *ee*) (Scheme 2.1B) and the electrooxidation of *p*-tolyl methyl sulfide **13** to the corresponding sulfoxide **14** (2% *ee*) (Scheme 2.1C). [2]

In another early attempt by Miller and co-workers (1976) to prepare a chiral electrode, (–)-camphoric acid was covalently anchored to a dimensionally stable anode (DSA), an electrode consisting of mixed metal oxides, or a SnO_2 electrode *via* a *γ*-aminopropyltriethoxysilane linker (Scheme 2.1D).[3] The oxidation of the thioanisole

derivative **15** with these electrodes afforded the corresponding sulfoxide **16** as a racemate. When comparing this report with a study from Komori and Nonaka (1984),[4] the question remains whether sterically demanding substituents on the sulfide would have had a positive influence on the enantiomeric excess.

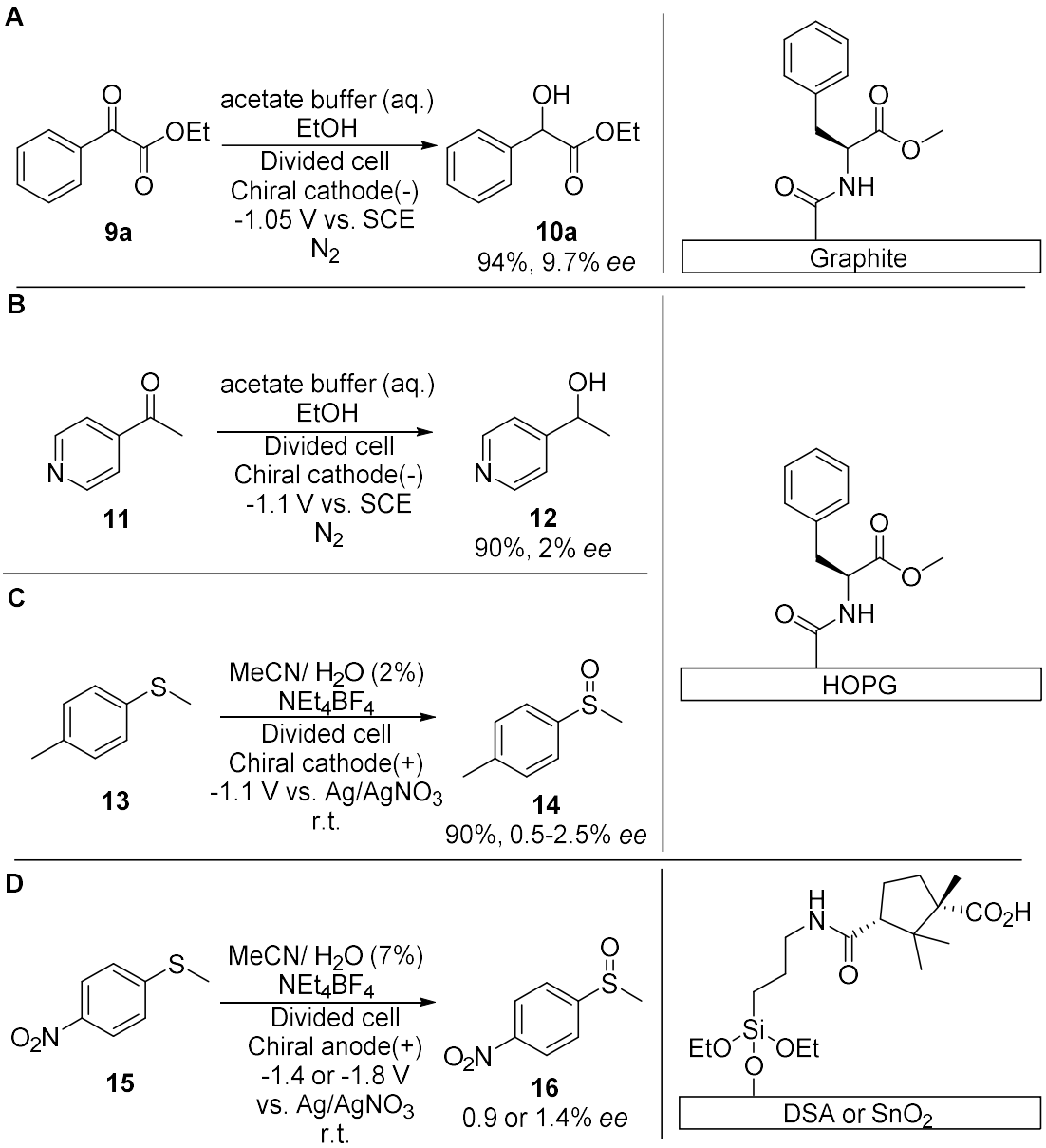

Scheme 2.1: Anodic and cathodic electrolysis with covalently modified chiral electrodes by Miller and co-workers.

These near racemic results indicate that either the coverage of the electrode with chiral selectors was too low or that the chiral selectors were not optimal for the presented substrates or reactions. Nevertheless, Miller and co-workers developed the idea and the first examples of chiral electrodes.

Lu and co-workers prepared chiral electrodes in a similar manner and provided a deeper insight into electrodes containing covalently linked amino acids as chiral modifiers (Scheme 2.2). Carboxylic acid moieties were generated on multi walled carbon nanotubes (MWCNTs) under oxidative conditions, transformed to acyl chloride groups with thionyl chloride and subsequently functionalised with amino acids. The functionalised MWCNTs were coated onto carbon paper. The chiral electrode was subsequently used as cathode for the reduction of ketones to the corresponding alcohols. The model amino acid in this study was L-lysine but the highest enantiomeric excess was obtained with arginine. Electrodes functionalised with L-arginine and D-arginine led to the (*R*)- (43% *ee*, 61% yield) and (*S*)-enantiomer (44% *ee*, 60% yield), respectively, when reducing 2,2,2-trifluoroacetophenone **17** to the corresponding alcohol **18** (Scheme 2.2A). The electrodes were recycled up to six times without loss of yield or *ee*. The authors assumed that the amino acids lysin and arginine were immobilised via the nucleophilic side chains. Based on that, they postulated a mechanism, in which a proton from the amino group in α-position of the amino acid forms a hydrogen bond with the carbonyl oxygen of the substrate and is then transferred during the electroreduction.[5]

Following a similar idea, D-phenylalanine functionalised MWCNTs were prepared by grafting the amino acid, D-4-amino-phenylalanine, onto MWCNTs *via* a diazo-reaction. The chiral material was immobilised on a glassy carbon electrode and utilised in the electroreduction of prochiral ketones. The most promising substrate, 2,2,2-trifluoroacetophenone **17**, was converted to the (*S*)-enantiomer of the corresponding alcohol **18** in 65% yield and 40% *ee* (Scheme 2.2B), which is comparable to the lysine and arginine electrodes described above.[6]

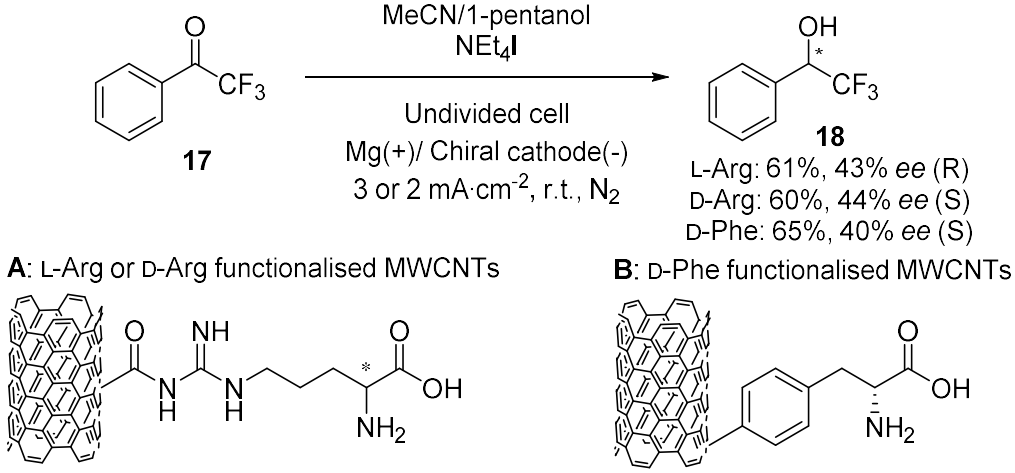

Scheme 2.2: Electrodes coated with amino acid functionalised MWCNTs.

Chiral polymer coated electrodes

Nonaka and co-workers investigated a new type of chiral electrodes based on poly-L-valine **19** (Scheme 2.3) in several reports. The project focused on the development of the electrode, the improvement of the stability and the possibilities and limitations for asymmetric organic electrosynthesis. This type of electrode could be used either as chiral cathode for the reduction of prochiral olefins, carbonyl compounds, oximes or halides or as chiral anode for the oxidation of sulfides to sulfoxides. Over the course of the project, they were able to prepare electrodes with remarkable stability and observed high stereoselectivities.

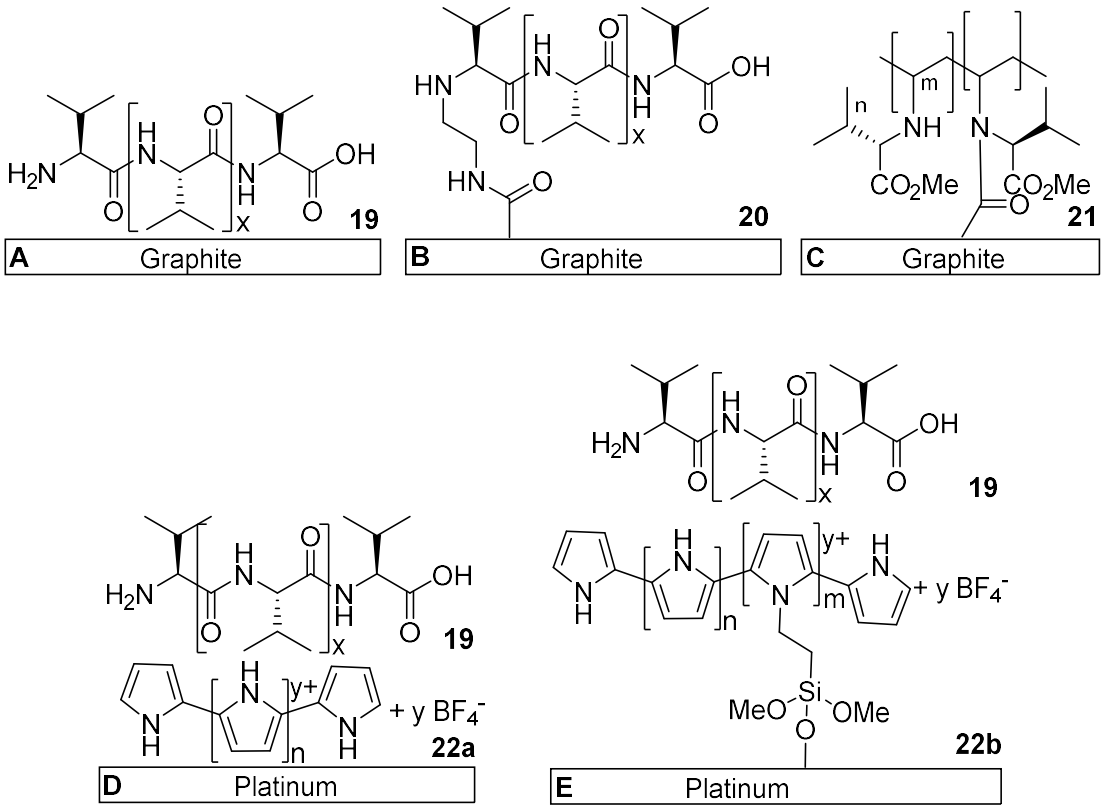

Scheme 2.3: Chiral electrodes coated with poly L-valine developed by Nonaka and co-workers.

The first report in the series by Abe *et al.* is one of the first examples for an electrode coated with a chiral polymer that was used in electrosynthesis (Scheme 2.3A). The electrode was prepared by dip-coating a graphite sheet in 0.5 w/v% or 1.0 w/v% solutions of poly-L-valine **19** in trifluoroacetic acid. The poly amino acid was synthesised by the *N*-carboxy anhydride (NCA) method *via* a ring opening polymerisation. The optical rotation was measured to be $[\alpha]_D^{20}$= -150° (c 1, trifluoroacetic acid), but only a rough estimate was given for the molecular weight (M_r = 2000). The electrode was used for asymmetric cathodic reductions of prochiral alkenes

23 (Scheme 2.4A). Citraconic acid **23a** was reduced to 2-methylsuccinic acid **24a** with 25% *ee* (determined by optical rotation). When the electrodes were tested in reuse experiments, no enantiomeric excess was detected after the fourth and sixth use for electrodes prepared with concentrations of 0.5 w/v% and 1.0 w/v% of poly-L-valine in the dip-coating solution, respectively. The reduction of 4-methylcoumarin **23b** resulted in up to 43% *ee* for 3,4-dihydro-4-methylcoumarin **24b**.[7]

Building up on initial results with the poly-L-valine electrode, Nonaka *et al.* explored the use of other optically active polymers on graphite electrodes. The electrodes were prepared with a similar dip-coating method as the aforementioned poly-L-valine coated electrode. Besides L-valine, the poly amino acids were based on D-valine, L-leucine, L-tryptophan and *γ*-benzyl L-glutamate. Poly(*N*-acroyloyl-L-valine methyl ester) was also investigated. The ability of these electrodes to induce an enantiomeric excess were tested with the electroreduction of citraconic acid **23a** to 2-methylsuccinic acid **24a** (Scheme 2.4A). Poly-L-valine gave the best stereocontrol, which was linked to its higher optical rotating power compared to the other polymers. Apart from different chiral polymers, a variety of reaction conditions were investigated. Different base electrodes like lead or zinc resulted in a lower enantiomeric excess. Factors like pH value, temperature, potential, current density and applied charge were also studied. The film thickness was investigated by recovering poly-L-valine **19** from the electrode, and it was found that an increase in thickness was detrimental to the reaction. It is hypothesised that substrates and protons travel through the non-conducting film and are then reduced at the interface to the graphite surface *via* an asymmetric electron transfer. After five uses the electrode lost all stereocontrol.[8]

Nonaka and co-workers expanded the reaction scope of their first poly-L-valine coated graphite electrode. Prochiral *α*-keto acids and esters **9** and the corresponding oximes **25** were converted to alcohols **10** and amins **26** with a low enantiomeric excess of up to 7% *ee* (Scheme 2.4B). The reduction of the *gem* dihalide 1,1-dibromo-2,2-diphenylcyclopropane **27** to 1-bromo-2,2-diphenylcyclopropane **28** proceeded with 16.6% *ee* (Scheme 2.4C). The low enantiomeric excess is explained with limitations of the electrode stability towards large amounts of charge over time.[9]

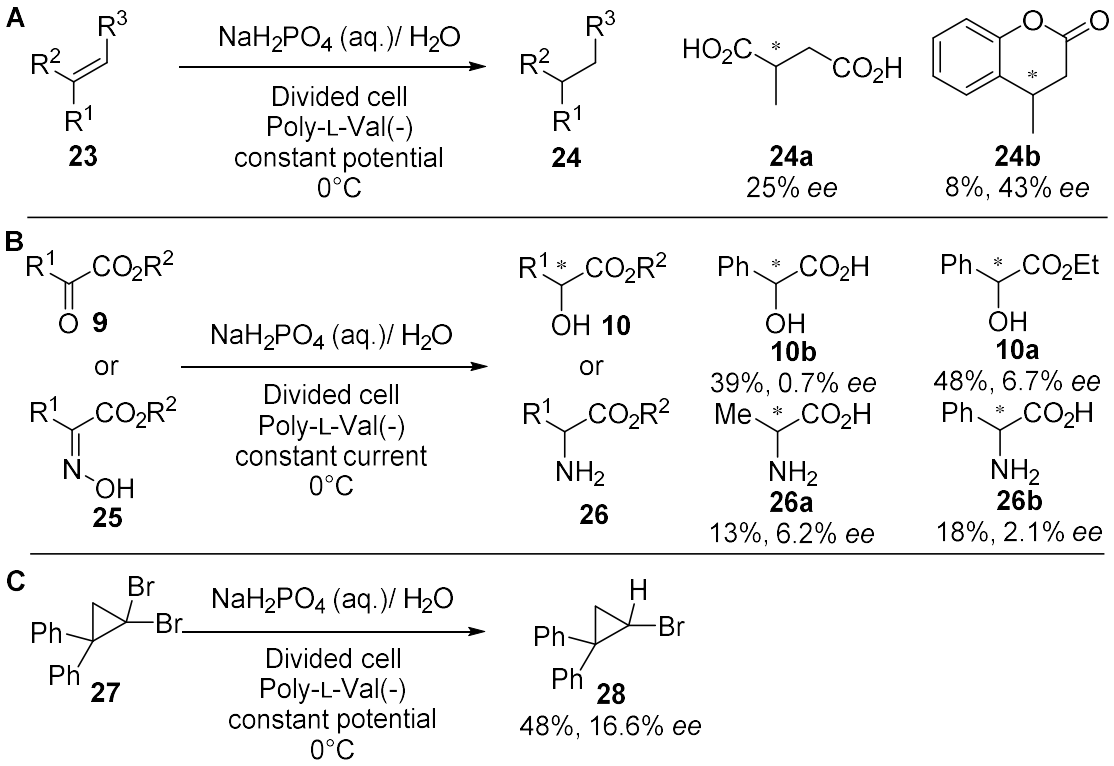

Scheme 2.4: Electrochemical reduction of alkenes (A), α-keto acids and esters, oxims (B) and *gem* halides (C) on poly L-valine/graphite cathodes.

Subsequently, Abe and Nonaka started to address the stability issue of the polymer film electrodes. Chemical modification of the graphite electrodes resulted in superior durability compared to dip coated electrodes. The electrodes were used and reused for the asymmetric electrochemical reduction of citraconic acid **23a** to 2-methylsuccinic acid **24a** (Scheme 2.4A). The modification was achieved by anchoring chiral polymers to the carboxylic acid residues of a graphite surfaces that had been activated with thionyl chloride. A poly-L-valine modified electrode **20** was prepared by initiating the polymerisation of the NCA of L-valine with 1,3-diaminopropane linkers on the electrode surface (Scheme 2.3B). The poly(N-acryloyl-L-valine methyl ester) modified electrode **21** were prepared by reacting the polymer with the previously activated surface oxide groups (Scheme 2.3C). The poly-L-valine modified electrode gave a higher enantiomeric excess of around 10% *ee* compared to the poly(N-acryloyl-L-valine methyl ester) modified electrode and outcompeted the dip-coated version after the third reuse.[10]

In another attempt to improve the electrode stability, Komori and Nonaka coated base electrodes with polypyrrole films before dip-coating with poly amino acids.[11] In their study, platinum electrodes were coated with polypyrrole by electropolymerisation (Scheme 2.3D) to obtain film **22a** or by the covalent anchoring of

((trimethoxysilyl)propyl))pyrrole monomers to the electrode surface before electropolymerisation to obtain film **22b** (Scheme 2.3E). These polypyrrole electrodes were compared with plain platinum after dip-coating in a TFA solution of poly-L-valine **19**. The electrodes were then tested for the oxidation of phenyl cyclohexyl sulfide **29f** to the corresponding sulfoxide **30f** (Scheme 2.5). The dip-coated plain platinum electrode gave the lowest enantiomeric excess with 28% *ee*. With the first polypyrrole **22a** coated electrode (Scheme 2.3D), the enantiomeric excess was increased to 40% *ee*. This was further improved to 54% by covalent anchoring of the polypyrrole film **22b** (Scheme 2.3E). The increase in enantiomeric excess was explained by an improved adhesion of the poly amino acid. The three differently modified platinum electrodes were further explored by Komori and Nonaka with a substrate scope (Scheme 2.5), a variety of chiral polymer coatings and reuse experiments.[4] Electrodes with polypyrrole films, that were covalently linked to the electrode surface, gave a higher stereoselectivity and had a better stability in reuse experiments compared to the other two modification methods. As observed before, poly-L-valine **19** outcompeted other chiral polymers when it came to stereocontrol. One of the most influential factors on the stereocontrol was the bulkiness of substituent groups. While thioanisole **29a** was oxidised to racemic phenyl methyl sulfoxide **30a**, *tert*-butyl phenyl sulfide **29e** was converted to the corresponding sulfoxide **30e** with up to 93% *ee*. The dip-coating concentration was analysed in a range between 1.0-0.1% w/v of poly-L-valine in TFA and the highest value was obtained at 0.25% w/v, which, in turn, highlighted the importance of the film thickness. Following these remarkable results, it would have been interesting to see these improved electrodes used in electrochemical reductions.

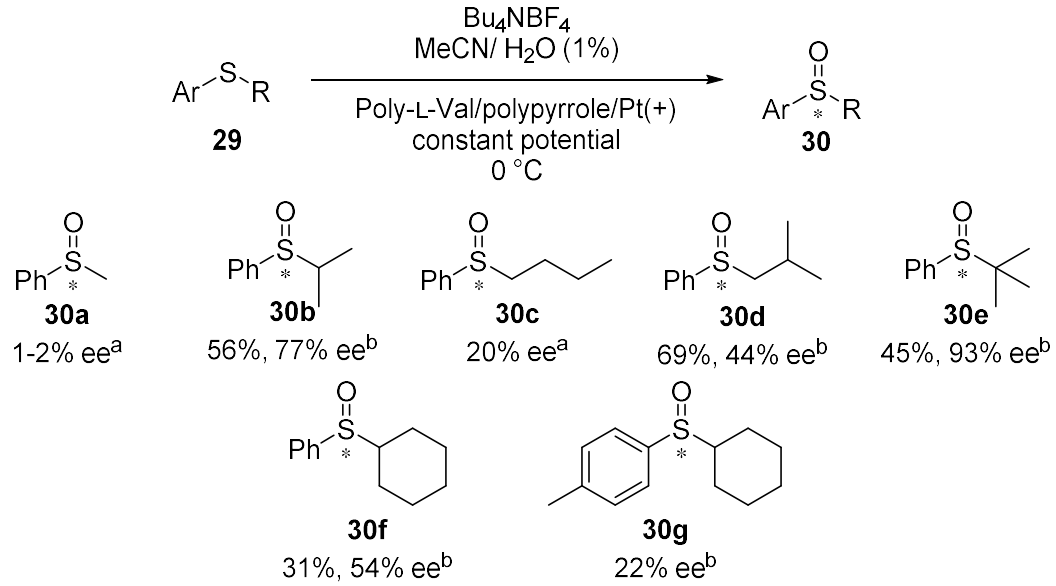

Scheme 2.5: Electrochemical oxidation of sulfides to sulfoxides on chiral poly amino acid/polypyrrole coated platinum electrodes (a: non-covalently bound polypyrrole film; b: covalently anchored polypyrrole film)

Furthermore, Nonaka and co-workers provided the first example of electrochemical kinetic resolution of racemic compounds (Scheme 2.6). The stereoselective oxidation of 2,2-dimethyl-1-phenyl-1-propanol **31** was performed with the previously reported platinum electrodes coated with polypyrrole **22b** poly-L-valine **19** (Scheme 2.3E). Initial results with the platinum electrodes showed a low stability over time at the required high potentials. Similar to platinum, lead dioxide electrodes were covalently coated with polypyrrole **22b** and dip-coated with poly-L-valine **19** to obtain a more durable chiral electrode. This electrode afforded the unreacted *S*-enantiomer of the alcohol **31** with an optical purity of 43% *ee*.[12]

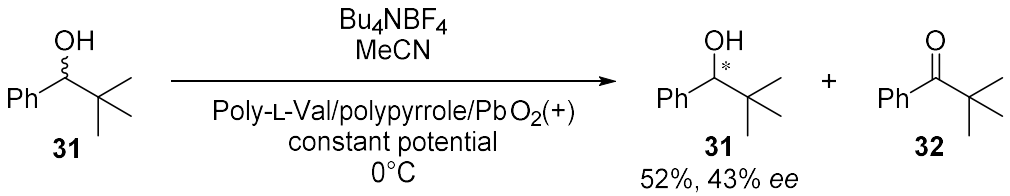

Scheme 2.6: Electrochemical kinetic resolution of 2,2-dimethyl-1-phenyl-1-propanol with poly L-valine coated electrodes.

In conclusion, Nonaka and co-workers established a method to prepare chiral electrodes based on poly amino acids immobilised on electrode surfaces. First generation electrodes prepared by dip-coating of graphite in a solution of poly-L-valine **19** in TFA gave promising results but suffered from a low stereoselectivity and stability in reuse experiments. Moving on from these results they improved the stability of the electrodes by tethering the chiral polymers to surface oxides of the graphite

electrode.[10] Another approach to increase stability was to deposit a polypyrrole **22a** film on the electrode surface by electro-polymerisation before dip-coating the electrode with poly-L-valine **19**.[11] The stability of this type of electrode was further improved by covalently linking the polypyrrole layer **22b** to electrode materials like platinum[4] or lead dioxide[12] leading to some of the highest stabilities and stereocontrol reported for chiral electrodes. The electrodes were successfully used for a broad scope of oxidations and reductions. Nonaka and co-workers also tested polymer coated electrodes based on different amino acids. The researchers investigated the effect of the electrodes on the enantioinduction in various reactions and reuse experiments meticulously. However, the electrode materials were not characterised in sufficient detail. Only a rough estimate for the molecular weight of the poly-L-valine **19** was given while the other chiral polymers remained uncharacterised. The characterisation of the electrode could be further improved with methodologies like circular dichroism, XPS or electron microscopy to obtain a deeper understanding of the surface structure and film thickness. Computational methods could be used to elucidate the interactions between the substrate and the chiral polymer that influence the asymmetric induction in the products.

Apart from these poly amino acid coated electrodes, other research groups have been investigating chiral polymers on electrode surfaces for organic synthesis as well. Several attempts have been reported regarding electrochemical polymerisation of pyrrole monomers substituted with chiral moieties and the use of the resulting electrodes in the asymmetric reduction of prochiral ketones.

Pleus and Schwientek derivatised pyrrole monomers with chiral moieties in the 3-position and *N*-position. They deposited the chiral monomers **33-36** (Scheme 2.7) on electrodes by means of electropolymerisation. The chiral moiety L-lactate was linked to the pyrrole via a spacer unit consisting of a variety of alkyl chains. The enantioselectivity of the electrodes was confirmed with differences in current density in cyclic voltammograms of (*S*)-(+)- and (*R*)-(–)-10-champhorsulfonic acid.[13,14] Following these first two reports, in which the electrodes were prepared and characterised, Pleus *et al.* tested the enantioselective properties of the electrodes in electroreduction experiments with prochiral ketones. They observed optical purities of up to 17% *ee* for the electroreduction of 4-methyl benzophenone **37a** to the corresponding alcohol **38a**. The enantiomeric excess was dependant on the electrolyte used during the

electrodeposition of the polymer. Only two substrates, 4-methyl benzophenone **33** and acetophenone **35**, have been tested with this electrode.[15,16]

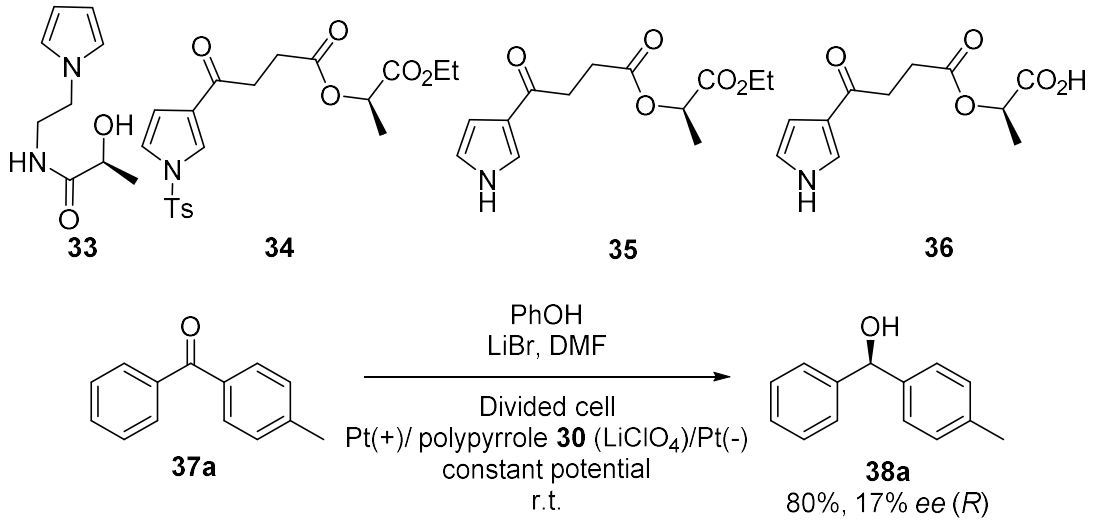

Scheme 2.7: Chiral pyrrole monomers and electrochemical reduction of 4-methyl benzophenone with a chiral polypyrrole coated cathode.

Seki and co-workers deposited palladium particles on a chiral polypyrrole (**39**) film electrode. The electrode was used as cathode for the electrocatalytic hydrogenation (ECH) of prochiral *α*-ketoesters **9**. The pyrrole monomer was *N*-substituted with L-lactate and electropolymerised in a similar fashion as described in the previous section. The ECH with methyl phenylglyoxylate **9c** afford the corresponding alcohol **10c** with a low optical purity of up to 14% *ee* (Scheme 2.8) and an excellent yield of 97%. They explained their highest enantiomeric excess with a decrease in particle size due to an increase in current density during the electrodeposition of palladium. Furthermore, the electrode could be reused without a significant decrease of enantiomeric excess.[17]

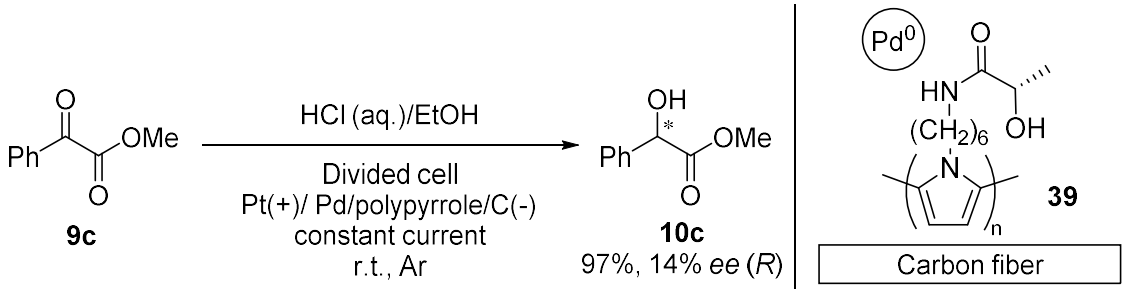

Scheme 2.8: ECH of methyl phenylglyoxylate **9c** with a chiral polypyrrole film/Pd electrode.

Immobilised electrocatalysts and mediators

The use of polymer films on electrodes enabled the immobilisation of chiral electrocatalysts and mediators on electrode surfaces for both enantioselective reductions and oxidations. This technique of heterogenisation of chiral catalysts can

help to reduce the amount of required catalyst, simplify the purification of products and recovery of catalyst. The concept of chiral polymer coatings on electrodes was used in the form of chiral polymeric ligands by Moutet *et al*. They used chiral bipyridyl ligands tethered to polypyrrole in order to immobilise rhodium(III) complexes **40** for ECH on a carbon cloth electrode (Scheme 2.9). The electrochemical and enantioselective properties of this electrode were investigated with cyclic voltammetry and the ECH of acetophenone **37b** (Scheme 2.9). The heterogeneous system turned out to exhibit higher efficiencies compared to the homogeneous catalyst as indicated by higher catalytic currents. Higher turnover numbers and good current efficiencies were observed and a reduction of film thickness was also favourable. Furthermore, a slightly higher enantiomeric excess for (*S*)-1-phenylethanol **38b** was observed (average: 18% *ee*) when using the coated electrode compared to the homogeneous catalyst. The durability and stability of the electrode was demonstrated with three reuses.[18,19]

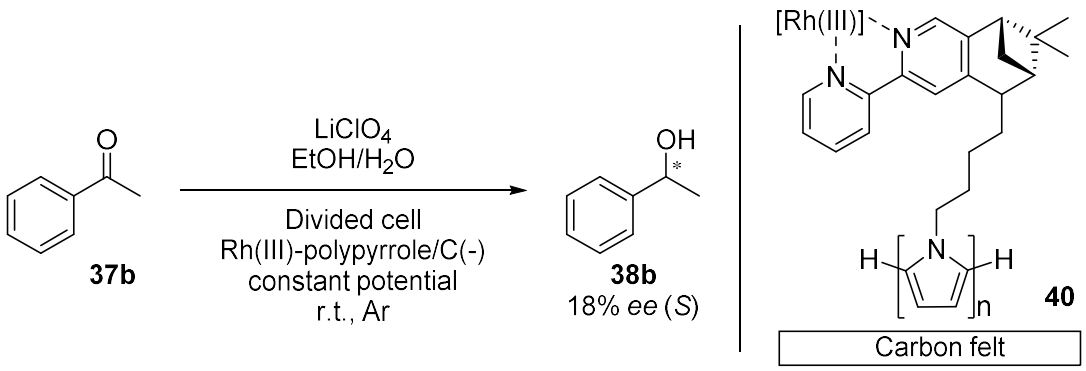

Scheme 2.9: Rhodium catalysed ECH with cathodes coated with chiral polymeric ligands.

Wong and co-workers reported chiral manganese-salen complexes **41a** and **41b**, which represents another example for chiral polymeric ligands (Scheme 2.10). The salen complex was immobilised on glassy carbon by electropolymerisation of vinyl substituents. These electrodes gave 65 – 77 % *ee* for the epoxidation of olefins **42a-c** with molecular oxygen. The turnover numbers for the immobilised manganese catalyst are also significantly higher compared to the homogeneous catalyst.[20]

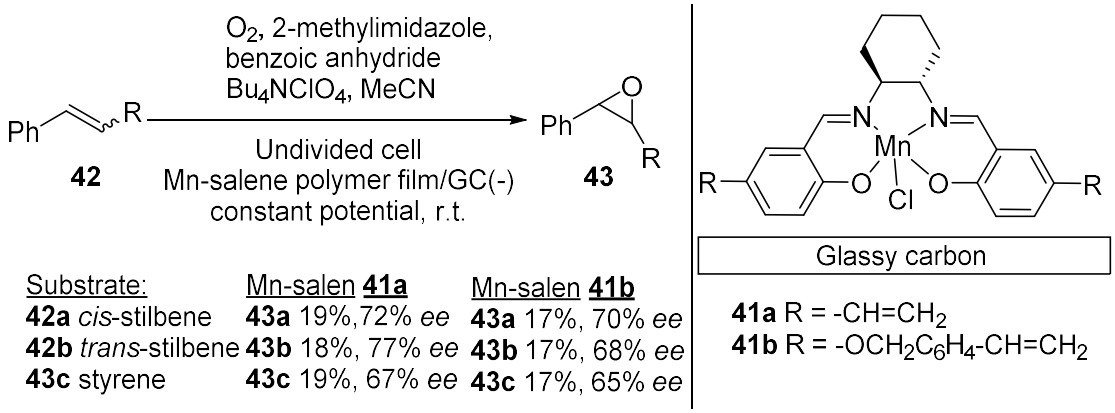

Substrate:	Mn-salen **41a**	Mn-salen **41b**
42a *cis*-stilbene	**43a** 19%,72% *ee*	**43a** 17%, 70% *ee*
42b *trans*-stilbene	**43b** 18%, 77% *ee*	**43b** 17%, 68% *ee*
43c styrene	**43c** 19%, 67% *ee*	**43c** 17%, 65% *ee*

Scheme 2.10: Manganese catalysed electrochemical epoxidation of alkenes with chiral polymeric salen ligand coated electrodes.

Another interesting polymer based chiral electrode, that falls into the category of immobilised chiral redox mediator was reported by Kashiwagi *et al.* (2003). A chiral N-oxyl radical mediator **44**, (6*S*,7*R*,10*R*)-4-amino-2,2,7-trimethyl-10-isopropyl-1-azaspiro[5.5]undecane *N*-oxyl, was covalently linked to poly acrylic acid on a graphite felt electrode for the asymmetric electrochemical transformation of diols **45** to lactones **46**. Various substrates **45a-d** were converted to the corresponding lactones **46a-d** with yields between 80% and 96% and enantiomeric excesses between 82% *ee* and 99% *ee* were reported. Unfortunately, only one prochiral substrate, diol **45b**, was used. All other substrates were used enantiomerically pure, which defeats the purpose of a chiral electrode. The stability of the electrode was only confirmed with cyclic voltammetry waves. A reuse of the electrode was indicated in the report, but the exact number of runs was not specified.[21]

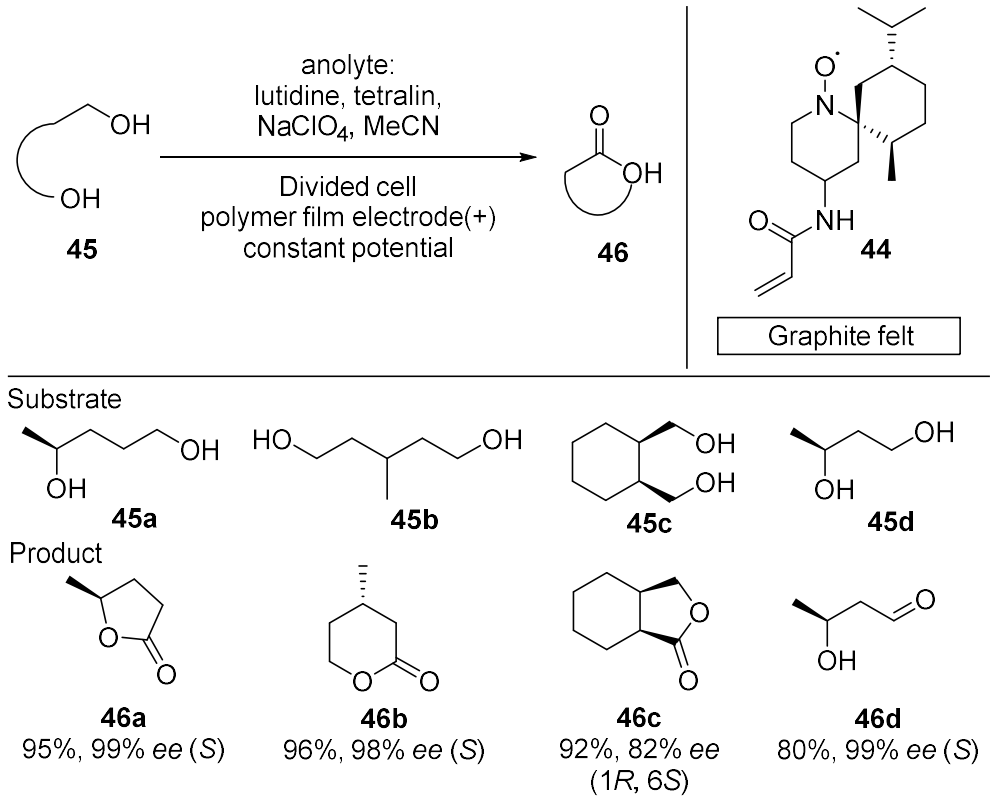

Scheme 2.11: Electrochemical lactonisation of diols **44** on electrodes coated with a chiral mediator modified electrode.

Chiral clay film electrodes – ion exchange

Yamagishi and Aramata developed an optically active clay-chelate film electrode that consisted of a chiral metal chelate complex immobilised in a clay thin film on a SnO_2 coated glass plate. The electrodes were prepared by coating the SnO_2 electrode with a sodium montmorillonite film. Subsequently, the sodium ions were exchanged for optically pure $Ru(phen)_3^{2+}$ ions (phen = 1,10-phenanthroline) to obtain the chiral electrodes.[22,23]

In their first report on this type of electrode, a Δ-$Ru(phen)_3^{2+}$ **47a** chelate complex was used in the clay film (Scheme 2.12A). Due to steric hindrance, only 50% of the surface sites are occupied with the Δ -isomer of the Ru chelate while the remaining sites are free to be taken by the Λ-isomer of the same or a similar complex. In this example a $Co(phen)_3^{2+}$ complex **48** is electrolysed to test the stereoselective properties. Potentiostatic oxidation of racemic $Co(phen)_3^{2+}$ **48** on the chiral clay-chelate film electrodes resulted in a full conversion to $Co(phen)_3^{3+}$ **49** and a low enantiomeric excess of 7%.[22]

In a second study, an electrode containing Λ-Ru(phen)$_3^{2+}$ **47b** was utilised to oxidise sulfides to sulfoxides under potentiostatic conditions (Scheme 2.12B).[23] Phenyl alkyl sulfides **29f** and **29h-j** with sterically demanding alkyl residues were converted to the corresponding *R*-sulfoxides **30f** and **30h-j** with a low enantiomeric excess. Stronger interactions between the *R*-enantiomer of phenyl cyclohexyl sulfoxide and a column of Λ-Ru(phen)$_3^{2+}$ **47b** on montmorillonite in comparison to the *S*-enantiomer were reported before.[24] It is rationalised in this study that this interaction leads to an excess of the *R*-enantiomer due to a better stabilisation of the intermediate.

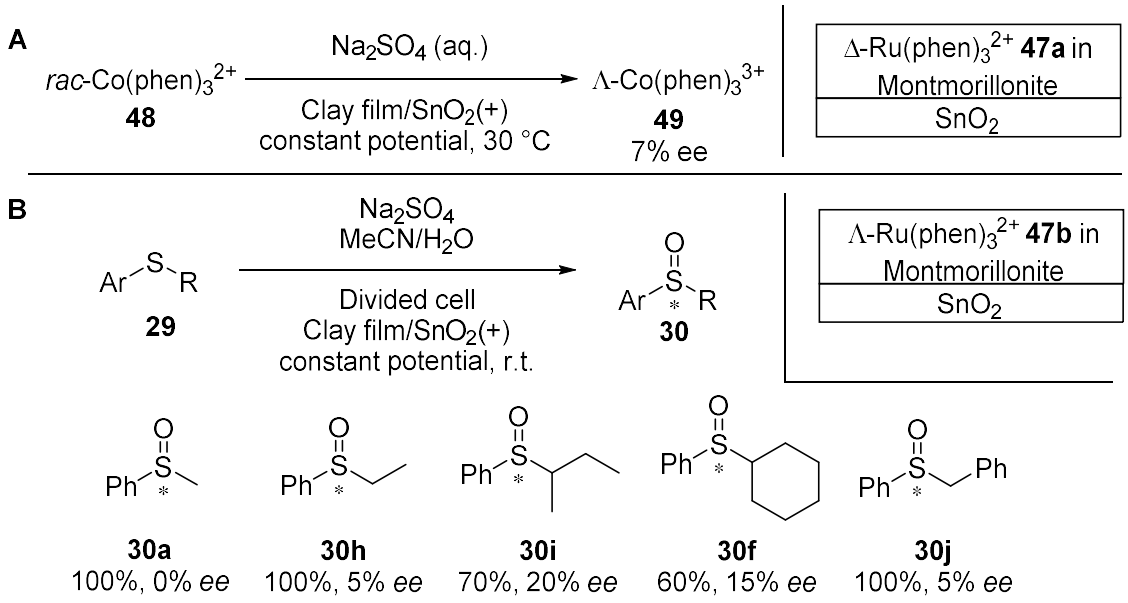

Scheme 2.12: Chiral electrodes based on chiral Ru(phen)$_3^{2+}$ immobilised in clay film. A) Electrochemical stereoselective oxidation of a Co(phen)$_3^{2+}$ chelate complex. B) Asymmetric electrochemical oxidation of sulfides to sulfoxides.

In these two studies potential leaching of the chelate complex from the electrode and thereby the durability of the chiral electrode is not discussed.

Chiral metals as electrode materials

The most recent methods for the preparation of chiral electrodes focused on the use of chiral metal. Lu and co-workers employed the concept of organically doped metals to entrap chiral modifiers, in particular cinchona alkaloids **50a-d** (Scheme 2.13B), within silver[25] and copper particles[26]. These chiral metal composites were pressed into coins and used as cathodes in ECH reactions of ketones. The highest *ee* values for the ECH of methyl phenylglyoxylate **9c** were achieved with cinchonine encapsulated in silver electrodes (CN@Ag) (60% *ee*, *S*) and cinchonidine in copper electrodes (CD@Cu) (78% ee, *R*) (Scheme 2.13A). The coin electrodes showed remarkable stability when

reused up to ten times without a significant loss of yield or enantiomeric excess. Interestingly, the enantiomeric configuration could be chosen depending on the cinchona alkaloid present within the metal: Cinchonidine **50a** and quinidine **50c** afforded the *R*-configuration while cinchonine **50b** and quinine **50d** gave the *S*-configuration of methyl mandelate **10c**. So far, a drawback of this type of electrode is the limited substrate and reaction scope. With CD@Cu cathodes high ee values were obtained for *α*-ketoesters **9a-c** and low yields and moderate enantiomeric excesses were afforded for ketones such as acetophenone **37b** (Scheme 2.13C). As a proof of concept, the use of organically doped metals as electrode materials offers a wide range of potential catalyst-metal combinations for asymmetric heterogeneous electrocatalysis.

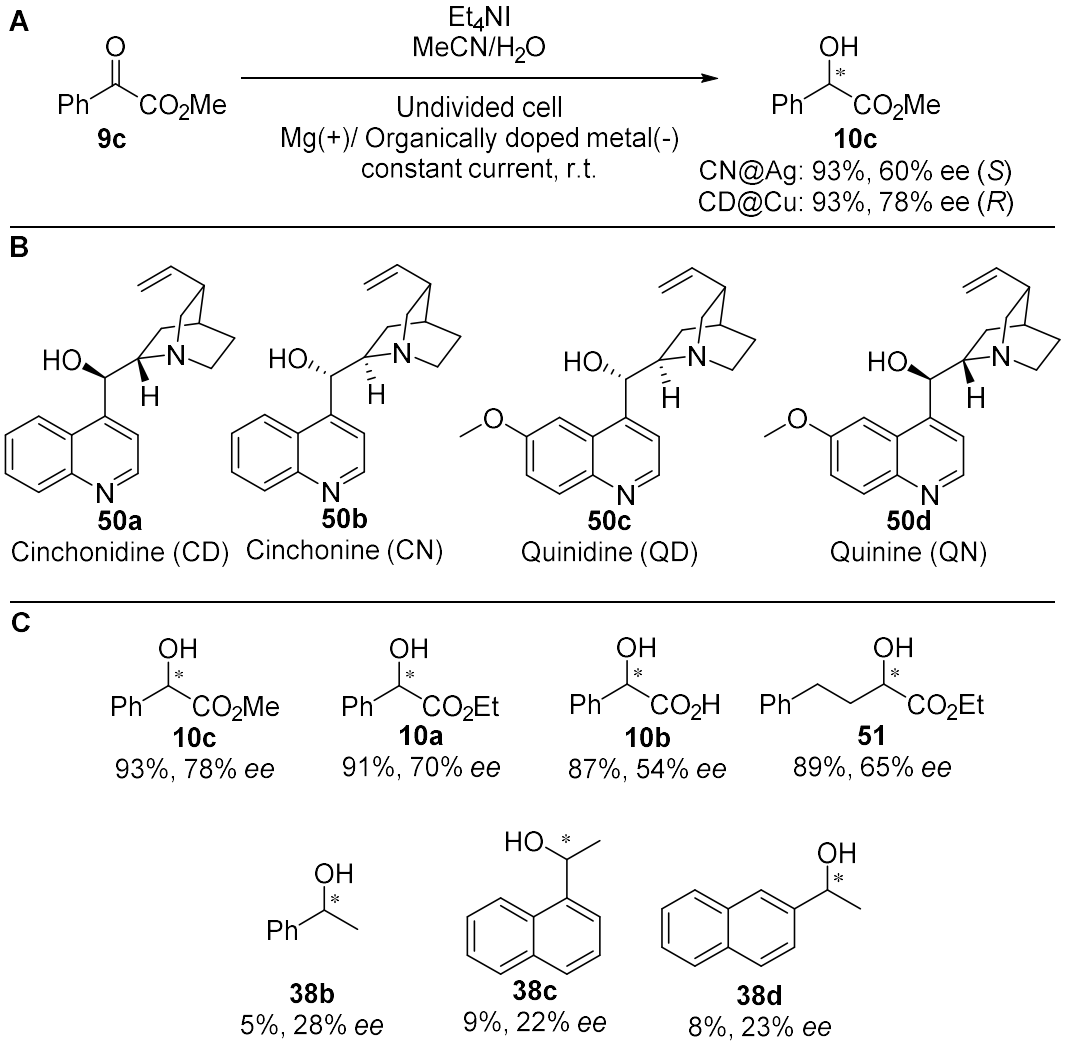

Scheme 2.13: A) ECH of methyl phenylglyoxylate with CN@Ag and CD@Cu cathodes. B) Cinchona alkaloids that were entrapped in silver and copper. C) Substrate scope for the ECH of ketones with a CD@Cu cathode.

By doping silver with a chiral cobalt complex, Lu and co-workers produced another chiral electrode based on the concept of organically doped metals (Scheme 2.14A).[27] They reduced silver cations with zinc powder in the presence of a chiral cobalt salen complexes **52a** and **52b**, which had been used previously as a homogeneous catalyst for the electrocatalytic asymmetric carboxylation of benzyl chlorides.[28] The entrapment in silver allowed the heterogenisation of the catalyst and its reuse, which was significantly easier to implement compared to the homogeneous system. The recyclability was demonstrated with up to seven uses of the same electrode without a significant loss of activity. In a small substrate scope (Scheme 2.14B), various racemic benzyl bromides were carboxylated with 20% *ee* to 73% *ee*. The model substrate (1-bromoethyl)benzene **53a** was converted to 2-phenylpropionic acid **54a** with up to 73% *ee*.

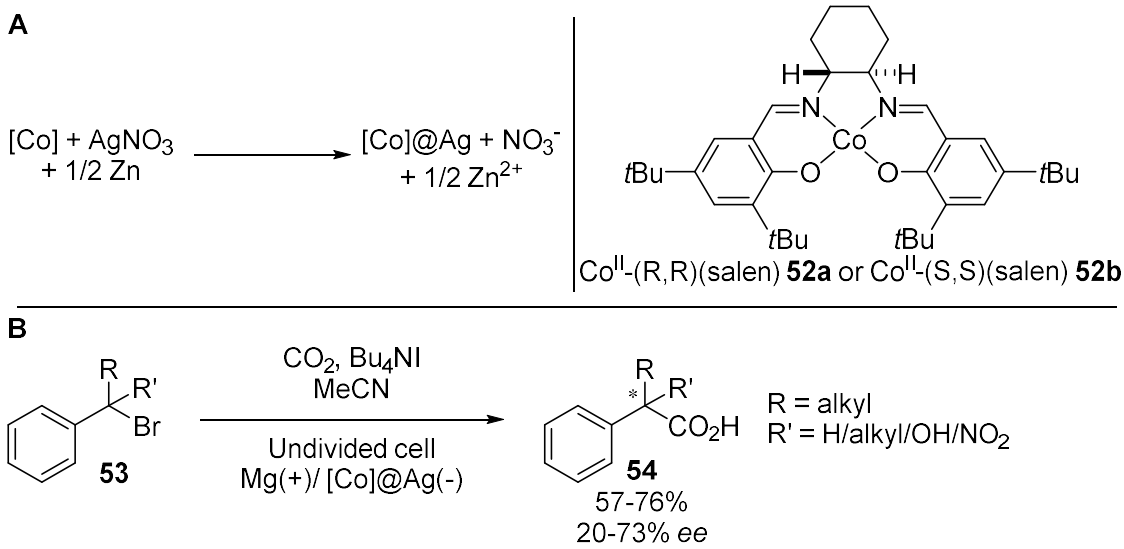

Scheme 2.14: Entrapment of a chiral cobalt salen complex in silver (A). Electrocatalytic asymmetric carboxylation of benzyl bromides with chiral [Co]@Ag electrodes (B).

Another approach, which utilised chiral metals as electrode materials, focused on chiral imprinted mesoporous platinum[29,30] and nickel[31]. The imprinting process included the reduction of the metal salt in the presence of a surfactant and a chiral template such as mandelic acid **10b** or 1-phenylethanol **38b**. The template and surfactant would then be washed off to leave a mesoporous metal structure with chiral cavities. Subsequently, the electroreduction of prochiral ketones such as phenylglyoxylic acid **9b**[29] and acetophenone **37b**[30] furnished the corresponding alcohols **10b** and **38b** with low enantiomeric excess (Scheme 2.15A). A sharp increase in enantiomeric excess of up to 91% *ee* for (*S*)-1-phenylethanol **38b** was achieved by using pulsed electrosynthesis compared to 13% *ee* in the steady state experiment (Scheme 2.15B).[30] The shortest

pulse time of 2 s followed by 120 s of relaxation time gave the best results. This increase was explained with the time it takes for the product to free up the chiral cavities within the mesoporous metal and the time for the next substrate molecule to fill the cavities again before the next conversion event. The platinum electrodes were reused with a decreasing stereocontrol over three runs. It was mentioned that the nickel electrodes[31] had inferior stability compared to platinum and an oxidation of the surface in the absence of applied potential would lead to a loss of chiral information.

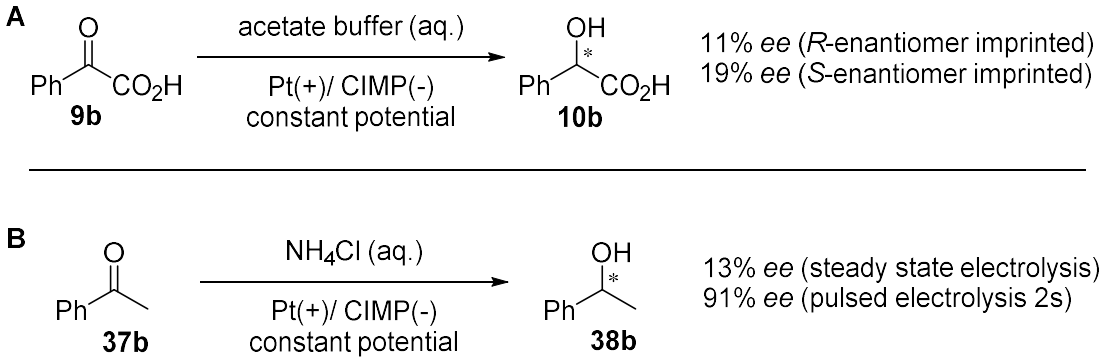

Scheme 2.15: Chiral imprinted mesoporous platinum (CIMP) electrodes were used for the electroreduction of phenylglyoxylic acid (A) and the pulsed electroreduction of acetophenone (B).

Since monometallic chiral imprinted electrodes exhibit problems regarding the stability and durability, due to reorganisation of surface atoms and loss of chiral information, Kuhn and co-workers developed electrodes based on alloys.[32] A platinum-iridium alloy was imprinted with optically pure 1-phenylethanol **38b** and used several times in pulsed electrosynthesis experiments to compare the stability with the previous platinum electrodes. The enantiomeric excess decreased only by 8% between the first (98% *ee*) and the third run (90% *ee*) with the chiral imprinted mesoporous alloy electrode, which constitutes a major improvement to the chiral imprinted mesoporous platinum[30] with a loss of 28% between first (67% *ee*) and third run (39% *ee*). Not only could the enantiomeric excess be increased compared to previous electrodes, but also the stability and durability of the electrode was significantly improved.

As the chiral information is only contained within the mesoporous material, a pulsed electrolysis approach with short pulse times and long relaxation times was necessary to furnish high enantioselectivity, leading to long reaction times. In an attempt to reduce the overall reaction times while obtaining high enantioselectivity, Kuhn and co-workers blocked the outer surface of the chiral imprinted mesoporous platinum electrode with a self-assembled monolayer (Figure 2.1).[33] A medium length linear alkanethiol, 1-heptanethiol **55**, was chosen as organosulfur ligand in order to cover the outer surface

of the mesoporous platinum and inhibit side reactions. Two methods for the preparation of the self-assembled monolayer have been investigated. For the first approach the electrode, which still contained surfactant and chiral template, was dipped into a solution of thiols. An increased time in the thiol solution led to a decrease of enantiomeric excess due to thiol ligands entering and blocking the chiral sites within the mesopores. In the second approach, the monolayer was transferred by micro printing onto the clean electrode surface *via* a rubber stamp. This method could be used to modify the electrode several times with a thiol monolayer without the loss of enantiomeric excess. In steady state electroreductions of acetophenone **37b**, bare platinum imprinted with (*S*)-1-phenylethanol **38b** gave only 29% *ee*. Electrodes modified in thiol solution and by micro printing afforded 93% *ee* and 90% *ee*, respectively, thus, maintaining high enantiomeric excess while reducing the reaction time significantly from one week to 13 hours.

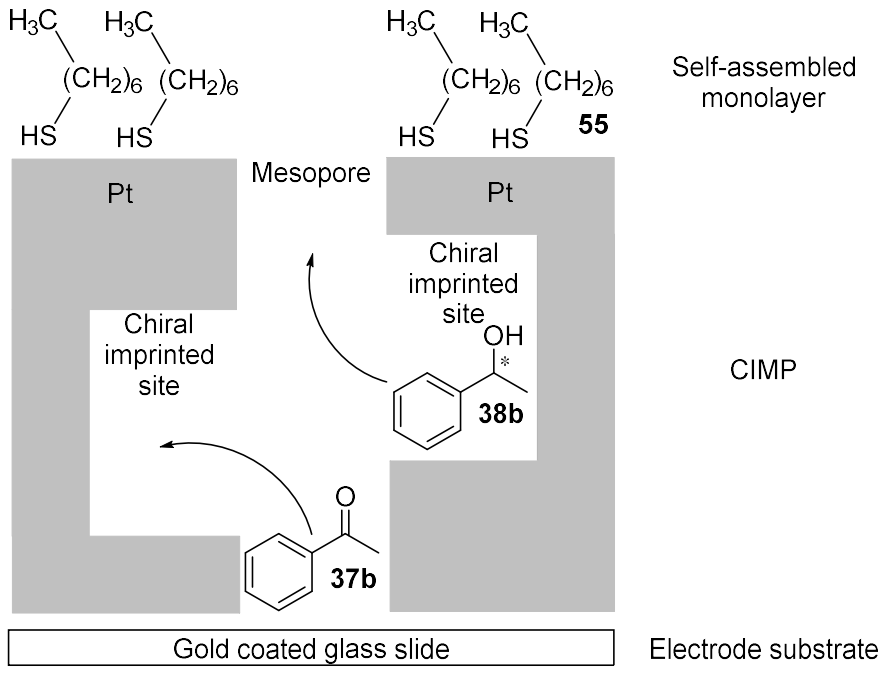

Figure 2.1: Schematic representation of a chiral imprinted mesopore in platinum metal electrode protected with a self-assembled monolayer.

Recently, Cong and co-workers presented a new type of chiral electrode for organic electrosynthesis based on a chiral macrocyclic compound, S-chiral multifarene[3,2,1] **56** (Scheme 2.16B).[34] This compound had been used before as a chiral selector for electrochemical sensors where it provided a chiral cavity on the electrode surface for enantiorecognition. The electrode for electrosynthesis was prepared by decorating gold nanoparticles on a glassy carbon electrode surface with the chiral macrocyclic compound. The electrode was subsequently used in the electroreduction of aryl

ketones **37** and *α*-ketoesters **9**. The best results were obtained for the reduction of acetophenone **37b** to 1-phenylethanol **38b** in 71% yield and 64% *ee* (Scheme 2.16A).

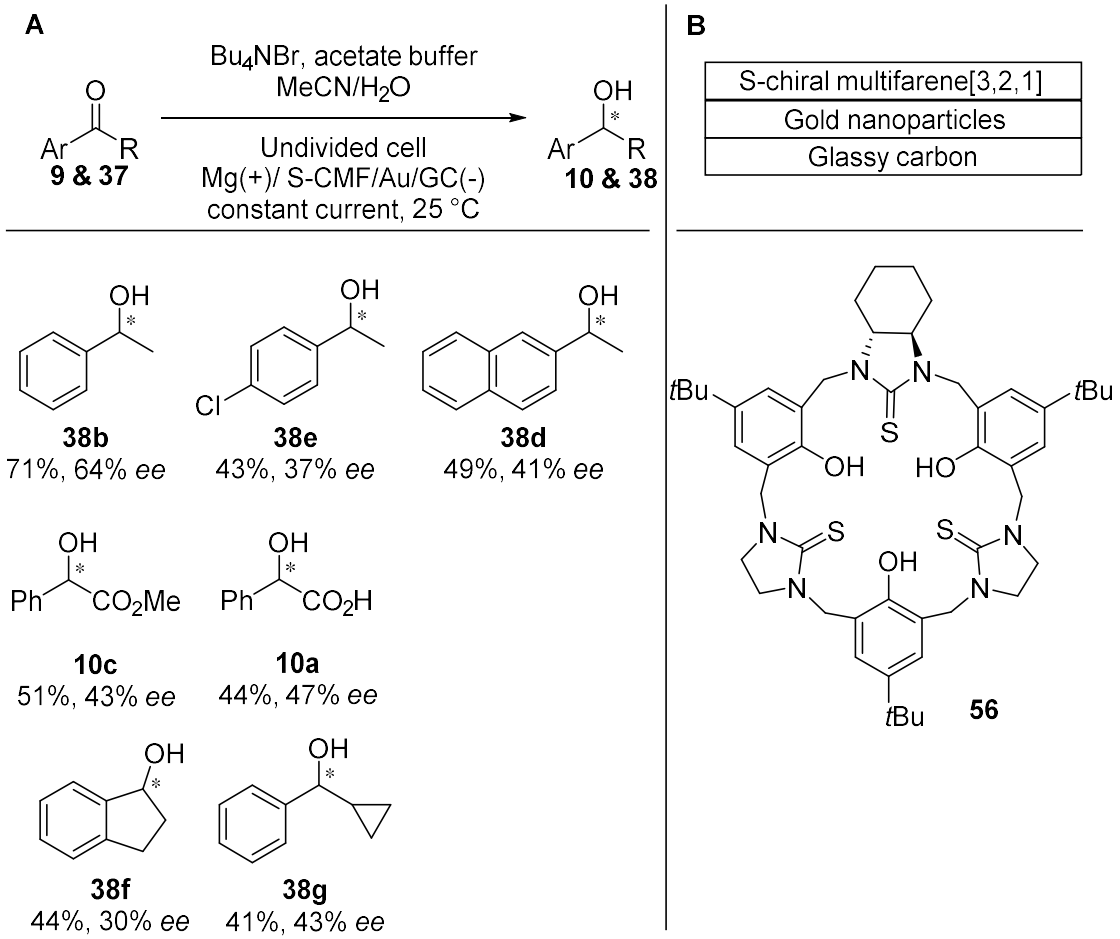

Scheme 2.16: Electrochemical reduction of ketones (A) with S-chiral multifarene [3,2,1] gold nanoparticle modified electrode (B).

Unfortunately, the scale of the experiments was not stated in the report. The claim that this method is superior to previous methods is not supported by the literature on chiral electrodes. For example, Kuhn and co-workers observed a significantly higher enantiomeric excess in the pulsed electroreduction of acetophenone **37b**.[30]

Enzymes immobilised on electrodes

The immobilisation of enzymes together with a mediator system on electrodes was performed by Yoneyama and co-workers. They immobilised D- or L-amino acid oxidase (AOx) together with 1-aminopropyl-1'-methyl-4,4'-dipyridinium iodide **57** (ADPy) as a mediator on glassy carbon electrodes by crosslinking with glutaraldehyde. The choice of the right mediator enabled the reverse reaction. These electrodes were used to reduce pyruvate **58** to D- or L-alanine **59** with an enantiomeric excess of close to 100% *ee* (Scheme 2.17).[35]

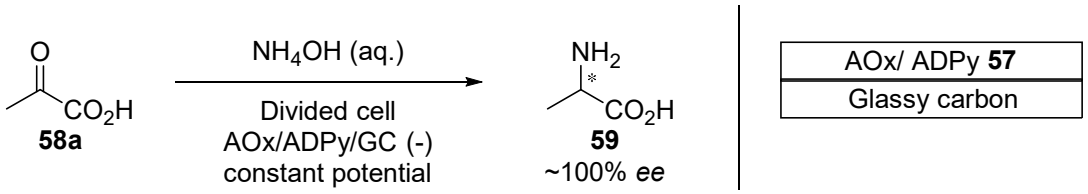

Scheme 2.17: Electrochemical conversion of ethyl pyruvate to D- or L-alanine with D- or L-amino acid oxidase immobilised on a glassy carbon electrode.

2.1.2 Organically Doped Nanoparticles

The idea of entrapping organic molecules within metal was introduced by Avnir and co-workers in 2002.[36] The so called organically doped metals are produced by reducing metal ions in the presence of soluble dopants like organic molecules, polymers or organometallic complexes. The metal cations are reduced to form nanocrystallites, which aggregate and entrap the dopant (Figure 2.2). Avnir and co-workers adopted the notation “dopant@metal” for this new type of composite material. The process of entrapment results in material properties that are different from mere adsorption. Dopants can often be extracted with certain solvents such as DMSO while leaching is not observed with other solvents in which the dopants would be soluble such as water in most examples. This type of composite material provides interesting opportunities for the immobilisation of catalysts as reactants are still able to enter the porous material to interact with the entrapped molecules.

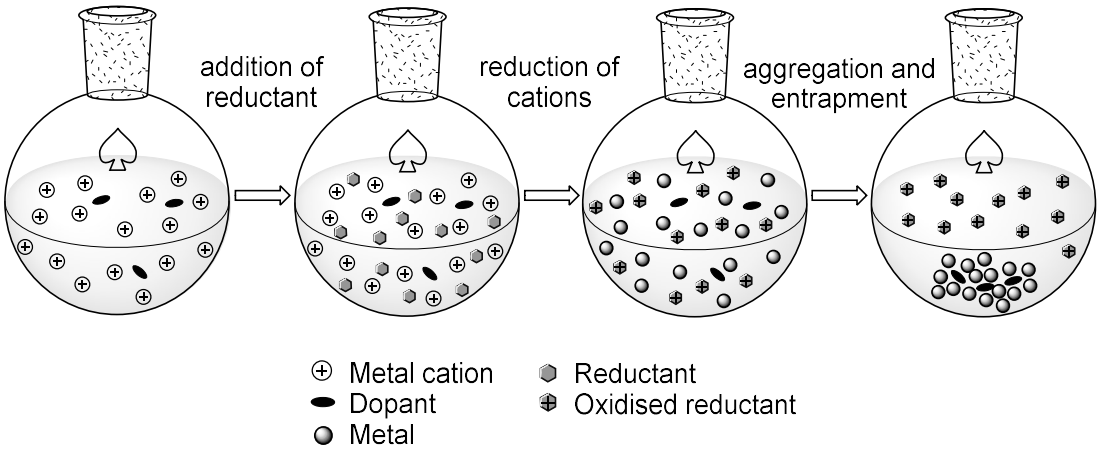

Figure 2.2: Process of entrapment process of organic molecules within metal to form organically doped metals.

Inspired by the concept of the sol-gel methodology, the entrapment of organic molecules in ceramics, Avnir and co-workers (2002) reduced silver cations in the presence of organic molecules to obtain organically doped metals (Scheme 2.18).

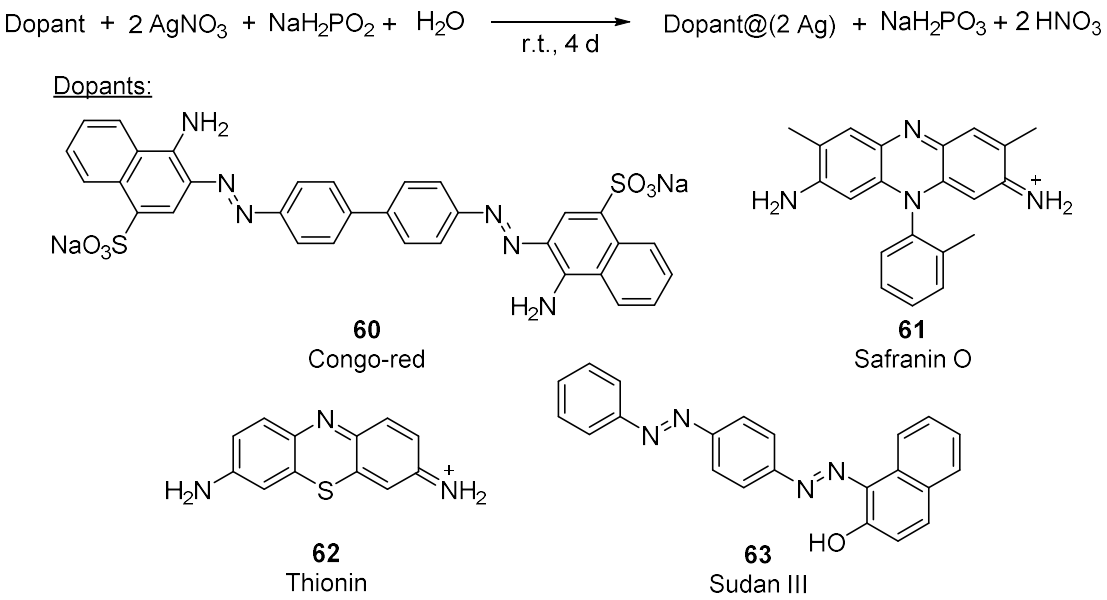

Scheme 2.18: Entrapment of organic molecules within silver.

Silver ions were reduced in aqueous media with sodium hypophosphite in the presence of Congo-red **60**, Safranin-O **61** and thionine **62**. Sodium dodecylsulfate (SDS) was used as a surfactant to solubilise and subsequently entrap hydrophobic Sudan III **63** within silver.[36]

In a second study, Avnir and co-workers demonstrated the entrapment of polymers such as poly(4-styrene sulfonic acid) (PSSA) **64** and poly(vinyl alcohol) (PVA) **65** in silver (Scheme 2.19A).[37] The water-soluble polymers could not be extracted with water but with DMSO. The characterisation of the materials further corroborated an entrapment of the polymers in mesoporous aggregated nanocrystallites in contrast to adsorption. Silver was also doped with a polymeric acid, Nafion® **66**, and a polymeric base, poly(vinylbenzyltrimethyl-ammonium hydroxide) (PVBA) **67**.[38] The ion exchange properties of the resulting doped metals were investigated. Furthermore, Nafion@Ag was utilised as an acidic catalyst for the conversion of pinacol **68** to pinacolone **69** and the dehydration of 1-phenylethanol **38b** to afford styrene **42c** (Scheme 2.19B). In these two examples the reactants enter the porous composite material to interact with Nafion® as catalyst.

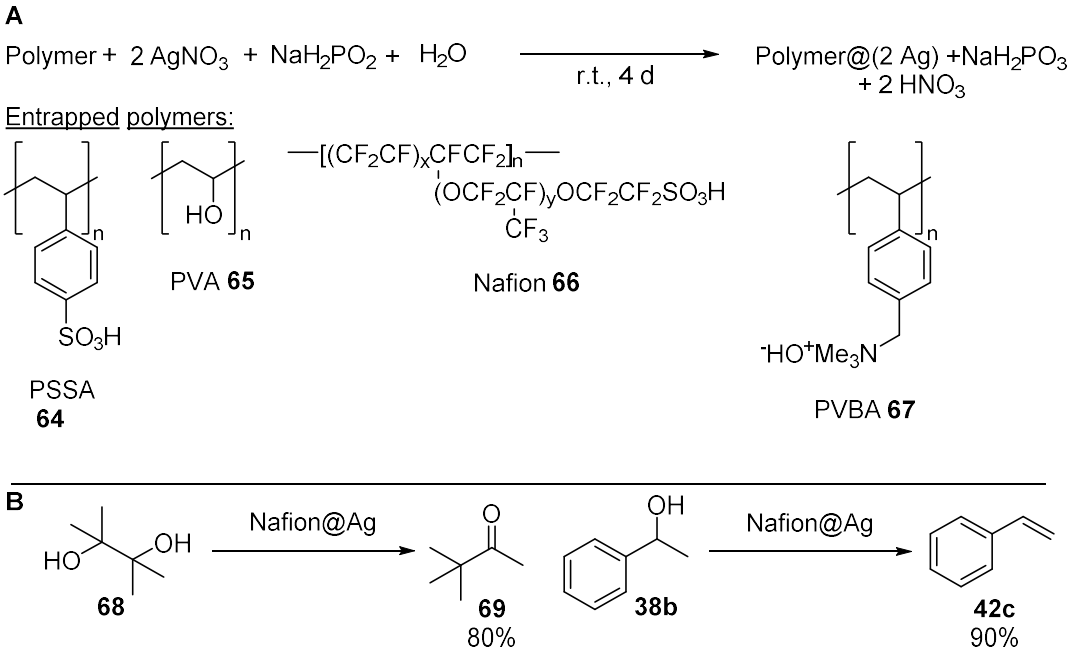

Scheme 2.19: Entrapment of polymers within silver (A). Pinacol rearrangement and dehydrogenation of 1-phenylethanol catalysed by Nafon@Ag (B).

Besides silver, an entrapment of thionine **62** and Nafion® **66** was also achieved in copper and gold with a heterogeneous reduction method. Copper and silver cations could be reduced with zinc powder in the presence of the dopants to obtain the organically doped metals. Gold cations were reduced with copper powder.[39] A similar reduction process was used to entrap the dyes thionine and neutral red in metal alloys such as Ag-Au, Cu-Pt and Cu-Pt.[40]

The concept of organically doped metals offers an interesting approach for the heterogenisation of homogeneous catalytic systems. An organometallic rhodium catalyst **70** was physically entrapped within silver (Scheme 2.20A). In contrast to the homogeneous use of this catalyst for the hydrogenation of styrene **42c** and diphenylacetylene **72**, the entrapped catalyst could be recovered and reused albeit with some loss of activity (Scheme 2.20B). When the rhodium complex was just adsorbed on silver, there was no catalytic activity observed for the recovered catalyst, which highlights the difference between adsorption and entrapment.[41]

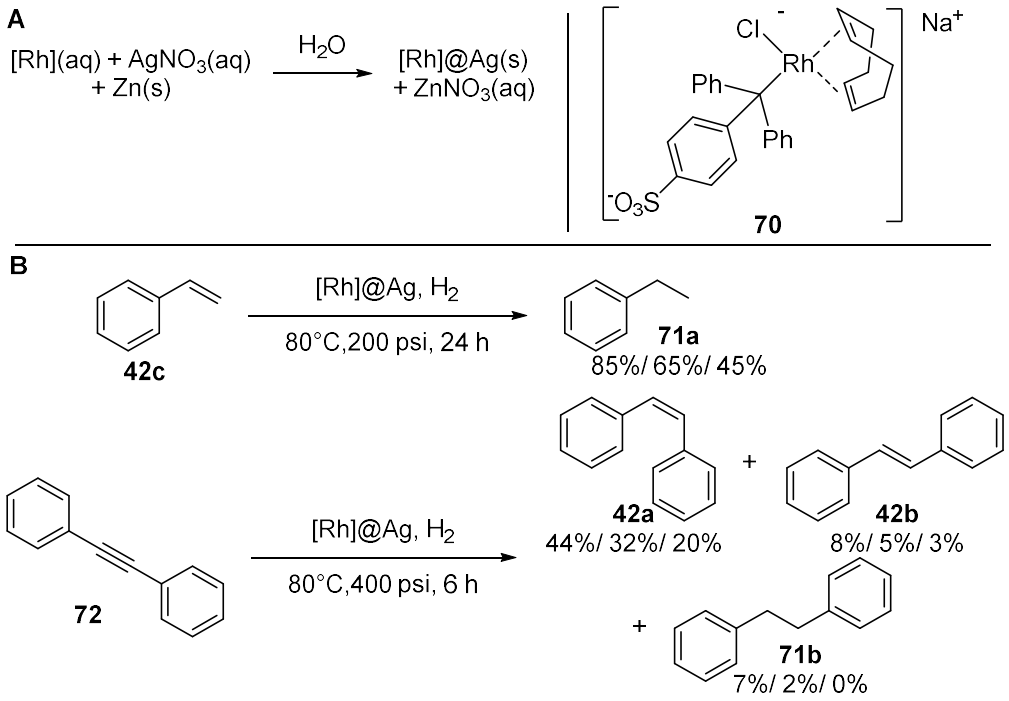

Scheme 2.20: Entrapment of a rhodium catalyst for homogeneous catalytic hydrogenation within silver (A). Heterogeneous catalytic hydrogenation with Rh@Ag catalyst (yields: 1st/2nd/3rd use) (B).

Chiral molecules such as L-glutathione, L-quinine, D- and L-tryptophan were used as dopants to induce chirality in gold and silver. As a characterisation method, samples were irradiated with clockwise or counter-clockwise circularly polarised UV-light and electron energy distribution profiles of the ejected photoelectrons were recorded. Differences between profiles recorded with clockwise and counter-clockwise circularly polarised light confirmed the induction of chirality into the metal.[42] Avnir and co-workers produced chiral metals by doping palladium with cinchona alkaloids **50a-d** (Scheme 2.21A). The alkaloids were solubilised with SDS sulfate and NaH_2PO_2 was chosen as reducing agent to avoid the reduction of dopants. The chiral composite materials were pressed into coins and tested in the catalytic hydrogenation of isophorone **73** to give **74** with 16% ee. The transfer hydrogenation of acetophenone **37b** and isopropanol **75** afforded 1-phenylethanol **38b** with 5% ee, respectively (Scheme 2.21B). Even when the cinchona alkaloids were extracted from the material with DMSO, a difference in photoelectron emission spectra with clock-wise or counter-clockwise circularly polarised light was observed. This indicates that the chiral information was imprinted in the metal even though the presence of the chiral modifier was necessary for the asymmetric hydrogenation.[43]

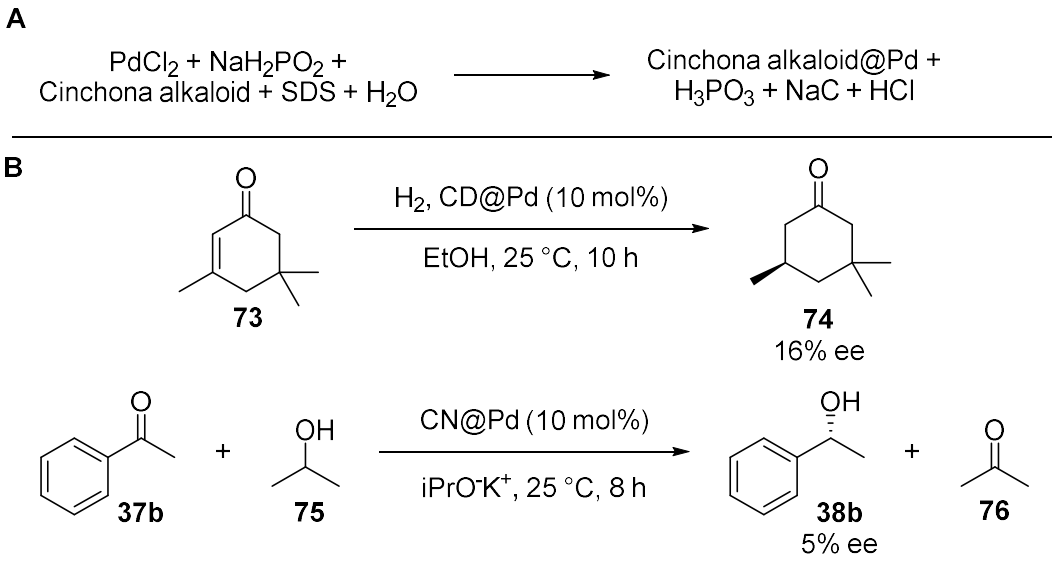

Scheme 2.21: Entrapment of cinchona alkaloids within palladium (A). Catalytic hydrogenation and transfer hydrogenation catalysed by alkaloid@Pd catalysts (CD: cinchonidine; CN: cinchonine) (B).

Organically doped metals have also been investigated as electrode materials. For this purpose, the metal powders are pressed into coins with a tablet press.

As discussed earlier, Lu and co-workers used metals doped with chiral molecules to produce chiral electrodes. The composite materials were pressed into coins and used as cathodes in undivided cells. Cinchona alkaloids were entrapped within silver and copper to prepare electrodes that were used in the ECH of ketones. The entrapment of a chiral cobalt catalyst as dopant in silver gave an electrode for the electrocatalytic asymmetric carboxylation of benzyl bromides.

By entrapping pyridine-based catalysts for the electrochemical reduction of CO_2, Lu and co-workers provided another example for the use of organically doped metals as electrodes. Pyridine had been used as a homogenous electrocatalyst for the reduction of CO_2 to methanol before.[44] The difficulty to separate the pyridine from the reaction mixture and the low recyclability, however, limit the usefulness of this system. Since pyridine would be too small for an entrapment in metal, Lu and co-workers introduced a bulky pyridine derivative **77** (PYD) as catalyst (Scheme 2.22B), which could be entrapped in palladium[45] and alloys such as palladium-copper[46] and platinum-copper.[47] The organically doped metals were pressed into coins and used in an H-type cell setup with an aqueous potassium chloride solution saturated with CO_2 (Scheme 2.22A). The PYD@Pd electrode resulted in the formation of methanol at a potential of -0.6 V vs. SCE. The copper alloy electrodes were able to catalyse the formation of different alcohols besides methanol. At a PYD@Cu-Pd electrode the production of methanol

was favoured at -0.04 V vs. RHE and the formation of ethanol at –0.64 V vs. RHE. The PYD@Cu-Pt electrode allowed the formation of ethanol at –1.2 V vs. SCE as the major product while a change in potential to –0.6 V vs. SCE resulted in a high selectivity for methanol.

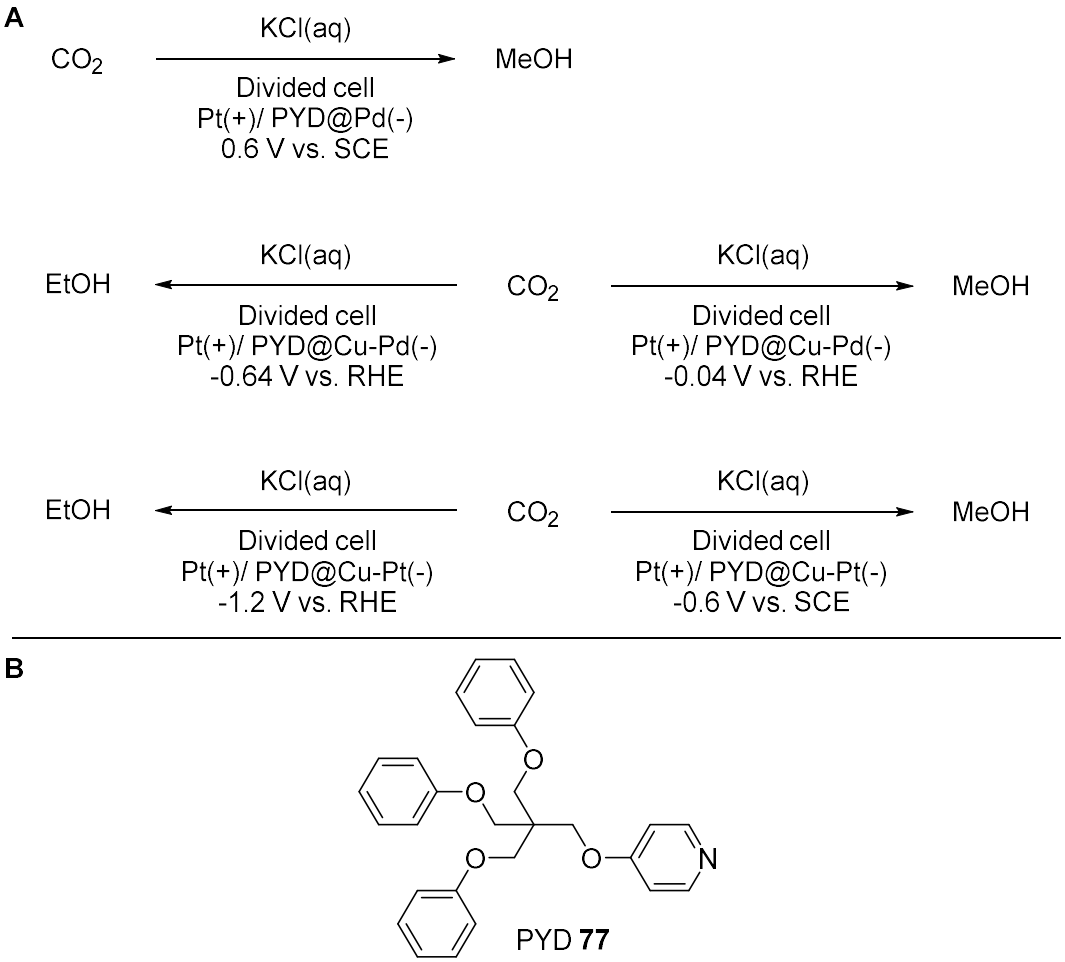

Scheme 2.22: Electrochemical reduction of CO_2 to alcohols with organically doped metal electrodes (A). Pyridine derivative as catalyst for the electrochemical reduction of CO_2 (B).

2.1.3 Preparation of Poly amino acids *via* the NCA Method

A popular synthetic route for the preparation of poly amino acid is the ring opening polymerisation of the *N*-carboxy anhydrides (NCA) of amino acids **78**.[48] NCAs are commonly synthesised by treating α-amino acids **79** with phosgene, diphosgene or triphosgene following the Fuchs-Farthing method (Scheme 2.23A).[49] According to the Leuchs method (Scheme 2.23B), urethane protected α-amino acids **80** are treated with halogenating agents like thionyl chloride, phosphorous pentachloride or phosphorous tribromide.[50] Other approaches include the reaction of α-amino acids **79** with di-*tert*-butyltricarbonate **81** (Scheme 2.23C)[51] and the reaction of the silyl esters of *N*-(*tert*-butoxycarbonyl) protected α-amino acids **82** with oxalylchloride (Scheme 2.23D).[52]

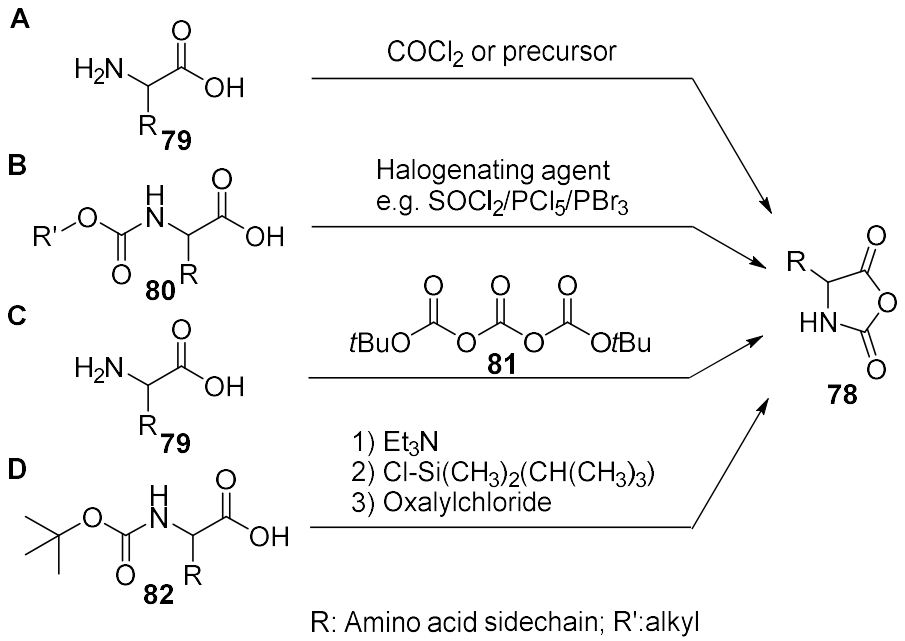

Scheme 2.23: Synthetic routes for the preparation of NCAs.

The ring opening polymerisation of NCAs can be started with basic or nucleophilic initiators. For example, Nonaka and co-workers demonstrated the formation of poly amino acid films by polymerisation of NCAs with electrogenerated bases.[53]

2.2 Aims and Objective

The use of chiral electrodes offers intriguing advantages to asymmetric electrocatalysis. The ideal electrode would allow for a significantly lower loading of chiral selectors and catalysts compared to homogeneous approaches. Furthermore, the heterogenisation of the chiral catalyst would also simplify the purification process and allow for a better recyclability and reuse. Flow electrochemical methods would be used for an easier scale up and faster screening of reaction conditions with the help of automation. Moreover, flow chemistry could enable the use of online analysis. This would not only allow faster screening of reaction parameters, but also offer a platform to test the stability of the electrodes over time. The stability of chiral electrodes is an important factor that determines their usefulness regarding reusability. Ideally, an electrode would not lose the immobilised chiral species and its ability to induce enantioselectivity. A thorough, standardised and time resolved investigation of this process could lead to the development of more stable electrodes.

Hence, the overall objective of this project was to identify a chiral electrode for asymmetric electrocatalysis that could be used in a microreactor in continuous flow. For this purpose, different concepts for the preparation of chiral electrodes would be

reproduced in a first step. In the second step, the most promising approach would be applied on an electrode that could fit into a microreactor like the Ion electrochemical reactor from Vapourtec.[54] The first concept was electrodes based on organically doped metals. Based on reports from Lu and co-workers (2016),[26] the starting point of the project was to encapsulate cinchonidine, a common chiral selector for asymmetric hydrogenation, in copper. As a first test, organically doped copper particles would then be pressed into coins and used for electrocatalytic hydrogenation of prochiral ketones. Since coin electrodes would not fit into the available microreactors, the electrode preparation would have to be adapted. A promising option could include the coating of electrodes with films containing heterogeneous catalysts in a way similar to the manufacture of fuel cell electrodes. Organically doped metals would be immobilised on a carbonaceous support with the help of binders such as Nafion®.[55,56] The electrodes would then be tested for their stability and activity in electrochemical batch and flow hydrogenation reactions.

Alternatively, electrodes would be coated with chiral polymers. Poly amino acids have been reported by Nonaka and co-workers for a variety of asymmetric transformations with a high stereoselectivity.[4,11] The highest enantiomeric excess was observed for the oxidation of prochiral sulfides to sulfoxides. Therefore, the aforementioned poly-L-valine electrodes would be prepared and used for the electrochemical oxidation of sulfides to sulfoxides. The determination of the enantiomeric excess of the sulfoxides and the reuse of the electrodes should elucidate whether this type of electrode is a suitable candidate for asymmetric catalysis in a flow electrochemical reactor.

2.3 Results and Discussion

2.3.1 Electrocatalytic Hydrogenation with Modified Electrodes

Preparation of CD@Cu coin electrodes

A particularly appealing approach for the production of chiral electrodes was reported by Lu and co-workers. Building up on their asymmetric hydrogenation protocols with coin electrodes manufactured from organically doped silver particles,[25] they were able to use cinchona alkaloids **50a-d** encapsulated in copper in a similar fashion.[26]

The original procedure for these functionalised materials appeared to be simple and straightforward (Scheme 2.24): An aqueous solution of $CuCl_2$ was mixed with an aqueous solution of cinchonidine **50a** and SDS. SDS was used as a surfactant to improve the water-solubility of cinchonidine. Zinc powder was then added to the

mixture to reduce Cu(II) to Cu(0). According to the concept of organically doped metals, the aggregation of copper particles leads to the encapsulation of cinchonidine. After filtration, washing steps and drying *in vacuo*, Lu and co-workers obtained CD@Cu as a red-brown powder. The copper particles were then pressed into a coin that could be used for the asymmetric electrocatalytic hydrogenation of prochiral ketones. The corresponding alcohols were afforded with high yields of up to 93% and up to 78% *ee*, respectively. No significant decline in yield and enantiomeric excess was observed after the electrode was reused ten times. Furthermore, copper has the advantage of a lower cost and higher abundancy compared to common metals in hydrogenation catalysis such as palladium and platinum.

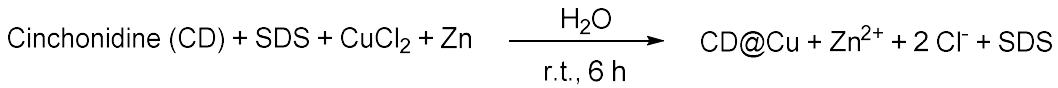

Scheme 2.24: Entrapment of cinchonidine (CD) in copper.

The initial reproduction of the original procedure afforded 3 mg of red-brown powder (Table 2.1, entry 1), which corresponds to the reduction of 1% of the copper salt. The amount of material was too low for a characterisation or its use as an electrode. A threefold scale up of the procedure gave 78 mg of material (Table 2.1, entry 2) which corresponds to a reduction of 6% of the copper salt. The powder-XRD pattern of CD@Cu02 (Figure 2.3C) indicated the absence of cinchonidine and the presence of Cu(0) compared to pure samples of cinchonidine **50a** and copper powder (Figure 2.3A & B). Extraction of the particles with DMSO-d6 and an investigation of the extract by ^{1}H-NMR spectroscopy confirmed the absence of cinchonidine **50a**. Recovered material from the filtrate showed the XRD-pattern of Cu(I)Cl (Figure 2.3D).[57] In conclusion, the sub-stochiometric use of zinc in comparison to the copper(II) salt in this procedure led to an incomplete reduction to Cu(0). It is assumed that the mixture of copper(0) and copper salts hindered the encapsulation of cinchonidine, which was then washed out in the filtration steps. Therefore, all following experiments were conducted with an excess of reductant.

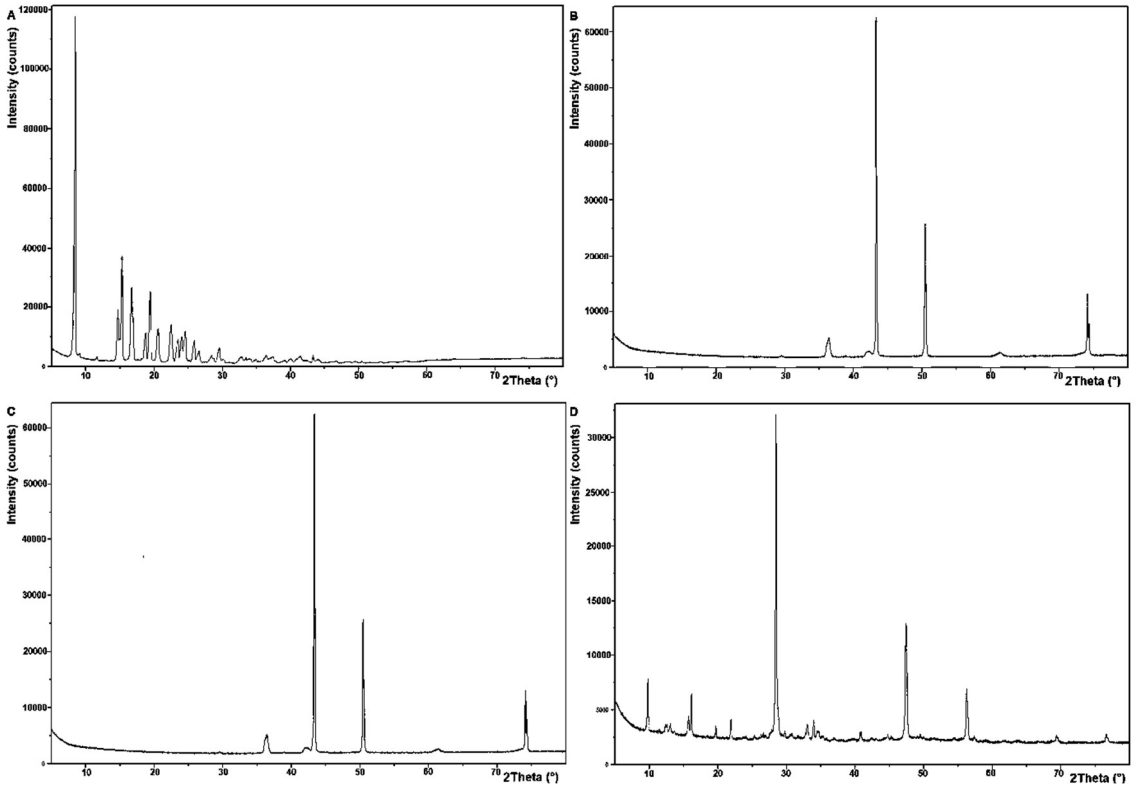

Figure 2.3: Powder XRD-patterns for cinchonidine (A), copper powder (B), CD@Cu02 (C), CD@Cu02 filtrate residues (D) (x-axis: 2θ angle [°]; y-axis: Intensity (counts)).

Subsequently, conditions such as the amount of reductant, the ratio of cinchonidine to copper and the solubilisation method for cinchonidine were changed in order to overcome the lack of encapsulation. At first, an excess of the reductant zinc was used to ensure a complete reduction of the copper salt to Cu(0) (Table 2.1, entry 3). The powder-XRD of the resulting material revealed the pattern for Cu(0) together with an impurity at a 2θ angle of 37°. However, the diffraction pattern for cinchonidine was not detected. In the next attempt SDS was omitted leading to a suspension of cinchonidine in water (Table 2.1, entry 4). The subsequent reduction with an excess of zinc gave a dark red powder. The powder XRD only showed the pattern for Cu(0) and impurities at 2θ angles between 35° and 40°. The amount of cinchonidine was then increased to 10 mol% (Table 2.1, entry 5). Mixing of cinchonidine and SDS resulted in a white suspension due to the large amount of dopant. Since powder XRD could not confirm the presence so far, the material was extracted with DMSO, which was reported to release cinchonidine from organically doped metals.[43] However, signals for cinchonidine were neither detected in IR spectra nor UV/Vis spectra of the DMSO extracts of CD@Cu05. For the next attempt (Table 2.1, entry 6), the amount of cinchonidine was kept at 10 mol% while using acetonitrile as a cosolvent instead of a surfactant. Prior to the addition of zinc, the reaction mixture was still a suspension,

which indicated a low solubility for cinchonidine. Powder-XRD, and IR or UV/Vis spectra of DMSO extracts indicated an absence of cinchonidine in the obtained material CD@Cu6. Reduction at a higher $CuCl_2$ concentration without additive (Table 2.1, entry 7) did not lead to an encapsulation of cinchonidine according to UV/Vis spectra of the DMSO extracts. In the case of ethanol as cosolvent (Table 2.1 entry 8), an encapsulation could not be confirmed either. The filtrate from the washing steps of CD@Cu07 and CD@Cu08 (Table 2.1, entries 7 & 8) was investigated by UV/vis spectroscopy. The spectra indicated the presence of cinchonidine in the solutions, which indicates that cinchonidine is not encapsulated or that it is leaching out of the composite material. The quantity of the lost chiral modifier was not calculated. DMSO extracts of the particles did not contain cinchonidine, which indicates that there was no encapsulated material. When sodium hypophosphite was used as reducing agent instead of zinc (Table 2.1, entry 9), no copper particles were obtained after the washing steps. The encapsulation of cinchonidine could also not be confirmed for particles produced with 2 equivalents of zinc (Table 2.1, entry 10). An attempt to adjust the pH value of the otherwise slightly acidic (pH4) reaction mixture to pH 9 (Table 2.1, entry 11) did not lead to the encapsulation of cinchonidine. In the case of CD@Cu10 (Table 2.1, entry 10), the filtrate of the washing steps was investigated by UV/Vis spectroscopy and cinchonidine was detected in solution.

In order to understand why the encapsulation of cinchonidine did not occur, the filtrate and washing step solutions were analysed by UV/Vis spectroscopy. Cinchonidine shows distinctive absorption maxima in neutral aqueous solutions at 315 nm, 289 nm (broad), 226 nm and 203 nm. In acidic solutions the maxima appear at 316 nm (broad) and 235 nm (Figure 2.4).

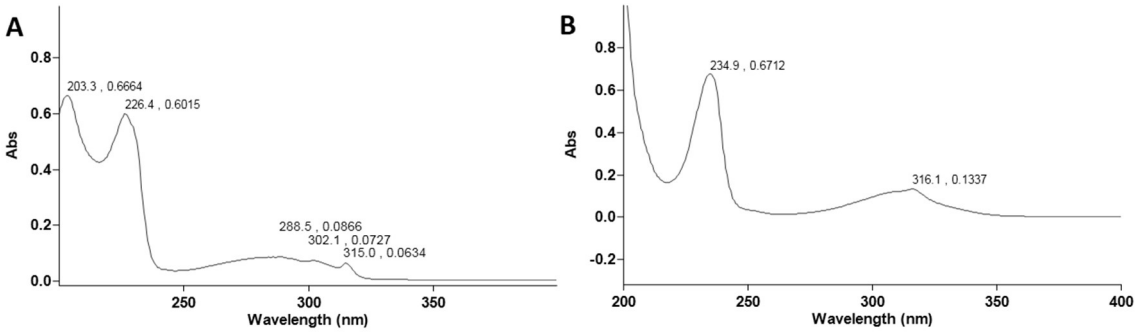

Figure 2.4: UV/Vis spectra of cinchonidine **50a** in neutral aqueous solution (5 mg·L^{-1}) (A) and cinchonidine **50a** in acidic aqueous solution (5 mg·L^{-1}) (B).

Table 2.1: Encapsulation of cinchonidine in copper by reduction in the presence of $CuCl_2$.

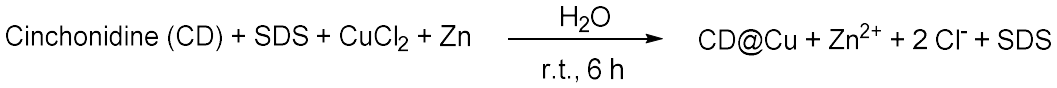

Entry	CD@Cu	H_2O [mL]	$CuCl_2$ [mmol]	Zn (eq.)	Additive (eq.)	CD[a] [mol%]	Characterisa-tion method[b]	CD[f]
1	01	50	6.4	0.85	SDS (0.5)	0.5	No Cu(0)	
2	02	150	19.2	0.85	SDS (0.5)	0.5	Powder XRD	-
							NMR (DMSO)	-
3	03	50	6.4	1.56	SDS (0.4)	1	Powder-XRD	-
							IR (DMSO)	-
							UV/Vis (DMSO)	-
4	04	50	6.0	1.26	-	2	Powder-XRD	-
5	05	32	3.9	1.25	SDS (0.5)	10	IR (DMSO)	-
							UV/Vis (DMSO)	-
6[c]	06	45	6.0	1.20	MeCN 5 mL	10	Powder-XRD	-
							IR (DMSO)	-
							UV/Vis (DMSO)	-
7	07	50	10.0	1.20	-	1	UV/Vis (DMSO)	-
							UV/Vis (reaction)	+
8	08	45	6.0	1.20	EtOH 5 mL	2	IR (DMSO)	-
							UV/Vis (DMSO)	-
							UV/Vis (reaction)	+
9	09	50	6.2	4[d]	SDS (0.5)	5	No Cu(0)	
10	10	50	6.1	2	SDS (0.5)	6	NMR (DMSO)	-
							UV/Vis (reaction)	+
11[e]	11	50	6.0	2	SDS 0.1 eq.	2	Powder-XRD	-
							UV/Vis (DMSO)	-
12	12	40	5.0	1.2	SDS (0.6)	0.6	UV/Vis (reaction)	+
13	13	50	5.0	1.1	SDS (0.6)	0.6	UV/Vis (reaction)	+

Reaction conditions: reaction time 6 h, r.t.; a) CD = Cinchonidine; b) (DMSO): DMSO extracts of the composite material; c) 35 °C instead of r.t.; d) $NaHPO_2 \times 2\ H_2O$ instead of Zn, 50 °C instead

of r.t.; e) 40 °C instead of r.t., pH 9 (instead of approximately pH 4); f) Detected cinchonidine (+: detected; -: not detected).

Two more encapsulation attempts with $CuCl_2$ and a slight excess of zinc powder were performed, followed by UV/Vis spectroscopy. This revealed a loss of cinchonidine over the filtration steps (Table 2.1, entries 12 & 13). Most of the cinchonidine was lost in the first filtration step. The subsequent washing solutions contained the rest of the cinchonidine. Calculations of the concentration based on absorption values indicated that at least 90% and 96% of cinchonidine was lost in the washing steps of the two reactions, respectively. Considering the experimental error, it is possible that no cinchonidine was retained in the copper particles.

A series of experiments investigated the reduction of $CuSO_4$ in water with zinc powder in the presence of cinchonidine (Table 2.2). For these experiments, SDS was not used as a surfactant. The experiments were followed by measuring UV/Vis spectra of the filtrate of the reaction mixture, the aqueous washing steps and the washing step with acetonitrile.

Without additives (pH 4) or with Na_2CO_3 as additive (pH 9) (Table 2.2, entries 1 & 2), cinchonidine was not completely dissolved. When hydrochloric acid was added dropwise to the solution (pH 3-4), cinchonidine could be solubilised (Table 2.2, entry 3). Even though the UV/Vis spectra of the filtrates suggested that some cinchonidine could have remained in the copper, powder XRD patterns could not confirm the presence of cinchonidine (Figure 2.5).

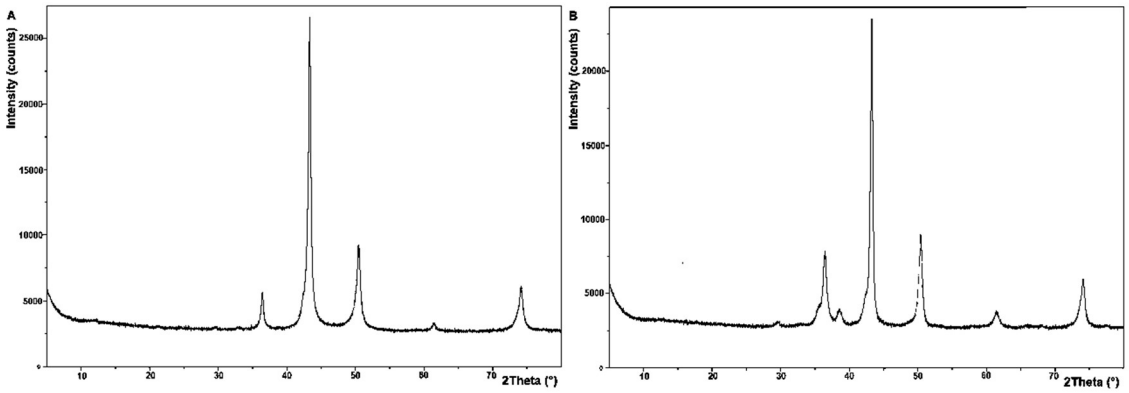

Figure 2.5: Powder XRD patterns for CD@Cu14 (A) and CD@Cu16 (B) (x-axis: 2θ angle [°]; y-axis: Intensity (counts)).

In subsequent experiments (Table 2.2, entries 4 to 6), cinchonidine was dissolved by adding hydrochloric acid and the addition of varying amounts of zinc powder were tested. The most promising result was obtained when 1.4 equivalents of zinc powder were added (Table 2.2, entry 6). In this case, cinchonidine was only observed in the

filtrate from the aqueous washing step. Furthermore, this is the only example where cinchonidine could be extracted from the composite material with DMSO. However, cinchonidine was found in all filtrates and could not be extracted when these conditions were repeated (Table 2.2, entry 7).

Table 2.2: Encapsulation of cinchonidine in copper by reduction in the presence of $CuSO_4$.

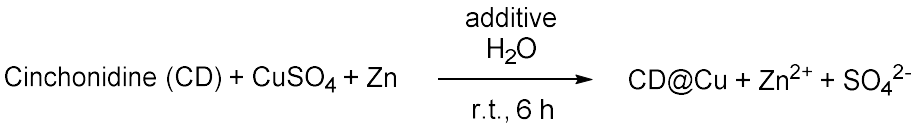

Entry	CD@Cu	H_2O [mL]	$CuCl_2$ [mmol]	Zn (eq.)	Additive	CD[a] [mol%]	Characterisation methods[b]	CD[c]
1	14	100	10.0	1.1	-	0.6	Powder XRD	-
							UV/Vis A	+
							UV/Vis B	+
							UV/Vis C	-
2	15	100	10.0	1.1	Na_2CO_3 (pH 9)	0.6	UV/Vis A	+
							UV/Vis B	+
							UV/Vis C	+
3	16	100	10.0	1.3	HCl (pH 3)	0.6	Powder XRD	-
							UV/Vis A	+
							UV/Vis B	+
							UV/Vis C	+
4	17	50	5.0	1.1	HCl (pH 3-4)	0.6%	UV/Vis A	+
							UV/Vis B	+
							UV/Vis C	+
5	18	50	5.0	1.2	HCl (pH 3-4)	0.6%	UV/Vis A	+
							UV/Vis B	+
6	19	50	5.0	1.4	HCl (pH 3-4)	0.6%	UV/Vis A	-
							UV/Vis B	+
							UV/Vis C	-
							UV/Vis (DMSO)	+
7	20	50	5.0	1.4	HCl	0.6%	UV/Vis A	+

	(pH 3-4)	UV/Vis B	+
		UV/Vis C	+
		UV/Vis (THF)	-

Reaction conditions: reaction time 6 h, r.t.; a) CD = Cinchonidine; b) UV/vis (DMSO): DMSO extracts of the composite material; UV/vis (THF): THF extracts of the composite material; UV/vis A: filtrate of the reaction mixture; UV/vis B: filtrate of the aqueous washing steps; C: Filtrate of the acetonitrile washing steps; c) Detected cinchonidine (+: detected; -: not detected).

While the calculated amount of cinchonidine in the filtrate of the reaction mixture and washing step solutions did not always account for all of the added cinchonidine, an entrapment of cinchonidine could only be confirmed in one case, which could not be reproduced in a second try. Another drawback of the composite material CD@Cu was its instability towards oxidation in air as indicated by signals for copper oxides in powder XRD patterns, an increase in weight over time and a colour change from red to black.

Nevertheless, selected batches of copper particles were pressed into coins and used as electrodes. Some coins were not stable enough and cracked immediately or when first mounted on the electrode holder. The instability might be explained with too little material and copper oxide impurities. Copper particles CD@Cu07, 14 and 16, were successfully pressed into coins and tested in electrochemical hydrogenation reactions (Scheme 2.25) according to the procedure from Lu and co-workers.[26] The copper coin was used as the cathode and a magnesium ribbon was used as sacrificial anode in an undivided cell. Tetraethyl ammonium bromide (100 mM) was used instead of iodide based on a previous report from Lu and co-workers.[58] In their report on the enantioselective electroreduction of acetophenone with cinchona alkaloids, tetraethylammonium bromide showed a higher enantiomeric excess for the alcohol product and similar dl/meso ratios for the pinacol product in direct comparison to the iodide salt. An acetonitrile/water mixture (9:1) was used as a solvent. Ethyl pyruvate **58b** was used as α-ketoester with a concentration of 50 mM. A charge of 3 $F \cdot mol^{-1}$ (150 C) was passed at a current of 10 mA. The exposed surface area of the copper coin was approximately 1 cm^2.

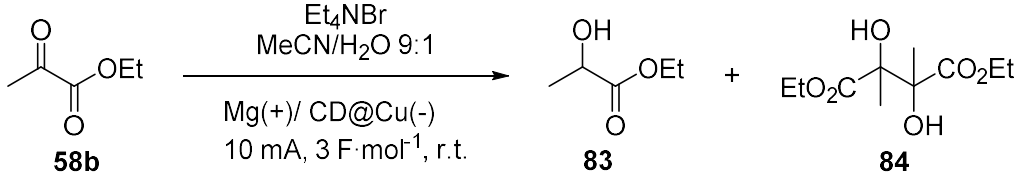

58b **83** **84**

Scheme 2.25: Electrochemical reduction of ethyl pyruvate with CD@Cu electrodes.

All investigated copper coins gave the diol **84** while the alcohol **83** was only observed in trace amounts. This indicates an electroreduction followed by a dimerisation rather than the proposed ECH mechanism (Scheme 2.26).[59] The small amounts of alcohol could not be isolated and ee-values were not measured.

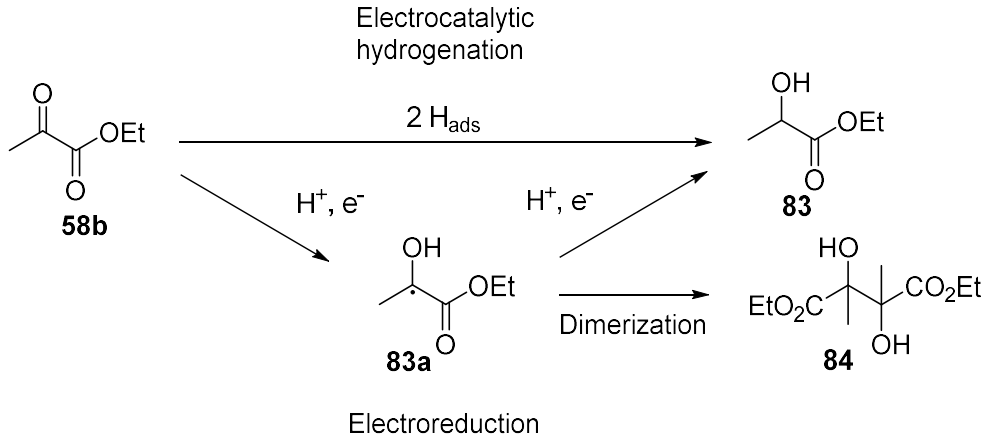

Volmer reaction: $H^+ \xrightarrow{e^-} H_{ads}$

Scheme 2.26: ECH vs Electroreduction of ethyl lactate.

The produced copper particles were not suitable as catalysts for the ECH of ethyl pyruvate **58b**. The CD@Cu composite material was unstable, indicated by oxidation of the metal and the loss of chiral modifier during the preparation. Even though the entrapment could be confirmed in one case, the procedure used here was not reliable enough to be reproduced. The instability of the CD@Cu copper coins towards mechanical pressure was difficult to handle in a batch setup but would have made the use in a flow electrochemical reactor under mechanical pressure impossible. Therefore, it was necessary to find other preparation methods that would result in stable electrodes that could be used in the pressurised assembly of a flow electrochemical reactor.

Preparation of Pd/C coated electrodes

The immobilisation of heterogeneous hydrogenation catalysts with binders on graphite sheets was chosen as a promising procedure to manufacture electrodes, that would be stable under the conditions of the flow electrochemical reactor. The initial ink formulation was inspired by the work of Sáez *et al*. on the hydrogenation of acetophenone in a polymer electrolyte membrane electrochemical reactor.[55] The catalyst inks that were tested consisted of Pd/C as hydrogenation catalyst and Nafion® or chitosan as binder. The ink formulations were spread onto graphite sheets, which were cut into dimensions that were suitable for the Electrasyn 2.0 device

(50mm × 8mm × 2mm) and the electrochemical reactor (50mm × 50mm × 1mm). The test setup with the Electrasyn 2.0 ensured more control over parameters such as surface area and interelectrode distance compared to the copper coins used in a homemade cell. While conditions for stable electrode coatings were explored, the ion exchange properties of Nafion® regarding the cinchonidinium ion also investigated.

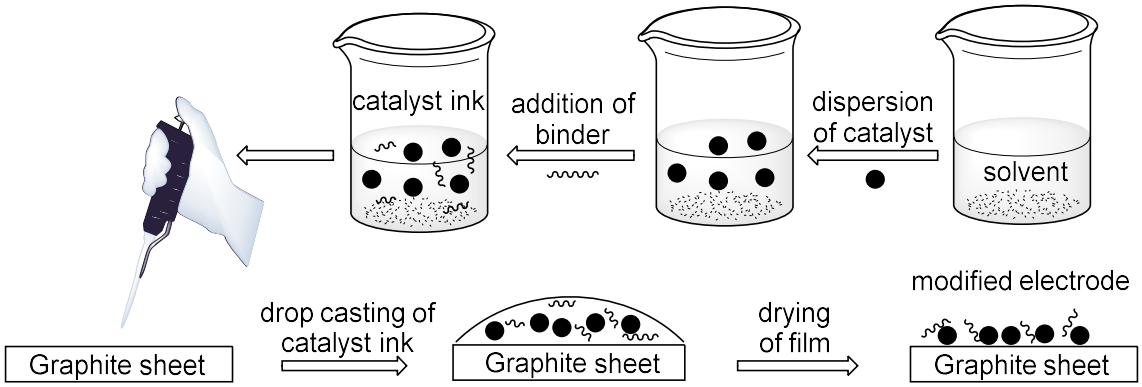

Figure 2.6: Ink preparation and drop casting process.

Initially, catalyst inks were prepared by dispersing Pd/C in isopropanol with a Nafion® 5 wt% solution as binder with a ratio of 60:40 (catalyst:binder) in isopropanol or isopropanol-water mixtures. In contrast to the procedure of Sáez *et al*., [55] the catalyst ink was not applied by air-brushing onto carbon fibre paper but by drop-casting onto a graphite sheets (Figure 2.6). At first, the films were dried at room temperature over night or heated to 125 °C after initial drying for variable amounts of time. These procedures led to films that were unstable in ethanol-water mixtures, the solvent systems used for the ECH of acetophenone by Sáez *et al*.[55] The instability was observed by visible loss of coated material. The stability of the films could be increased by heating the films to 140 °C on a hotplate after drop casting. The use of a catalyst ink consisting of Pd/C and Nafion (weight ratio 60:40) in dimethylformamide (DMF) followed by heating to 140 °C resulted in electrodes, that were stable in the alcohol-water mixtures used for ECH reactions. This observation is in alignment with the literature on the casting of Nafion® films from solution, which suggested that the use of high boiling point solvents such as DMF and DMSO and drying at temperatures above 125 °C are required to obtain films that are stable in polar solvent systems.[60,61]

Attempts were also made to cast films containing cinchonidine **50a** in the protonated form as a cinchonidinium ion. Since Nafion has been used as an ion exchange polymer on electrodes,[62] its ability to immobilise cinchonidinium ions in the Pd/C-Nafion film was investigated. Inks were prepared based on IPA or DMF, and cinchonidine was added either dissolved in ethanol or in 1 M hydrochloric acid. The electrodes were used in

ECH reactions with a low enantiomeric excess during the first use and the formation of racemic products in reuse experiments. When this type of electrode was immersed into alcohol water mixtures, the catalyst film appeared to be stable. However, UV/Vis spectra of the solvent revealed the presence of cinchonidine, which indicates that cinchonidine could not be immobilised as cinchonidinium ions in the ion exchange polymer.

As an alternative to Nafion®, the biopolymer chitosan was tested as an environmentally friendly binder. Chitosan had been used as binder to immobilise nanoparticles on sensors and to prepare Pd/C based electrodes for borohydride fuel cells.[63,64] The catalyst ink was prepared by mixing a dispersion of Pd/C in an isopropanol-water mixture with a 0.5% solution of chitosan in 2% (v/v) aqueous acetic acid. The ink was applied by drop casting onto graphite, dried at room temperature and treated with sodium hydroxide solution. This procedure gave stable modified electrodes, that were usable in batch and flow electrolysis without a visual loss of coating. It is noteworthy, that the Pd/C-chitosan electrodes show higher stability towards the mechanical pressure in the Ion electrochemical reactor than Pd/C-Nafion electrodes since the catalyst was not found on the PTFE spacer.

ECH with Pd/C Electrodes

Electrodes that were stable in alcohol water mixtures were also tested as cathodes in electrochemical experiments. The ECH batch reactions were performed in an undivided cell with a constant current and platinum anode. Methanol was used as solvent together with acetic acid and sodium acetate as supporting electrolyte. Acetophenone **37b** was chosen as the model substrate. It was possible to afford the product 1-phenylethanol **38b** in 32% yield with the Pd/C-chitosan electrode (Table 2.3, entry 1). The chiral biopolymer did not have a chirality inducing effect on the product. Electrodes coated with a Pd/C-Nafion film were investigated for their retention of cinchonidine in the film. Two electrodes with 0.1 $mg \cdot cm^{-2}$ of cinchonidine, which was applied to the ink in a 1 M hydrochloric acid solution, were tested. The first electrode, which was prepared with an IPA based ink, gave a racemic product with 7% yield (Table 2.3, entry 2). The second electrode, which was coated with a DMF based ink, afforded the product with 14% *ee* but a reuse of the electrode gave a racemic product with yields of 13% and 15%, respectively (Table 2.3, entries 3 & 4). A similar observation was made for an electrode with a surface amount of 0.5 $mg \cdot cm^{-2}$ of cinchonidine **50a**, which was prepared by adding the modifier in ethanol to the ink. A

low enantiomeric excess of 11% *ee* was observed for the first use but a reuse of the electrode gave a racemic product (Table 2.3, entries 5 & 6).

Table 2.3: Batch ECH of acetophenone with Pd/C coated electrodes.

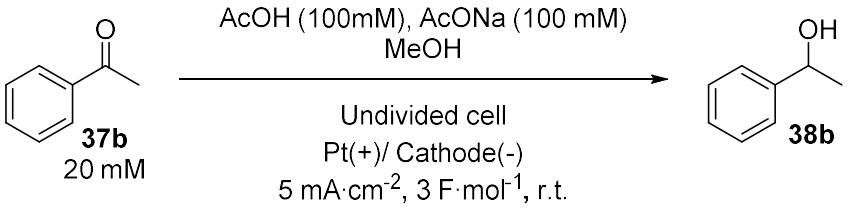

Entry	Cathode	Yield [%]	% *ee*
1	A	32	2
2	B-1	7	2
3	B-2	13	14
4	B-2 (reuse)	15	0
5	C-1	8	11
6	C-1 (reuse)	Not measured	0

Reaction conditions: Acetophenone (20 mM), AcOH(100 mM), AcONa (100 mM), MeOH (5 mL); Anode: Pt; Current density: 5 mA·cm^2; Charge: 3 F·mol^{-1}; Cathodes: A) Pd/C-chitosan (80:20); B) Pd/C-Cinchonidine (10:1), C) Pd/C-Cinchonidine (2:1).

Electrodes coated with Pd/C were also used in the Ion electrochemical reactor. When Pd/C-Nafion coated electrodes were equipped, black particles stuck to the PTFE spacer that forms the channel. This observation indicates, that the Pd/C-Nafion electrode is not stable enough towards mechanical force. The Pd/C-chitosan electrode exhibited a suitable stability and was used for several ECH reactions in the electrochemical reactor. A solution of acetophenone in methanol with acetic acid and sodium acetate as supporting electrolyte was passed through the reactor. At a flow rate of 0.1 mL·min^{-1}, 1-phenylethanol **38b** was obtained in 10% yield when a charge of 2 F·mol^{-1} was passed (Table 2.4, entry 1). An increase in charge to 3 F·mol^{-1} gave the product in 14% yield (Table 2.4, entry 2). A higher flow rate of 0.2 mL·min^{-1} led to a reduction of the yield to 7% (2 F·mol^{-1}) and 4% (3 F·mol^{-1}) (Table 2.4, entries 3 & 4). Initial yields were low and the reaction conditions would have to be further optimised. Nevertheless, the coating of graphite with a Pd/C catalyst and chitosan as binder provided an electrode that can be used in the Ion electrochemical reactor for ECH reactions. Further tests would have to show whether electrodes coated with modified heterogeneous catalysts could be used under similar conditions.

Table 2.4: ECH of acetophenone with a Pd/C-chitosan cathode in flow.

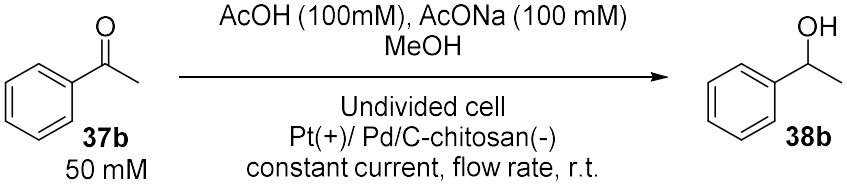

Entry	Solvent system	Flow rate [mL·min^{-1}]	Charge [F·mol^{-1}]	Current [mA]	Yield [%]
1	MeOH	0.1	2	16	10
2	MeOH	0.1	3	24	14
3	MeOH	0.2	2	32	7
4	MeOH	0.2	3	48	4

Reaction conditions: Acetophenone (50 mM), AcOH (100 mM), AcONa (100 mM); Undivided cell; Anode: Pt foil; Cathode: Pd/C-chitosan.

Electrocatalytic hydrogenation with CN&Ag & CD@Pd electrodes

Building up on the encapsulation of cinchonidine in copper, procedures for two other organically doped metals with cinchona alkaloids were followed. The first composite material was the encapsulation of cinchonine in silver similar to Lu and co-workers.[25] The second method was reported by Rothenberg and co-workers (2009) on chiral imprinted palladium.[43]

Silver particles were prepared by adding sodium hypophosphite as reducing agent to an acidic solution of silver(I)oxide and cinchonine in water. An entrapment of chiral modifier within silver could not be confirmed. Nevertheless, the silver particles were dispersed in DMF together with Nafion® in a ratio of 25:75 (w/w) and coated onto a surface area of 2.4 cm^2 on a graphite sheet. This electrode was stable in mixtures of water with alcohols or acetonitrile.

The palladium particles were synthesised according to the procedure from Rothenberg and co-workers.[43] The metal salt $PdCl_2$ was reduced with zinc powder in the presence of cinchonidine and SDS. Even though the entrapment of the chiral molecules within the metal could not be confirmed, the particles were immobilised on graphite sheets to be used in initial tests as electrodes. Metal to binder ratios of 50:50 (w/w) resulted in brittle and instable films for both chitosan and Nafion®. A stable composite electrode was obtained with a 25:75 (w/w) ratio of CD@Pd particles to Nafion®.

The CD@Pd electrode was fitted into a Electrasyn 2.0 device and used for the electrocatalytic hydrogenation in an undivided cell (Scheme 2.27). The immersed surface area of the CD@Pd electrode was 2.4 cm^2. The electrode was used in an acetonitrile-water mixture with tetraethyl ammonium tetrafluoroborate as supporting electrolyte and a magnesium anode. At a current density of 3 $mA \cdot cm^{-2}$ the ECH of ethyl benzoylformate **9a** gave the corresponding alcohol **10a** in 15% yield as a racemate. Under the same conditions, acetophenone **37b** could not be converted to 1-phenylethanol **38b**. However, the ECH of acetophenone with CD@Pd cathode and a platinum foil anode in methanol with acetic acid and sodium acetate as supporting electrolyte gave the racemic product with a low yield of 6%.

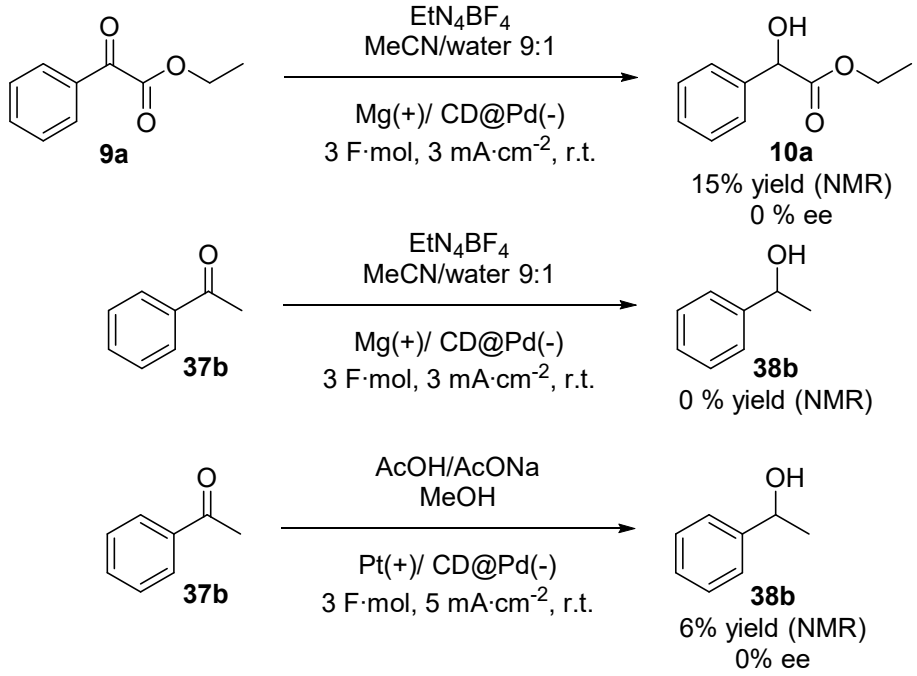

Scheme 2.27: ECH with a CD@Pd electrode.

2.3.2 Electrochemical Sulfoxidation with Modified Electrodes

Poly-L-valine Coated Electrodes

The chiral electrode modifier poly-L-valine **19** was prepared *via* the *N*-carboxy anhydride route from L-valine according to a procedure adapted from Nonaka and co-workers (1983). The amino acid was cyclised with triphosgene instead of diphosgene in dry THF. The solvent was removed in *vacuo* and the N-carboxy anhydride of L-valine was polymerised with triethyl amine in dry dioxane. The specific optical rotation of the polymer, $[\alpha]_D^{20}$= -82° (c = 1, trifluoroacetic acid), differed from the literature value ($[\alpha]_D^{20}$=: -150 ° (c = 1, trifluoroacetic acid)). The IR data confirmed the formation of the amide bond and the NMR signals corresponded to data from the literature. Mass

spectrometry with the MALDI technique only showed signals with a m/z ratio below 900. The highest intensity was observed at 535.185 m/z, which would account for no more than 5 monomer units of L-valine (exact mass: 99.07) together with H_2O and Na^+.

According to literature on the preparation of NCAs, a purification step like recrystallisation or anhydrous column chromatography is important to remove impurities that arise from the use of triphosgene.[48] The method described here was lacking such a purification step after the preparation of the NCA of L-valine as did the original report by Nonaka and co-workers.[7] Side reactions catalysed by impurities might explain the difference in specific optical rotation and the low molecular weight as indicated by MALDI mass spectrometry.

Polypyrrole films **22a** were formed on glassy carbon electrodes by constant current electrolysis. The thin film covered the whole electrode, but irregular optical interference phenomena were observed (Figure 2.7A). The polypyrrole **22a** coated electrodes were dipped into a 0.5 % solution of poly-L-valine **19** in trifluoroacetic acid to produce poly-L-valine modified electrodes (Figure 2.7B).

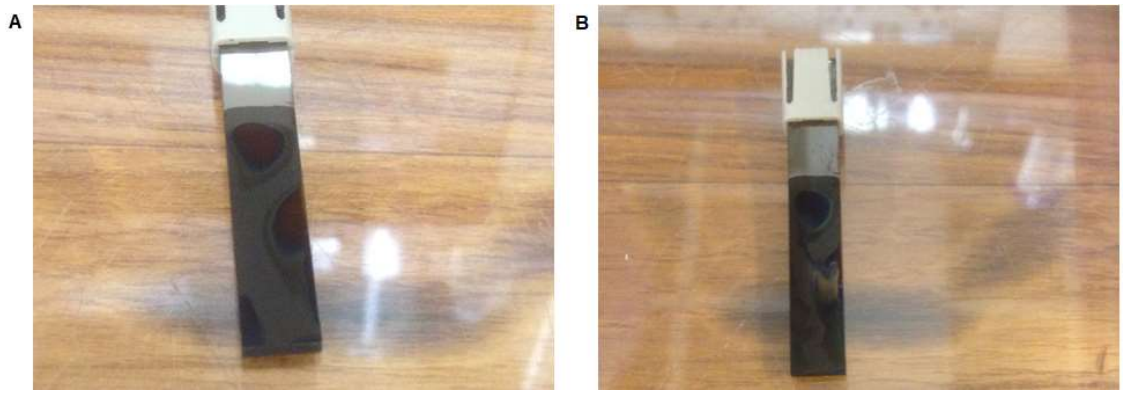

Figure 2.7: Glassy carbon electrode after electropolymerisation with polypyrrole (A) and dip-coating with poly- L -valine (B).

A permanent immobilisation of the electrodes with poly- L -valine could not be confirmed and the film thickness could not be determined.

Electrochemical Sulfoxidation

The oxidation of sulfides was tested with an adapted procedure from Nonaka and co-workers. Instead of constant potential electrolysis, sulfides were oxidised to sulfoxides under constant current electrolysis in an undivided cell. It is not clear from the reports whether Nonaka and co-workers used a divided or an undivided cell.[4,11]

Thioanisole **29a** (10 mM) was converted to methyl phenyl sulfoxide **30a** in 71% yield with platinum as anode (Table 2.5, entry 1). Since the best results for enantiomeric

excess were reported for sulfides with bulky residues, *tert*-butyl phenyl sulfide **29e** was prepared and used for the electrochemical sulfoxidation. When *tert*-butyl phenyl sulfide was oxidised under the same conditions, only trace amounts of product **30e** were observed by ^{1}H NMR (Table 2.5, entry 2). Increasing the charge to 3 F mol^{-1} at a sulfide concentration of 20 mM did not have a positive effect on the yield (Table 2.5, entry 3). The use of glassy carbon instead of platinum electrodes afforded the *tert*-butyl phenyl sulfoxide only in trace amounts (Table 2.5, entries 4 & 5). A higher substrate concentration of 50 mM with platinum electrodes gave the sulfoxide **30e** with a low NMR yield of 21% (Table 2.5, entry 6). The electrolysis of *tert*-butyl phenyl sulfide **29e** (20 mM) was also performed with a constant potential of 2.0 V (vs. Ag/AgCl) according to the literature procedure (Table 2.5, entry 7). Instead of the modified electrode, a platinum anode and cathode were used. After 10 hours a charge of 2 F·mol^{-1} was passed, however, no sulfoxide could be detected by ^{1}H NMR spectroscopy. The ^{1}H NMR spectrum showed peaks that might indicate the presence of starting material and the corresponding sulfone.

Table 2.5: Electrochemical oxidation of sulfides to sulfoxides.

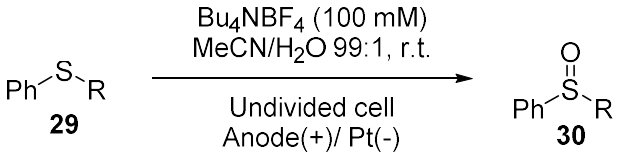

Entry	Substituent R	Sulfide conc. [mM]	Anode	Current density [mA·cm^{-2}]	Charge [F·mol^{-1}]	Yield [%][c]
1[a]	methyl	10	Pt	3.2 (4.8 mA)	2	70
2	*tert*-butyl	10	Pt	3.2 (4.8 mA)	2	< 5
3[b]	*tert*-butyl	20	Pt	3.0 (4.5 mA)	3	< 5
4[b]	*tert*-butyl	20	Glassy carbon	5.0 (12 mA)	3	< 5
5[b]	*tert*-butyl	20	Glassy carbon	2.0 (4.8 mA)	3	< 5
6[b]	*tert*-butyl	50	Pt	3.0 (4.5 mA)	2	21
7[b]	*tert*-butyl	20	Pt	(2.0 V)[d]	2	not detected

Reaction conditions: 5 mL vial (Electrasyn 2.0); Bu_4NBF_4 (100 mM) in MeCN/H_2O (99:1); cathode: Pt; Surface area: Pt (1.5 cm^2), GC (2.4 cm^2); a*)* Substrate: Thioanisole; b) Substrate:*Tert*-butyl phenyl sulfide; c) Yields are determined by NMR with 1,3,5-trimethoxybenzene as internal standard; d) Potentiostatic electrolysis: 2.0 V vs. Ag/AgCl (reaction time approximately 10 h).

When poly-L-valine electrodes were used, no significant quantity of the *tert*-butyl phenyl sulfoxide **25e** could be isolated. The small amount that was obtained did not allow for a reliable HPLC chromatogram to determine the enantiomeric excess (Table 2.6, entries 1 & 2). The reaction with thioanisole **24a** gave the corresponding sulfoxide **25a** as a racemic mixture in 8% and 18% yield when a charge of 2 F mol^{-1} was passed (Table 2.6, entries 3 & 4). In accordance with these findings, Nonaka and co-workers observed racemic mixtures of sulfoxide when converting sulfides with less sterically demanding groups such as methyl substituents.

Table 2.6: Electrochemical oxidation of sulfides with poly-L-valine coated electrodes.

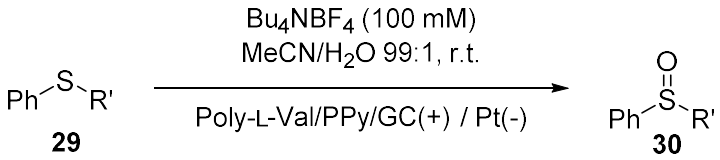

Entry	Substituent R	Use	Yield [%][c]	*ee* [%]
1[a]	*tert*-butyl	1	- (0)	-
2[a]	*tert*-butyl	2	- (0)	-
3[b]	methyl	3	8	0
4[b]	methyl	4	18	0

Reaction conditions: 5 mL vial (Electrasyn 2.0), sulfide (20 mM), Bu_4NBF_4 (100 mM), $MeCN/H_2O$ (99:1), r.t.; Anode: Poly-L-valine-polypyrrole electrode (2.4 cm^2); Cathode: (1.5 cm^2); Current density: 2 $mA \cdot cm^{-2}$ (4.8 mA); a) Charge: 3 $F \cdot mol^{-1}$; b) Charge: 2 $F \cdot mol^{-1}$; c) Yields are determined by 1H NMR with 1,3,5-trimethoxybenzene as internal standard (isolated yield in brackets).

2.4 Conclusion

A variety of concepts were investigated in order to produce chiral electrodes: Metals were doped with cinchona alkaloids as chiral selectors and used as catalysts in the ECH of prochiral ketones. The common hydrogenation catalyst Pd/C was immobilised on electrodes with Nafion®, an ion exchange resin, and the composite material was modified with cinchonidinium ions. ECH electrodes were prepared by utilising the chiral biopolymer chitosan as binder to immobilise Pd/C on a graphite surface. And finally, poly-L-valine was coated on electrodes for the asymmetric electrochemical oxidation of sulfides to sulfoxides. However, a chiral electrode could not be produced or reproduced in this work.

2.4.1 Electrocatalytic hydrogenation

The principle of organically doped metal electrodes was applied to encapsulate chiral modifiers such as cinchonidine **50a** in copper to obtain chiral electrodes for the asymmetric ECH of α-ketoesters. The original method for the encapsulation of cinchonidine in copper failed to produce CD@Cu particles due to a sub-stoichiometric amount of reductant. The encapsulation of cinchonidine in copper was partially achieved after the optimisation of the reaction conditions. The presence of the dopant could be confirmed in one case by extraction with DMSO. This experiment, however, could not be reproduced reliably. The resulting materials were still pressed into copper coins and used as electrodes for the ECH of ethyl pyruvate **58b**. Ethyl lactate **83** was only detected in trace amounts while the diol **84** was observed as the main product. This observation indicated an electroreduction mechanism followed by dimerisation rather than an ECH mechanism. Since CD@Cu particles could not be used successfully for ECH and would oxidise quite easily, the focus of the project was shifted to other metals.

Subsequently, the conversion of prochiral ketones to alcohols was investigated with electrodes coated with catalyst inks consisting of Pd/C as ECH catalyst and Nafion® or chitosan as binder and acetophenone **37b** as model substrate. The modification of electrodes with catalyst ink is commonly used in fuel cell applications.

Electrodes coated with a composite of Pd/C, Nafion® and cinchonidinium ions induced enantioselectivity in the ECH of acetophenone to 1-phenylethanol **38b**. However, those most promising attempts suffered from a low enantiomeric excess of no more than 14% *ee*. Furthermore, a reuse of these electrodes turned out to furnish racemic products. An immersion of this type of electrode in an alcohol water mixture followed by UV/vis spectrometry revealed a loss of cinchonidine into the solution. It can be concluded that cinchonidine or the corresponding cinchonidinium ion were not sufficiently immobilised in the ion exchange polymer. The dimerisation product was not observed with properly coated Pd/C electrodes but the yields for the alcohol were low even after optimisation attempts.

Pd/C-chitosan electrodes were also used for ECH reactions. Even though chitosan is a chiral biopolymer, the electrolysis of **37b** with this type of electrode gave **38b** as a racemate. In contrast to Pd/C-Nafion® films, Pd/C-chitosan electrodes were mechanically stable in the electrochemical reactor and could be used for ECH reactions in flow. As a biopolymer chitosan offers interesting opportunities for further

investigations as a more sustainable alternative to the perfluorinated binder Nafion®. Moreover, chitosan had been reported as a chiral polymeric ligand for metals such as ruthenium. The resulting catalysts were successfully used in enantioselective hydrogenation reactions.[65] It could be possible to coat films of these materials onto conducting materials to obtain chiral electrodes for ECH reactions similar to previous reports on rhodium(III) complexes with immobilised chiral polymeric ligands.[19]

The encapsulation of cinchonine and cinchonidine in silver and palladium was attempted but could not be confirmed. Nevertheless, CD@Pd was coated onto a graphite electrode with Nafion® as binder and used in the ECH of prochiral ketones. The racemic products led to the assumption that the chiral modifier was either absent or inaccessible for the reaction. Further investigations would be required to reproduce and characterise the chiral materials and use them in ECH reactions in batch and flow.

2.4.2 Poly Amino Acid Coated Electrodes

Finally, the asymmetric sulfoxidation procedure from Nonaka and co-workers was followed.[4] Poly-L-valine **19** was applied onto a polypyrrolepyrrole **22a** coated electrode by a dipcoating method. The electrode was tested for the oxidation of sulfides to sulfoxides. Methyl phenyl sulfide **29a** was converted to the corresponding sulfoxide **30a** in good yields but without enantiomeric excess, which is in accordance with the literature. The modified electrode was also tested with the more promising *tert*-butyl phenyl sulfide **29e** for which a high stereoselectivity was reported in literature. The electrolysis of this substrate with the modified electrode afforded the corresponding sulfoxide only in trace amounts, which prevented a reliable determination of the enantiomeric excess.

Any future attempt to reproduce this type of polymer coated electrode should start with a detailed characterisation and investigation of the electrode material and electrode surface. A start would be to use a cleaner preparation method for the poly amino acid synthesis and to determine the molecular weight with MALDI. Subsequently, the thickness of the film and the amount of the poly amino acid on the dip coated electrode should be investigated. Furthermore, the reaction conditions for the sulfoxidation have to be improved to facilitate a reliable conversion of substrates with sterically demanding functional groups such as *tert*-butyl phenyl sulfide **29e** to the corresponding sulfoxides. The mechanical stability of the chiral electrode in the electrochemical reactor would have to be investigated. Frictions between the electrode and the PTFE-spacer in the assembled reactor might rupture the film. The stability of the film under flow conditions

would have to be monitored as well. A related strategy would be the use of chiral poly pyrrole monomers. In this case the chiral moieties are covalently linked to the electropolymerised film, which might improve the stability of the chiral coating.

2.4.3 Final conclusion

In conclusion, none of the investigated methods offered a way to reproduce or produce a chiral electrode that could be used and reused for batch or flow electrolysis. In order to afford chiral electrodes for asymmetric electrochemistry, the next methods that could be tested would be the immobilisation of catalysts with chiral polymeric ligands, the coating of electrodes with polymer tethered mediators and the preparation of chiral imprinted mesoporous metals.

Apart from the studies conducted by Nonaka and co-workers, most examples of chiral electrodes appear to be a proof of concept rather than an intensively studied and reliable system. Another good example for a well-studied chiral electrode is the mesoporous imprinted chiral platinum, which Kuhn and co-workers developed and optimised in recent years. In general, the field of chiral electrodes for electrosynthesis would require exhaustive studies on the durability and reusability of existing electrode types while also offering a wide range of reactions and substrates to choose from. A thorough investigation and characterisation of the materials will be essential to understand underlying mechanisms and to improve the electrode systems. Moreover, simple, cheap and reliable preparation methods would be necessary for a wider acceptance of chiral electrodes in organic electrochemistry.

2.5 References

(1) Watkins, F. B.; Behling, J. R.; Kariv, E.; Miller, L. L. A Chiral Electrode. *J. Am. Chem. Soc.* **1975**, *97*, 3549–3550. https://doi.org/10.1021/ja00845a061.

(2) Firth, B. E.; Miller, L. L.; Mitani, M.; Rogers, T.; Lennox, J.; Murray, R. W. Anodic and Cathodic Reactions on a Chemically Modified Edge Surface of Graphite. *J. Am. Chem. Soc.* **1976**, *98*, 8271–8272. https://doi.org/10.1021/ja00441a069.

(3) Firth, B. E.; Miller, L. L. Oxidations on DSA and Chirally Modified DSA and SnO_2 Electrodes. *J. Am. Chem. Soc.* **1976**, *98*, 8272–8273. https://doi.org/10.1021/ja00441a070.

(4) Komori, T.; Nonaka, T. Electroorganic Reactions on Organic Electrodes. 6. Electrochemical Asymmetric Oxidation of Unsymmetric Sulfides to the Corresponding Chiral Sulfoxides on Poly(Amino Acid)-Coated Electrodes. *J. Am. Chem. Soc.* **1984**, *106*, 2656–2659. https://doi.org/10.1021/ja00321a028.

(5) Yue, Y.-N.; Meng, W.-J.; Liu, L.; Hu, Q. L.; Wang, H.; Lu, J.-X. Amino Acid-Functionalized Multi-Walled Carbon Nanotubes: A Metal-Free Chiral Catalyst for the Asymmetric Electroreduction of Aromatic Ketones. *Electrochim. Acta* **2018**, *260*, 606–613. https://doi.org/10.1016/j.electacta.2017.12.058.

(6) Yue, Y.-N.; Zeng, S.; Wang, H.; Wang, S.; Wang, H.; Lu, J.-X. One-Pot Synthesis of d-Phenylalanine-Functionalized Multiwalled Carbon Nanotubes: A Metal-Free Chiral Material for the Asymmetric Electroreduction of Aromatic Ketones. *ACS Appl. Mater. Interfaces* **2018**, *10*, 23055–23062. https://doi.org/10.1021/acsami.8b04589.

(7) Abe, S.; Nonaka, T.; Fuchigami, T. Electroorganic Reactions on Organic Electrodes. 1. Asymmetric Reduction of Prochiral Activated Olefins on a Poly-L-Valine-Coated Graphite. *J. Am. Chem. Soc.* **1983**, *105*, 3630–3632. https://doi.org/10.1021/ja00349a046.

(8) Nonaka, T.; Abe, S.; Fuchigami, T. Electro-Organic Reactions on Organic Electrodes. Part 2. Electrochemical Asymmetric Reduction of Citraconic and Mesaconic Acids on Optically-Active Poly(Amino Acid)-Coated Electrodes. *Bull. Chem. Soc. Jpn.* **1983**, *56*, 2778–2783. https://doi.org/10.1246/bcsj.56.2778.

(9) Abe, S.; Fuchigami, T.; Nonaka, T. Electrochemical Asymmetric Reduction of Prochiral Carbonyl Compounds, Oximes and a Gem-Dihalide on a Poly-L-Valine

Coated Graphite Electrode. *Chem. Lett.* **1983**, *12*, 1033–1036. https://doi.org/10.1246/cl.1983.1033.

(10) Abe, S.; Nonaka, T. Durable Chiral Graphite Electrodes Modified Chemically with Poly(L-Valine) and Poly(*N*-Acryloyl-L-Valine Methyl Ester). *Chem. Lett.* **1983**, *12*, 1541–1542. https://doi.org/10.1246/cl.1983.1541.

(11) Komori, T.; Nonaka, T. Electroorganic Reactions on Organic Electrodes. 3. Electrochemical Asymmetric Oxidation of Phenyl Cyclohexyl Sulfide on Poly(L-Valine)-Coated Platinum Electrodes. *J. Am. Chem. Soc.* **1983**, *105*, 5690–5691. https://doi.org/10.1021/ja00355a029.

(12) Komori, T.; Nonaka, T. Electrochemical Enantiomer-Differentiating Oxidation of a Racemic Alcohol on Poly(L-Valine)-Coated Electrodes. *Chem. Lett.* **1984**, *13*, 509–512. https://doi.org/10.1246/cl.1984.509.

(13) Pleus, S.; Schwientek, M. Design of Chiral Poly(Pyrroles). *Synth. Commun.* **1997**, *27*, 2917–2930. https://doi.org/10.1080/00397919708004998.

(14) Pleus, S.; Schwientek, M. Enantioselective Electrodes: Synthesis and Use of Polypyrroles Prepared from Chiral Pyrrole Derivatives. *Synth. Met.* **1998**, *95*, 233–238. https://doi.org/https://doi.org/10.1016/S0379-6779(98)00063-0.

(15) Schwientek, M.; Pleus, S.; Hamann, C. H. Enantioselective Electrodes: Stereoselective Electroreduction of 4-Methylbenzophenone and Acetophenone. *J. Electroanal. Chem.* **1999**, *461*, 94–101. https://doi.org/https://doi.org/10.1016/S0022-0728(98)00039-4.

(16) Pleus, S.; Schulte, B. Poly(Pyrroles) Containing Chiral Side Chains: Effect of Substituents on the Chiral Recognition in the Doped as Well as in the Undoped State of the Polymer Film. *J. Solid State Electrochem.* **2001**, *5*, 522–530. https://doi.org/10.1007/s100080000181.

(17) Takano, N.; Seki, C. Preparation of Chiral Polypyrrole Film-Coated Electrode Incorporating Palladium Metal and Asymmetric Hydrogenation of α-Keto Esters. *Electrochemistry* **2006**, *74*, 596–598. https://doi.org/10.5796/electrochemistry.74.596.

(18) Moutet, J.-C.; Duboc-Toia, C.; Ménage, S.; Tingry, S. A Chiral Poly(2,2′-Bipyridyl Rhodium(III) Complex) Film Electrode for Asymmetric Induction in Electrosynthesis. *Adv. Mater.* **1998**, *10*, 665–667.

https://doi.org/https://doi.org/10.1002/(SICI)1521-4095(199806)10:9<665::AID-ADMA665>3.0.CO;2-5.

(19) Moutet, J.-C.; Cho, L. Y.; Duboc-Toia, C.; Ménage, S.; Riesgo, E. C.; Thummel, R. P. Heterogeneous and Homogeneous Asymmetric Electrocatalytic Hydrogenation with Rhodium(III) Complexes Containing Chiral Polypyridyl Ligands. *New J. Chem.* **1999**, *23*, 939–944. https://doi.org/10.1039/a904477i.

(20) Guo, P.; Wong, K.-Y. Enantioselective Electrocatalytic Epoxidation of Olefins by Chiral Manganese Schiff-Base Complexes. *Electrochem. Commun.* **1999**, *1*, 559–563. https://doi.org/10.1016/S1388-2481(99)00110-1.

(21) Kashiwagi, Y.; Kurashima, F.; Chiba, S.; Anzai, J.; Bobbitt, J. M. Asymmetric Electrochemical Lactonization of Diols on a Chiral 1-Azaspiro[5.5]Undecane N-Oxyl Radical Mediator-Modified Graphite Felt Electrode. *Chem. Commun.* **2003**, 114–115. https://doi.org/https://doi.org/10.1039/B209871G.

(22) Yamagishi, A.; Aramata, A. A Clay-Modified Electrode with Stereoselectivity. *J. Chem. Soc., Chem. Commun.* **1984**, 452–453. https://doi.org/10.1039/C39840000452.

(23) Yamagishi, A.; Aramata, A. Asymmetric Electrooxidation of Phenyl Alkyl Sulfide on an SnO_2-Glass Electrode Coated with a Film of Λ-$Ru(Phen)_3^{2+}$-Montmorillonite. *J. Electroanal. Chem* **1985**, *191*, 449–452. https://doi.org/https://doi.org/10.1016/S0022-0728(85)80039-5.

(24) Yamagishi, A. Chromatographic Resolution of Enantiomers Having Aromatic Groups by an Optically Active Clay-Chelate Adduct. *J. Am. Chem. Soc.* **1985**, *107*, 732–734. https://doi.org/https://doi.org/10.1021/ja00289a051.

(25) Yang, H.-P.; Chi, D.; Sun, Q.; Sun, W.; Wang, H.; Lu, J.-X. Entrapment of Alkaloids within Silver: From Enantioselective Hydrogenation to Chiral Recognition. *Chem. Commun.* **2014**, *50*, 8868–8870. https://doi.org/10.1039/c4cc02823f.

(26) Yang, H.-P.; Fen, Q.; Wang, H.; Lu, J.-X. Copper Encapsulated Alkaloids Composite: An Effective Heterogeneous Catalyst for Electrocatalytic Asymmetric Hydrogenation. *Electrochem. Commun.* **2016**, *71*, 38–42. https://doi.org/10.1016/j.elecom.2016.08.004.

(27) Yang, H. P.; Yue, Y. N.; Sun, Q. L.; Feng, Q.; Wang, H.; Lu, J. X. Entrapment of a Chiral Cobalt Complex within Silver: A Novel Heterogeneous Catalyst for Asymmetric

Carboxylation of Benzyl Bromides with CO_2. *Chem. Commun.* **2015**, *51*, 12216–12219. https://doi.org/10.1039/c5cc04554a.

(28) Chen, B.-L.; Zhu, H.-W.; Xiao, Y.; Sun, Q.-L.; Wang, H.; Lu, J.-X. Asymmetric Electrocarboxylation of 1-Phenylethyl Chloride Catalyzed by Electrogenerated Chiral [CoI(Salen)]- Complex. *Electrochem. Commun.* **2014**, *42*, 55–59. https://doi.org/10.1016/j.elecom.2014.02.009.

(29) Yutthalekha, T.; Wattanakit, C.; Lapeyre, V.; Nokbin, S.; Warakulwit, C.; Limtrakul, J.; Kuhn, A. Asymmetric Synthesis Using Chiral-Encoded Metal. *Nat. Commun.* **2016**, *7*, 12678. https://doi.org/10.1038/ncomms12678.

(30) Wattanakit, C.; Yutthalekha, T.; Asssavapanumat, S.; Lapeyre, V.; Kuhn, A. Pulsed Electroconversion for Highly Selective Enantiomer Synthesis. *Nat. Commun.* **2017**, *8*, 2087. https://doi.org/10.1038/s41467-017-02190-z.

(31) Assavapanumat, S.; Ketkaew, M.; Kuhn, A.; Wattanakit, C. Synthesis, Characterization, and Electrochemical Applications of Chiral Imprinted Mesoporous Ni Surfaces. *J. Am. Chem. Soc.* **2019**, *141*, 18870–18876. https://doi.org/10.1021/jacs.9b10507.

(32) Butcha, S.; Assavapanumat, S.; Ittisanronnachai, S.; Lapeyre, V.; Wattanakit, C.; Kuhn, A. Nanoengineered Chiral Pt-Ir Alloys for High-Performance Enantioselective Electrosynthesis. *Nat. Commun.* **2021**, *12*, 1314. https://doi.org/10.1038/s41467-021-21603-8.

(33) Butcha, S.; Lapeyre, V.; Wattanakit, C.; Kuhn, A. Self-Assembled Monolayer Protection of Chiral-Imprinted Mesoporous Platinum Electrodes for Highly Enantioselective Synthesis. *Chem. Sci.* **2022**, *13*, 2339–2346. https://doi.org/10.1039/d2sc00056c.

(34) Xue, Y. F.; Li, H.; Ge, Q.; Liu, M.; Tao, Z.; Cong, H. Supramolecular Chiral Electrochemical Reduction of Acetophenone with Hybridization of a Chiral Multifarene and Au Nanoparticles. *J. Catal.* **2021**, *404*, 529–536. https://doi.org/10.1016/j.jcat.2021.10.037.

(35) Kawabata, S.; Iwata, N.; Yoneyama, H. Asymmetric Electrosynthesis of Amino Acid Using an Electrode Modified with Amino Acid Oxidase and Electron Mediator. *Chem. Lett.* **2000**, *29*, 110–111. https://doi.org/10.1246/cl.2000.110.

(36) Behar-Levy, H.; Avnir, D. Entrapment of Organic Molecules within Metals: Dyes in Silver. *Chem. Mater.* **2002**, *14*, 1736–1741. https://doi.org/10.1021/cm011558o.

(37) Behar-Levy, H.; Shter, G. E.; Grader, G. S.; Avnir, D. Entrapment of Organic Molecules within Metals. 2. Polymers in Silver. *Chem. Mater.* **2004**, *16*, 3197–3202. https://doi.org/10.1021/cm049824w.

(38) Behar-Levy, H.; Avnir, D. Silver Doped with Acidic/Basic Polymers: Novel, Reactive Metallic Composites. *Adv. Funct. Mater.* **2005**, *15*, 1141–1146. https://doi.org/10.1002/adfm.200400370.

(39) Yosef, I.; Avnir, D. Metal-Organic Composites: The Heterogeneous Organic Doping of the Coin Metals-Copper, Silver, and Gold. *Chem. Mater.* **2006**, *18*, 5890–5896. https://doi.org/10.1021/cm0615368.

(40) Ben-Efraim, Y.; Avnir, D. Entrapment of Organic Molecules within Binary Metal Alloys. *J. Mater. Chem.* **2012**, *22*, 17595–17603. https://doi.org/10.1039/c2jm34032a.

(41) Yosef, I.; Abu-Reziq, R.; Avnir, D. Entrapment of an Organometallic Complex within a Metal: A Concept for Heterogeneous Catalysis. *J. Am. Chem. Soc.* **2008**, *130*, 11880–11882. https://doi.org/10.1021/ja804112z.

(42) Behar-Levy, H.; Neumann, O.; Naaman, R.; Avnir, D. Chirality Induction in Bulk Gold and Silver. *Adv. Mater.* **2007**, *19*, 1207–1211. https://doi.org/10.1002/adma.200601702.

(43) Durán Pachón, L.; Yosef, I.; Markus, T. Z.; Naaman, R.; Avnir, D.; Rothenberg, G. Chiral Imprinting of Palladium with Cinchona Alkaloids. *Nat. Chem.* **2009**, *1*, 160–164. https://doi.org/10.1038/nchem.180.

(44) Hori, Y. Electrochemical CO_2 Reduction on Metal Electrodes. In *Modern Aspects of Electrochemistry*; Springer New York: New York, NY, 2008; pp 89–189. https://doi.org/10.1007/978-0-387-49489-0_3.

(45) Yang, H. P.; Qin, S.; Wang, H.; Lu, J. X. Organically Doped Palladium: A Highly Efficient Catalyst for Electroreduction of CO_2 to Methanol. *Green Chem.* **2015**, *17*, 5144–5148. https://doi.org/10.1039/c5gc01504a.

(46) Yang, H. P.; Qin, S.; Yue, Y. N.; Liu, L.; Wang, H.; Lu, J. X. Entrapment of a Pyridine Derivative within a Copper-Palladium Alloy: A Bifunctional Catalyst for Electrochemical Reduction of CO_2 to Alcohols with Excellent Selectivity and

Reusability. *Catal. Sci. Technol.* **2016**, *6*, 6490–6494. https://doi.org/10.1039/c6cy00971a.

(47) Yang, H.-P.; Yue, Y. N.; Qin, S.; Wang, H.; Lu, J.-X. Selective Electrochemical Reduction of CO2 to Different Alcohol Products by an Organically Doped Alloy Catalyst. *Green Chem.* **2016**, *18*, 3216–3220. https://doi.org/10.1039/c6gc00091f.

(48) Khuphe, M.; Thornton, P. D. Poly(Amino Acids). In *Engineering of Biomaterials for Drug Delivery Systems: Beyond Polyethylene Glycol*; Elsevier Ltd, 2018; pp 199–228. https://doi.org/10.1016/B978-0-08-101750-0.00007-6.

(49) Katakai, R.; Iizuka, Y. An Improved Rapid Method for the Synthesis of *N*-Carboxy α-Amino Acid Anhydrides Using Trichloromethyl Chloroformate. *J. Org. Chem.* **1985**, *50*, 715–716. https://doi.org/10.1021/jo00205a039.

(50) Wilder, R.; Mobashery, S. The Use of Triphosgene in Preparation of *N*-Carboxy-α-Amino Acid Anhydrides. *J. Org. Chem.* **1992**, *57*, 2755–2756. https://doi.org/10.1021/jo00035a044.

(51) Nagai, A.; Sato, D.; Ishikawa, J.; Ochiai, B.; Kudo, H.; Endo, T. A Facile Synthesis of N-Carboxyanhydrides and Poly(α-Amino Acid) Using Di-Tert-Butyltricarbonate. *Macromolecules* **2004**, *37*, 2332–2334. https://doi.org/10.1021/ma0498464.

(52) Mobashery, S.; Johnston, M. A New Approach to the Preparation of *N*-Carboxy α-Amino Acid Anhydrides. *J. Org. Chem.* **1985**, *50*, 2200–2202.

(53) Komori, T.; Nonaka, T.; Fuchigami, T.; Zhang, K. Electrochemical Synthesis of Poly(Amino Acid)s, Poly(Amino Acid) Urethane Copolymers, and Electroconductive Poly(Amino Acid)-Polypyrrole Complex Films. *Bull. Chem. Soc. Jpn.* **1987**, *60*, 3315–3320. https://doi.org/10.1246/bcsj.60.3315.

(54) Vapourtec Ltd. *Ion electrochemical reactor*. https://www.vapourtec.com/products/flow-reactors/ion-electrochemical-reactor-features/, (accessed September 2022).

(55) Sáez, A.; García-García, V.; Solla-Gullón, J.; Aldaz, A.; Montiel, V. Electrocatalytic Hydrogenation of Acetophenone Using a Polymer Electrolyte Membrane Electrochemical Reactor. *Electrochim. Acta* **2013**, *91*, 69–74. https://doi.org/10.1016/j.electacta.2012.12.097.

(56) Mulero, C. M.; Sáez, A.; Iniesta, J.; Montiel, V. An Alternative to Hydrogenation Processes. Electrocatalytic Hydrogenation of Benzophenone. *Beilstein J. Org. Chem.* **2018**, *14*, 537–546. https://doi.org/10.3762/bjoc.14.40.

(57) Mayoral, A.; Sakamoto, Y.; Anderson, P. A. Synthesis of Copper Chloride Nanowires by Thermal Treatment in the Presence of Zeolite X. *Cryst. Eng. Comm.* **2010**, *12*, 3012–3018. https://doi.org/10.1039/c004261g.

(58) Chen, B. L.; Xiao, Y.; Xu, X.-M.; Yang, H.-P.; Wang, H.; Lu, J.-X. Alkaloid Induced Enantioselective Electroreduction of Acetophenone. *Electrochim. Acta* **2013**, *107*, 320–326. https://doi.org/10.1016/j.electacta.2013.06.082.

(59) Chadderdon, X. H.; Chadderdon, D. J.; Matthiesen, J. E.; Qiu, Y.; Carraher, J. M.; Tessonnier, J.; Li, W. Mechanisms of Furfural Reduction on Metal Electrodes: Distinguishing Pathways for Selective Hydrogenation of Bioderived Oxygenates. *J. Am. Chem. Soc.* **2017**, *139*, 14120–14128. https://doi.org/10.1021/jacs.7b06331.

(60) Moore, R. B.; Martin, C. R. Procedure for Preparing Solution-Cast Perfluorosulfonate Ionomer Films and Membranes. *Anal. Chem.* **1986**, *58*, 2569–2570. https://doi.org/10.1021/ac00125a046.

(61) Zook, L. A.; Leddy, J. Density and Solubility of Nafion: Recast, Annealed, and Commercial Films. *Anal. Chem.* **1996**, *68*, 3793–3796. https://doi.org/10.1021/ac960604e.

(62) Szentirmay, M. N.; Martin, C. R. Ion-Exchange Selectivity of Nafion Films on Electrode Surfaces. *Anal. Chem.* **1984**, *56*, 1898–1902. https://doi.org/10.1021/ac00275a031.

(63) Kaushik, A.; Khan, R.; Solanki, P. R.; Pandey, P.; Alam, J.; Ahmad, S.; Malhotra, B. D. Iron Oxide Nanoparticles-Chitosan Composite Based Glucose Biosensor. *Biosens. Bioelectron.* **2008**, *24*, 676–683. https://doi.org/10.1016/j.bios.2008.06.032.

(64) Choudhury, N. A.; Ma, J.; Sahai, Y.; Buchheit, R. G. High Performance Polymer Chemical Hydrogel-Based Electrode Binder Materials for Direct Borohydride Fuel Cells. *J. Power Sources* **2011**, *196*, 5817–5822. https://doi.org/10.1016/j.jpowsour.2011.03.004.

(65) Szőllősi, G.; Kolcsár, V. J. Highly Enantioselective Transfer Hydrogenation of Prochiral Ketones Using Ru(II)-Chitosan Catalyst in Aqueous Media. *ChemCatChem* **2019**, *11*, 820–830. https://doi.org/doi:10.1002/cctc.201801602.

Chapter 3: Electrochemical Oxychlorination of Alkenes

3.1 Introduction

3.1.1 Oxygen Reduction Reaction

The oxygen reduction reaction has been studied intensively in applications like fuel cells or metal air batteries. In the presence of water, a reduction of oxygen will give either water or hydrogen peroxide.[1,2] The oxygen reduction reaction in organic aprotic solvents has not been studied in similar depth. In the absence of protons, the increased lifetime of the superoxide anion enables its use for subsequent organic reactions. In this case, the characteristic properties of the superoxide anion, such as basicity, nucleophilicity or its radical character can be exploited.[1,3]

In 1983, Baizer and Sugawara reported the use of electrogenerated superoxide as a base. They had found that electrogenerated superoxide ions could convert *sec*-nitriles to ketones **37** and primary nitriles to carboxylic acids **86** (Scheme 3.1). Aldehydes are formed in the presence of acetic anhydride, and trapped as the diacetate **88** (Scheme 3.2). The molecular oxygen, that was bubbled through the catholyte, was reduced in a divided cell at a mercury cathode at 1.0 V vs SCE. Ethyl cyanoacetate **85h** and diethyl cyanomalonate **85g** could be converted to ethyl glyoxalate **87a** and diethyl ketomalonate **37h** respectively.[4]

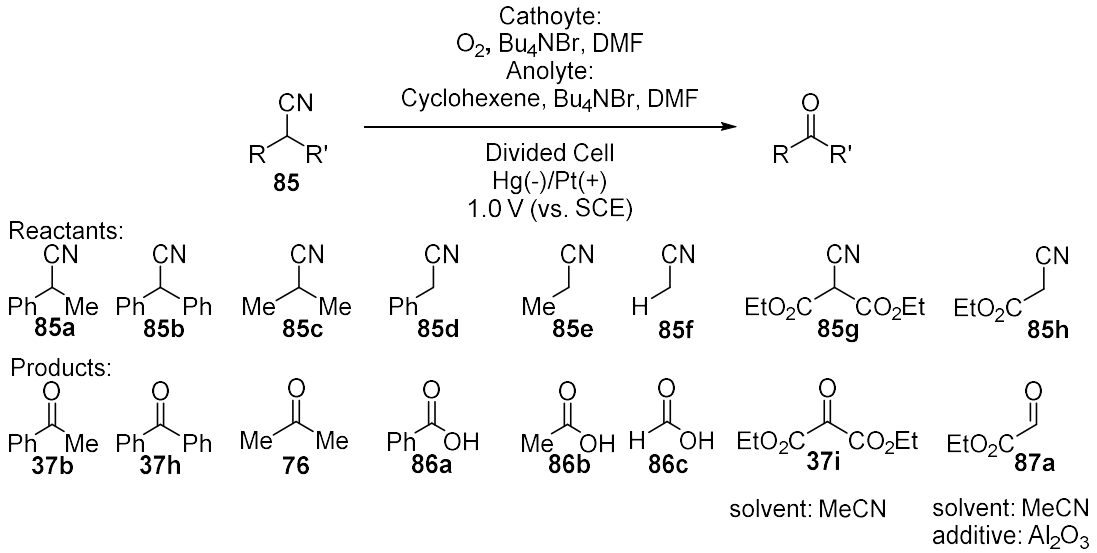

Scheme 3.1: Electrochemical oxidation of nitriles to ketones and carboxylic acids.

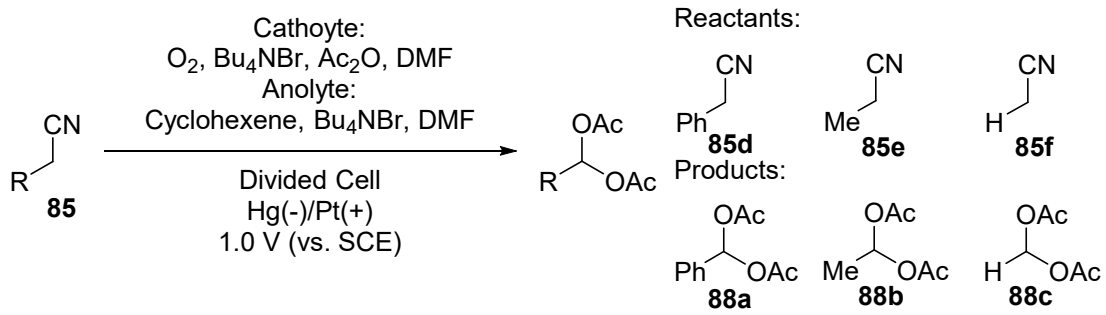

Scheme 3.2: Electrochemical conversion of primary nitriles **85** to diacetates **88**.

Electrogenerated superoxide was also used as a base to promote the autoxidation of sec-nitroalkanes **89** to the corresponding ketones **37** (Scheme 3.3). Primary nitroalkanes **90** could be used as acyl anion equivalents for Michael additions. The oxygen was reduced at a mercury-pool cathode in a divided cell in a MeCN/Bu_4NBr electrolyte. Cyclohexene was added to the anodic chamber to trap the bromine generated in the anodic reaction. Care was taken to dry the oxygen before passing it into the cathodic chamber.[5]

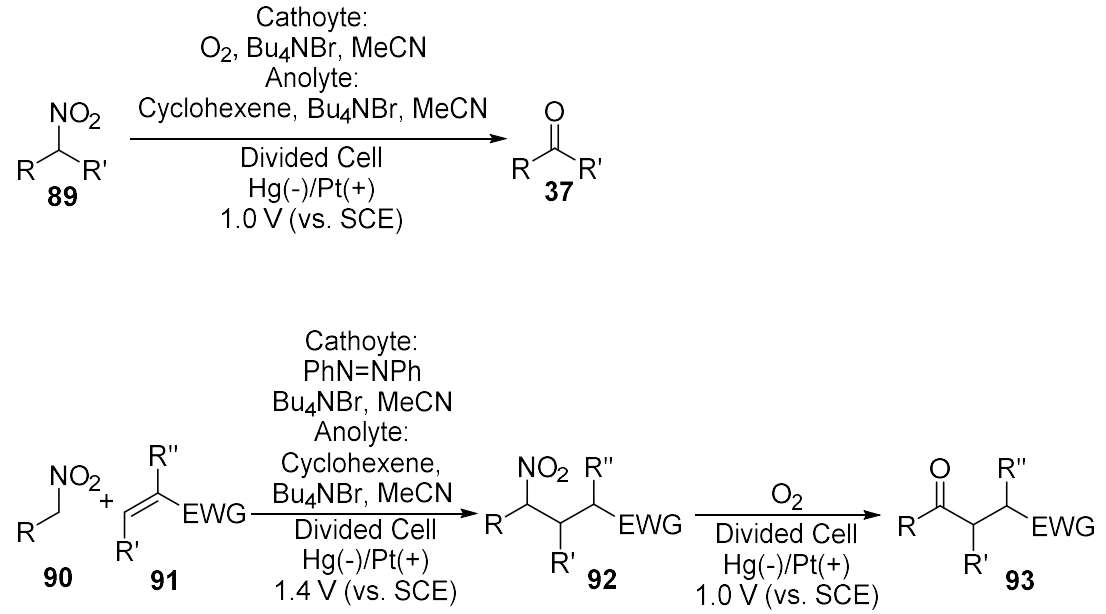

Scheme 3.3: Electrogenerated superoxide promoted oxidation of nitroalkanes.

Electrochemically generated superoxide radicals have been investigated for their nucleophilicity as early as 1970. Peover and co-workers employed this reactivity in nucleophilic substitution reactions with *n*-alkyl halides **94** to di-*n*-alkyl peroxides **95** (Scheme 3.4A). In the case of tertiary alkyl halides, they observed an elimination of the halide. Furthermore, the addition of superoxide to activated double bonds was observed.[6] Sawyer and co-workers also observed a nucleophilic substitution reaction of

superoxide with alkyl halides to form peroxide radicals **96** and subsequently hydroperoxides **97** in DMSO/NEt_4ClO_4 electrolytes (Scheme 3.4B).[7]

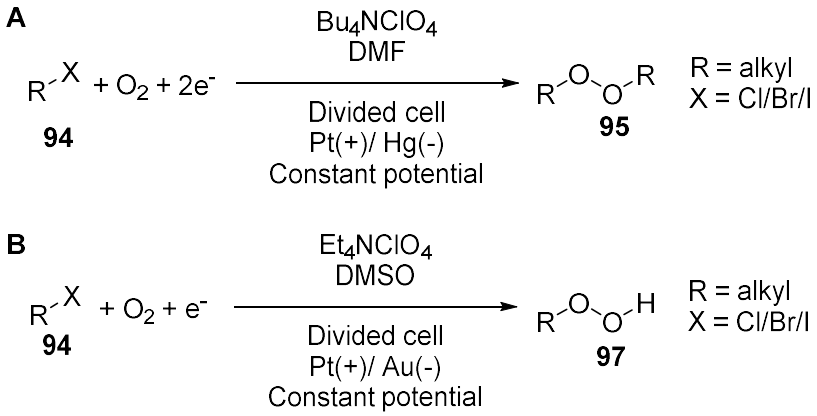

Scheme 3.4: Nucleophilic reactions of electrogenerated superoxide ions with halides lead to the formation of hydroperoxides (A) and di-alkyl peroxides (B).

The nucleophilicity of superoxide had been exploited for its reaction with carbon dioxide to form $C_2O_6^{2-}$ **98c** (Scheme 3.5). Evidence was found for an oxo-bridge rather than a peroxide linkage between the two carbon atoms.[8] Casadei *et al.* reported the reaction of electrogenerated superoxide with carbon dioxide to give the carboxylating reagent **98c**. The mild reaction conditions allowed the conversion of amines (**99** and **101**) to linear carbamates **100** and cyclic carbamates **102,** if an appropriate leaving group was present at an alkyl chain (Scheme 3.6).[9]

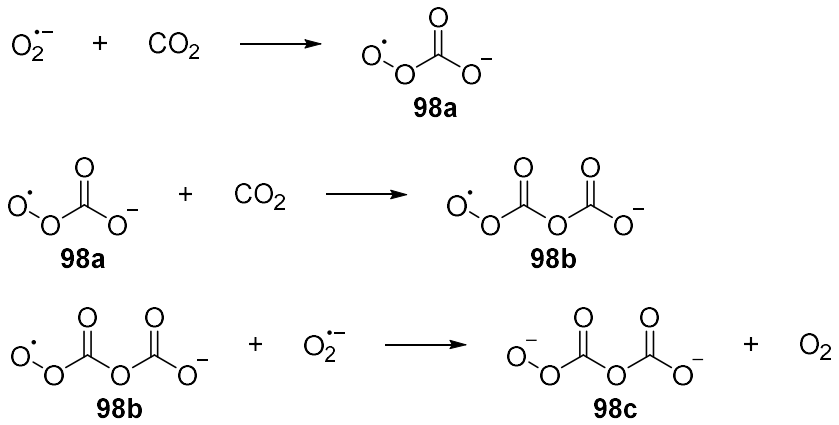

Scheme 3.5: Nucleophilic reaction of superoxide with carbon dioxide.

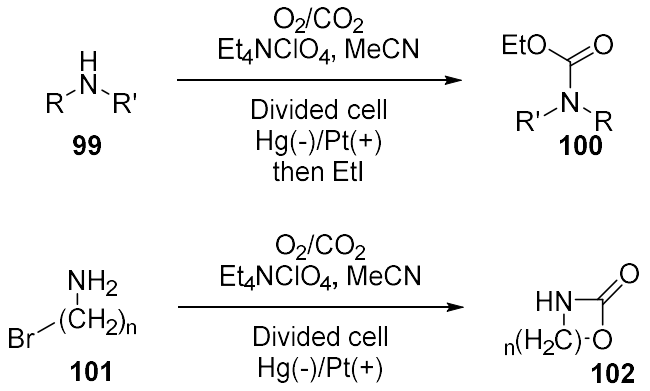

Scheme 3.6: Electrochemical carboxylation with O_2/CO_2 to form linear and cyclic carbamates.

Lund and co-worker demonstrated benzylic oxidations with electrogenerated superoxide (Scheme 3.7). *Ortho*- and *para*-nitrotoluene (**99a** & **99b**) reacted to give nitrobenzoic acids (**86d** & **86e**). The reaction with *p*-nitroethylbenzene **99c** afforded *p*-nitroacetophenone **37j** and 1-*p*-(nitrophenyl)ethanol **38h**.[10]

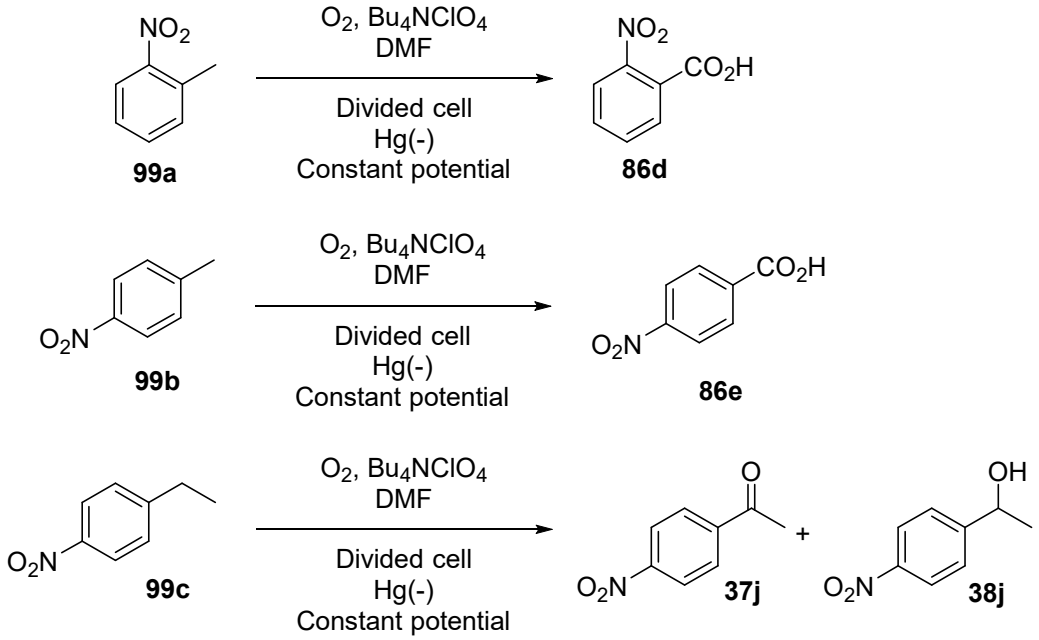

Scheme 3.7: Benzylic oxidations with electrogenerated superoxide ions.

Chen and co-workers reported a manganese or cobalt catalysed paired electrolysis of styrene derivatives **42** to the corresponding 2-chloroacetophenone derivatives **103** to in the presence of oxygen and chloride salts (Scheme 3.8). The anodic reaction with the transition metal catalyst would provide chlorine radicals for the reaction with the alkene. The resulting radical intermediate reacted with the electrogenerated superoxide ion and further oxidation of the intermediary 1-phenylethanol derivative **104** gave the final product.[11,12]

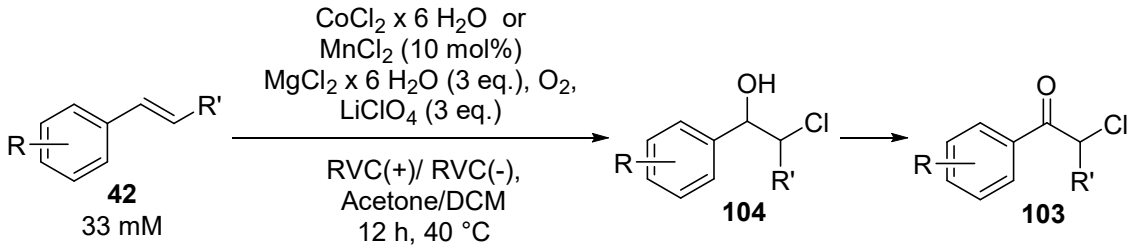

Scheme 3.8: Electrochemical oxychlorination of alkenes.

In water or other protic solvents superoxide ions will rapidly disproportionate to oxygen and hydroperoxide ions.[1,2] Chan and co-workers demonstrated the electrochemical generation of hydrogen peroxide from molecular oxygen in a mixture of the ionic liquid [bmim][BF_4] and water. The reaction was performed in an electrochemical microreactor under recirculating conditions (Figure 3.1). Platinum was equipped as anode and a RVC electrode as cathode. The two cell compartments were separated by a Nafion® membrane. *In situ* generated hydrogen peroxide was used in the subsequent epoxidation of alkenes. The ionic liquid could be recovered and reused.[13] An electrochemical epoxidation in an aqueous $NaHO_3$ solution employed a similar microreactor setup.[14] In this example, a manganese catalyst and the alkene were already added to the electrolyte. The addition of *tert*-butanol enabled the epoxidation of lipophilic alkenes as well.

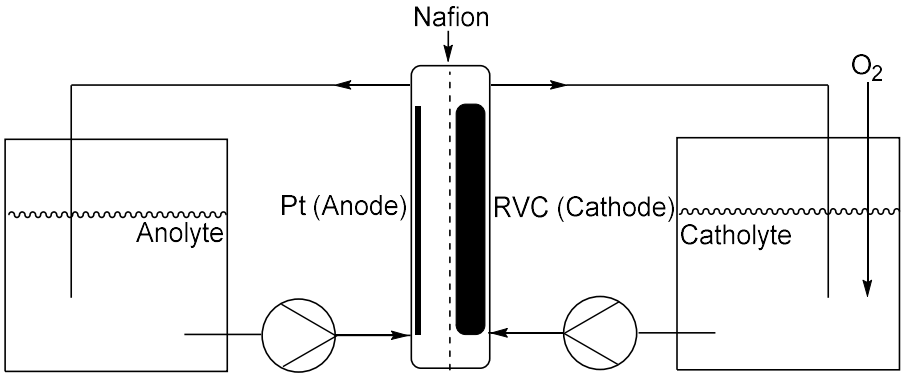

Figure 3.1: Reactor setup for the electrochemical generation of H_2O_2 and epoxidation of alkenes.

Collman and co-workers modified electrodes with a polymeric ligand and immobilised ruthenium catalyst. The electrodes were employed to reduce molecular oxygen, in the presence of benzoic acid, to hydrogen peroxide, which would then be utilised in a manganese catalysed epoxidation of olefins in the solution (Scheme 3.9).[15]

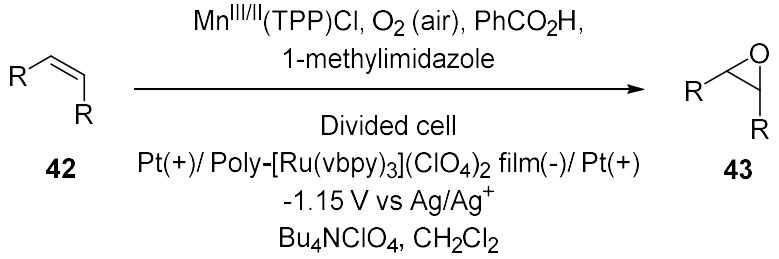

Scheme 3.9: Epoxidation of olefins with manganese meso-tetraphenyl porphyrin catalyst and H_2O_2 generated at poly-[$Ru(vbpy)_3(ClO_4)_2$ film electrodes.

3.1.2 Use of Molecular Oxygen in Continuous Flow Reactors

Molecular oxygen can serve as a green reagent and terminal oxidant in aerobic oxidations. The benefits of oxygen include its abundance and low cost, but also the generally high atom economy and low waste production compared to other oxidants. However, there are certain challenges when it comes to the use of oxygen in organic solvents. Mass-transfer effects at the gas-liquid interface require efficient mixing, which becomes increasingly difficult when scaling up reactions. Highly flammable mixtures of oxygen organic vapours, especially in the headspace of batch reactors, is a safety concern. The exothermic nature of oxidations involving oxygen requires a precise control of the temperature. The use of continuous flow reactors can provide a solution to most of these problems and can also enable a safer scale up process. The small channel dimensions of the reactor can help to give better control over the reaction temperature. Furthermore, the increased surface area at the gas-liquid interface in the reactor allows for more efficient mixing and minimises mass-transfer limitations. Pressurising continuous flow reactors can be easily achieved, thereby the solubility of oxygen in organic solvents can be increased. Moreover, the precise control of reaction parameters under continuous conditions can help to minimise overoxidation.[16]

Several microreactor designs can be employed to perform gas liquid reactions. Single-channel microreactors can be utilised to implement segmented or annular flow regimes. In a falling-film reactor, a gas phase interacts with a flowing thin film, which is created by gravity. Mesh microreactors can also be used to create a large interfacial area. Another strategy to saturate the solvents with oxygen under continuous flow conditions is the tube-in-tube reactor.[17] In this case, the gas phase is separated from the liquid phase by a permeable membrane. Generally, Teflon is used as a gas-permeable polymer for the membrane of the inner tube.[18]

The use of air and oxygen in continuous flow processes is already employed in the production of several commodity chemicals.[19] There are also some initiatives under

way to promote the implementation of continuous reactions involving oxygen in the pharmaceutical industry.[20]

Stahl and co-workers developed a continuous flow method for the aerobic palladium catalysed oxidation of alcohols to aldehydes and ketones (Scheme 3.10). The risk of explosions was mitigated by using a diluted mixture of oxygen in nitrogen. The use of a tube reactor reduced the decomposition of the catalyst by efficient mixing in a segmented flow regime. They could demonstrate the versatility of the reaction on a 1 kg scale with a 7 L coil made from stainless steel.[21]

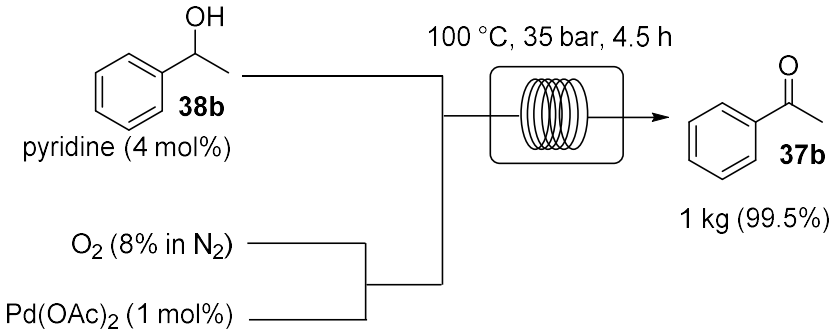

Scheme 3.10: Palladium catalysed aerobic oxidation in continuous flow using diluted oxygen.

An *anti*-Markovnikov Wacker oxidation was realised under continuous conditions with a tube-in-tube reactor (Scheme 3.11). The flow setup reduced the overoxidation of the product. Furthermore, the synthesis of aryl acetaldehydes **105** from styrene derivatives **42** could be performed on a multi-gram scale.[22]

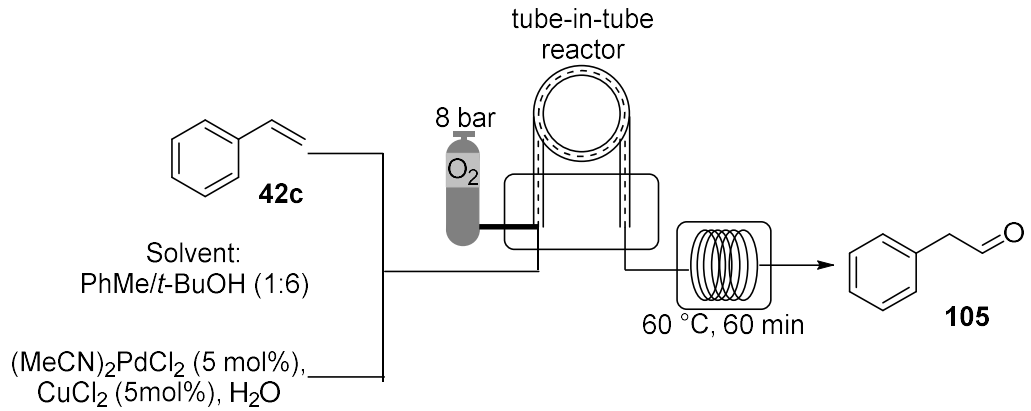

Scheme 3.11: Aerobic *anti*-Markovnikov Wacker oxidation in continuous flow using pure O_2 and a tube-in-tube reactor.

Green *et al.* identified PTFE tubing as a suitable material for a so called “tube-in-shell” reactor due to its low cost and oxygen permeability. The tube was led through a stainless-steel shell pressurised with oxygen. A homogeneous Cu(OTf)/TEMPO system was used to catalyse the aerobic oxidation of alcohols in excellent yields

(Scheme 3.12). A packed bed reactor loaded with $Ru(OH)_x/Al_2O_3$ as heterogeneous catalyst was also used for the oxidation of benzyl alcohol to benzaldehyde within the shell.[23]

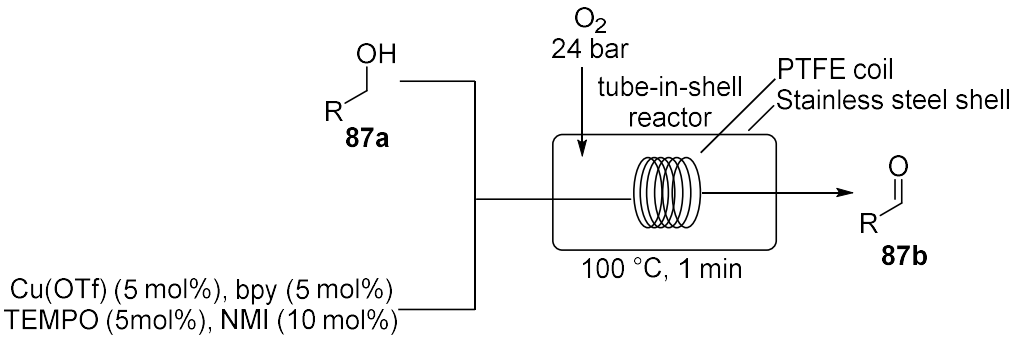

Scheme 3.12: Copper catalysed aerobic oxidation using a tube-in-shell reactor with gas-permeable PTFE tubing.

3.2 Aims and Objectives

The aim of this project was to implement the use of molecular oxygen in a flow electrochemical reactor in order to benefit from the previously described advantages.

The electrochemical oxychlorination of alkenes was chosen as a potential model reaction. This reaction combines the reduction of superoxide at the cathode and the oxidation of chloride complexes at the anode in a paired electrolysis. The first aim was to reproduce the batch reaction reported by Chen and co-workers. Subsequently, the reaction conditions would be adapted and optimised in a single-pass flow electrochemical setup. The use of oxygen in the ion electrochemical microreactor would aid in mitigating the risk arising from the combination of oxygen with organic vapours, establish a better control over reaction parameters and ensure a higher interfacial area. The supply of oxygen would be controlled using a mass flow controller.

3.3 Results and Discussion

3.3.1 Oxychlorination of alkenes

Recently, Chen and co-workers described the oxychlorination of alkenes with molecular oxygen in the presence of a chloride source. Their best results were obtained with both cobalt(II) chloride[12] or manganese(II) chloride[11] as a catalyst. Their reactions were conducted in an undivided cell (10 mL) filled with 6 mL of solvent, containing the alkene **42** (0.2 mmol, 33 mM), catalyst (10 mol%), $MgCl_2$ (100 mM) as chloride source and $LiClO_4$ (100 mM) as supporting electrolyte. The cell was flushed with oxygen prior to the electrolysis. Pencil lead (diameter: 2 mm; immersion depth: 10

mm; active surface area: 0.63 cm^2) was used as the electrode material for the optimisation of the cobalt catalysed reaction. With these electrodes, a current of 5 mA was applied for 5 hours which corresponds to a transferred charge of 4.66 $F \cdot mol^{-1}$ (90 C). The current density was calculated to be approximately 8 $mA \cdot cm^{-2}$. Manganese catalysed experiments and substrate scopes were performed with RVC electrodes (100 PPI, dimensions: 10 mm × 10 mm × 2 mm). In this case, the current of 5 mA was applied for 12 hours for full conversion, which resulted in a transferred charge of 11.2 $F \cdot mol^{-1}$ (216 C). Reactions were performed in a mixture of acetone (5.9 mL) and CH_2Cl_2 (0.1 mL), which was heated to 40 °C for several hours. This would suggest there was a considerable loss of solvent during the reaction even in a vessel sealed with a rubber septum. For the substrate scope of the cobalt catalysed reaction, 2 equivalents of sulfuric acid were added to the reaction mixture. This addition did not lead to an increase in yield in the optimisation and was not discussed in detail. Furthermore, the presence of acid questions the role of the super oxide radical anions in the proposed reaction mechanism, given the disproportion of superoxide ions in protic systems.

Reproduction of these experiments served as the starting point for this project. The molecular oxygen was fed into the reaction mixture by means of a balloon. Electrasyn 2.0 vials equipped with the corresponding cap were used as the reaction vessel. The cap was sealed with a rubber septum which was punctured with a needle attached to the oxygen balloon. Carbon based materials like graphite and RVC were used as anode materials. Graphite, RVC and platinum were investigated as cathode materials. Generally, the flask was loaded with $CoCl_2 \times 6\ H_2O$ as catalyst (10 mol%), $MgCl_2$ (100 mM, 3 eq.) and $LiClO_4$ (100 mM). Subsequently, the reaction vessel was sealed, flushed with oxygen and filled with acetone-CH_2Cl_2 mixtures (5.9 : 0.1) or acetonitrile as solvent and styrene **42c** (33 mM, 0.165 mmol) as substrate. The reaction mixture was purged with oxygen while a constant current was applied.

Chen and co-workers reported a good yield of 63% for 2-chloroacetophenone **103a** when the reaction was performed at room temperature.[12] Therefore, the initial experiments were conducted at ambient temperatures with graphite electrodes (active surface area: 2.4 cm^2) and $CoCl_2 \times 6\ H_2O$ as catalyst. In a first experiment (Table 3.1, entry 1) the current density was set to 10 $mA \cdot cm^{-2}$ and a charge of 3 $F \cdot mol^{-1}$ was passed to give the desired compound **103a** in only 5% yield. A second attempt (Table 3.1, entry 2) with a current density of 5 $mA \cdot cm^{-2}$ and $MgCl_2 \times 6\ H_2O$ as chloride salt

resulted in a yield of 15%. Two side products, 2-chloro-1-phenylethanol **104a** and 1,2-dichloroethylbenzene **106a**, were detected in 8% yield and trace amounts, respectively. By using RVC electrodes and heating the reaction mixture to 40 °C (Table 3.1, entry 3) a mixture of ketone **103a** and alcohol **104a** in 5% and 18% yield, respectively, was afforded. Under the reported conditions, the chloride salt is not completely soluble, which would be important for a flow electrochemistry setup. To help with the solubility of the chloride salt, acetonitrile was chosen as solvent. When the reaction was performed in acetonitrile, the chloride salt was still not dissolved sufficiently and 2-chloroacetophenone **103a** was obtained in only 10% yield (Table 3.1, entry 4). By using RVC electrodes and heating the acetonitrile-based reaction mixture to 40 °C (Table 3.1, entry 5), the alcohol **104a** was furnished in 7% yield while ketone **103a** and dichloride **106a** were only detected in trace amounts.

Table 3.1: Oxychlorination – initial experiments.

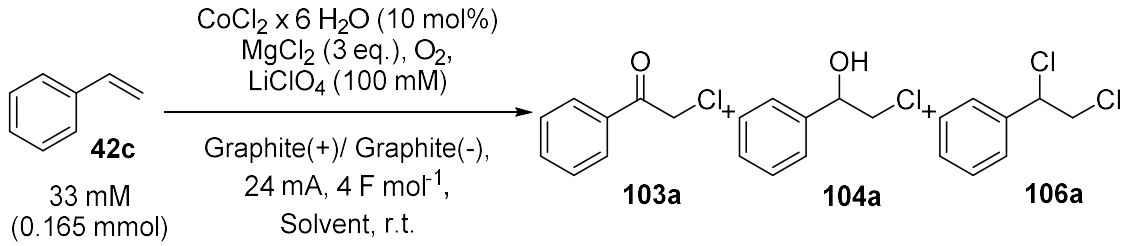

Entry	Solvent	Cl^- source (eq.)	Electrodes	Charge [F·mol^{-1}]	Current [mA]	**103a** [%]	**104a** [%]	**106a** [%]
1	Acetone CH_2Cl_2[a]	$MgCl_2$ (3)	Graphite	3	24	5[b]	-	-
2	Acetone CH_2Cl_2[a]	$MgCl_2 \times 6H_2O$ (3)	Graphite	2.2	12	15	8	2
3[c]	Acetone CH_2Cl_2[a]	$MgCl_2$ (4.5)	Graphite	4	24	5	18	2
4	MeCN	$MgCl_2 \times 6H_2O$ (3)	Graphite	4	12	10	4	3
5[c]	MeCN	$MgCl_2$ (3)	RVC	4	12	2	7	2

Reaction conditions: Styrene **42c** (0.165 mmol, 33 mM), chloride source, solvent (5 mL), $CoCl_2 \times 6\ H_2O$ (10 mol%), $LiClO_4$ (100 mM), 4 F mol^{-1}, r.t., O_2 atmosphere; Graphite electrodes (Immersed surface area: 2.4 cm^2); RVC electrode (Dimensions of immersed electrode material: 30 mm × 8 mm × 2 mm); Internal standard: 1,3,5-trimethoxybenzene; a) Acetone/CH_2Cl_2 5.9:0.1; b) Isolated yield; c) 40 °C instead of r.t.

Subsequently, the focus was placed on the solubility and performance of different chloride salts in acetonitrile at room temperature. The use of tetraethylammonium chloride (Table 3.2, entry 1), which served as chloride source and electrolyte, did not

afford any product. Both potassium chloride and sodium chloride (Table 3.2, entries 2 & 3) suffered from low solubility and gave low yields. Even though lithium chloride (Table 3.2, entry 4) was not completely soluble, an increase in yield to 20% for **103a** was observed. Unfortunately, the yield of the dichloride **106a** was also significantly increased to 23%. When the amount of lithium chloride was reduced to 2 equivalents (Table 3.2, entry 5), the salt was dissolved completely over the course of the reaction. A reduction to 1 equivalent of lithium chloride (Table 3.2, entry 6) allowed complete solubility. On the other hand, the reduction of lithium chloride resulted in lower ketone **103a** yields of 12% and 13%, respectively, while the ratio of ketone **103a** to dichloride **106a** remained at approximately 1:1. Increasing the current density from 5 $mA \cdot cm^{-2}$ to 10 and 15 $mA \cdot cm^{-2}$ (Table 3.2, entries 7 & 8) afforded an increase in yield to 24% and a reduction to 11%, respectively. When the solvent was purged with nitrogen and the oxygen balloon was replaced for a nitrogen balloon (Table 3.2, entry 9), the ketone **103a** and alcohol **104a** were obtained in 7% and 11% yield, respectively. Interestingly, the production of the dichloride **106a** could be increased to 55% yield in the absence of oxygen. When the reaction vessel was open to air (Table 3.2, entry 10), the oxygenated products were furnished in trace amounts and the dichloride **106a** in 16% yield. The addition of 2.5% of water to the acetonitrile (Table 3.2, entry 11) resulted in the predominant formation of the alcohol **104a** with a yield of 10%.

Table 3.2: Oxychlorination – chloride salt tests.

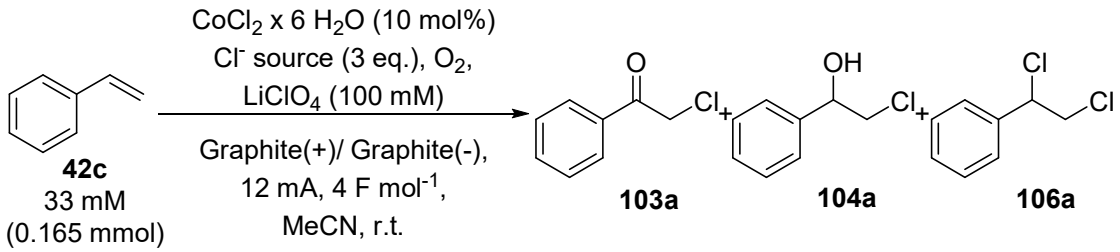

Entry	Cl^- source (eq.)	Current [mA]	**103a** [%]	**104a** [%]	**106a** [%]
1[a]	E_4NCl (3)	36	0	0	0
2	KCl (3)	12	9	4	3
3	NaCl (3)	12	4	2	2
4	LiCl (3)	12	20	5	23
5	LiCl (2)	12	12	3	11
6	LiCl (1)	12	13	5	14
7	LiCl (3)	24	24	17	27

8	LiCl (3)	36	11	3	3
9[b]	LiCl (3)	24	7	11	55
10[c]	LiCl (3)	24	1	3	16
11[d]	LiCl (3)	12	2	10	1

Reaction conditions: Styrene **42c** (0.165 mmol, 33 mM), MeCN (5 mL), $CoCl_2 \times 6\ H_2O$ (10 mol%), chloride source, $LiClO_4$ (100 mM), 4 $F \cdot mol^{-1}$, r.t., O_2 atmosphere, graphite electrodes (immersed surface area: 2.4 cm^2); Internal standard: 1,3,5-trimethoxybenzene; a) No supporting electrolyte, 6.2 $F \cdot mol^{-1}$; b) N_2 atmosphere instead of O_2; c) Reaction vessel was open to air; d) H_2O (2.5%) in MeCN.

RVC has been used as electrode material due to its high surface area. The major challenge of this electrode material, however, is its instability under mechanical pressure. Hence, the implementation of RVC in a flow reactor would be challenging, given its dependence on pressure sealing.[24] The challenge here lies in the fixation of the electrode material to the contact while keeping it away from the opposite electrode to avoid a short circuit. A solution for this problem was identified for electrochemical epoxidation reactions with molecular oxygen in protic solvents. The RVC cathode was separated from the anodic compartment in the electrochemical microreactor with a Nafion membrane. The catholyte had been saturated with oxygen before being passed over the cathode in a recirculating fashion.[13,14]

Several test reactions were performed at 40 °C with $CoCl_2 \times 6\ H_2O$ as catalyst and RVC electrodes instead of graphite. The current was adjusted to 12 mA based on the dimensions of the RVC electrodes (30 mm × 8 mm × 2 mm) in comparison to the current (5 mA) and dimensions (10 mm × 10 mm × 2 mm) described by Chen and co-workers.[11,12] A current of 10 mA was applied when the immersion depth of the RVC electrode was only 25 mm (Dimensions of immersed electrode: 25 mm × 8 mm × 2 mm). After the reaction with magnesium chloride in acetonitrile, product **103a** was isolated in 23% yield (Table 3.3, entry 1). As observed before with graphite electrodes, the use of tetraethylammonium chloride did not afford the product (Table 3.3, entry 2). An increase in charge from 4 to 11.5 $F \cdot mol^{-1}$ gave the product **103a** with a yield of 22% (Table 3.3, entry 3).

Subsequently, DMF was used, which facilitated the dissolving of the magnesium chloride completely. Under these conditions, an applied charge of 4 and 8 $F \cdot mol^{-1}$ (Table 3.3, entries 4 & 5) gave the product **103a** only in 6% yield and trace amounts respectively.

The $CoCl_2 \times 6\ H_2O$ catalyst system failed to give good yields and a high selectivity for 2-chorocetophenone **103a** which stands in contrast to previous reports.[12] There could be several reasons for this like the quality of the used $CoCl_2 \times 6\ H_2O$ or differences in the reaction setup. Therefore, another protocol for the electrochemical oxychlorination developed by Chen and co-workers was followed, in which manganese(II) chloride was used as catalyst and RVC electrodes served as anode and cathode. With the original solvent system developed by Chen and co-workers, the ketone **103a** was obtained in 31% and the corresponding alcohol **104a** in 22% yield (Table 3.3, entry 6). A yield of 36% for the ketone **103a** and 15% for the alcohol **104a** was obtained with acetonitrile as solvent (Table 3.3, entry 7). In both cases, the dichloride was only observed in trace amounts. Finally, the use of DMF together with manganese catalyst (Table 3.3, entry 8) did not afford the desired product **103a**. Even though magnesium chloride can be completely dissolved in DMF, this solvent is not suitable for the oxychlorination. Even though the yields with the manganese catalyst are still low, higher yields can be achieved in comparison to the $CoCl_2 \times 6\ H_2O$ used (Table 3.3, entries 1 & 7).

Table 3.3: Oxychlorination with RVC electrodes

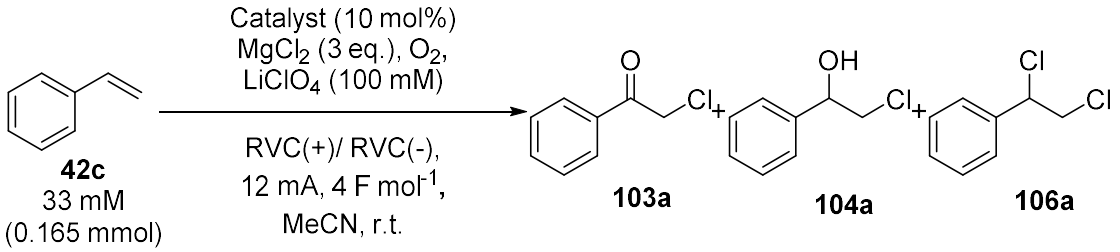

Entry	Solvent	Catalyst	Cl^- source	Charge [$F \cdot mol^{-1}$]	Current [mA]	**103a** [%]	**104a** [%]	**106a** [%]
1	MeCN	$CoCl_2 \times 6\ H_2O$	$MgCl_2$	4	12	23[a]	-	-
2	MeCN	$CoCl_2 \times 6\ H_2O$	Et_4NCl	4	12	0[a]	-	-
3	MeCN	$CoCl_2 \times 6\ H_2O$	$MgCl_2$	11.5	12	22[a]	-	-
4[b]	DMF	$CoCl_2 \times 6\ H_2O$	$MgCl_2$	4	10	6	7	4
5[b]	DMF	$CoCl_2 \times 6\ H_2O$	$MgCl_2$	8	10	trace	5	4
6[b]	Acetone/ CH_2Cl_2[c]	$MnCl_2 \times 4\ H_2O$	$MgCl_2$	11.2	10	31	22	3

7	MeCN	$MnCl_2 \times 4 H_2O$	$MgCl_2$	4	10	36	15	2
8[b]	DMF	$MnCl_2 \times 4 H_2O$	$MgCl_2$	4	10	0	3	2

Reaction conditions: Styrene **42c** (0.33 mmol, 33 mM), MeCN (10 mL), catalyst (10 mol%), chloride source (100 mM, 3 eq.), $LiClO_4$ (100 mM), 4 $F \cdot mol^{-1}$, 40 °C., O_2 atmosphere, RVC electrode (Dimensions of immersed electrode material: 30 mm × 8 mm × 2 mm for 12 mA, 25 mm × 8 mm × 2 mm for 10 mA); Internal standard: 1,3,5-trimethoxybenzene; a) Isolated yield; b) Styrene (0.165 mmol, 33 mM), solvent (5 mL); c) Acetone/DCM 5.9:0.1.

Other electrochemical transition metal catalysed chlorination reactions, as described by Lin and co-workers[25] or Morrill and co-workers,[26] employed a solvent system based on acetonitrile and acetic acid to solubilise magnesium chloride. Subsequently, reaction conditions described by Lin and co-workers for the manganese catalysed dichlorination of alkenes were followed.[25] Styrene (80 mM) and magnesium chloride (160 mM, 2 eq.) were dissolved in 10 mL of an acetonitrile-acetic acid mixture (5:1) in an undivided cell equipped with RVC anode and platinum cathode. Under a nitrogen atmosphere, the dichloride **106a** could be obtained with a yield of 54% (Table 3.4, entry 1) after a charge of 3 $F \cdot mol^{-1}$ was passed. The current was adjusted to 24.5 mA based on the dimensions of the RVC electrodes (30 mm × 8 mm × 2 mm). Interestingly, an acetate ester, 2-chloro-1-phenylethyl acetate **107a** was isolated in 3% yield. The new side product can be explained with an involvement of acetic acid in the reaction. When the dichlorination reaction conditions were performed with an oxygen balloon and a charge of 2 $F \cdot mol^{-1}$ was passed, 2-chloroacetophenone **103a** was isolated in 25% and 2-chloro-1-phenylethanol **104a** in 6% yield (Table 3.4, entry 2). An increase of the applied charge to 3 $F \cdot mol^{-1}$ (Table 3.4, entry 3) gave the desired product **103a** with 29% yield while the alcohol **104a** was detected in 6%, the dichloride **106a** in 4% yield, and the ester **107a** in trace amounts. When the reaction was performed in a 5 mL vial, the yield for product **103a** decreased to 9% (Table 3.4, entry 4) even though a higher charge of 4 $F \cdot mol^{-1}$ was passed. The lower amount of substrate results in a shorter overall reaction time even with a slightly higher applied charge of 4 $F \cdot mol^{-1}$. However, it is not entirely clear as to why the yield dropped in a smaller vessel. Going back to the previously investigated styrene (33 mM) and $MgCl_2$ (100 mM, 3 eq.) concentrations, the desired product **103a** was obtained in 24% yield and the side products in trace amounts after passing a charge of 8 $F \cdot mol^{-1}$ at a current of 12 mA (Table 3.4, entry 5). Employing graphite anode and cathode with a current density of 10 $mA \cdot cm^{-2}$ at a styrene concentration of 33 mM and an applied charge of 4 $F \cdot mol^{-1}$ (Table 3.4, entry 6), resulted in the formation of the ketone in 17% yield and an increased amount of side

products. The corresponding alcohol **104a**, dichloride **106a**, and chloro-ester **107a** were detected in 7%, 9%, and 7% yield, respectively. The use of a lower $LiClO_4$ concentration of only 50 mM afforded the ketone in lower yields (Table 3.4, entries 7 & 8). Finally, Bu_4NClO_4 (50 mM) turned out to be a viable supporting electrolyte and the product **103a** was isolated with an increase in yield to 30% (Table 3.4, entry 9). When the reaction would be adapted under continuous conditions, the investigation of different supporting electrolytes and electrolyte concentrations would make an important part of the optimisation process. Ideally, the shorter interelectrode distance in the microreactor would allow for a sufficient conductivity so that the supporting electrolyte can be omitted.

Table 3.4: Oxychlorination with MeCN/AcOH mixtures

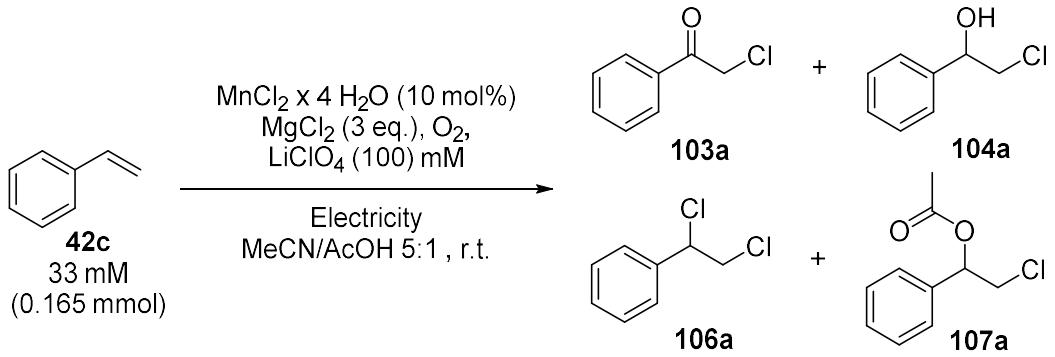

Entry	Styrene [mM]	$MgCl_2$ [mM]	Anode/ Cathode	Charge [F mol^{-1}]	Current [mA]	**103a** [%]	**104a** [%]	**106a** [%]	**107a** [%]
1[a]	80	160	RVC/Pt	3	24.5	-	-	54[b]	4[b]
2[c]	80	160	RVC/Pt	2	24.5	25[b]	6[b]	-	-
3[c]	80	160	RVC/Pt	3	24.5	29	6	4	1
4[cd]	80	160	RVC/Pt	4	24.5	9	2	0	trace
5[de]	33	100	RVC/Pt	8	12	24	4	2	trace
6	33	100	Graphite	4	24	17	7	9	7
7[de]	33	100	Graphite	4	12	11	2	trace	3
8[e]	33	120	Graphite	4	12	14	3	2	1
9[f]	33	120	Graphite	4	12	30[b]	-	-	-

Reaction conditions: Styrene **42c**, MeCN/AcOH (5:1, 10 mL), $MnCl_2 \times 4\ H_2O$ (10 mol%), $LiClO_4$ (100 mM), r.t., O_2 atmosphere; RVC electrode (Dimensions of immersed electrode material: 30 mm × 8 mm × 2 mm), Pt electrode (immersed surface area: 1.5 cm^2); Graphite electrodes (immersed surface area: 2.4 cm^2) Internal standard: 1,3,5-trimethoxybenzene; a) $CoCl_2 \times 6\ H_2O$ (5 mol%), N_2 atmosphere, 40 °C; b) Isolated yield; c) Catalyst: 5 mol%; d) MeCN/AcOH (5:1, 5 mL); e) $LiClO_4$ (50 mM); f) Bu_4NClO_4 (50 mM).

3.3.2 Mechanistic considerations for the oxychlorination of alkenes

In general, it can be concluded from the experiments, that there are at least two competing reaction mechanisms, which lead to a mixture of products.

The anodic oxidation of the transition metal complex, in this example cobalt(II)chloride (Scheme 3.13), leads to the release of a chlorine radical, which reacts with styrene to give a carbon centred radical **I** as an intermediate. The reduction of oxygen at the cathode gives the superoxide ion, which reacts with the carbon centred radical **I** to form a peroxo species **II**. Decomposition of the peroxo species by heterolytic cleavage of the O-O bond results in the formation of the alcohol 2-chloro-1-phenylethanol **104a**, which was isolated as a side product. Further superoxide mediated oxidation of the alcohol **104a** leads to the formation of the desired product 2-chloroacetophenone **103a**. A second chlorine radical transfer to the carbon centred radical **I,** results in the formation of 1,2-dichloro-1-phenylethane **106a** as another side product.[12,25]

Alternatively, a manganese complex was used to generate the chlorine radicals.[11]

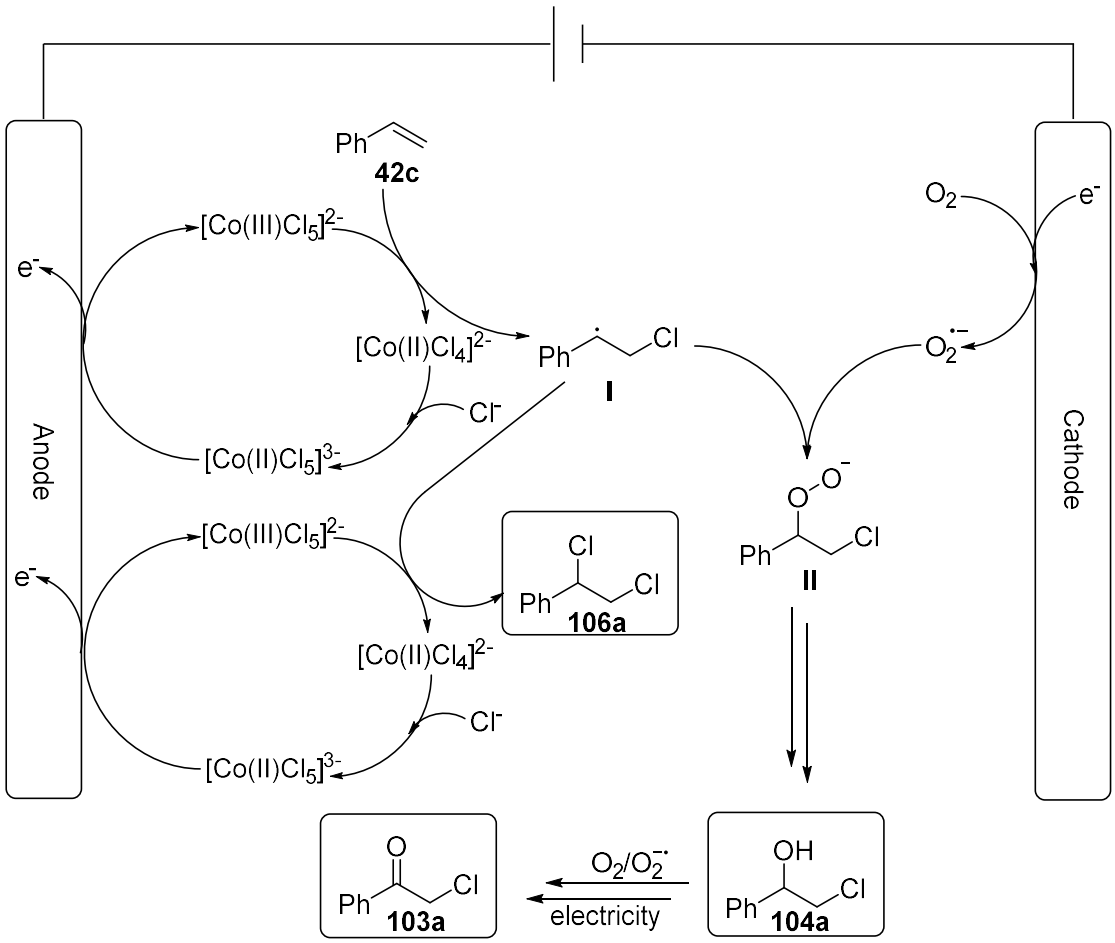

Scheme 3.13: Reaction mechanism for the cobalt catalysed electrochemical paired oxychlorination of styrene.

The ratio of roughly 1:1 between 2-chloroacetophenone **103a** and 1,2-dichloro-1-phenylethane **106a** indicates a low selectivity for the desired oxychlorination reaction mechanism under the chosen reaction conditions. The reason for the low yields of 2-chloroacetophenone **103a** might be a low concentration of superoxide ions in the reaction, which could arise from a low solubility of oxygen or superoxide in the reaction mixture or a low efficiency for the cathodic reaction. The comparably high yield for 1,2-dichloro-1-phenylethane **106a** might be assigned to a high chlorine radical concentration. This could be, among other reasons, due to a large amount of chlorine source equivalents or a high solubility. The compound, 2-chloro-1-phenylethanol **104a**, might be an intermediate in the formation of 2-chloroacetophenone **103a** according to previously proposed reaction mechanisms. If it is assumed that superoxide radicals lead to the oxidation of 2-chloro-1-phenylethanol **104a** to 2-chloroacetophenone **103a**, a low concentration of these could lead to an incomplete oxidation of the intermediate and in turn a high prevalence of the alcohol side product. The electrochemical oxidation of alcohols to ketones under oxygen atmosphere has to be researched in more depth. Proper elucidation of this mechanism could give clues as to why the reaction investigated here does not proceed completely to the ketone **103a**.[12,25]

The use of acetic acid as co-solvent was chosen to help with the solubility of the chlorine source $MgCl_2$. The presence of a protic solvent, however, has a great impact on the life time of the superoxide ion that is formed at the cathode. A reaction with protons followed by disproportion would lead to the formation of hydrogen peroxide. Nevertheless, with this solvent system the selectivity could be slightly tweaked in favour of 2-chloroacetophenone **103a** and the low solubility issue of the chlorine source was overcome. On the other hand, the presence of acetic acid led to the formation of another side product, 2-chloro-1-phenylethyl acetate **107a**, which constitutes an additional competing reaction pathway (Table 3.4).

3.3.3 Oxybromination of Alkenes

The use of potassium bromide instead of a chloride source was also investigated in two experiments. Manganese(II) acetate was chosen as the catalyst (10 mol%) and styrene **42c** (33 mM) was kept as the substrate. In the first experiment (Scheme 3.14), the reaction conditions were similar to the conditions for the oxychlorination in acetonitrile with RVC electrodes (Table 3.3, entry 7). An amount of 3 eq. of potassium bromide compared to the substrate was used, however, the bromide salt was only partially dissolved. Before and during the electrolysis, molecular oxygen was passed through

the reaction mixture, which was provided with a balloon. The current was set to 10 mA and applied until a charge of 4 F·mol^{-1} was passed. The yield was determined by ^{1}H NMR spectroscopy with an internal standard. The main product, 1,2-dibromoethylbenzene **108a**, was detected with a yield of 60%. The alcohol, 2-bromo-1-phenylethanol **109a**, was obtained in 6% yield. The NMR spectrum indicated only trace amounts of the desired compound, 2-bromoacetophenone **110a**. Under these conditions, the dibromination of the alkene is clearly favoured and proceeds to give 1,2-dibromoethylbenzene **108a** with a good yield.

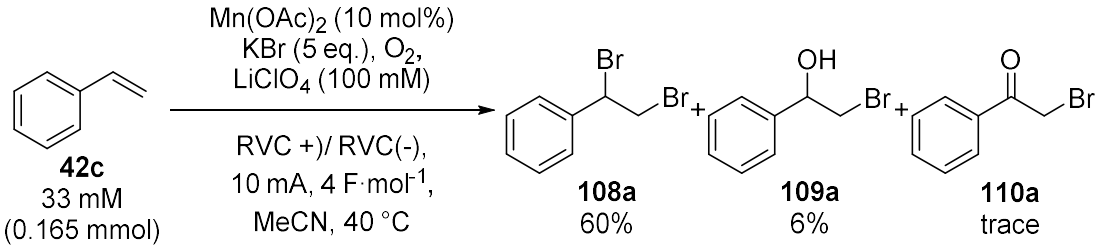

Scheme 3.14: Oxybromination of styrene **42c** in MeCN. (Internal standard 1,3,5-trimethoxybenzene).

The second experiment with potassium bromide was performed in a mixture of acetonitrile and acetic acid (5:1) under an oxygen atmosphere (Scheme 3.15). Graphite electrodes were used as cathode and anode and a current density of 5 mA·cm^{-2} was applied until a charge of 4 F·mol^{-1} was passed. Interestingly, 2-bromo-1-phenylethyl acetate **111a** was isolated with a yield of 9%. A TLC of the crude product indicated the presence of 1,2-dibromoethylbenzene **108a**, however, this could not be confirmed with the ^{1}H NMR spectrum of the isolated compound. The initially chosen amount of potassium bromide could not be dissolved completely in the acetonitrile-acetic acid mixture. In future experiments, the equivalents of brominating agent would have to be reduced or replaced with a more soluble bromide source.

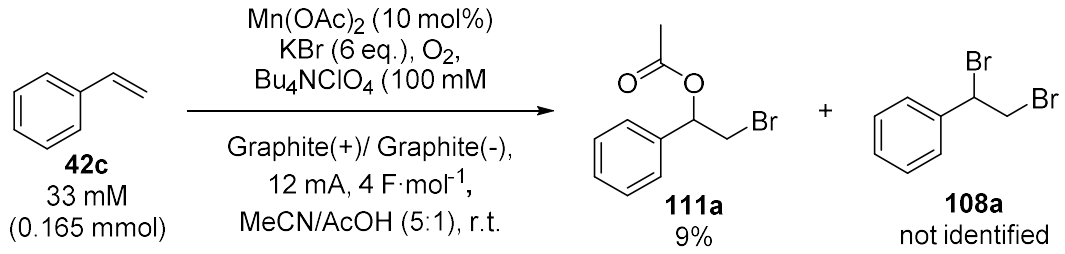

Scheme 3.15: Oxybromination of styrene **42c** in MeCN/AcOH.

The two results indicated that an oxybromination was not viable under the investigated conditions. Nevertheless, the observation of the dibromination and the

bromoesterification of alkenes in acetonitrile and acetonitrile-acetic acid mixtures could provide an interesting starting point for further investigations.

3.4 Conclusion

The electrochemical oxychlorination of styrene was reproduced to give 2-chloroacetophenone in significantly lower yields compared to the original reports.[11,12] The use of $MgCl_2$ was not feasible in flow as this chlorine source does not readily dissolve in the acetone-CH_2Cl_2 mixture, or acetonitrile. The use of a chlorine source like Et_4NCl, which is readily soluble in acetonitrile, was discouraged as no product could be observed. Among the alkali metal salts, LiCl exhibited the best solubility in acetonitrile and gave the highest yields. However, this chlorine source was still not completely dissolved in the system. Reducing the LiCl equivalents to a completely soluble amount in acetonitrile led to a decline in yield. On the other hand, a mixture of acetic acid and acetonitrile turned out to be a viable solvent for $MgCl_2$. In this case, the lifetime of the generated superoxide species would be shortened significantly and the reduced oxygen would most likely react to form hydrogen peroxide. This reaction medium would ultimately lead to a different mechanistic pathway than what was proposed by Chen and co-workers.[11,12] Nevertheless, positive results were obtained with this electrolyte regarding the electrochemical oxychlorination of alkenes. The remaining drawback of this solvent mixture is the formation of three different side products besides 2-chloroacetophenone.

The use of potassium bromide as a bromide source for a potential electrochemical oxybromination led to the predominant formation of the corresponding dibromide in acetonitrile and the formation of the 2-bromo-1-phenylethyl acetate in a mixture of acetonitrile and acetic acid. Even though the desired product 2-bromoacetophenone was not obtained, the results indicate an interesting side reaction with the formation the ester. A thorough investigation could lead to reaction conditions that would promote this pathway.

The low yield of the desired product and the suppression of persisting side reactions remains a major challenge for the successful electrochemical oxychlorination of alkenes. Another remaining problem is the low reproducibility of the results. The flow of oxygen can vary a lot because it is determined by the quality of the reaction vessel sealing, which can differ from reaction to reaction. This challenge might be overcome with flow chemistry and the use of a mass flow controller since the use of a balloon allows only for a limited control of oxygen flow through the reaction mixture.

Unfortunately, the solubility issue of the chlorine source and the lack of selectivity for the desired reaction pathway could not be solved on a reasonable timescale for an adaptation of the reaction under single-pass flow conditions. Acetonitrile and acetic acid in combination with $MnCl_2$, $MgCl_2$, $LiClO_4$, and styrene would have been used as rection mixture. Acetic acid was essential as the solubility of the electrolyte and chloride salt is inevitable for an adaption of the rection in continuous flow. Since reasonable yields had been obtained with graphite electrodes in batch, this material would be used for first flow reactions. However, a thorough screening of electrode materials in flow would be a crucial part of the optimisation process. The initial strategy for the reaction in the electrochemical microreactor would have been a segmented flow regime. As an alternative, the rection mixture could be saturated with oxygen in a tube-in-tube reactor before being passed through the electrochemical reactor.

3.5 References

(1) Hayyan, M.; Hashim, M. A.; Alnashef, I. M. Superoxide Ion: Generation and Chemical Implications. *Chem. Rev.* **2016**, *116*, 3029–3085. https://doi.org/10.1021/acs.chemrev.5b00407.

(2) Sawyer, D. T.; Chlerlcato, G.; Angells, C. T.; Nanni, E. J.; Tsuchlya, T. Effects of Media and Electrode Materials on the Electrochemical Reduction of Dioxygen. *Anal. Chem.* **1982**, *54*, 1720–1724. https://doi.org/10.1021/ac00248a014.

(3) Han, X.; Wang, K.; Zhang, G.; Gao, W.; Chen, J. Application of the Electrochemical Oxygen Reduction Reaction (ORR) in Organic Synthesis. *Adv. Synth. Catal.* **2019**, *361*, 2804–2824. https://doi.org/10.1002/adsc.201900003.

(4) Sugawara, M.; Baizer, M. M. Electrogenerated Bases VII. Novel Syntheses of Ethyl Glyoxylate and Diethyl Ketomalonate Via Electrogenerated Superoxide. *Tetrahedron Lett.* **1983**, *24*, 2223–2226. https://doi.org/10.1016/S0040-4039(00)81889-4.

(5) Monte, W. T.; Baizer, M. M.; Little, D. R. Electrogenerated Superoxide-Initiated Autoxidation. A Convenient Electrochemical Method for the Conversion of Secondary Nitroalkanes to Ketones and the Use of Primary Nitroalkanes as Acyl Anion Equivalents in Michael Reactions. *J. Org. Chem.* **1983**, *48*, 803–806. https://doi.org/10.1021/jo00154a009.

(6) Dietz, R.; Forno, A. E. J.; Larcombe, B. E.; Peover, M. E. Nucleophilic Reactions of Electrogenerated Superoxide Ion. *J. Chem. Soc. (B)* **1970**, 816–820. https://doi.org/10.1039/J29700000816.

(7) Merritt, M. v.; Sawyer, D. T. Electrochemical Studies of the Reactivity of Superoxide Ion with Several Alkyl Halides in Dimethyl Sulfoxide. *J. Org. Chem.* **1970**, *35*, 2157–2159. https://doi.org/10.1021/jo00832a011.

(8) Roberts, J. L.; Calderwood, T. S.; Sawyer, D. T. Nucleophilic Oxidation of Carbon Dioxide by Superoxide Ion in Aprotic Media to Form the $C_2O_6^{2-}$ Species. *J. Am. Chem. Soc.* **1984**, *106*, 4667–4670. https://doi.org/10.1021/ja00329a003.

(9) Casadei, M. A.; Moracci, F. M.; Zappia, G.; Inesi, A.; Rossi, L. Electrogenerated Superoxide-Activated Carbon Dioxide. A New Mild and Safe Approach to Organic Carbamates. *J. Org. Chem.* **1997**, *62*, 6754–6759. https://doi.org/10.1021/jo970308h.

(10) Sagae, H.; Fujihira, M.; Osa, T.; Lund, H. Oxidation of Nitroalkylbenzene with Electro-Generated Superoxide Ion. *Chem. Lett.* **1977**, 793–796. https://doi.org/10.1246/cl.1977.793.

(11) Tian, S.; Jia, X.; Wang, L.; Li, B.; Liu, S.; Ma, L.; Gao, W.; Wei, Y.; Chen, J. The Mn-Catalyzed Paired Electrochemical Facile Oxychlorination of Styrenes: Via the Oxygen Reduction Reaction. *Chem. Commun.* **2019**, *55*, 12104–12107. https://doi.org/10.1039/c9cc06746a.

(12) Tian, S.; Lv, S.; Jia, X.; Ma, L.; Li, B.; Zhang, G.; Gao, W.; Wei, Y.; Chen, J.; Gmbh, C. W. V.; Kgaa, C.; Tian, S.; Lv, S.; Jia, X.; Ma, L.; Li, B.; Zhang, G.; Gao, W.; Wei, Y. CV-Driven Optimization: Cobalt-Catalyzed Electrochemical Expedient Oxychlorination of Alkenes via ORR. *Adv. Synth. Catal.* **2019**, *361*, 5626–5633. https://doi.org/10.1002/adsc.201901260.

(13) Tang, M. C. Y.; Wong, K. Y.; Chan, T. H. Electrosynthesis of Hydrogen Peroxide in Room Temperature Ionic Liquids and in Situ Epoxidation of Alkenes. *Chem. Commun.* **2005**, *10*, 1345–1347. https://doi.org/10.1039/b416837b.

(14) Ho, K. P.; Chan, T. H.; Wong, K. Y. An Environmentally Benign Catalytic System for Alkene Epoxidation with Hydrogen Peroxide Electrogenerated in Situ. *Green Chem.* **2006**, *8*, 900–905. https://doi.org/10.1039/b605009c.

(15) Nishihara, H.; Pressprich, K.; Murray, R. W.; Coliman, J. P. Electrochemical Olefin Epoxidation with Manganese Meso-Tetraphenylporphyrin Catalyst and Hydrogen Peroxide Generation at Polymer-Coated Electrodes. *Inorg. Chem.* **1990**, *29*, 1000–1006. https://doi.org/10.1021/ic00330a020.

(16) Hone, C. A.; Roberge, D. M.; Kappe, C. O. The Use of Molecular Oxygen in Pharmaceutical Manufacturing: Is Flow the Way to Go? *ChemSusChem* **2017**, *10*, 32–41. https://doi.org/10.1002/cssc.201601321.

(17) Noël, T.; Hessel, V. Membrane Microreactors: Gas-Liquid Reactions Made Easy. *ChemSusChem* **2013**, *6*, 405–407. https://doi.org/10.1002/cssc.201200913.

(18) Brzozowski, M.; O'Brien, M.; Ley, S. v.; Polyzos, A. Flow Chemistry: Intelligent Processing of Gas-Liquid Transformations Using a Tube-in-Tube Reactor. *Acc. Chem. Res.* **2015**, *48*, 349–362. https://doi.org/10.1021/ar500359m.

(19) Cavani, F.; Teles, J. H. Sustainability in Catalytic Oxidation: An Alternative Approach or a Structural Evolution? *ChemSusChem* **2009**, *2*, 508–534. https://doi.org/10.1002/cssc.200900020.

(20) Leahy, D. K.; Tucker, J. L.; Mergelsberg, I.; Dunn, P. J.; Kopach, M. E.; Purohit, V. C. Seven Important Elements for an Effective Green Chemistry Program: An IQ Consortium Perspective. *Org. Process Res. Dev.* **2013**, *17*, 1099–1109. https://doi.org/10.1021/op400192h.

(21) Ye, X.; Johnson, M. D.; Diao, T.; Yates, M. H.; Stahl, S. S. Development of Safe and Scalable Continuous-Flow Methods for Palladium-Catalyzed Aerobic Oxidation Reactions. *Green Chem.* **2010**, *12*, 1180–1186. https://doi.org/10.1039/c0gc00106f.

(22) Bourne, S. L.; Ley, S. v. A Continuous Flow Solution to Achieving Efficient Aerobic Anti-Markovnikov Wacker Oxidation. *Adv. Synth. Catal.* **2013**, *355*, 1905–1910. https://doi.org/10.1002/adsc.201300278.

(23) Greene, J. F.; Preger, Y.; Stahl, S. S.; Root, T. W. PTFE-Membrane Flow Reactor for Aerobic Oxidation Reactions and Its Application to Alcohol Oxidation. *Org. Process Res. Dev.* **2015**, *19*, 858–864. https://doi.org/10.1021/acs.oprd.5b00125.

(24) Vapourtec Ltd. *Ion electrochemical reactor*. https://www.vapourtec.com/products/flow-reactors/ion-electrochemical-reactor-features/, (accessed September 2022).

(25) Fu, N.; Sauer, G. S.; Lin, S. Electrocatalytic Radical Dichlorination of Alkenes with Nucleophilic Chlorine Sources. *J. Am. Chem. Soc.* **2017**, *139*, 15548–15553. https://doi.org/10.1021/jacs.7b09388.

(26) Allen, B. D. W.; Hareram, M. D.; Seastram, A. C.; McBride, T.; Wirth, T.; Browne, D. L.; Morrill, L. C. Manganese-Catalyzed Electrochemical Deconstructive Chlorination of Cycloalkanols via Alkoxy Radicals. *Org. Lett.* **2019**, *21*, 9241–9246. https://doi.org/10.1021/acs.orglett.9b03652.

Chapter 4: Flow Electrochemical Bromination of Alkenes

Parts of this work have been published:

J. Seitz, T. Wirth, *Organic & Biomolecular Chemistry* **2021**, *19*, 6892-6896: "Electrochemical bromofunctionalization of alkenes in a flow reactor"

4.1 Introduction

4.1.1 Electrochemical Bromination of Organic Compounds

The bromination of organic compounds has been studied extensively. Nevertheless, there is still a demand for safer and greener methodologies, which can increase atom economy, avoid waste and minimise the risks that come with the use of corrosive and hazardous elemental bromine. One way to solve these challenges is the electrochemical generation of bromine from bromide salts *in situ*.[1–3]

Torii *et al.* reported an electrochemical procedure to convert enol acetates, enol ethers or silyl enol ethers **112** to halo-ketones **113** and acetals **114** (Scheme 4.1). The electrolysis was performed with platinum electrodes in acetonitrile-water mixtures containing NH_4Cl, NH_4Br or NH_4I.[4]

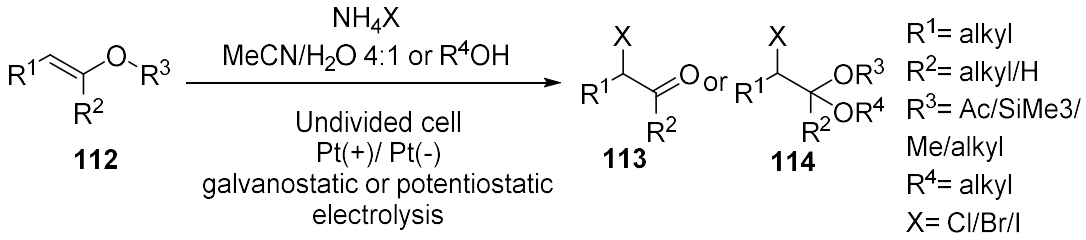

Scheme 4.1: Electrochemical halogenation of enol acetates, enol ethers and silyl enol ethers to halo-ketones and acetals.

In 1981, Torii and co-workers demonstrated the electrochemical conversion of olefins to bromohydrins **109**, epoxides **43** and dibromides **108** in acetonitrile-water mixtures with NaBr as bromine source and electrolyte (Scheme 4.2). The reaction was performed with platinum electrodes under constant current electrolysis. However, only a limited substrate scope with three alkenes was investigated.[5] Similar reaction conditions were used with isosafrole and 3-methyl-2-phenyl-8-(1-propenyl)-4H-1-benzopyran-4-one.[6,7] The electrochemical bromohydroxylation of indene in acetonitrile-water mixtures was decried by Torii et al.[8]

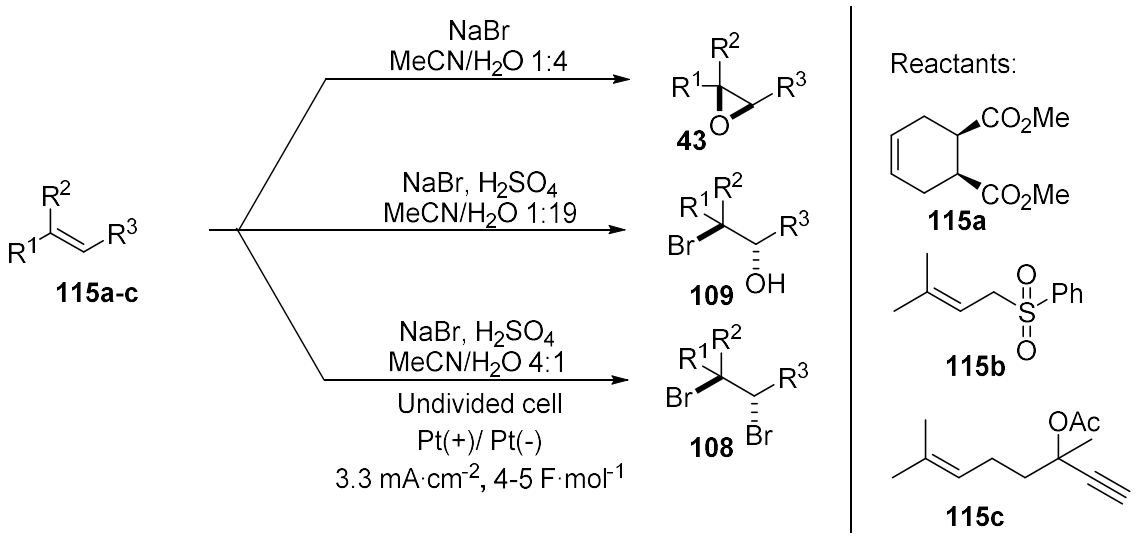

Scheme 4.2: Electrochemical conversion of olefins to epoxides, bromohydrins and dibromides.

Yoshida and co-workers stabilised electrogenerated Br^+ and I^+ ions with DMSO with a cation-pool method for the subsequent difunctionalisation of alkenes to halo-ketones **113a**, halohydrins **113b** or epoxides **43** (Scheme 4.3).[9,10]

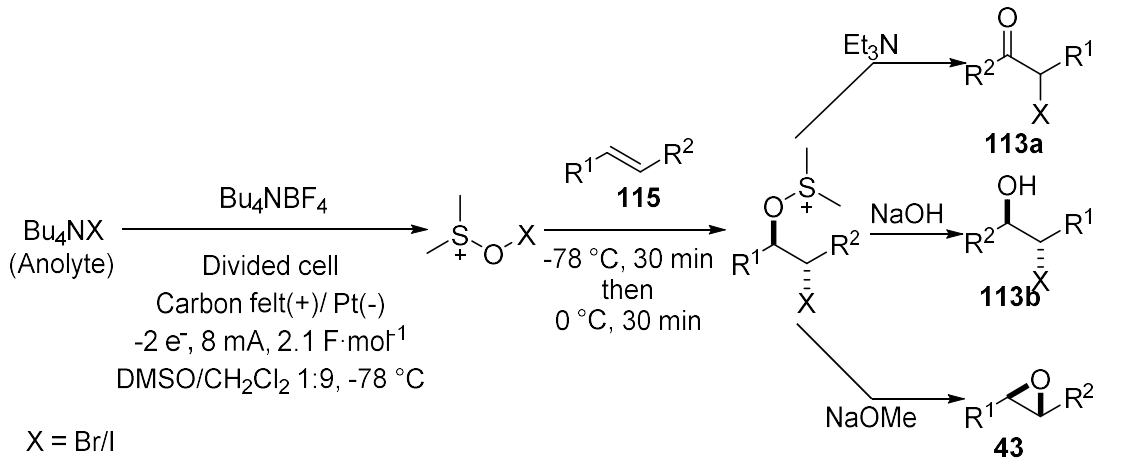

Scheme 4.3: Stabilisation of electrogenerated Br^+ and I^+ with DMSO and subsequent reactions with alkenes to form halo-ketones, halohydrins and epoxides.

In 2021, Bityukov *et al.* electrolysed mixture of alkenes and KBr in DMSO with water or alcohol as nucleophile and acetic acid as additive (Scheme 4.4). They could obtain the corresponding bromohydrins **109** and bromohydrin ethers **116** with good to excellent yields after constant current electrolysis with glassy carbon anode and platinum cathode.[11]

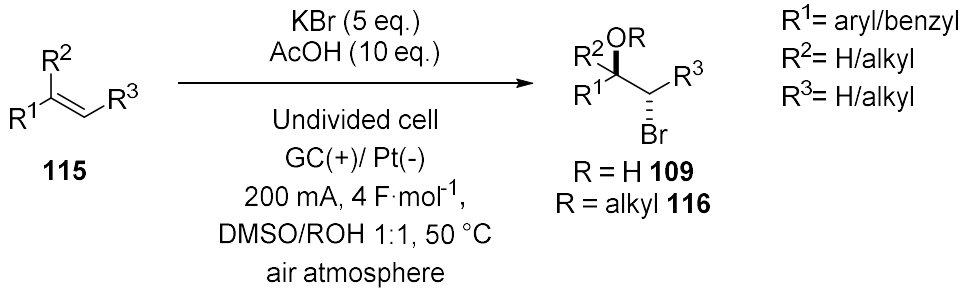

Scheme 4.4: Electrochemical conversion of alkenes to bromohydrins and bromohydrin ethers in DMSO solvent mixtures.

Nikishin and co-workers could afford bromohydrin ethers **116** by electrolysis of NH_4Br and alkenes in the corresponding alcohols, which served as nucleophiles (Scheme 4.5).[12]

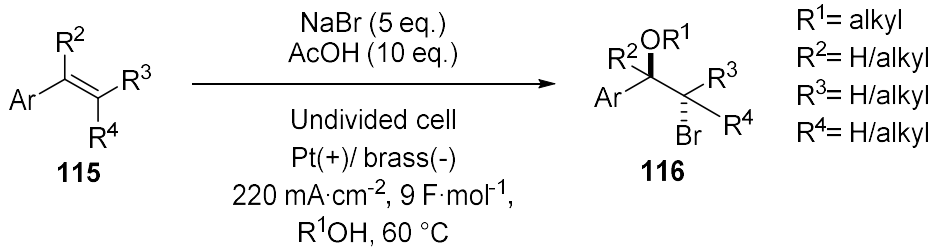

Scheme 4.5: Electrochemical conversion of styrene derivatives to bromohydrin ethers.

The electrochemical dibromination of alkenes under biphasic conditions (Scheme 4.6) was performed by Kulangiappar *et al.* The platinum electrodes were dipped into the aqueous phase containing NaBr and sulfuric acid while the dibromination took place in the organic phase consisting of chloroform.[13]

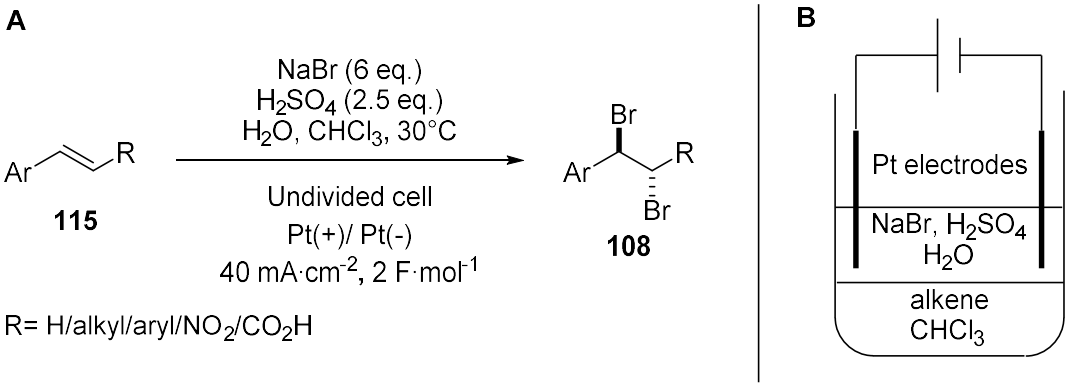

Scheme 4.6: A) Biphasic electrochemical dibromination of alkenes. B) Schematic representation of biphasic reaction setup.

Lei and co-workers employed the anodic oxidation of chloride and bromide salts for a variety of transformations (Scheme 4.7). They could demonstrate the chlorination and bromination of aromatic heterocycles **117** and the dibromination of alkenes **113** and alkynes **119**.[14]

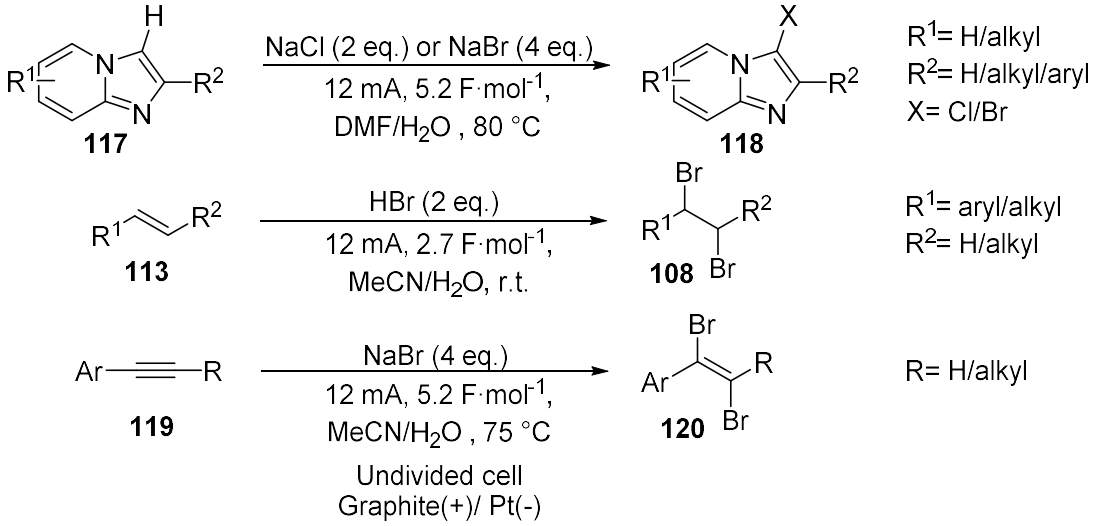

Scheme 4.7: Electrochemical halogenation of heterocycles and electrochemical bromination of alkenes and alkynes.

Recently, current efficiencies of up to 190% were achieved by Hilt and co-workers for the dibromination of alkenes with a paired electrolysis strategy (Scheme 4.8). Bromide ions were oxidised to bromine at the anode and molecular oxygen was reduced to hydrogen peroxide at the cathode, which in turn could oxidise bromide to bromine leading to potential current efficiencies of up to 200%.[15]

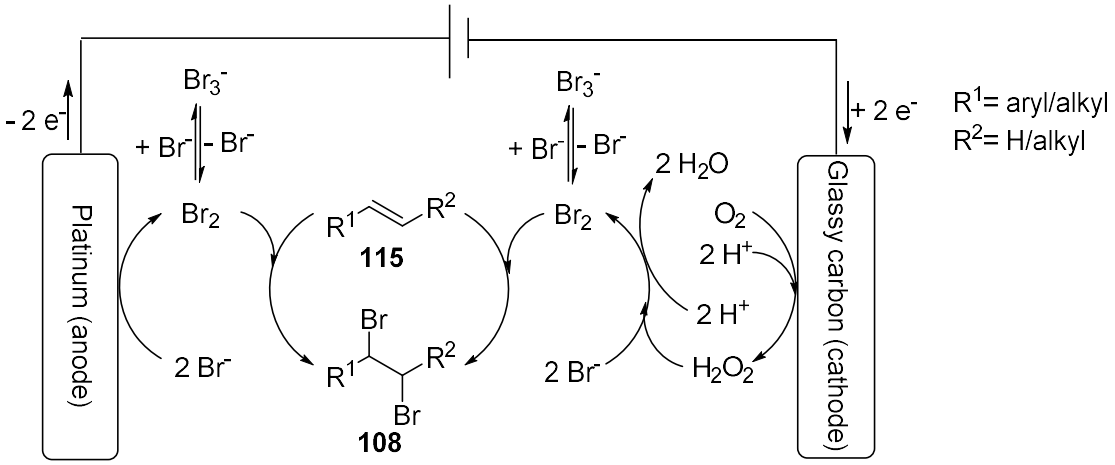

Scheme 4.8: Electrochemical bromination of alkenes with a paired electrolysis strategy under oxygen atmosphere. Reaction conditions: Bu_4NBr (4 eq.), H_2SO_4 (0.2 M), MeCN, 10 mA, 1 F·mol^{-1}, 0 °C.

4.1.2 Bromination in Electrochemical Microreactors

The electrochemical bromination of late-stage intermediates and drug molecules (Scheme 4.9) such as cytidine **121** and uridine **122** or Tenofovir **123**, MK-4618 **124** or Sch 48973 **125** under recirculating flow conditions, was demonstrated by Tan *et al.* The electrolysis was performed in a divided cell microreactor with platinum anode and copper cathode on a small scale.[16]

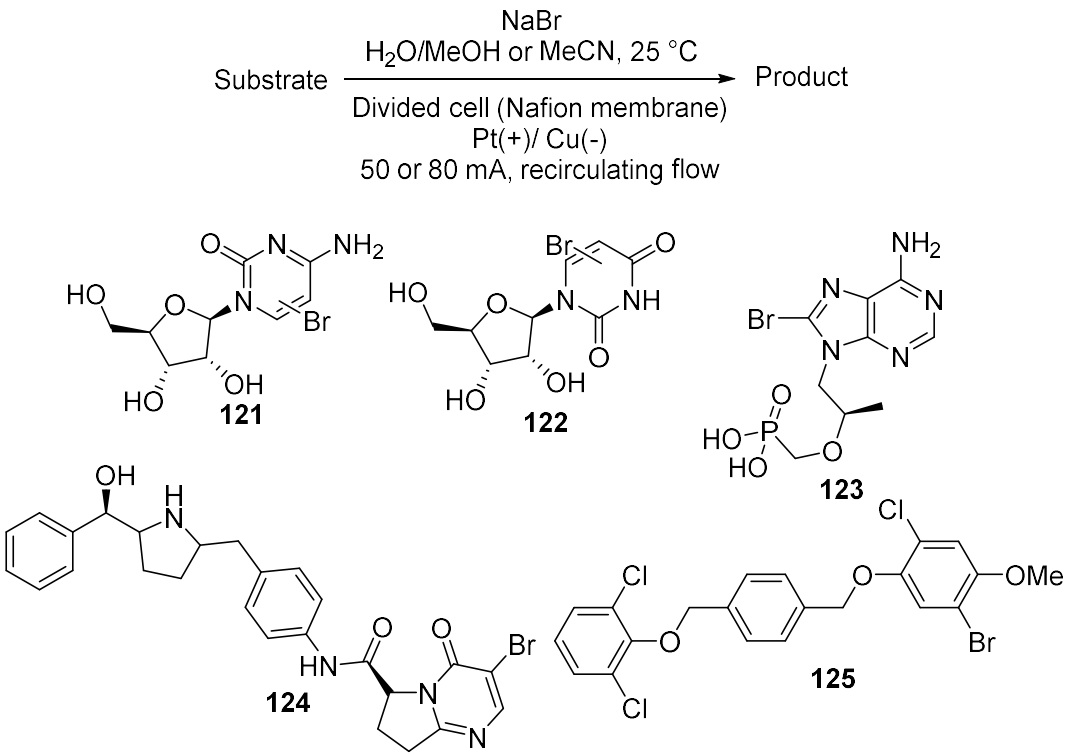

Scheme 4.9: Electrochemical bromination of late-stage intermediates and drug molecules under recirculating flow conditions.

Vasudevan *et al.* utilised flow electrochemical conditions for the decagram synthesis of eosin **126** and erythrosine **127** from fluorescein **128** (Scheme 4.10). The reaction was conducted in a microreactor equipped with stainless steel cathode and a DSA under recirculating conditions.

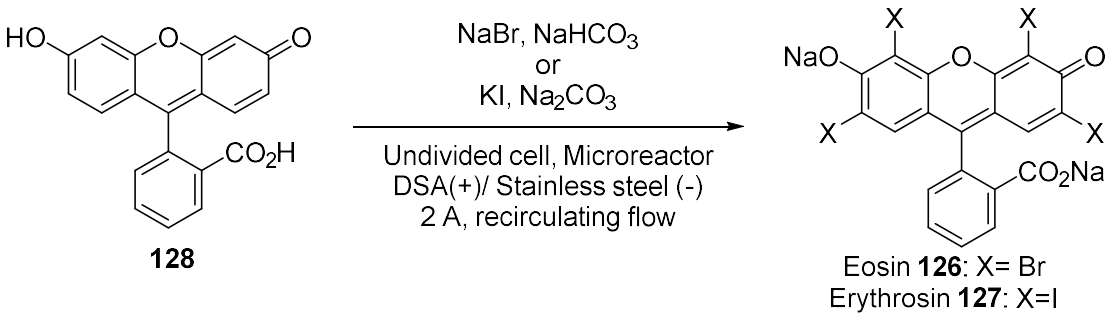

Scheme 4.10: Electrochemical conversion of fluorescein to eosin **126** and erythrosine **127** in a microreactor with batch recirculation.

Recently, Rueping and co-workers developed an electrochemical oxybromination of β,γ-unsaturated ketoximes **129** for batch electrolysis and continuous flow conditions (Scheme 4.11). Electrogenerated bromine is stabilised by DMSO and reacts with the double bond to form a bromonium species, which is then attacked by the oxime moiety in the substrate to form an isoxazoline ring. Flow electrochemical experiments were

conducted under single pass conditions. The microreactor was equipped with graphite anode and stainless steel cathode.[17]

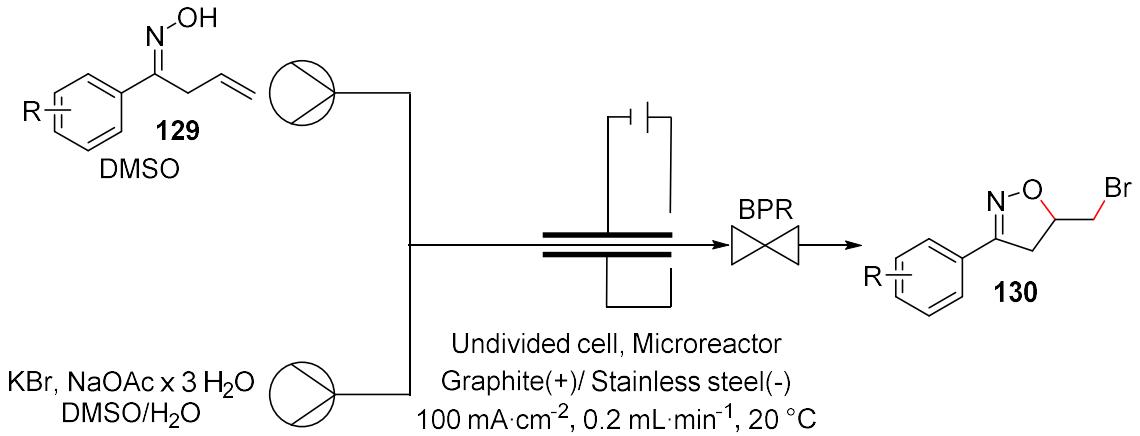

Scheme 4.11: Electrochemical synthesis of isoxazolines **130** *via* oxybromination of β,γ-unsaturated ketoximes **129** in continuous flow.

4.1.3 Preparation of Bromohydrins

Early strategies for the preparation of bromohydrins from alkenes were carried out in water using elemental bromine (Scheme 4.12A). Read and Reid reported the use of this reaction mixture to convert olefins like styrene, anethole, safrole, and eugenol to the corresponding bromohydrins in 1928.[18] Zabicky and Nutkovitch investigated the reaction of cyclohexene and bromine in aqueous reaction mixtures with focus on the selectivity for either the dibromination or bromohydroxylation of the alkene.[19] Another popular strategy is the use of *N*-bromosuccinimide (NBS) in water as demonstrated by Guss and Rosenthal in 1955 (Scheme 4.12B).[20] Dalton *et al.* employed NBS in wet DMSO to obtain bromohydrins from the corresponding alkenes (Scheme 4.12 C).[21,22] Gupta and co-workers reacted alkenes with *N*-bromo- and *N*-iodo-succinimide in mixtures of water with the ionic liquid [bmim]BF_4 to obtain halohydrins (Scheme 4.12D). Ishii and co-workers generated hypohalous acids from the reduction of $HBrO_3$ and H_5IO_6 with sodium sulfite (Scheme 4.12E), which could then react with akenes to form the corresponding bromohydrin and iodohydrin derivatives.[23] Another brominating reagent that had been used to prepare bromohydrins and bromohydrin ethers was bromodichloroisocyanuric acid **131** in water or the corresponding alcohol (Scheme 4.12F).[24] A particularly interesting strategy for the preparation of bromohydrins was developed by Jiao and co-workers in 2015 (Scheme 4.12G). They heated mixtures of aqueous HBr in DMSO with alkenes as substrate at 60 °C under an argon atmosphere for 18 hours to obtain the corresponding bromohydrins in good to excellent yield. Besides DMSO, no additional oxidant was neccessary.[25]

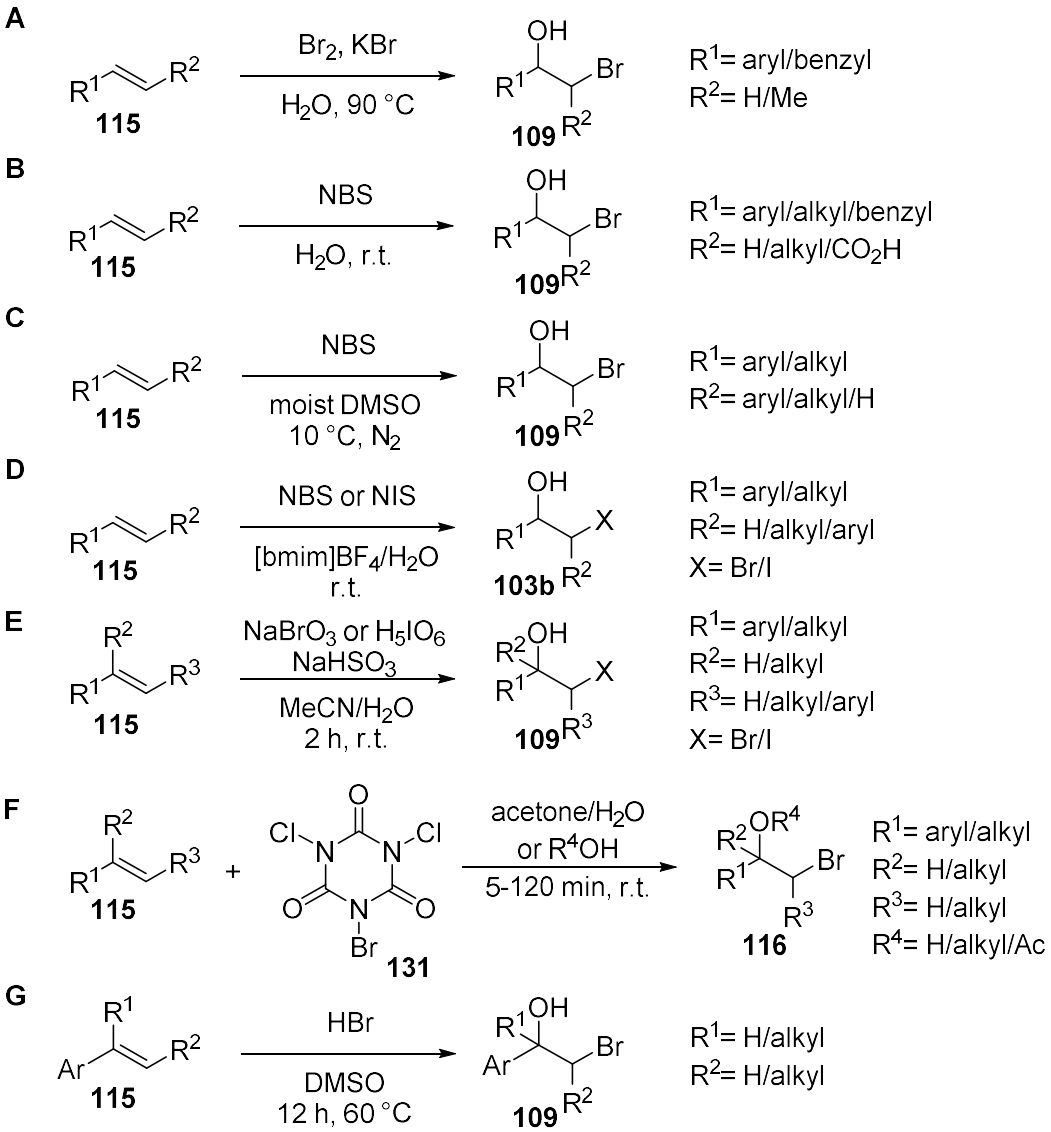

Scheme 4.12: Chemical methods for the transformation of alkenes to bromohydrins.

4.2 Aims and Objectives

The aim of the project was to develop electrochemical bromination strategies for single pass flow conditions. The flow setup should enable a safer use of bromine than in conventional batch processes. The electrochemical generation of bromine *in situ* would not only further minimise the chance of coming into contact with the hazardous intermediate, but also avoid the use of chemical oxidants. Thereby the atom economy could be increased and the production of waste would be reduced. The next step was to demonstrate the versatility of the process. Small changes in the composition of the solvent mixture would enable a high control over the reaction outcome. Depending on the concentration of water in acetonitrile, the reaction of the electrogenerated bromine with alkenes would either yield the corresponding dibromide **108** or bromohydrin **109**.

The use of alcohols instead of water as nucleophile would furnish bromohydrin ethers **116** while substrates with internal nucleophiles would lead to cyclisation reactions.

4.3 Results and Discussion

4.3.1 Synthesis of Dibromides

Batch Electrochemical Experiments

Initially, the conditions for the dibromination of olefins as reported by Lei and co-workers[14] were adapted to be used in a 5 mL Electrasyn 2.0 vial (Scheme 4.13). The cell was equipped with a platinum foil cathode (surface area: 1.5 cm^2) and a graphite anode (surface area: 2.4 cm^2). A current of 17 mA was applied corresponding to a current density of 7.08 mA/cm^2 at the anode, which was chosen based on the exposed surface area of the graphite rod reported in the original procedure. The adapted reaction mixture consisted of styrene (46 mM), hydrobromic acid (90 mM) and *tetra*-butyl ammonium tetrafluoroborate (9.2 mM) in a mixture of 2% water in acetonitrile. The product 1,2-dibromo-1-phenylethane **108a** was obtained in 45% yield on average (Literature: 73% yield). [14]

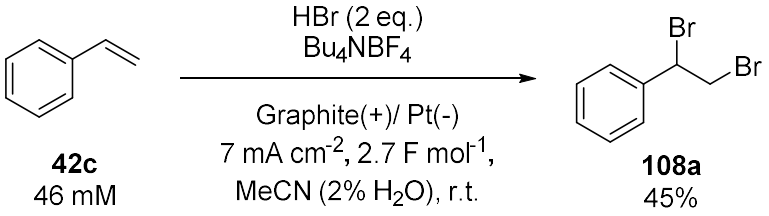

Scheme 4.13: Electrochemical bromination of styrene in batch.

Flow Electrochemical Experiments - Optimisation

Flow electrochemical experiments were carried out in an Ion Electrochemical Reactor from Vapourtec Ltd.[26] The platinum foil cathode and graphite anode were separated by a 500 µm fluorinated ethylene propylene (FEP) spacer with a channel that resulted in a reactor volume of 600 µL and an exposed electrode surface area of 12 cm^2. The initial concentration of hydrobromic acid in acetonitrile was 200 mM. In contrast to the batch experiment, additional water and supporting electrolyte was avoided due to the significantly smaller interelectrode gap. At a flow rate of 0.1 $mL \cdot min^{-1}$, an applied current of 48 mA and a styrene concentration of 100 mM, which corresponds to a charge of 3.0 $F \cdot mol^{-1}$, the dibromide **108a** was observed as main product in 54% yield and the bromohydrin **109a** in 17% yield (Table 4.1, entry 1). Excess bromine was quenched with aqueous $Na_2S_2O_3$ or aqueous Na_2SO_3 upon collection.

Parameters such as electrode materials, concentration of hydrobromic acid and styrene, applied charge and the flow rate were investigated in the optimisation process. At higher hydrobromic acid concentrations of 400 mM and 600 mM, **108a** was obtained with a yield of 74% and 80%, respectively, while the formation of the side product **109a** was reduced (Table 4.1, entries 2 & 3). When employing glassy carbon and platinum foil as anode materials, **108a** was obtained in 73% and 79% yield, respectively (Table 4.1, entries 4 & 5). A higher charge of 3.5 F·mol^{-1} led to a yield of 92% (Table 4.1, entry 6). Further increasing the charge to 4 F·mol^{-1} and 4.5 F·mol^{-1} gave declining yields of 86% and 80% (Table 4.1, entries 7 & 8). Higher flow rates of 0.2 mL·min^{-1} and 0.4 mL·min^{-1} still afforded the product in 78% yield and 79% yield (Table 4.1, entries 9 & 10). For the optimal conditions a platinum coated on titanium was used as cathode material to improve the cathodic reaction. At the optimal concentration of 600 mM of hydrobromic acid, 4 F·mol^{-1} and 0.4 mL·min^{-1}, the product **108a** was isolated with a yield of 86% (Table 4.1, entry 11).

Table 4.1: Optimisation of the reaction conditions for the flow electrochemical dibromination of styrene.

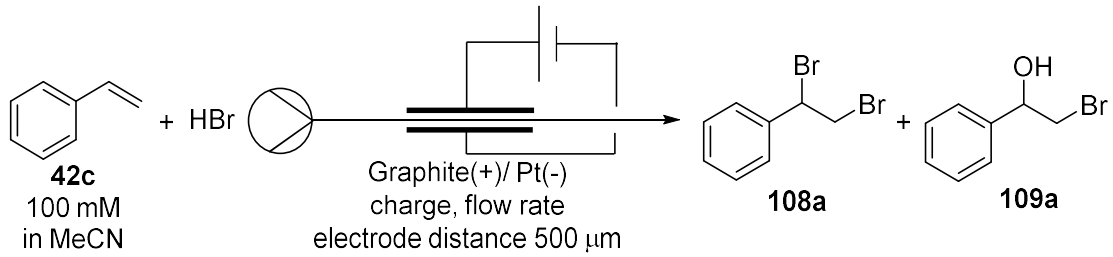

Entry	HBr [mM]	Charge [F·mol^{-1}]	Current [mA]	Flow rate [mL·min^{-1}]	**108a** [%][a]	**109a** [%][a]
1	200	3	48	0.1	54	17
2	400	3	48	0.1	74	6
3	600	3	48	0.1	80	3
4[b]	600	3	48	0.1	73	17
5[c]	600	3	48	0.1	79	13
6	600	3.5	56	0.1	92	4
7	600	4	64	0.1	86	3
8	600	4.5	72	0.1	80	4
9	600	4	129	0.2	78	8

10	600	4	257	0.4	79	9
11[d]	600	4	257	0.4	86[e]	

Reaction conditions: styrene (100 mM), hydrobromic acid; Acetonitrile (MeCN); constant current; undivided cell; Graphite anode (surface area: 12 cm^2); Pt foil cathode. a) Yields are determined by ^1H NMR with 1,3,5-trimethoxybenzene as internal standard; b) Glassy carbon anode; c) Pt foil anode; d) Pt coated Ti cathode; e) Isolated yield.

Flow Electrochemical Experiments – Substrate Scope

Besides styrene, the optimised conditions for the dibromination of alkenes were applied to allylbenzene to give the corresponding dibromide **108b** in 64% yield (Scheme 4.14). The unactivated alkene, 2-(pent-4-en-1-yl)isoindoline-1,3-dione, was converted to the corresponding dibromide **108c** in 84% yield. 1,4-cyclohexadiene was converted to the tetrabrominated compound **108d** with a yield of 34% under the optimised conditions.

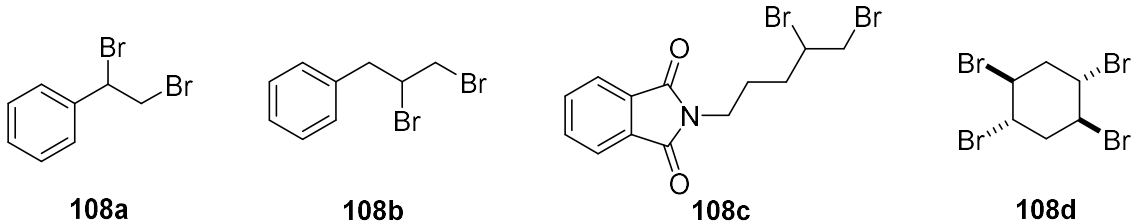

108a 86% **108b** 64% **108c** 84% **108d** 34%

Scheme 4.14: Substrate scope for the electrochemical dibromination of alkenes in flow. Reaction conditions: alkene (0.1 M, 0.7 mmol), hydrobromic acid (48% w/w in water, 0.6 M); MeCN; 0.4 $mL \cdot min^{-1}$, 4 $F \cdot mol^{-1}$ (257 mA); constant current; undivided cell; graphite anode (surface area: 12 cm^2); Pt coated Ti cathode.

Multi-gram-scale Experiment in Flow

The dibromination of styrene **41c** was selected for a large-scale experiment. In a first attempt, the reaction mixture consisting of hydrobromic acid (0.6 M) and styrene (0.1 M) in acetonitrile was fed into the reactor from one reservoir (Scheme 4.15). The output from the microreactor was quenched immediately in a reservoir filled with aqueous $Na_2S_2O_3$ after leaving the reactor. Under these conditions, the product **108a** was isolated in only 47% yield after 9 hours (545.5 min) of experiment time together with 19% of bromohydrin **109a** and 22% of 1-phenylethanol **38b**. To identify the cause for the second side product, a mixture of hydrobromic acid (600 mM) and styrene (100 mM) in acetonitrile was stirred at room temperature for 9 hours. The side product 1-phenylethanol **38b** was detected in 22% yield by ^1H NMR. This observation suggests that the prolonged experiment time led to an acid catalysed side reaction in the feeding reservoir.

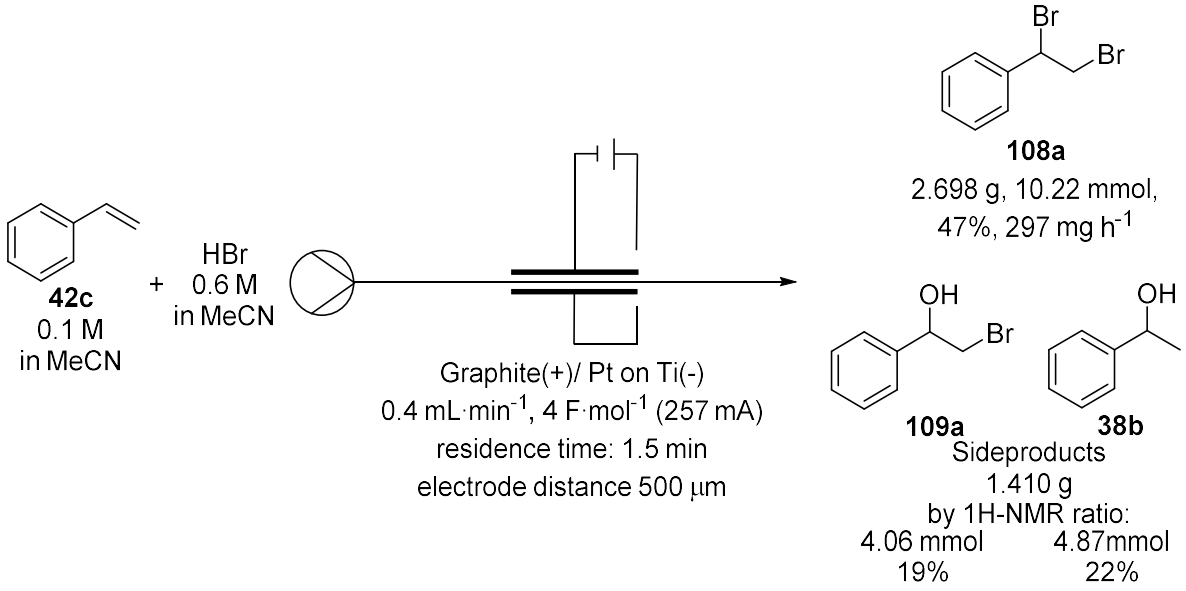

Scheme 4.15: Large-scale electrochemical dibromination of styrene **42c** in flow with one pump.

To avoid a side reaction in the reservoir, a solution of hydrobromic acid in acetonitrile and a solution of styrene in acetonitrile were pumped from two separate reservoirs. The two solutions were joined with a T-piece mixer before entering the reactor. With this setup, the acid catalysed formation of 1-phenylethanol from styrene could be supressed successfully. Over the course of 9.5 hours (571 min), 3.93 g of **108a** were isolated corresponding to a yield of 65% (Scheme 4.16). The experiment was monitored by collecting aliquots of 0.4 mL at the beginning (**108a**, 87%), after 3.5 h (**108a**, 83%), after 7 h (**108a**, 74%) and towards the end of the experiment after 9.5 h (**108a**, 76%) (Table 4.2). The yields were determined by ^{1}H-NMR spectroscopy with an internal standard. Over the course of the experiment, a gradual decline in yield was observed (Table 4.2). This could indicate a passivation on the electrode surface, which interferes slightly with the reaction after prolonged reaction times. Indeed, the formation of a black brown film was observed on the graphite anode, which could be wiped off with ease. Nevertheless, compound **108a** was produced on a multi-gram scale under the optimised conditions. To avoid passivation, an alternating current could be employed. However, this would require the use of the same electrode material for anode and cathode. A follow up experiment could make use of graphite anode and cathode as this would allow the use of alternating current. Furthermore, this could bring down the cost of the electrode material, which would be favourable from a process chemistry point of view. Further optimisation of the reaction setup could be realised with inline quenching. For this purpose, an aqueous solution of Na_2SO_3 would be joined

with the stream to deactivate excess bromine. Quenching with aqueous Na_2SO_3 would be chosen instead of aqueous $Na_2S_2O_3$ as this would avoid the formation of elemental sulfur particles, which could block the channel.[27]

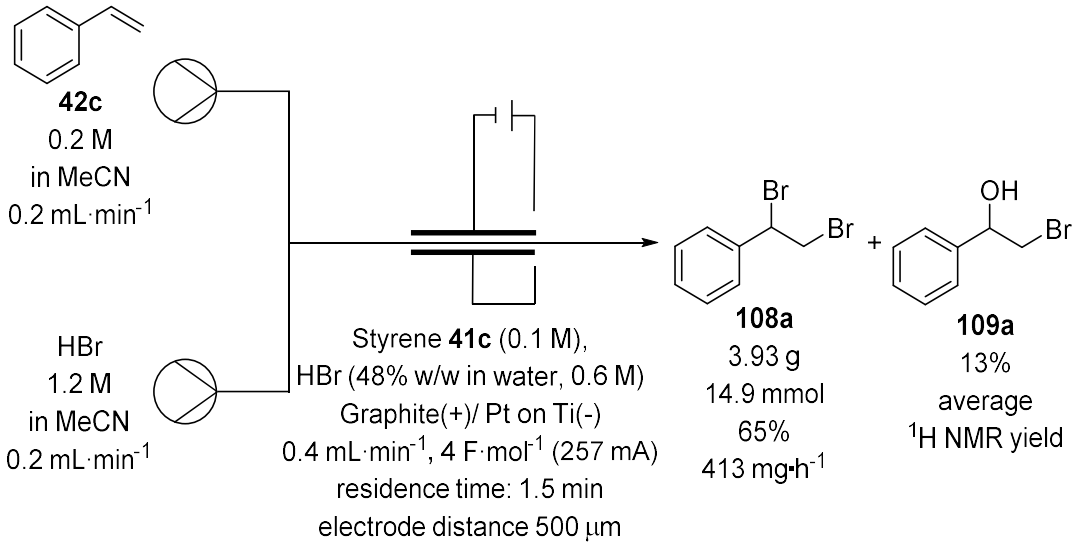

Scheme 4.16: Large-scale dibromination of styrene **42c** in flow with separated reservoirs for hydrobromic acid and styrene **42c**.

Table 4.2: Monitoring of the flow electrochemical dibromination of styrene **42c** on multi-gram-scale.

Entry	Collection time	**108a** [%]	**109a** [%]
1	0h 0min – 0h 1min	87	15
2	3h 36 min – 3h 37 min	83	12
3	6h 48min – 6h 49min	74	12
4	9h 26min – 9h 27min	76	13

Large-scale electrochemical dibromination of styrene **42c** in flow with separated reservoirs for bromine source and stubstrate. Reaction conditions: styrene **42c** (0.1 M), hydrobromic acid (48% w/w in water, 0.6 M); MeCN; 0.4 mL·min^{-1}, 4 F·mol^{-1}; constant current; undivided cell; Graphite anode (surface area: 12 cm^2); Pt coated Ti cathod; Reactor volume: 600 µL; 500 µm spacer; Yields were determined by NMR with 1,3,5-trimethoxybenzene as internal standard.

4.3.2 Synthesis of Bromohydrins

Flow Electrochemical Experiments – Optimisation

Based on the initial conditions for the dibromination of styrene in a flow electrochemical reactor (Table 4.1, entry 1), the investigation of the bromohydroxylation was started by altering the concentration of additional water content. At a water concentration of 5%, bromohydrin **109a** was observed in 40% yield and the dibromide **108a** in 29% yield

(Table 4.3, entry 1). An increase in water concentration in steps of 5% led to an increase in product yield and a decrease of the side product **108a** (Table 4.3, entries 2 and 3). Between 20% and 30% the yield of **108a** stagnated at 79-80% (Table 4.3, entries 4 to 6). However, the yield started to decline at higher water concentrations (Table 4.3, entries 7 & 8).

Table 4.3: Optimisation of the water concentration in the electrochemical bromohydroxylation of styrene in flow.

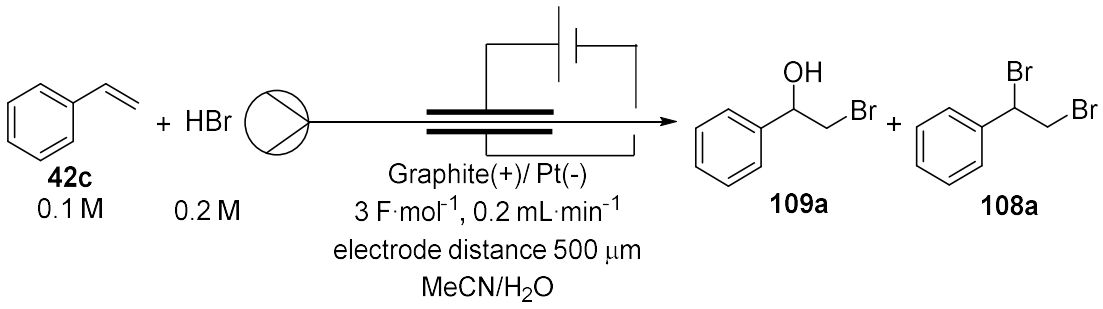

Entry	Additional H_2O	**109a** [%]	**108a** [%]
1	5%	40	29
2	10%	53	30
3	15%	63	18
4	20%	79	14
5	25%	81	9
6	30%	81	7
7	35%	66	2
8	40%	68	3

Reaction conditions: styrene **42c** (100 mM), hydrobromic acid (48% w/w in water, 200 mM); 0.2 $mL \cdot min^{-1}$; 3 $F \cdot mol^{-1}$; constant current; undivided cell; Pt foil cathode, Graphite anode (surface area: 12 cm^2); Yields are determined by NMR with 1,3,5-trimethoxybenzene as internal standard.

Subsequently, the effect of the concentration of hydrobromic acid was investigated at an additional water concentration of 20%. At a concentration of 100 mM of hydrobromic acid **109a** was obtained in 31% yield while only trace amounts of side product **108a** were detected (Table 4.4, entry 1). Higher concentrations of 150 mM, 160 mM and 170 mM gave **109a** in 55%, 63% and 66% yield, respectively (Table 4.4, entries 2 to 4). The highest yields for **109a** were observed at 180 mM and 190 mM of hydrobromic acid with 85% and 84% (Table 4.4, entries 5 & 6) together with increasing yields for the side product **108a**.

A change in styrene concentration either down to 50 mM or up to 150 mM resulted in a lower yield of **109a** with 52% and 72%, respectively (Table 4.4, entries 7 & 8).

The choice of bromide source had a great impact on the reaction. While a yield of 6% of product **109a** was detected with LiBr (Table 4.4, entry 10), no conversion to **109a** could be detected with NaBr (Table 4.4, entry 11). Selecting ammonium bromide still furnished **109a** in a moderate yield of 49% (Table 4.4, entry 10).

Table 4.4: Optimisation of bromide concentration in the electrochemical bromohydroxylation of styrene **41c** in flow.

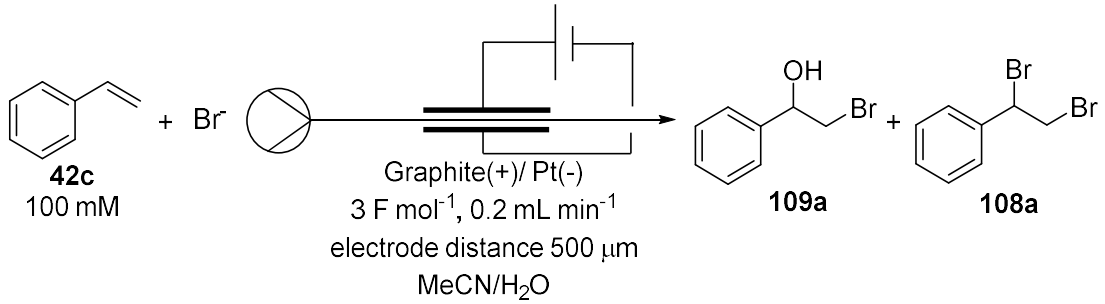

Entry	Br^- source	Br^- [mM]	Additional H_2O	**109a** [%]	**108a** [%]
1	HBr	100	20%	31	1
2	HBr	150	20%	55	4
3	HBr	160	20%	63	7
4	HBr	170	20%	66	8
5	HBr	180	20%	85	9
6	HBr	190	20%	84	13
7[a]	HBr	180	20%	52	13
8[b]	HBr	180	20%	72	5
9	HBr	180	30%	85	8
10	LiBr	180	30%	6	6
11	NaBr	180	30%	0	0
12	NH_4Br	180	30%	49	9

Reaction conditions: styrene **42c** (100 mM); hydrobromic acid (48% w/w in water); 0.2 mL·min^{-1}; 3 F·mol^{-1} (97 mA); constant current; undivided cell; Pt foil cathode, Graphite anode (surface area: 12 cm^2); Yields are determined by NMR with 1,3,5-trimethoxybenzene as internal standard. a) styrene (50 mM); b) 150 (mM).

Next, various anode and cathode materials were tested. Different cathode materials like platinum coated on titanium (85%), nickel (75%), graphite (82%) (Table 4.5, entries 1 to 3) only have a minor impact on the yield. Different anode materials such as Panasonic carbon (67%), glassy carbon (72%) or platinum foil (2%) gave **109a** in lower yield (Table 4.5, entries 4 to 6). Switching the electrodes to graphite cathode and platinum anode gave product **109a** with 75% yield (Table 4.5, entry 7).

Table 4.5: Optimisation of electrode materials in the electrochemical bromohydroxylation of styrene **42c** in flow.

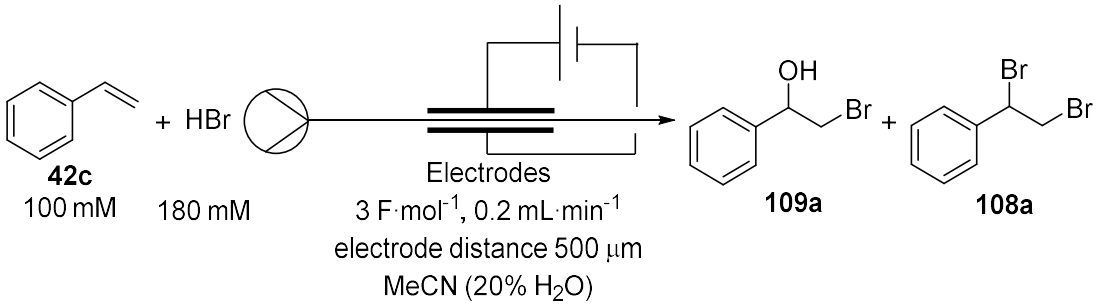

Entry	Cathode	Anode	**109a** [%]	**108a** [%]
1	Pt on Ti	Graphite	85	13
2	Ni	Graphite	75	6
3	Graphite	Graphite	82	12
4	Pt	Panasonic Carbon	67	9
5	Pt	Glassy Carbon	72	6
6	Pt	Pt	2	25
7	Graphite	Pt	75	14

Reaction conditions: styrene **42c** (100 mM), hydrobromic acid (48% w/w in water, 180 mM); additional H_2O in MeCN 20%; 0.2 mL·min^{-1}; 3 F·mol^{-1} (97 mA); constant current; undivided cell; working electrode (surface area: 12 cm^2); Pt on Ti: Platinum coated on titanium; Ni: Nickel foil; Yields are determined by NMR with 1,3,5-trimethoxybenzene as internal standard.

The optimal charge was identified as 4 F·mol^{-1} with a bromohydrin **109a** yield of 86% (Table 4.6, entry 2). A lower (2 F·mol^{-1}) or higher charge (5 F·mol^{-1}) had a negative impact on the yield (Table 4.6, entries 1 & 3). At a flow rate of 0.4 mL·min^{-1} and a charge of 3 F·mol^{-1}, a high yield of 81% was still obtained, but further decline was observed at 4 F·mol^{-1} with 75% yield (Table 4.6, entry 4 & 5). At 0.6 mL·min^{-1} the yield went down to 72% (3 F·mol^{-1}) and 70% (4 F·mol^{-1}) (Table 4.6, entry 6 & 7).

Table 4.6: Optimisation of charge and flow rate in the electrochemical bomohydroxylation in flow.

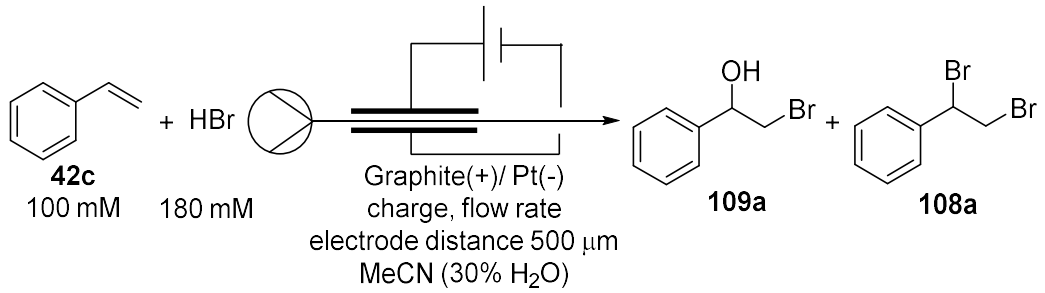

Entry	Charge [F·mol^{-1}]	Current [mA]	Flow rate [mL·min^{-1}]	**109a** [%]	**108a** [%]
1	2	64	0.2	63	9
2	4	129	0.2	86	4
3	5	161	0.2	68	3
4	3	193	0.4	81	7
5	4	257	0.4	75	6
6	3	290	0.6	72	6
7	4	386	0.6	70	6

Reaction conditions: styrene **42c** (100 mM), hydrobromic acid (48% *w/w* in water, 180 mM); additional H_2O in MeCN 30%; constant current; undivided cell; Pt foil cathode, Graphite anode (surface area: 12 cm^2); Yields are determined by NMR with 1,3,5-trimethoxybenzene as internal standard.

Flow Electrochemical Experiments – Substrate Scope

The optimised conditions for the flow electrochemical bromohydroxylation of alkenes were utilised to convert a selection of activated and unactivated alkenes to the corresponding bromohydrins (Scheme 4.17). The highest yields for styrene were obtained with method A (Table 4.6, entry 2: 4 F·mol^{-1}, 0.2 ml·min^{-1}). However, the yield for **109a** did not drop significantly when using method B (Table 4.6, entry 4: 3 F·mol^{-1}, 0.4 ml·min^{-1}), while increasing the flow rate and thereby the productivity (g·h^{-1}). Styrene derivatives were converted to the corresponding bromohydrins **109a-f** in good to excellent yields. In the case of 4-methoxystyrene, a bromination of the aromatic ring in *ortho*-position to the methoxy group afforded the bromohydrin side product **109f'** in 13% yield. Due to solubility issues, 4-vinylbiphenyl (80 mM) was converted in a water/acetonitrile/tetrahydrofuran mixture (3:3:4) to give the product **109g** in 65% yield. The solubility issue of indene in the acetonitrile-water mixture was solved by using tetrahydrofuran instead of acetonitrile. Compounds **109i-k** were obtained in moderate

yield using method B at a higher flow rate of 0.4 mL min^{-1}. Methyl cinnamate was converted to the bromohydrin **109l** in a moderate yield. Two α,β-unsaturated ketones gave the products **109m** and **109n** in moderate yields. Compound **109o** was obtained in 56% yield from cinnamyl alcohol. Allylbenzene reacted to give a 1.78:1.00 ratio of regioisomers (**109p**:**109p'**) using method A and B in 43% and 46% yields, respectively. The unactivated alkenes 1-hexene and 1-decene both gave mixtures of regioisomers. The bromohydrins formed from 1-hexene were obtained in 33% yield and with a ratio of 3.76:1.00 (**109q**:**109q'**). The conversion of 1-decene to bromohydrins proceeded with 59% yield and a 1.00:1.04 ratio of regioisomers (**109r**:**109r'**). Cyclohexene reacted to give compound **109s** in 43% (method A) and 37% (method B) yield. Furthermore, the use of graphite as cheaper cathode material compared to platinum was explored (method C). Pleasingly, product **109a** was obtained in 78% yield by using method C, which is in the same range as the yield from method A (77-81%). However, other substrates like *para*-methyl styrene and β-methyl styrene were converted to the corresponding bromohydrins with significantly lower yields compared to method A. By employing method C, compound **109b** was obtained in 61% yield (method A: 76%) and compound **109j** in 46% yield (method A: 74%).

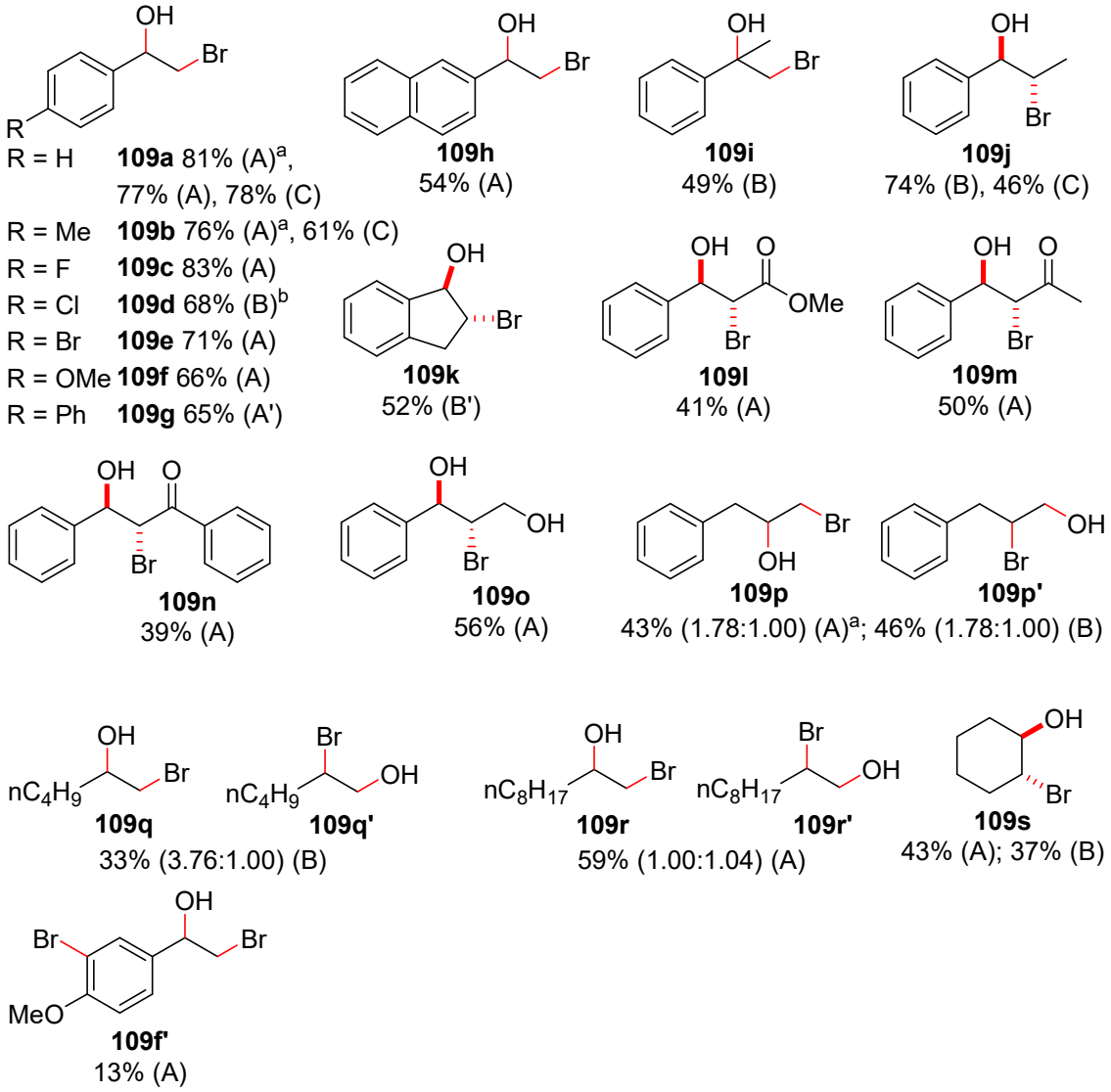

Scheme 4.17: Substrate scope for the electrochemical bromohydroxylation of alkenes in flow. Reaction conditions: alkene (100 mM, 0.7 mmol), hydrobromic acid (48% w/w in water, 180 mM), additional H_2O/MeCN 3 : 7; Method A: 0.2 mL·min^{-1}, 4 F·mol^{-1}, constant current 129 mA, Pt plated Nb cathode, graphite anode (surface area: 12 cm^2), A': alkene (80 mM) in H_2O/MeCN/THF 3 : 3 : 4; Method B: 0.4 mL·min^{-1}, 3 F·mol^{-1}, constant current 193 mA, Pt foil cathode, graphite anode (surface area: 12 cm^2), B': THF instead of MeCN; C: 0.2 mL·min^{-1}, 4 F·mol^{-1}, constant current 129 mA, graphite anode and cathode (surface area: 12 cm^2); a) Pt foil cathode; b) Pt plated Nb cathode.

4.3.3 Synthesis of Bromohydrin Ethers and Bromo-Cyclisation Products

By changing the co-solvent from water to alcohols, the formation of bromohydrin ethers could be furnished. In the presence of methanol and ethanol the corresponding ethers **116a** and **116b** were obtained from styrene in moderate yields at a flow rate of 0.4 mL·min^{-1}, 4 F·mol^{-1} and a hydrobromic acid concentration of 150 mM (Scheme 4.17).

Pleasingly, internal nucleophiles reacted to give cyclised products under conditions, which were derived from the bromohydroxylation method A (180 mM hydrobromic acid,

0.2 mL·min^{-1}, 4 F·mol^{-1}) (Scheme 4.18). Unsaturated carboxylic acids were cyclised to the corresponding lactones **111b** in 74% yield and **111c**/**111c'** in 57% yield. In the case of 2-vinylbenzoic acid, a 9:1 mixture of regioisomers (**111c**/**111c'**) was observed. The major isomer **111c** was the result of a 5-*exo*-*trig* cyclisation and the minor isomer **111c'** can be explained with a 6-*endo*-*trig* cyclisation. The internal nitrogen nucleophile in *N*-(2-allylphenyl)-4-methylbenzenesulfonamide reacted with the allyl group to form two products with newly formed 5-membered rings. Compound **132a** was isolated in 22% yield after a 5-*exo*-*trig* cyclisation. Interestingly, the electron rich aromatic ring of compound **132a** was further brominated in *para*-position to the nitrogen substituent to give **132b** as a side product in 21% yield. The double bond in 2-allyl-6-methylphenol reacted with the *in situ* generated bromine and the phenolic hydroxy group to give a mixture of cyclised products. Furthermore, the electron rich aromatic ring was brominated in *para*-position to the phenol ether moiety. The double bond reacted to give either a 5-membered ring (**133a**, 5-*exo*-*trig*) or a 6-membered ring (**133b**, 6-*endo*-*trig*). The products were isolated in a 2.33:1.00 mixture of regioisomers (**133a**/**133b**) in 22% yield. A conclusion about the selectivity of both the aromatic bromination and the cyclisation cannot be drawn due to a challenging and only partially successful separation procedure by column chromatography and overlapping NMR signals in the crude mixture.

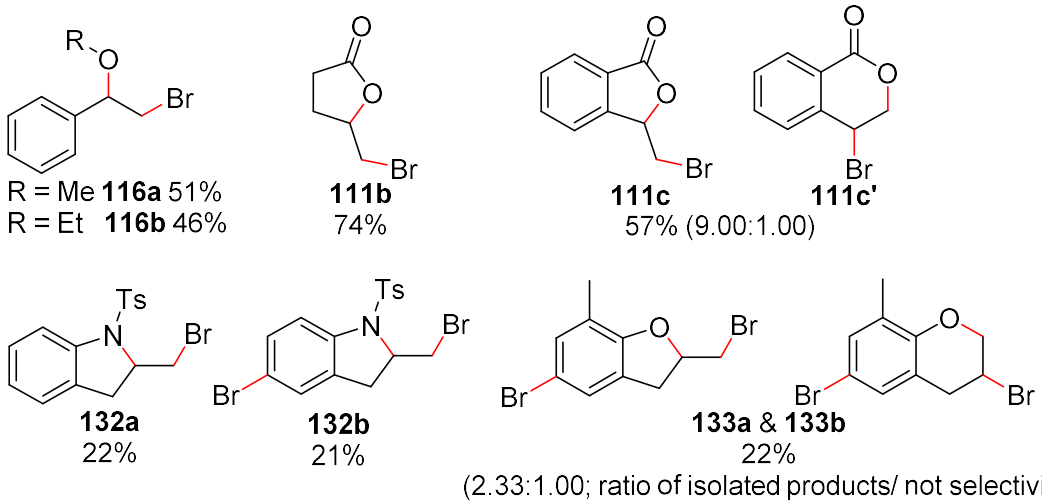

Scheme 4.18: Electrochemical bromoalkoxylation and cyclisation of alkenes in flow. Reaction conditions (alkoxylation): alkene (100 mM, 0.7 mmol), hydrobromic acid (48% w/w in water, 150 mM), 30% alcohol in MeCN; 0.4 mL·min^{-1}, 4 F·mol^{-1}, constant current 257 mA; Pt foil cathode, graphite anode (surface area: 12 cm2); reaction conditions (cyclisation): alkene (100 mM), HBr (180 mM), H_2O/MeCN, 0.2 mL·min^{-1}, 4 F·mol^{-1}, constant current 129 mA. **111b** & **133a/133b**: 0% H_2O; **111c/111c'**: 30% H_2O, 0.4 mL·min^{-1}, 3 F·mol^{-1}; **132a/132b**: 5% H_2O.

4.3.4 Biphasic Flow Electrochemical Reaction Setup

Inspired by the electrochemical dibromination of alkenes under biphasic conditions (water/ chloroform) reported by Kulangiappar *et al.* (2016)[13], biphasic conditions were adapted in the Ion Electrochemical Reactor. Based on the reported batch conditions, a 400 mM solution of styrene in chloroform and an acidic solution of NaBr (2.43 M) were both pumped at a flow rate of 0.2 mL·min^{-1} (Scheme 4.19). The solutions were joined with a T-piece mixer and passed through a reactor equipped with platinum foil electrodes. At a charge of 2 F·mol^{-1} (257 mA), the corresponding dibromide **2a** was detected in 40% yield and the bromohydrin **3a** in 10% yield.

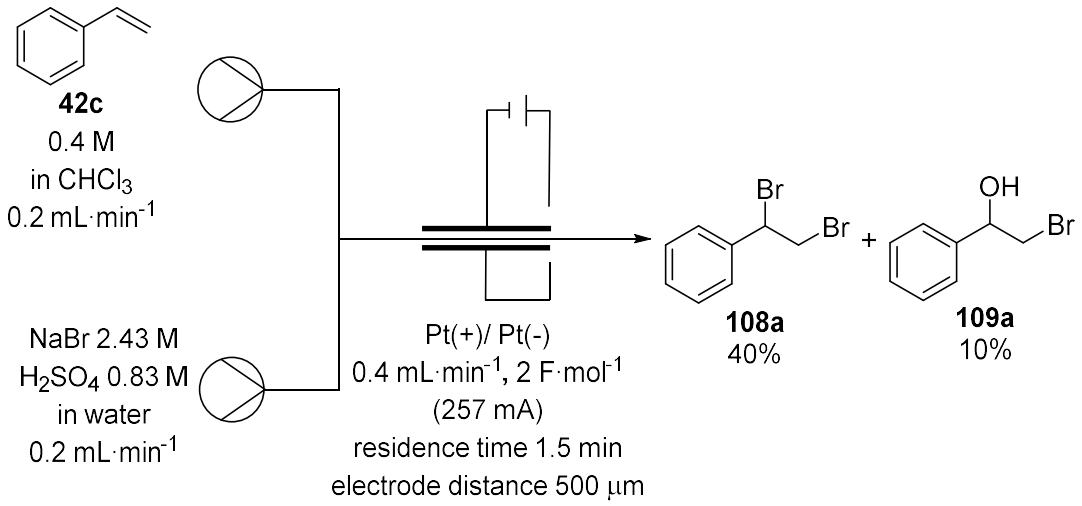

Scheme 4.19: Biphasic electrochemical bromination of styrene **42c** under single-pass flow conditions.

Subsequently, the concentrations were changed to be more comparable to the conditions for the electrochemical dibromination and bromohydroxylation in flow. A solution of styrene in organic solvent (200 mM) and an apeueous solution of hydrobromic acid (400 mM) were both joined by a T-piece mixer at flowrates of 0.2 mL·min^{-1}, which resulted in a flow rate of 0.4 mL·min^{-1} in the reactor. The current was fixed at 129 mA (2 F·mol^{-1}).

In this experimental setup, the effect of various organic solvents on the yield and chemoselectivity were investigated. The formation of the bromohydrin **109a** was favoured in water soluble solvents like dimethylsulfoxide (64%), acetonitrile (60%), tetrahydrofurane (53%) (Table 4.7, entries 1 to 3). These solvents are miscible with water, therefore no biphasic conditions should be expected. However, a phase separation in the syringe (reservoir) was observed at a water concentration of 50% in acetonitrile in the presence of styrene (100 mM). The formation of the dibromide was

suppressed to trace amounts in dimethylsulfoxide and acetonitrile, but in tetrahydrofurane **108a** was obtained in 10% yield as a sideproduct. When using ethyl acetate, both products were observed in equal amounts of 31% (**108a**) and 29% (**109a**) yield (Table 4.7, entry 4). The highest yields for the dibromide **108a** were furnished in diethyl ether (48%) and methyl *tert*-butyl ether (56%) (Table 4.7, entries 5 & 6). On the other hand, the highest selectivities for the dibromide were acomplished by using CH_2Cl_2 with a 6.57:1.00 ratio and toluene with a 4.25:1.00 ratio of products **108a** and **109a** (Table 4.7, entries 7 & 9). The selectivity of the reaction towards the formation of **108a** in chloroform (Table 4.7, entry 8) was only slightly better compared to methyl *tert*-butyl ether with a lower dibromide yield of 36%. Nonpolar solvents such as cyclohexane and *n*-pentane gave low yields of 22% and 27% for **108a** and showed lower selectivities for the dibromination (Table 4.7, entries 10 & 11).

Table 4.7: Electrochemical bromination of styrene in solvent-water mixtures.

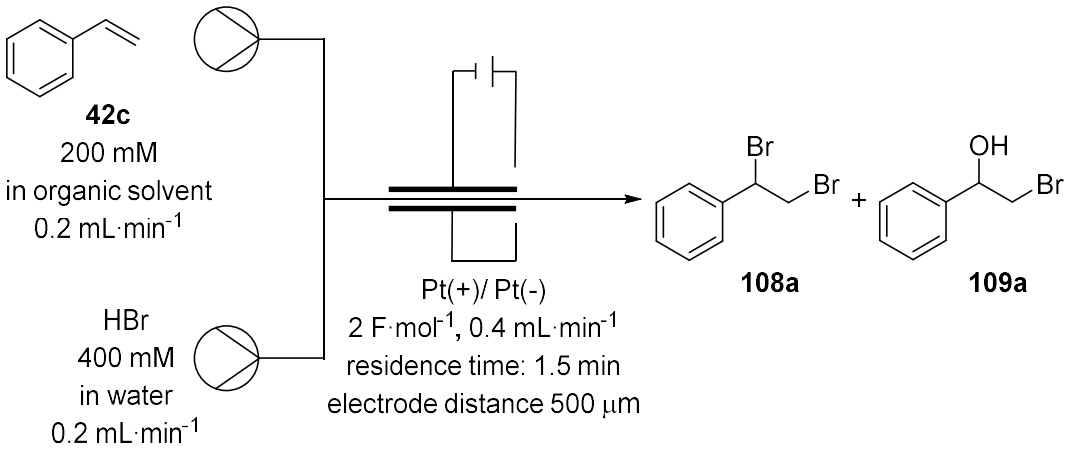

Entry	Organic Solvent	logP	**108a** [%]	**109a** [%]	**108a:109a**
1	dimethylsulfoxide	-1.35	1	64	1.00 : 64.00
2	acetonitrile	-0.45	4	60	1.00 : 15.00
3	tetrahydrofurane	0.33	10	53	1.00 : 5.30
4	ethyl acetate	0.71	31	29	1.07 : 1.00
5	diethyl ether	0.98	48	18	2.67 : 1.00
6	methyl *tert*-butyl ether	1.15	56	19	2.95 : 1.00
7	dichloromethane	1.19	46	7	6.57 : 1.00
8	chloroform	1.75	36	11	3.27 : 1.00
9	toluene	2.68	34	8	4.25 : 1.00

10	cyclohexane	3.39	22	15	1.47 : 1.00
11	*n*-pentane	3.41	27	17	1.59 : 1.00

Reaction conditions: Solution 1: 400 mM HBr in water, 0.2 mL·min^{-1}; Solution 2: 200 mM styrene **42c** in solvent, 0.2 mL·min^{-1}; Solution 1 and 2 were joined via a T-piece before entering the reactor; Reactor: Platinum anode and cathode, 2 F·mol^{-1}, 500µm FEP spacer (600µL reactor volume).

The yields of bromohydrin **109a** and dibromide **108a** were correlated to the LogP values of the investigated solvents (Figure 4.1). When plotting the yield against the LogP value of the solvents, it was observed that at lower LogP values the bromohydroxylation was favoured, while it was suppressed at higher LogP values. This might be explained by the required presence of water as nucleophile for the bromohydroxylation, which is favoured in solvents that are miscible with water. In the case of the dibromination of styrene, the highest yield was observed at logP values between 1 and 1.2. Higher logP values had a negative effect on the yield and selectivity for **108a** and in solvents with LogP values below 0 compound **108a** was only detected in trace amounts.

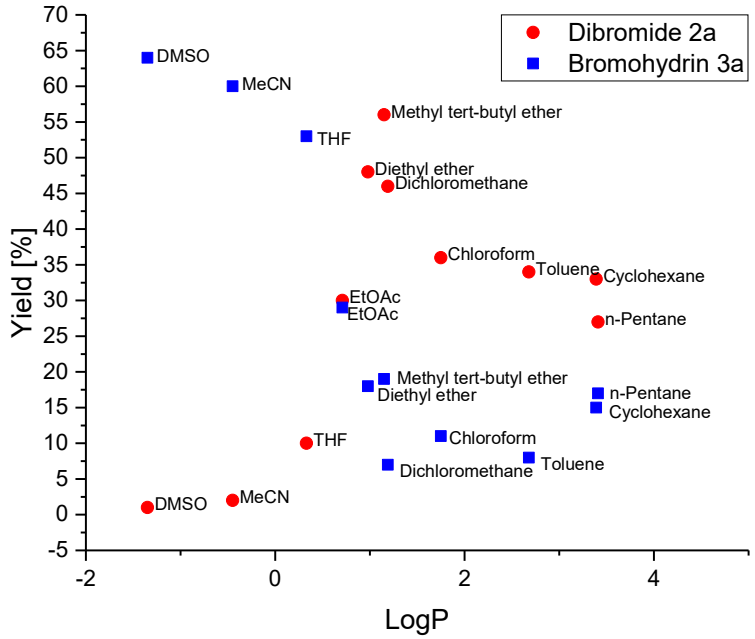

Figure 4.1: Correlation of dibromide **108a** and bromohydrin **109a** yields vs. LogP values of the co-solvent.

In conclusion, the highest yields and selectivities for the bromohydroxylation of styrene **42c** were observed with dimethylsulfoxide and acetonitrile. In the case of the dibromination, the highest yield was obtained with methyl *tert*-butyl ether and the

highest selectivity with dichloromethane. The two reservoir setup with a T-piece mixer before the reactor enabled the use of various water imiscible organic solvents under biphasic segmented flow conditions. This setup in combination with some of the investigated solvents can also serve as a useful addition to the electrochemical bromohydroxylation protocols under single pass flow conditions for substrates that are not readily soluble in the optimised water-acetonitrile mixture as discussed above.

4.3.5 Mechanism for the Electrochemical Bromination of Alkenes

The mechanism for electrochemical bromination of alkenes (Scheme 4.20) starts with the anodic oxidation of bromide ions. This leads to the formation of elemental bromine.[28,29] The reaction of bromine with alkenes **115** results in the formation of a cyclic bromonium ion **I** as intermediate.[30,31] The bromonium species is subsequently attacked by a nucleophile such as a bromide ion or water to form the dibromide or bromohydrin respectively.[11,30] Since hydrobromic acid is used for the protocols described above, protons are reduced to hydrogen gas as the counter reaction at the cathode. The use of aqueous hydrobromic acid results in the formation of bromohydrin as a side product even when no additional water is used. Increasing the bromide concentration shifts the reaction pathway to the formation of **108** while the addition of water promotes the formation of **109**.

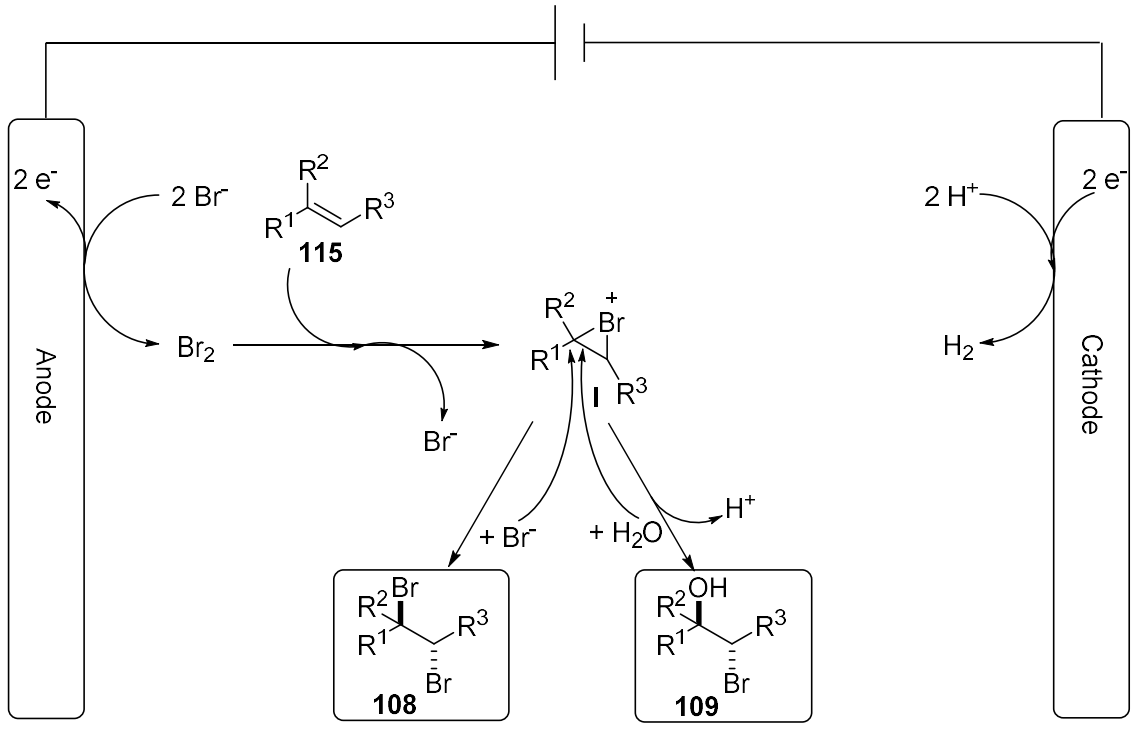

Scheme 4.20: Reaction mechanism for the electrochemical dibromination or bromohydroxylation of alkenes.

Starting materials with nucleophilic moieties **134** could react to give cyclised products **135** and **135'** (Scheme 4.20), which differ in ring size by one atom due to *exo* and *endo* ring closures. In this case, the electrogenerated bromine reacts with the alkene to give the cyclic bromonium ion **I'**, which is then attacked by the nucleophile in an intramolecular fashion. In this work, carboxylic acids, tosylamides and phenols were used as internal nucleophiles.[30,31]

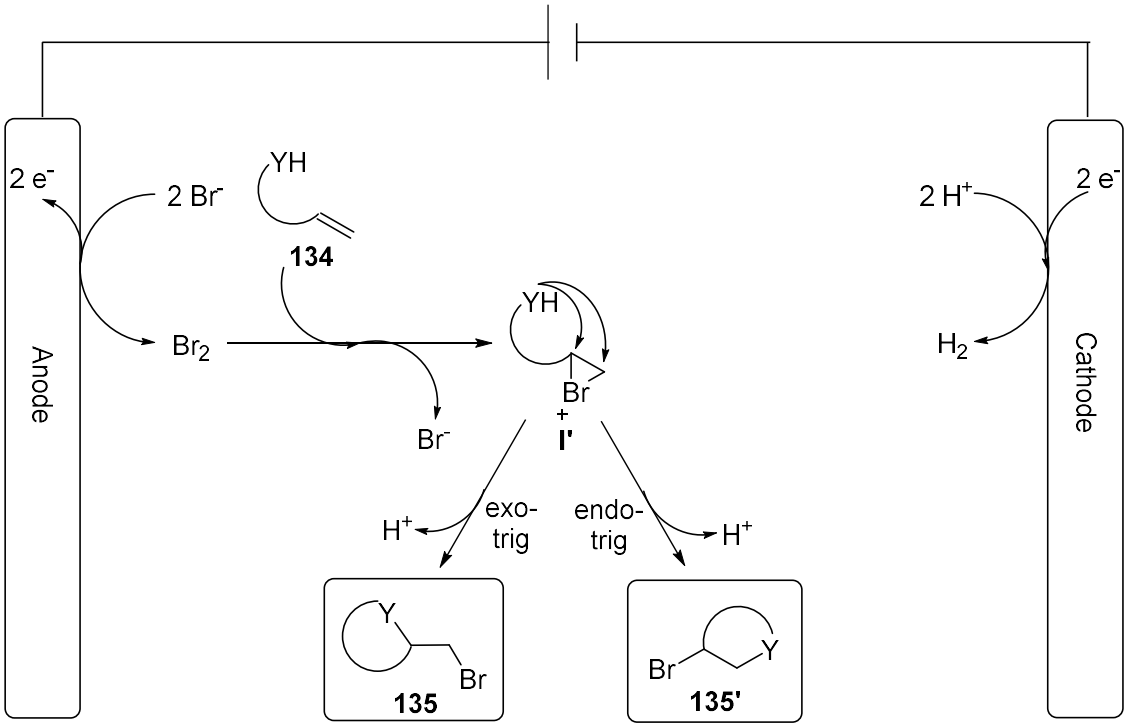

Scheme 4.21: Reaction mechanism for the electrochemical bromo-cyclisation of alkenes with intramolecular nucleophilic moieties.

4.4 Conclusion

A flow electrochemical methodology for the bromination of alkenes under single pass conditions was developed. The generation of bromine from hydrobromic acid and electricity *in situ* within the microreactor and quenching of the leftover bromine with sodium sulfite solution at the outlet, provided a safe reaction setup where the risk of a potential contact with the hazardous reagent could be mitigated.

The electrolysis of hydrobromic acid in acetonitrile, acetonitrile-water mixtures and acetonitrile-alcohol mixtures enabled the selective formation of dibromides, bromohydrins and bromohydrin ethers in moderate to excellent yields. Activated alkenes such as styrene derivatives as well as unactivated alkenes such as cyclohexene, 1-hexene and 1-decene could be engaged successfully in the investigated reactions.

Furthermore, alkenes with internal nucleophiles like carboxylic acids, tosylamides or phenols could be converted to cyclised products.

A setup with two pumps enabled the investigation of various solvents in combination with water and their effect on the selectivity of the reaction pathway in the electrochemical bromination of styrene with hydrobromic acid. Water-soluble solvents such as DMSO, acetonitrile and acetone predominantly gave the bromohydrin product. Solvents that were immiscible with water resulted in a higher selectivity for the dibromide.

In this work, only the reactions of electrochemically *in situ* generated bromine or hypobromous acid have been investigated. The electrochemical oxidation of bromide in electrochemical microreactors could be further investigated with an extension of the substrate and reaction scope. A potential starting point could be the dibromination or oxybromination of alkynes or the bromination of electron rich aromatic rings. Furthermore, the oxidation of iodide and chloride salts could also be used to functionalise alkenes in a similar fashion. Moreover, the use of chiral catalysts could give rise to flow electrochemical asymmetric halogenation procedures.

4.5 References

(1) Eissen, M.; Lenoir, D. Electrophilic Bromination of Alkenes: Environmental, Health and Safety Aspects of New Alternative Methods. *Chem. Eur. J.* **2008**, *14*, 9830–9841. https://doi.org/10.1002/chem.200800462.

(2) Saikia, I.; Borah, A. J.; Phukan, P. Use of Bromine and Bromo-Organic Compounds in Organic Synthesis. *Chem. Rev.* **2016**, *116*, 6837–7042. https://doi.org/10.1021/acs.chemrev.5b00400.

(3) Scheide, M. R.; Nicoleti, C. R.; Martins, G. M.; Braga, A. L. Electrohalogenation of Organic Compounds. *Org. Biomol. Chem.* **2021**, *19*, 2578–2602. https://doi.org/10.1039/d0ob02459g.

(4) Torii, S.; Inokuchi, T.; Misima, S. Highly Convenient Electrolysis Procedure for the Preparation of -Halogenated Ketones and Acetals from Enol Acetates, Enol Ethers, and Silyl Enol Ethers Troublesome Halogenating Reagents. *J. Org. Chem.* **1980**, *45*, 2731–2735. https://doi.org/10.1021/jo01301a044.

(5) Torii, S.; Uneyama, K.; Tanaka, H.; Yamanaka, T.; Yasuda, T.; Ono, M.; Kohmoto, Y. Efficient Conversion of Olefins into Epoxides, Bromohydrins, and Dibromides with Sodium Bromide in Water-Organic Solvent Electrolysis Systems. *J. Org. Chem.* **1981**, *46*, 3312–3315. https://doi.org/10.1021/jo00329a032.

(6) Uneyama, K.; Masatsugu, Y.; Torii, S. Electrochemical Epoxidation and Carbon-Carbon Bond Cleavage for the Preparation of 3-Methy-4-Oxo-2phenyl-4H-1-Benzopyran-8-Carboxylic Acid from 3-Methyl-2-Phenyl-8-(1-Propenyl)-4H-1-Benzopyran-4-One. *Bull. Chem. Soc. Jpn.* **1985**, *58*, 2361–2365. https://doi.org/10.1246/bcsj.58.2361.

(7) Torii, S.; Uneyama, K.; Ueda, K. Electrochemical Procedure for a Practical Preparation of Piperonal from Isosafrole. *J. Org. Chem.* **1984**, *49*, 1830–1832. https://doi.org/10.1021/jo00184a033.

(8) Torii, S.; Kubo, Y.; Miyawaki, Y.; Tanaka, H. Electrochemical Bromohydroxylation of Indene for Manufacturing of Indene Derivatives. In *Reactive Intermediates in Organic and Biological Electrochemistry*; Peters, D. G., Schäfer, H. J., Workentin, M. S., Yoshida, J., Eds.; The Electrochemical Society, 2001; pp 29–32.

(9) Ashikari, Y.; Shimizu, A.; Nokami, T.; Yoshida, J. Halogen and Chalcogen Cation Pools Stabilized by DMSO. Versatile Reagents for Alkene Difunctionalization. *J. Am. Chem. Soc.* **2013**, *135*, 16070–16073. https://doi.org/10.1021/ja4092648.

(10) Shimizu, A.; Hayashi, R.; Ashikari, Y.; Nokami, T.; Yoshida, J. Switching the Reaction Pathways of Electrochemically Generated β-Haloalkoxysulfonium Ions - Synthesis of Halohydrins and Epoxides. *Beilstein J. Org. Chem.* **2015**, *11*, 242–248. https://doi.org/10.3762/bjoc.11.27.

(11) Bityukov, O. v.; Vil', V. A.; Nikishin, G. I.; Terent'ev, A. O. Alkene, Bromide, and ROH – How To Achieve Selectivity? Electrochemical Synthesis of Bromohydrins and Their Ethers. *Adv. Synth. Catal.* **2021**, *363*, 3070–3078. https://doi.org/10.1002/adsc.202100161.

(12) Élinson, M. N.; Makhova, I. v.; Nikishin, G. I. Selective Electrochemical Bromoalkoxylation of Aryl Olefins. *Bull. Acad. Sci. USSR, Div. Chem. Sci.* **1988**, *37*, 1636–1641. https://doi.org/10.1007/BF00961113.

(13) Kulangiappar, K.; Ramaprakash, M.; Vasudevan, D.; Raju, T. Electrochemical Bromination of Cyclic and Acyclic Enes Using Biphasic Electrolysis. *Synth. Commun.* **2016**, *46*, 145–153. https://doi.org/10.1080/00397911.2015.1125498.

(14) Yuan, Y.; Yao, A.; Zheng, Y.; Gao, M.; Zhou, Z.; Qiao, J.; Hu, J.; Ye, B.; Zhao, J.; Wen, H.; Lei, A. Electrochemical Oxidative Clean Halogenation Using HX/NaX with Hydrogen Evolution. *iScience* **2019**, *12*, 293–303. https://doi.org/10.1016/j.isci.2019.01.017.

(15) Strehl, J.; Abraham, M. L.; Hilt, G. Linear Paired Electrolysis—Realising 200 % Current Efficiency for Stoichiometric Transformations—The Electrochemical Bromination of Alkenes. *Angew. Chem. Int. Ed.* **2021**, *60*, 9996–10000. https://doi.org/10.1002/anie.202016413.

(16) Tan, Z.; Liu, Y.; Helmy, R.; Rivera, N. R.; Hesk, D.; Tyagarajan, S.; Yang, L.; Su, J. Electrochemical Bromination of Late Stage Intermediates and Drug Molecules. *Tetrahedron Lett.* **2017**, *58*, 3014–3018. https://doi.org/10.1016/j.tetlet.2017.06.019.

(17) Prabhakar Kale, A.; Nikolaienko, P.; Smirnova, K.; Rueping, M. Intramolecular Electrochemical Oxybromination of Olefins for the Synthesis of Isoxazolines in Batch and Continuous Flow. *Eur. J. Org. Chem.* **2021**, *2021*, 3496–3500. https://doi.org/10.1002/ejoc.202100640.

(18) Read, J.; Reid, W. G. CXCVI.—The Action of Bromine Water on Certain Olefinic Hydrocarbons and Ethers. *J. Chem. Soc.* **1928**, 1487–1493. https://doi.org/10.1039/JR9280001487.

(19) Zabicky, J.; Nutkovitch, M. Reactions of Bromine and Cyclohexene in Aqueous Media. Selectivity of Bromohydrin Vs. Dibromo Adduct Formation. *Ind. Eng. Chem. Prod. Res. Dev.* **1986**, *25*, 372–375. https://doi.org/10.1021/i300022a041.

(20) Guss, C. O.; Rosenthal, R. Bromohydrins from Olefins and N-Bromosuccinimide in Water. *J. Am. Chem. Soc.* **1955**, *77*, 2549–2549. https://doi.org/10.1021/ja01614a056.

(21) Dalton, D. R.; Dutta, V. P. Bromohydrin Formation in Aqueous Dimethyl Sulphoxide; Electronic and Steric Effects. *J. Chem. Soc. (B)* **1971**, 85–89. https://doi.org/10.1039/J29710000085.

(22) Dalton, D. R.; Dutta, V. P.; Jones, D. C. Bromohydrin Formation in Dimethyl Sulfoxide. *J. Am. Chem. Soc.* **1968**, *90*, 5498–5501. https://doi.org/10.1021/ja01022a030.

(23) Masuda, H.; Takase, K.; Nishio, M.; Hasegawa, A.; Nishiyama, Y.; Ishii, Y. A New Synthetic Method of Preparing Iodohydrin and Bromohydrin Derivatives through in Situ Generation of Hypohalous Acids from H_5IO_6 and $NaBrO_3$ in the Presence of $NaHSO_3$. *J. Org. Chem.* **1994**, *59*, 5550–5555. https://doi.org/10.1021/jo00098a012.

(24) de Almeida, L. S.; Esteves, P. M.; de Mattos, M. C. S. Efficient Electrophilic Cobromination of Alkenes and Bromination of Activated Arenes with Bromodichloroisocyanuric Acid under Mild Conditions. *Synlett* **2007**, *11*, 1687–1690. https://doi.org/10.1055/s-2007-982575.

(25) Song, S.; Huang, X.; Liang, Y. F.; Tang, C.; Li, X.; Jiao, N. From Simple Organobromides or Olefins to Highly Value-Added Bromohydrins: A Versatile Performance of Dimethyl Sulfoxide. *Green Chem.* **2015**, *17*, 2727–2731. https://doi.org/10.1039/c5gc00184f.

(26) Vapourtec Ltd. *Ion electrochemical reactor*. https://www.vapourtec.com/products/flow-reactors/ion-electrochemical-reactor-features/, (accessed September 2022).

(27) van Kerrebroeck, R.; Naert, P.; Heugebaert, T. S. A.; D'hooghe, M.; Stevens, C. v. Electrophilic Bromination in Flow: A Safe and Sustainable Alternative to the Use of Molecular Bromine in Batch. *Molecules* **2019**, *24*, 2116. https://doi.org/10.3390/molecules24112116.

(28) Raju, T.; Kulangiappar, K.; Anbu Kulandainathan, M.; Uma, U.; Malini, R.; Muthukumaran, A. Site Directed Nuclear Bromination of Aromatic Compounds by an Electrochemical Method. *Tetrahedron Lett.* **2006**, *47*, 4581–4584. https://doi.org/10.1016/j.tetlet.2006.04.152.

(29) Čolović, M.; Vukićević, M.; Šegan, D.; Manojlović, D.; Sojic, N.; Somsák, L.; Vukićević, R. D. Electrochemical Bromination of Peracetylated Glycals. *Adv. Synth. Catal.* **2008**, *350*, 29–34. https://doi.org/10.1002/adsc.200700310.

(30) Martins, N. S.; Alberto, E. E. Dibromination of Alkenes with LiBr and H_2O_2 under Mild Conditions. *New J. Chem.* **2018**, *42*, 161–167. https://doi.org/10.1039/c7nj04300g.

(31) Ding, R.; Li, J.; Jiao, W.; Han, M.; Liu, Y.; Tian, H.; Sun, B. A Highly Efficient Method for the Bromination of Alkenes, Alkynes and Ketones Using Dimethyl Sulfoxide and Oxalyl Bromide. *Synthesis* **2018**, *50*, 4325–4335. https://doi.org/10.1055/s-0037-1609560.

Chapter 5: Experimental Part

5.1 General Methods

Solvents and Reagents

Solvents and reagents were used as provided by suppliers (Sigma Aldrich, Alfa Aesar, Acros Organic, VWR and FluoroChem) without further purification or drying, unless otherwise specified.

Dry diethyl ether, THF, n-hexane, toluene and acetonitrile were used from a MB SPS-800 solvent purification system from MBRAUN. Dry dichloromethane was prepared by distillation over calcium hydride under a nitrogen atmosphere.

Deionised water (15.0 MΩ·cm resistivity at 18 °C) was collected from a PURELAB Option water purification system from ELGA.

Laboratory Equipment

Standard laboratory equipment was used for the reactions. Lower temperatures were achieved with an ice/water bath (0 °C)

Solvents were evaporated with rotary evaporators from Heidolph or Büchi. Compounds were further dried on a high vacuum system.

Chromatography

Thin layer chromatography was performed on pre-coated aluminium sheets of Merck silica gel 60 F254 (0.20 mm) and visualized by UV radiation (254 nm) or by staining with ceric ammonium molybdate solution. Flash column chromatography was performed on Biotage® Isolera Four using Biotage® cartridges SNAP Ultra 10 g or 25 g and Biotage® cartridges Sfär 10 g or 25 g. Non-UV-visible compounds were separated by manual flash chromatography using silica gel (Sigma-Aldrich, technical grade, pore size 60 Å, 230-400 mesh particle size, 40-63 µm particle size).

NMR spectroscopy

^{1}H NMR, ^{13}C NMR and ^{19}F NMR spectra were recorded on a Bruker Fourier 300 apparatus and referenced relative to the residual solvent peaks (^{1}H: $CDCl_3$, δ 7.26 ppm; ^{13}C: $CDCl_3$, δ 77.2 ppm). The chemical shifts δ values are given in parts per million (ppm). The multiplicity of the signals was declared as followed: s = singlet, d = doublet, t = triplet, q = quartet, quin = quintet, sex = sextet, hep = septet, dd = doublet of doublets, m = multiplet, b = broad; and coupling constants (*J*) in Hertz.

UV/vis spectroscopy

UV/vis spectra were recorded on a Cary 60 UV-Vis Spectrophotometer from Agilent Technologies.

Mass Spectrometry

Mass spectrometry was performed by Cardiff University Analytical Service on a Water LCR Premier XE-TOF mass spectrometer. Ions were generated by Electron Ionisation (EI) and Chemical Ionisation (CI).

Powder XRD

Powder X-ray diffraction was performed on an PANalytical X'Pert Pro diffractometer.

IR spectroscopy

Infrared spectroscopy was conducted with a Shimadzu FTIR Affinity-1S apparatus. Wavenumbers are quoted in cm^{-1}. All compounds were measured neat directly on the crystal of the IR machine.

Polarimetry

Optical Rotation values were measured with a Schmidt+Haensch Uni Pol L polarimeter at 20 °C in a cuvette with a path length of 50 mm and a sodium light source (589.30 nm).

Melting point

Melting points were measured using a Gallenkamp variable heater with samples in open capillary tubes.

Cyclic Voltametry

Cyclic Voltammetry was performed with equipment from OrigaLys consisting of a power supply (OrigaFlex OGFPWR) and a potentiostat-galvanostat (OrigaFlex OGF500) controlled with Origa Master 5 software.

A glassy carbon (3 mm diameter) working electrode, Ag/AgCl (3 M KCl) reference electrode and a platinum wire auxiliary electrode were used with a VC-2 voltammetry cell from BASi.

Glassy carbon electrodes were polished with electrode polishing alumina suspension (0.05 µm) on an alumina polishing pad from BASi.

HPLC analysis

HPLC analysis was performed on a Shimadzu system consisting of following modules: DGU 20A 5R (degassing unit), LC-20 AT (liquid chromatograph), SIL-20A HT (auto sampler), CBM-20A (communications bus module), CTO-20A (column oven), SPD-M20A (diode array detector).

The 2D-HPLC measurements were conducted on a 1290 Infinity II 2D-LC system (Agilent) consisting of following modules: G7129A (1290 vial sampler), G1312 (1D binary pump), G1322A (degasser), G7120A (1290 high speed 2D binary pump), G1316A (1260 column oven), G7115A (1260 diode array detector).

Electrochemical batch experiments

Electrasyn 2.0: Batch electrochemical experiments were carried out with an Electrasyn 2.0 device. Graphite (5 cm x 0.8 cm x 0.2 cm) electrodes were cut by Cardiff University workshop. Platinum foil (5 cm x 0.5 cm), glassy carbon (5 cm x 0.8 cm x 0.2 cm) and copper (5 cm x 0.8 cm x 0.2 cm) electrodes were purchased from IKA. Sacrificial magnesium anodes (50 mm × 3 mm × 0.2 mm) were cut from a magnesium ribbon and fixated in the Electrasyn 2.0 cap with electrode holders. The electrodes were used in 5 mL or 10 mL Electrasyn 2.0 vials and were immersed 3 cm deep into the solution

Batch electrochemistry with copper coins: Reactions with coin electrodes were performed in a 10 mL round bottom flask (joint: ST/NS 29/32). Copper coins were manufactured with a hydraulic press under a pressure of 3 tons. The copper coins (diameter: 13 mm) and magnesium ribbon electrodes were mounted to electrode holders with platinum contacts that were connected to an Aim-TTi EX354RD Dual bench power supply.

Electrochemical flow reactor

Flow chemistry was conducted with KR Analytical Ltd Fusion 100 Touch syringe pumps and FEP tubing (OD: 1/16''; ID: 0.8 – 1.0 mm).

Flow electrochemical experiments were carried out with an Ion electrochemical reactor from Vapourtec Ltd.[1]

Either an Aim-TTi EX354RD Dual power supply or a GW Instek PSU 300-5 bench power supply were used for flow electrochemical experiments.

The following electrodes (5 x 5 cm^2) were used in the ion electrochemical reactor separated by a 0.5 mm thick FEP spacer resulting in a reactor volume of 600 µL and

exposed electrode surface area of 12 cm^2: graphite, platinum foil (Goodfellow); platinum plated on niobium, platinum coated on titanium, nickel, glassy carbon (GC), panasonic carbon (Vapourtec Ltd).

5.2 Experimental Data for Chapter 2

Magnesium ribbon (3 mm × 0.2 mm, 25 g) was purchased from Acros Organics.

5.2.1 Preparation of Organically doped Metals

Table 2.1:

CD@Cu01 (Table 2.1, entry 1)

CD@Cu was prepared according to a literature procedure:[2]

A solution of $CuCl_2$ (863 mg, 6.42 mmol, 1 eq.) in 25 mL of deionised water was poured into a stirred solution of SDS (900 mg, 3.12 mmol, 0.49 eq.) and cinchonidine (9 mg, 0.03 mmol, 0.5 mol%) in 25 mL of deionised water. Subsequently, zinc powder (364 mg, 5.57 mmol, 0.87 eq.) was added and the mixture was stirred at room temperature (colour change from blue solution to red-brown suspension). After 3 hours, the reaction mixture was filtered off and the precipitate was washed with 1 M hydrochloric acid (10 mL), deionised water (50 mL) and acetonitrile (3 × 20 mL). The resulting light green precipitate was washed with 1 M hydrochloric acid (2 × 5 mL), deionised water (3 × 5 mL). The remaining precipitate was dried *in vacuo* to yield 3 mg of red powder.

Characterisation:

A characterisation of the product was not possible.

CD@Cu02 (Table 2.1, entry 2)

A solution of $CuCl_2$ (2.55 g, 19.0 mmol, 1 eq.) in 75 mL of deionised water was poured into a stirred solution of SDS (2.72 g, 9.44 mmol, 0.5 eq.) and cinchonidine (27 mg, 0.09 mmol, 0.5 mol%) in 75 mL of deionised water. Subsequently, zinc powder (1.05 g, 16.1 mmol, 0.85 eq.) was added and the mixture was stirred at room temperature (colour change from blue solution to red-brown suspension). After 6 hours, the reaction mixture was filtered off and the orange precipitate was washed with 1 M hydrochloric acid (30 mL), deionised water (50 mL) and acetonitrile (2 × 50 mL). The remaining precipitate was dried *in vacuo* to yield 78 mg of red powder. The acetonitrile from the filtrate was removed to give 1.27 g of a brown solid.

Characterisation:

Powder XRD of solids recovered from the filtrate: Cu(I)Cl.

Powder XRD of the precipitate: no cinchonidine pattern could be observed.

After extraction of the particles with DMSO-d6, the cinchonidine could not be detected by ^{1}H-NMR spectroscopy.

CD@Cu03 (Table 2.1, entry 3)

Prior to use, the deionised water was ultrasonicated for 5-10 minutes. A solution of $CuCl_2$ (865 mg, 6.43 mmol, 1 eq.) in 25 mL of deionised water was poured into a stirred solution of SDS (795 mg, 2.76 mmol, 0.43 eq.) and cinchonidine (17 mg, 0.06 mmol, 1 mol%) in 25 mL of deionised water. Subsequently, zinc powder (658 mg, 10.1 mmol, 1.56 eq.) was added and the mixture was stirred at room temperature (colour change from blue solution to colourless solution with black precipitate). After 6 hours, the reaction mixture was filtered off and the precipitate was washed with 1 M hydrochloric acid (3 × 15 mL), deionised water (3 × 20 mL) and acetonitrile (2 × 20 mL). The precipitate was dried *in vacuo* to yield 428 mg of red powder.

Characterisation:

Powder XRD: no cinchonidine pattern could be observed.

After extraction of the particles with DMSO-d6, the copper particles could not be separated from the solution to conduct ^{1}H NMR spectroscopy.

After extraction of the particles with DMSO, cinchonidine was not detected by IR spectroscopy.

CD@Cu04 (Table 2.1, entry 4)

Prior to use, the deionised water was ultrasonicated for 5-10 minutes. A solution of $CuCl_2$ (807 mg, 6.00 mmol, 1 eq.) in 25 mL of deionised water was poured into a stirred suspension of cinchonidine (36 mg, 0.12 mmol, 2 mol%) in 25 mL of deionised water. Subsequently, zinc powder (493 mg, 7.54 mmol, 1.26 eq.) was added and the mixture was stirred at room temperature (colour change from blue solution to colourless solution with black precipitate). After 5 hours, the reaction mixture was filtered off and the precipitate was washed with 1 M hydrochloric acid (2 × 25 mL), deionised water (3 × 20 mL) and acetonitrile (20 mL). The precipitate was dried *in vacuo* to yield 407 mg of red powder.

Characterisation:

Powder XRD: no cinchonidine pattern could be observed.

CD@Cu05 (Table 2.1, entry 5)

A solution of $CuCl_2$ (529 mg, 3.93 mmol, 1 eq.) in 16 mL of deionised water was poured into a stirred solution of SDS (567 mg, 1.97 mmol, 0.5 eq.) and cinchonidine (113 mg, 0.38 mmol, 10 mol%) in 16 mL of deionised water. Subsequently, zinc powder (340 mg, 5.20 mmol, 1.32 eq.) was added and the mixture was stirred at room temperature (colour change from blue solution to colourless solution with black precipitate). After 2.5 hours, the reaction mixture was filtered off and the precipitate was washed with 1 M hydrochloric acid (2 × 25 mL), deionised water (2 × 10 mL) and acetonitrile (15 mL). The remaining precipitate was dried *in vacuo* to yield 187 mg of greenish powder.

Characterisation:

After extraction of the particles with DMSO, cinchonidine was not detected by IR spectroscopy or UV/Vis spectroscopy.

CD@Cu06 (Table 2.1, entry 6)

Prior to use, the deionised water was ultrasonicated for 5-10 minutes. A solution of $CuCl_2$ (808 mg, 6.00 mmol, 1 eq.) in 25 mL of deionised water was poured into a stirred solution of cinchonidine (176 mg, 0.60 mmol, 10 mol%) in a mixture of acetonitrile and water (1:4, 25 mL). The reaction mixture was heated to 35 °C. Zinc powder (473 mg, 7.20 mmol, 1.2 eq.) was added and the mixture was stirred at room temperature (colour change from blue solution to colourless solution with black precipitate). After 6 hours, the reaction mixture was filtered off and the precipitate was washed with 1 M hydrochloric acid (2 × 25 mL), deionised water (3 × 20 mL) and acetonitrile (2 × 20 mL). The precipitate was dried *in vacuo* to yield 300 mg of red powder.

Characterisation:

Powder XRD: no cinchonidine pattern could be observed.

After extraction of the particles with DMSO, cinchonidine was not detected by IR or UV/Vis spectroscopy.

CD@Cu07 (Table 2.1, entry 7)

Prior to use, the deionised water was ultrasonicated for 5-10 minutes. A solution of $CuCl_2$ (1.35 g, 10.0 mmol, 1 eq.) in 50 mL of deionised water was poured into a stirred solution of cinchonidine (30 mg, 0.10 mmol, 1 mol%) in deionised water (50 mL). Zinc

powder (473 mg, 7.20 mmol, 1.2 eq.) was added in portions over 30 minutes. The mixture was stirred at room temperature for another 4 hours (colour change from blue to colourless solution with precipitation). The reaction mixture was then filtered off and the precipitate was washed with 1 M hydrochloric acid (2 × 25 mL), deionised water (3 × 20 mL) and acetonitrile (2 × 20 mL). The precipitate was dried *in vacuo* to yield 506 mg of red powder.

Characterisation:

Cinchonidine was detected in the filtrate from the reaction mixture and the aqueous washing step by UV/Vis spectroscopy.

After extraction of the particles with DMSO, cinchonidine was not detected by UV/Vis spectroscopy.

CD@Cu08 (Table 2.1, entry 8)

Prior to use, the deionised water was ultrasonicated for 5-10 minutes. A solution of $CuCl_2$ (812 mg, 6.00 mmol, 1 eq.) in 25 mL of deionised water was poured into a stirred solution of cinchonidine (36 mg, 0.12 mmol, 2 mol%) in a mixture of ethanol and water (1:4, 25 mL). Zinc powder (473 mg, 7.20 mmol, 1.2 eq.) was added in small portions over 20 minutes. The mixture was stirred at room temperature for another 4 hours (colour change from blue solution to colourless solution with precipitation). The reaction mixture was filtered off and the precipitate was washed with 1 M hydrochloric acid (20 mL), deionised water (3 × 10 mL) and acetonitrile (2 × 20 mL). The precipitate was dried *in vacuo* to yield 242 mg of red powder.

Characterisation:

Cinchonidine was detected in the filtrate from the reaction mixture but not in the aqueous solution from the washing step by UV/Vis spectroscopy.

After extraction of the particles with DMSO, cinchonidine was not detected by IR or UV/Vis spectroscopy.

CD@Cu09 (Table 2.1, entry 9)

Prior to use, the deionised water was ultrasonicated for 5-10 minutes. A solution of $CuCl_2$ (830 mg, 6.17 mmol, 1 eq.) in 25 mL of deionised water was poured into a stirred solution of SDS (900 mg, 3.12 mmol, 0.5 eq.) and cinchonidine (97 mg, 0.3 mmol, 5 mol%) in water (25 mL). $NaHPO_2 \times H_2O$ (1.29 g, 12.2 mmol, 2 eq.) was added as the

reductant. The mixture was heated to 65 °C temperature for 5 hours. The appearance of the reaction mixture changed from a blue solution to an orange suspension. After addition of another 1.25 g (11.8 mmol, 2 eq.) of $NaHPO_2 \times H_2O$, the mixture was heated to 50 °C for 6 hours. The orange slurry was filtrated and washed with 1 M hydrochloric acid (50 mL). After the acidic washing step, no precipitate was left in the filter to be isolated.

Characterisation:

A characterisation of the product was not possible.

CD@Cu10 (Table 2.1, entry 10)

Prior to use, the deionised water was ultrasonicated for 5-10 minutes. A solution of $CuCl_2$ (814 mg, 6.06 mmol, 1.00 eq.) in 25 mL of deionised water was poured into a stirred solution of SDS (905 mg, 3.14 mmol, 0.52 eq.) and cinchonidine (88 mg, 0.30 mmol, 5 mol%) in 25 mL of deionised water. Subsequently, zinc powder (394 mg, 6.03 mmol, 1.00 eq.) was added and the mixture was stirred at room temperature. After 6 hours, 5 mL of concentrated hydrochloric acid were added and the reaction mixture was filtered off. The precipitate was washed with deionised water (3 × 20 mL). The precipitate was dried *in vacuo* to yield 301 mg of brick-red powder.

Characterisation:

Cinchonidine was detected in the filtrate from the reaction mixture and in the aqueous washing steps by UV/Vis spectroscopy.

Extraction of the material (12 mg) with DMSO-d6 and analysis by ^1H NMR spectroscopy did not confirm the presence of cinchonidine.

After extraction of the particles with DMSO, cinchonidine was not detected by IR spectroscopy.

CD@Cu11 (Table 2.1, entry 11)

Prior to use, the deionised water was ultrasonicated for 5-10 minutes. A solution of $CuCl_2$ (807 mg, 6.00 mmol, 1.00 eq.), SDS (200 mg, 0.69 mmol, 0.1 eq.) and cinchonidine (35 mg, 0.12 mmol, 2 mol%) in deionised water (40 mL) was adjusted to pH 9 by adding Na_2CO_3. Subsequently, zinc powder (472 mg, 7.22 mmol, 1.20 eq.) was added and the mixture was heated to 40 °C under stirring. After 5 hours, $NaH_2PO_2 \times H_2O$ (330 mg, 3.11 mmol, 0.52 eq.) was added and the reaction mixture was stirred

for another 30 minutes. Then the reaction mixture was filtered off and the precipitate was washed with 1 M hydrochloric acid (20 mL) and deionised water (3 × 20 mL). The precipitate was dried *in vacuo* to yield 516 mg of dark-red powder.

Characterisation:

Powder XRD: no cinchonidine pattern could be observed.

After extraction of the particles with DMSO, cinchonidine was not detected by UV/vis spectroscopy.

CD@Cu12 (Table 2.1, entry 12)

Prior to use, the deionised water was ultrasonicated for 5-10 minutes. A solution of $CuCl_2$ (678 mg, 5.04 mmol, 1.00 eq.) in 20 mL of deionised water was dripped into a stirred solution of SDS (900 mg, 3.12 mmol, 0.62 eq.) and cinchonidine (9 mg, 0.03 mmol, 1 mol%) in 20 mL of deionised water. Zinc powder (402 mg, 6.14 mmol, 1.22 eq.) was added and the reaction mixture was stirred at room temperature for 6 hours. Then the reaction mixture was filtered off and the precipitate was washed with 1 M hydrochloric acid (10 mL), deionised water (4 × 10 mL) and acetonitrile (2 × 10 mL). The precipitate was dried *in vacuo* to yield 322 mg of red-brown powder.

Characterisation:

Cinchonidine was detected in the filtrate from the reaction mixture and in the washing steps by UV/Vis spectroscopy. The calculation of the cinchonidine concentration in the filtrate indicated that over 90% of cinchonidine was leached out of the material.

CD@Cu13 (Table 2.1, entry 13)

A solution of $CuCl_2$ (672 mg, 5.00 mmol, 1.00 eq.) in 25 mL of deionised water was poured into a stirred solution of SDS (900 mg, 3.12 mmol, 0.62 eq.) and cinchonidine (9 mg, 0.38 mmol, 10 mol%) in deionised water (25 mL). Subsequently, zinc powder (360 mg, 5.50 mmol, 1.10 eq.) was added and the reaction mixture (pH 3-4) was stirred at room temperature for 6 hours, the reaction mixture was filtered off and the precipitate was washed with 1 M hydrochloric acid (10 mL), deionised water (3 × 10 mL) and acetonitrile (3 × 10 mL). After drying *in vacuo*, the product was obtained as a red powder (344 mg).

Characterisation:

Cinchonidine was detected in the UV/Vis spectrum of the filtrate from the reaction mixture and in the washing steps. Based on concentration calculations, it was estimated that no more than 4% of cinchonidine might remain in the material.

Table 2.2:

CD@Cu14 (Table 2.2, entry 1) Prior to use, the deionised water was ultrasonicated for 5-10 minutes. A solution of $CuSO_4 \times 5\ H_2O$ (2.50 g, 10.00 mmol, 1.00 eq.) in 50 mL of deionised water was poured into a solution of cinchonidine (18 mg, 0.06 mmol, 1 mol%) in deionised water (50 mL). Zinc powder (723 mg, 11.1 mmol, 1.11 eq.) was added and the reaction mixture was stirred at room temperature for 5 hours. Then the reaction mixture was filtered off and the precipitate was washed with 1 M hydrochloric acid (10 mL), deionised water (3 × 10 mL) and acetonitrile (3 × 10 mL). The precipitate was dried *in vacuo* to yield 367 mg of grey-brown powder.

Characterisation:

Cinchonidine was detected in the filtrate from the reaction mixture steps by UV/Vis spectroscopy. The calculation of the concentration in the filtrate indicated a loss of 70% of cinchonidine.

Powder XRD: No pattern for cinchonidine was observed.

CD@Cu15 (Table 2.2, entry 2)

Prior to use, the deionised water was ultrasonicated for 5-10 minutes. A solution of $CuSO_4 \times 5\ H_2O$ (2.50 g, 10.00 mmol, 1.00 eq.) in 50 mL of deionised water was poured into a solution of cinchonidine (18 mg, 0.06 mmol, 1 mol%) in deionised water (50 mL). The pH value was adjusted to pH 9 by adding Na_2CO_3. Zinc powder (719 mg, 11.1 mmol, 1.11 eq.) was added and the reaction mixture was stirred at room temperature for 10 hours. When there was no change to the cloudy blue suspension, hydrochloric acid was added dropwise to adjust to pH 7. Within a few minutes a black precipitate was observed. After 2 hours, more zinc powder (265 mg, 4.05 mmol, 0.41 eq.) was added and the rection mixture was stirred for another 3 hours. Then the reaction mixture was filtered off and the precipitate was washed with 1 M hydrochloric acid (10 mL), deionised water (3 × 10 mL) and acetonitrile (3 × 10 mL). The precipitate was dried *in vacuo*. The precipitate weight of 1.50 g indicated the presence of impurities. The material was washed again with 1 M hydrochloric acid (10 mL),

deionised water (3 × 10 mL) and acetonitrile (3 × 10 mL). After drying *in vacuo*, the product was obtained as a red powder (385 mg).

Characterisation:

Cinchonidine was detected in the filtrate from the reaction mixture steps by UV/Vis spectroscopy. The calculation of the concentration in the filtrate indicated a loss of 75% of cinchonidine.

CD@Cu16 (Table 2.2, entry 3)

Prior to use, the deionised water was ultrasonicated for 5-10 minutes. A solution of $CuSO_4 \times 5\ H_2O$ (2.50 g, 10.00 mmol, 1.00 eq.) in 50 mL of deionised water was poured into a solution of cinchonidine (18 mg, 0.06 mmol, 1 mol%) in deionised water (50 mL). The dissolving of cinchonidine was enhanced by adding concentrated hydrochloric acid (10 drops). Zinc powder (848 mg, 11.1 mmol, 1.11 eq.) was added and the reaction mixture was stirred at room temperature for 6 hours. Then the reaction mixture was acidified with hydrochloric acid to pH 3. The precipitate was filtered off, washed with deionised water (50 mL) and acetonitrile (4 × 10 mL). The precipitate was dried *in vacuo* to yield 600 mg of grey-brown powder.

Characterisation:

Cinchonidine was detected in the filtrate from the aqueous washing steps by UV/Vis spectroscopy. Cinchonidine was not observed in the filtrate of the reaction mixture and the acetonitrile washing step. The calculation of the concentration in the filtrate indicated that up to 80% of cinchonidine might remain in the material.

Powder XRD: No pattern for cinchonidine was observed.

The material (100 mg) was extracted with THF (10 mL) and the organic solvent was removed. The residue was dissolved in water and the solution was acidified with hydrochloric acid. The UV/Vis spectrum of the solution could not confirm the encapsulation of cinchonidine.

CD@Cu17 (Table 2.2, entry 4)

Prior to use, the deionised water was ultrasonicated for 5-10 minutes. Cinchonidine (9 mg, 0.03 mmol, 1 mol%) and zinc powder (359 mg, 5.49 mmol, 1.10 eq.) were mixed in deionised water (25 mL). A drop of concentrated hydrochloric acid was added to help solubilising cinchonidine. A solution of $CuSO_4 \times 5\ H_2O$ (1.25 g, 5.00 mmol, 1.00 eq.) in

25 mL of deionised water was poured into the suspension and the reaction mixture was stirred at room temperature for 6 hours. Subsequently, the reaction mixture was filtered off and the precipitate was washed with 1 M hydrochloric acid (10 mL), deionised water (3 × 10 mL) and acetonitrile (3 × 10 mL). After drying *in vacuo*, the product was obtained as a red powder (283 mg).

Characterisation:

Cinchonidine was detected in the UV/Vis spectrum of the filtrate from the reaction mixture and in the washing steps. Based on concentration calculations, it was estimated that around 50% of cinchonidine might remain in the material.

CD@Cu18 (Table 2.2, entry 5)

Prior to use, the deionised water was ultrasonicated for 5-10 minutes. Cinchonidine (9 mg, 0.03 mmol, 1 mol%) and zinc powder (393 mg, 6.01 mmol, 1.20 eq.) were mixed in deionised water (25 mL). Concentrated hydrochloric acid (2 drops) was added to help solubilising cinchonidine. A solution of $CuSO_4 \times 5\ H_2O$ (1.25 g, 5.00 mmol, 1.00 eq.) in 25 mL of deionised water was dripped into the suspension over the course of 5 minutes and the reaction mixture was stirred at room temperature for 6 hours. Subsequently, the reaction mixture was filtered off and the precipitate was washed with 1 M hydrochloric acid (10 mL), deionised water (3 × 10 mL) and acetonitrile (3 × 10 mL). After drying *in vacuo*, the product was obtained as a red powder (339 mg).

Characterisation:

Cinchonidine was detected in the UV/Vis spectrum of the filtrate from the reaction mixture and in the washing steps. Based on concentration calculations, it was estimated that around 40% of cinchonidine might remain in the material.

CD@Cu19 (Table 2.2, entry 6)

Prior to use, the deionised water was ultrasonicated for 5-10 minutes. Cinchonidine (9 mg, 0.03 mmol, 1 mol%) and zinc powder (465 mg, 7.11 mmol, 1.41 eq.) were mixed in deionised water (25 mL). A drop of concentrated hydrochloric acid was added to help solubilising cinchonidine. A solution of $CuSO_4 \times 5\ H_2O$ (1.25 g, 5.03 mmol, 1.00 eq.) in 25 mL of deionised water was dripped into the suspension over the course of 5 minutes and the reaction mixture was stirred at room temperature for 6 hours. Subsequently, the reaction mixture was filtered off and the precipitate was washed with 1 M

hydrochloric acid (10 mL), deionised water (4 × 10 mL) and acetonitrile (3 × 10 mL). After drying *in vacuo*, the product was obtained as a red powder (321 mg).

Characterisation:

Cinchonidine was not detected in the UV/Vis spectrum of the filtrate from the reaction mixture. The UV/vis spectra from the aqueous and organic washing steps indicated a minor loss of cinchonidine, which could indicate an encapsulation of up to 90% of cinchonidine.

The destruction of particles (20 mg and 10 mg) with hydrochloric acid and analysis with UV/vis spectroscopy indicated the presence of cinchonidine in the material. However, the observed concentrations indicated an encapsulation of 52% and 14% of cinchonidine in contrast to the amount calculated from the washing solutions.

CD@Cu20 (Table 2.2, entry 7)

Prior to use, the deionised water was ultrasonicated for 5-10 minutes. Cinchonidine (9 mg, 0.03 mmol, 1 mol%) and zinc powder (449 mg, 6.87 mmol, 1.37 eq.) were mixed in deionised water (25 mL). A drop of concentrated hydrochloric acid was added to help solubilising cinchonidine. A solution of $CuSO_4 \times 5\ H_2O$ (1.25 g, 5.00 mmol, 1.00 eq.) in 25 mL of deionised water was poured into the suspension and the reaction mixture was stirred at room temperature for 6 hours. Subsequently, the reaction mixture was filtered off and the precipitate was washed with 1 M hydrochloric acid (10 mL), deionised water (3 × 10 mL) and acetonitrile (3 × 10 mL). After drying *in vacuo*, the product was obtained as a red powder (301 mg).

Characterisation:

Cinchonidine was detected in the UV/Vis spectrum of the filtrate from the reaction mixture and the washing steps. Based on concentration calculations, it was estimated that around 50% of cinchonidine might remain in the material.

Extraction of the particles with THF or destruction with concentrated hydrochloric acid followed by UV/Vis spectroscopy did not confirm the encapsulation of cinchonidine.

CD@Pd

CD@Pd was prepared according to a literature procedure, the reaction was scaled down by a factor of 10:[3]

$PdCl_2$ (100 mg, 0.56 mmol, 1.00 eq.) was dissolved in deionised water (12.5 mL). The resulting suspension was poured into a solution of cinchonidine (1.0 mg, 0.0034 mmol, 1 mol%) and SDS (95 mg, 0.33 mmol, 0.59 eq.) in deionised water (5 mL). Subsequently, $NaH_2PO_2 \times H_2O$ (123 mg, 1.16 mmol, 2.06 eq.) was added and the reaction mixture was stirred at room temperature for 2 hours. The reaction mixture was filtered off and the precipitate was washed with water (3 × 10 mL). After drying *in vacuo*, the product was obtained as a black powder (72 mg).

Characterisation:

Cinchonidine was not detected in the filtrates by UV/Vis spectroscopy.

The material (11 mg) was extracted with THF. Subsequent analysation by UV/Vis spectroscopy did not confirm the presence of cinchonidine.

CN@Ag

A mixture of Ag_2O (119 mg, 0.51 mmol, 1 eq. Ag^+) and cinchonine (CN) (3.5 mg 0.012 mmol, 1 mol% compared to Ag^+) was prepared in deionised water (20 mL). Concentrated sulfuric acid was added dropwise (5 drops) to solubilise cinchonine and the silver salt. The solution was heated to 30 °C and NaH_2PO_2 (278 mg, 2.62 mmol, 5.14 mmol. 5.04 eq. compared to Ag^+) was added over the course of 10 minutes and the reaction mixture was stirred for 21 hours. The reaction mixture was filtered off and the precipitate was washed with diluted hydrochloric acid (50 mL), water (100 mL), ethanol (3 × 10 mL) and acetonitrile (3 × 10 mL). After drying in vacuo, the product was obtained as a brown powder (85 mg, 77% yield compared to Ag^+).

Characterisation:

-

5.2.2 Preparation of Electrodes with Heterogeneous Catalysts

Preparation of Copper Coins

Copper coins were manufactured by pressing organically doped copper particles, generally 300-500 mg, in a hydraulic press under a pressure of 3 t (CD@Cu 7/11/14/16) or 5 t (CD@Cu 17/18/19/20) for 10 s. The coins had a diameter of 13 mm (Surface area: 1.33 cm^2).

Preparation of Pd/C modified electrodes

Catalyst inks were prepared by mixing commercial hydrogenation catalysts ore organically doped metals with a binder like Nafion or chitosan. The catalyst inks were drop cast onto graphite sheets to be used for batch electrosynthesis with the Electrasyn 2.0 (Electrode dimensions: 2 mm × 8 mm × 50 mm; covered surface: 30 mm × 8 mm = 2.4 cm^2) or for flow electrosynthesis with the Ion Electrochemical Reactor from Vapourtec Ltd (Electrode dimensions: 1 mm × 50 mm × 50 mm; covered surface area: 50 mm × 50 mm = 25 cm^2).

Pd/C-Nafion® catalyst ink in alcohol-water mixtures

Method A1

Pd/C (2.4 mg) was dispersed in 5 % Nafion® solution (aliphatic alcohols (36.6 µL, 1.6 mg ionomer) by ultrasonication. The weight ratio of Pd/C to Nafion® was 60:40. The resulting catalyst ink was drop cast onto a surface of 2.4 cm^2 (30 mm × 8 mm) on a graphite sheet (2 mm × 8 mm × 50 mm) and dried at room temperature overnight. Subsequently, the electrode was heated to 125 °C in the oven for 0.0 h (a)/ 0.5 h (b)/ 1.0 h (c)/ 2.5 h (d). The amount of Pd/C on the electrode was estimated to be 1 $mg \cdot cm^{-2}$.

Visible loss of catalyst was observed when the electrode was dipped into ethanol or water. The electrode was instable when used for ECH experiments.

Method A2

Pd/C (4.8 mg) was dispersed in 5 % Nafion® solution (73.2 µL, 3.2 mg ionomer) by ultrasonication. The weight ratio of Pd/C to Nafion® was 60:40. The resulting catalyst ink was drop cast onto a surface of 2.4 cm^2 (30 mm × 8 mm) on a graphite sheet (2 mm × 8 mm × 50 mm) and dried at room temperature overnight. Subsequently, the electrode was heated to 125 °C in the oven for 18 hours. The amount of Pd/C on the electrode was estimated to be 2 $mg \cdot cm^{-2}$.

Apart from minor swelling, the electrode appeared stable in ethanol and water. The electrode was instable when used for ECH experiments.

Method A3

Pd/C (2.4 mg) was dispersed with 5 % Nafion® solution (36.6 µL, 1.6 mg ionomer) and IPA (24 µL) by ultrasonication. The weight ratio of Pd/C to Nafion® was 60:40. The resulting catalyst ink was drop cast onto a surface of 2.4 cm^2 (30 mm × 8 mm) on a graphite sheet (2 mm × 8 mm × 50 mm) and dried at room temperature overnight.

Subsequently, the electrode was heated to 125 °C in the oven for 5-10 minutes. The amount of Pd/C on the electrode was estimated to be 1 mg·cm^{-2}.

Visible loss of catalyst was observed when the electrode was dipped into ethanol or water. Nevertheless, the electrode was used in electrocatalytic experiments.

Method A4

Pd/C (6.5 mg) was dispersed with 5 % Nafion® solution (100 µL, 4.37 mg ionomer), water (300 µL) and IPA (250 µL) by ultrasonication. The weight ratio of Pd/C to Nafion® was 60:40. A volume of 60 µL (a)/ 120 µL (b)/ 240 µL (c) of the resulting catalyst ink was drop cast onto a surface of 2.4 cm^2 (30 mm × 8 mm) on a graphite sheet (2 mm × 8 mm × 50 mm) and dried at room temperature overnight. The amount of Pd/C on the electrode was estimated to be 0.25 mg·cm^{-2} (a)/ 0.5 mg·cm^{-2} (b)/ 1.0 mg·cm^{-2} (c).

Visible loss of catalyst was observed when the electrode was dipped into ethanol or water.

Method A5

Pd/C (8.5 mg) was dispersed with 5 % Nafion® solution (131 µL, 5.71 mg ionomer), water (300 µL) and IPA (250 µL) by ultrasonication. The weight ratio of Pd/C to Nafion® was 60:40. A volume of 240 µL of the resulting catalyst ink was drop cast onto a surface of 2.4 cm^2 (30 mm × 8 mm) on a graphite sheet (2 mm × 8 mm × 50 mm) and dried at room temperature overnight. Subsequently, the electrode was heated to 140 °C on a hotplate for 2.5 h. The amount of Pd/C on the electrode was estimated to be 1 mg·cm^{-2}.

The stability of the electrode in alcohol water mixtures was uncertain.

Pd/C-Nafion® catalyst ink in DMF

Method B1

Pd/C (7 mg) was dispersed in 5 % Nafion® solution (107 µL, 4.67 mg ionomer) and DMF (700 µL) by ultrasonication. The weight ratio of Pd/C to Nafion® was 60:40. A volume of 240 µL of resulting catalyst ink (2.1 mg of Pd/C) was drop cast onto a surface of 2.4 cm^2 (30 mm × 8 mm) on a graphite sheet (2 mm × 8 mm × 50 mm). Subsequently, the electrode was heated to 140 °C on a hotplate for 2 h. The amount of Pd/C on the electrode was estimated to be 0.88 mg·cm^{-2}.

The electrode was used for ECH experiments in ethanol-water mixtures without visual loss of catalyst.

Method B2 (batch)

Pd/C (6.6 mg) was dispersed in 5 % Nafion® solution (100.7 µL, 4.4 mg ionomer) and DMF (660 µL). The lower aliphatic alcohols from the Nafion® solution were removed on the rotary evaporator and the catalyst ink was stirred and ultrasonicated. The weight ratio of Pd/C to Nafion® was 60:40. A volume of 240 µL of resulting catalyst ink (2.1 mg of Pd/C) was drop cast onto a surface of 2.4 cm^2 (30 mm × 8 mm) on a graphite sheet (2 mm × 8 mm × 50 mm). Subsequently, the electrode was heated to 140 °C on a hotplate for 1 h. The amount of Pd/C on the electrode was estimated to be 1 $mg \cdot cm^{-2}$.

The electrode was stable under ECH reaction conditions in methanol.

Method B2 (flow)

Pd/C (28 mg) was dispersed in 5 % Nafion® solution (382 µL, 16 mg ionomer) and DMF (2.5 mL). The weight ratio of Pd/C to Nafion® was 60:40. The lower aliphatic alcohols from the Nafion® solution were removed on the rotary evaporator and the catalyst ink was stirred and ultrasonicated. The resulting catalyst ink was drop cast onto a surface of 25 cm^2 (50 mm × 50 mm) on a graphite sheet (1 mm × 50 mm × 50 mm). Subsequently, the electrode was heated to 140 °C on a hotplate for 1 h. The amount of Pd/C on the electrode was estimated to be 1.1 $mg \cdot cm^{-2}$.

The electrode was stable in a 1:1 mixture of ethanol and water but the loss of catalyst was observed in a 9:1 mixture. After the electrode was used in the electrochemical reactor under mechanical pressure, particles from the electrode were observed sticking to the FEP spacer.

Pd/C- Nafion®-cinchonidine catalyst ink in IPA

Method C1 Pd/C (2.5 mg) and cinchonidine (0.25 mg) in 1M hydrochloric acid (25 µL) were dispersed in IPA (225 µL) by ultrasonication. The catalyst ink was drop cast onto a surface of 2.4 cm^2 (30 mm × 8 mm) on a graphite sheet (2 mm × 8 mm × 50 mm) and dried at room temperature for 10 minutes. Subsequently, a 5 % Nafion® solution (38.1 µL, 1.67 mg ionomer) was drop cast onto the dry catalyst layer and the electrode was heated to 140 °C on a hotplate for 10 minutes. The amount of Pd/C on the electrode was estimated to be 1 $mg \cdot cm^{-2}$ and the amount of cinchonidine was 0.1 $mg \cdot cm^{-2}$.

Method C2

Cinchonidine (1.2 mg, 0.004 mmol) was dissolved in ethanol (120 µL) and added to a dispersion of Pd/C (2.5 mg) in 5 % Nafion® solution (36.6 µL, 1.6 mg ionomer), IPA (102 µL) and water (102 µL). The weight ratio of Pd/C to Nafion® was 60:40. The resulting catalyst ink was ultrasonicated and drop cast onto a surface of 2.4 cm^2 (30 mm × 8 mm) on a graphite sheet (2 mm × 8 mm × 50 mm). Subsequently, the electrode was heated to 140 °C on a hotplate for 2 h. The amount of Pd/C on the electrode was estimated to be 1 $mg \cdot cm^{-2}$ and the amount of cinchonidine was 0.5 $mg \cdot cm^{-2}$.

Pd/C- Nafion®-cinchonidine catalyst ink in DMF

Method D1 Cinchonidine (0.24 mg) was dissolved in 1M hydrochloric acid (24 µL) and added to a dispersion of Pd/C (2.4 mg) in a 5% Nafion® solution (36.6 µL, 1.6 mg ionomer). The solvent was removed on the rotary evaporator and DMF (240 µL) was added and the mixture was ultrasonicated. The weight ratio of Pd/C to Nafion® was 60:40. The resulting catalyst ink was drop cast onto a surface of 2.4 cm^2 (30 mm × 8 mm) on a graphite sheet (2 mm × 8 mm × 50 mm). Subsequently, the electrode was heated to 140 °C on a hotplate for 0.5 h. The amount of Pd/C on the electrode was estimated to be 1 mg cm^{-2} and the amount of cinchonidine was 0.1 $mg \cdot cm^{-2}$.

When used for ECH experiments in methanol, there was no visible loss of catalyst.

Method D2

Cinchonidine (2.1 mg, 0.007 mmol) was dissolved in ethanol (50 µL) and added to a dispersion of Pd/C (2.8 mg) in 5 % Nafion® solution (42.8 µL, 1.87 mg ionomer) and DMF (280 µL). The weight ratio of Pd/C to Nafion® was 60:40. The resulting catalyst ink was ultrasonicated and drop cast onto a surface of 2.4 cm^2 (30 mm × 8 mm) on a graphite sheet (2 mm × 8 mm × 50 mm). Subsequently, the electrode was heated to 140 °C on a hotplate for 1 h. The amount of Pd/C on the electrode was estimated to be 1.17 $mg \cdot cm^{-2}$ and the amount of cinchonidine was 0.89 $mg \cdot cm^{-2}$.

The electrode was dipped into water, water-ethanol (1:1) and water-ethanol (1:9). Even though there was no visible loss of catalyst, UV/vis spectroscopy of these solutions revealed the loss of the chiral modifier. When used for ECH experiments in ethanol-water mixtures, there was no visible loss of catalyst.

Pd/C-chitosan catalyst ink in acetic acid solution

Method E1 (batch) Pd/C (2.4 mg) was dispersed in IPA (60 µL) and water (60 µL) by ultrasonication. Then, a solution of chitosan (0.6 mg, 1 wt%) in 1% acetic acid (60 µL) was added (Pd/C-chitosan ratio 80:20). The resulting catalyst ink was drop cast onto a surface of 2.4 cm^2 (30 mm × 8 mm) on a graphite sheet (2 mm × 8 mm × 50 mm). Subsequently, the electrode was dried *in vacuo*. The electrode was dipped into 1M NaOH solution, deionised water, ethanol and methanol. The amount of Pd/C on the electrode was estimated to be 1 $mg \cdot cm^{-2}$.

When used for ECH experiments in methanol, there was no visible loss of catalyst.

Method E2 (flow) Pd/C (25 mg) was dispersed in a solution of chitosan (6 mg, 0.5 wt%) in acetic acid (2%, 1.2 mL) by ultrasonication. The resulting catalyst ink was drop cast onto a surface of 25 cm^2 (50 mm × 50 mm) on a graphite sheet (1 mm × 50 mm × 50 mm). The electrode was dried at room temperature overnight and for 5 hours in vacuo. Subsequently, the electrode was treated with 1 M NaOH solution, deionised water and methanol. The amount of Pd/C on the electrode was estimated to be 1 $mg \cdot cm^{-2}$.

After the electrode was used in the electrochemical reactor under mechanical pressure, no particles from the electrode were observed sticking to the FEP spacer indicating a higher stability compared to the Nafion® based electrodes.

Organically doped metal-Nafion® catalyst ink in IPA

Method F1 CD@Pd particles (2.1 mg) were dispersed in a 5% Nafion® solution (54.9 µL, 2.4 mg ionomer) and IPA (60 µL) by ultrasonication (Pd/Nafion® ratio: 0.9:1). The resulting catalyst ink was drop cast onto a surface of 2.4 cm^2 (30 mm × 8 mm) on a graphite sheet (2 mm × 8 mm × 50 mm) and dried at room temperature. Subsequently, DMF (60 µL) was applied onto the film and the electrode was heated to 140 °C on a hotplate for 1 hour. The amount of palladium on the electrode was estimated to be 0.92 $mg \cdot cm^{-2}$.

The resulting film was stable in water. However, a loss of particles was observed in methanol. An effort to use the electrode for ECH reactions resulted in the visible loss of more catalyst.

Method F2a CD@Pd particles (4.0 mg) were dispersed in IPA (100 µL) by ultrasonication. A 5% Nafion® solution (274.6 µL, 12 mg ionomer) was added

(Pd/Nafion® ratio: 1:3). A volume of 220 µL of the resulting catalyst ink (2.35 mg of Pd) was drop cast onto a surface of 2.4 cm^2 (30 mm × 8 mm) on a graphite sheet (2 mm × 8 mm × 50 mm) and dried at room temperature. Subsequently, DMF (240 µL) was applied on the film and the electrode was heated to 140 °C on a hotplate for 1 hour. The amount of palladium on the electrode was estimated to be 0.98 $mg \cdot cm^{-2}$.

The electrode was stable when dipped into ethanol.

Method F2b CD@Pd particles (4.0 mg) were dispersed in IPA (100 µL) by ultrasonication. A 5% Nafion® solution (274.6 µL, 12 mg ionomer) was added (Pd/Nafion® ratio: 1:3). A volume of 80 µL of the resulting catalyst ink (0.85 mg of Pd) was drop cast onto a surface of 2.4 cm^2 (30 mm × 8 mm) on a graphite sheet (2 mm × 8 mm × 50 mm) and dried at room temperature. Subsequently, DMF (60 µL) was applied on the film and the electrode was heated to 140 °C on a hotplate for 1 h. The amount of palladium on the electrode was estimated to be 0.35 $mg \cdot cm^{-2}$.

The electrode was stable when dipped into ethanol. The electrode was used in ECH reactions in alcohol and acetonitrile/water media.

Method F3 CN@Ag particles (2.7 mg) were dispersed in a 5% Nafion® solution (185.4 µL, 8.1 mg ionomer) was added (Ag/Nafion® ratio: 1:3). The resulting catalyst ink was drop cast onto a surface of 2.4 cm^2 (30 mm × 8 mm) on a graphite sheet (2 mm × 8 mm × 50 mm) and dried at room temperature. Subsequently, DMF (240 µL) was applied on the film and the electrode was heated to 150 °C on a hotplate for 1 h. The amount of silver on the electrode was estimated to be 1.13 $mg \cdot cm^{-2}$.

The electrode was stable when immersed in water and acetonitrile mixtures and when used under ECH reaction conditions.

Organically doped metal-chitosan catalyst ink in acetic acid solution

Method G CD@Pd particles (2.1 mg) were dispersed in a solution of chitosan (2.4 mg, 0.5 wt%) in 2% acetic acid (480 µL) by ultrasonication (Pd/Chitosan ratio: 0.9:1). The resulting catalyst ink was drop cast onto a surface of 2.4 cm^2 (30 mm × 8 mm) on a graphite sheet (2 mm × 8 mm × 50 mm). Subsequently, the electrode was dried on a hotplate at 80 °C for 1 h. The amount of palladium on the electrode was estimated to be 0.88 $mg \cdot cm^{-2}$.

The electrode was treated with 1 M NaOH solution, water and methanol without loss of particles. However, the electrode coating was unstable and brittle when dry.

5.2.3 General Procedures - ECH Reaction

Method A1 Ethyl pyruvate (0.5 mmol, 50 mM, 58 mg, 55 µL) was added to a solution of tetraethyl ammonium bromide (1 mmol, 100 mM, 210 mg) in a mixture of acetonitrile and water (10 mL, 9:1). The reaction mixture was purged with nitrogen prior to the electrolysis. A CD@Cu-coin-electrode was used as cathode (radius: 6.5 mm; surface area: 1.33 cm^2; immersed surface area: approximately 1 cm^2) and a magnesium ribbon was used as a sacrificial anode (immersed surface area: approximately 1 cm^2). The electrodes were clamped into holders with platinum contacts and inserted into a 10 mL round bottom flask (joint: ST/NS 29/32) to set up the electrochemical cell.

A constant current of 10 mA was applied for 4 h 10 min to pass a charge of 3 $F \cdot mol^{-1}$ (150 C). After the electrolysis the co-solvent was removed and water (10 mL) was added. The aqueous phase was extracted with ethyl acetate (3 × 10 mL). The combined organic layers were washed with brine (30 mL), dried over $MgSO_4$ and concentrated *in vacuo* to obtained the crude product.

The resulting product was analysed by ^1H NMR.

Method A2 Methyl benzoylformate (0.125 mmol, 25 mM, 18 µL) was added to a solution of tetraethylammonium bromide (0.5 mmol, 100 mM, 105 mg) in an acetonitrile-water mixture (5 mL, 9:1). A 5 mL Electrasyn 2.0 vial was equipped with stirring bar, sacrificial magnesium anode (dimensions: 50 mm × 3 mm × 0.2 mm; immersion depth: 30 mm) and catalyst coated cathode (immersed surface area: 2.4 cm^2). A current of 7.2 mA (current density: 3 mA cm^{-2}) was applied for 1 h 27 min 05 s (5225 s) to passe a charge of 3.12 F mol^{-1} (37.6 C). Subsequently the solvent was removed, saturated $NaHCO_3$ solution (10 mL) was added and extracted with ethyl acetate (3 × 10 mL). The organic layer was evaporated and the resulting crude product was obtained.

The yield was determined by ^1H NMR with 1,3,5-trimethoxybenxene as internal standard. The ee value was determined on an Agilent 1290 Infinity II 2D-LC system.

Method B Acetophenone (0.1 mmol, 20 mM, 12 µL) was added to a solution of acetic acid (0.5 mmol, 100 mM, 29 µL) and AcONa × 3 H_2O (0.5 mmol, 100 mM, 68 mg) in methanol (5 mL). A 5 mL Electrasyn 2.0 vial was equipped with stirring bar, platinum foil anode (immersed surface area: 1.5 cm^2) and catalyst coated cathode (immersed surface area: 2.4 cm^2). A current of 12 mA (current density: 5 mA cm^{-2}) was applied for 40 min 12 s (2412 s) to pass a charge of 3 F mol^{-1} (28.9 C). Subsequently the solvent

was removed, aqueous saturated $NaHCO_3$ solution (10 mL) was added and the aqueous phase was extracted with ethyl acetate (3 × 10 mL). The organic layer was evaporated and the resulting crude product was obtained.

The yield was determined by ^1H NMR with 1,3,5-trimethoxybenzene as internal standard. The crude product was purified by preperative-TLC before determining the enantiomeric excess on a Shimadzu system.

Method C (flow) A solution of acetophenone (0.1 mmol, 0.05 M), acetic acid (0.1 M) and sodium acetate (0.1 M) in methanol (10 mL) was prepared. The reaction mixture was passed through the Ion electrochemical reactor (FEP spacer: 0.5mm; reactor volume 0.6 mL) equipped with platinum anode and catalyst coated cathode (immersed surface area: 12 cm^2) at a flow rate of 0.1 ml min^{-1}. A current of 24 mA was applied to pass a charge of 3 F mol^{-1}. The first 1 – 2 reactor volumes were discarded to account for the stabilisation of the reaction. Subsequently, 5 mL of reaction mixture were collected. The solvent was evaporated, aqueous saturated $NaHCO_3$ (20 mL) was added and extracted with ethyl acetate (3 × 20 mL). The combined organic layers were washed with brine (30 mL), dried over $MgSO_4$ and concentrated in vacuum to obtain the crude product.

5.2.4 Characterisation of Compounds from Chapter 2.1

Ethyl lactate (83)

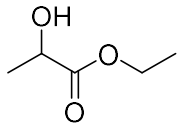

ECH reactions with ethyl pyruvate were compared to spectra of commercially available ethyl lactate.

^1H NMR (300 MHz, $CDCl_3$) δ 4.35 – 4.17 (m, 3H), 2.84 (s, 1H), 1.41 (d, *J* = 6.9 Hz, 3H), 1.30 (t, *J* = 7.1 Hz, 3H).

Diethyl 2,3-dihydroxy-2,3-dimethylsuccinate (84)

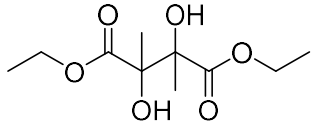

The dl:meso ratio of compound **84** was 1.28:1.00 (dl:meso). The spectral data are in agreement with the literature.[4]

^{1}H NMR (400 MHz, $CDCl_3$) δ 4.28 (qd, *J* = 7.1, 1.8 Hz, 4H, **dl**), 4.23 (q, *J* = 7.2 Hz, 4H, **meso**), 1.52 (s, 6H, **dl**), 1.50 (s, 6H, **meso**), 1.33 (t, *J* = 7.1 Hz, 6H, **dl**), 1.30 (t, *J* = 7.2 Hz, 6H, **meso**).

1-Phenylethanol (38b)

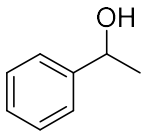

ECH reactions with acetophenone were compared to spectra of commercially available 1-phenylethanol.

^{1}H NMR (400 MHz, $CDCl_3$) δ = 7.41 – 7.32 (m, 4H), 7.30 – 7.26 (m, 1H), 4.91 (qd, *J* = 6.5, 3.6 Hz, 1H), 1.78 (d, *J* = 3.6 Hz, 1H), 1.51 (d, *J* = 6.5 Hz, 3H).

HPLC analysis:

HPLC (Shimadzu): CHIRALCEL® OD-H (250 mm × 4.6 mm, 5 μm) *n*-hexane/isopropanol 95:5 (v/v) 0.4 mL·min^{-1}, 25 °C, λ = 190 nm, t_R ((*R*)-**38a**) = 19.8 min, t_R ((*S*)-**38a**) = 22.6 min.

2D-HPLC (Agilent): ^{1}D Varian Si-5 μm (250 mm × 4.6 mm) *n*-hexane/isopropanol 9:1 (v/v) 1.0 mL·min^{-1}, 20 °C, λ = 254 nm, t_R(**38a**) = 4.3 min; ^{2}D CHIRALCEL® OD-H (250 mm × 4.6 mm, 5 μm) *n*-hexane/isopropanol 9:1 (v/v) 0.4 mL·min^{-1}, 20 °C, λ = 254 nm, t_R ((*R*)-**38a**) = 18.1 min, t_R ((*S*)-**38a**) =19.5 min.

2,3-diphenylbutane-2,3-diol (38b')

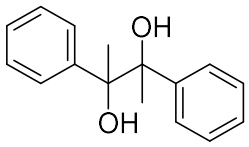

The spectral data are in agreement with the literature.[4]

^{1}H NMR (400 MHz, $CDCl_3$) δ = 7.26 – 7.17 (m, 20H, **dl & meso**), 2.55 (s, 2H, **dl**), 2.25 (s, 2H, **meso**), 1.59 (s, 6H, **meso**), 1.51 (s, 6H, **dl**).

Ethyl mandelate (10a)

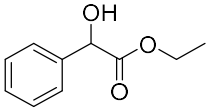

The spectral data are in agreement with the literature.[5]

^{1}H NMR (400 MHz, $CDCl_3$) δ = 7.41 – 7.28 (m, 5H), 5.14 (d, *J* = 5.4 Hz, 1H), 4.27 – 4.09 (m, 2H), 1.19 (t, *J* = 7.1 Hz, 3H).

HPLC (Shimadzu): CHIRALCEL® OD-H (250 mm × 4.6 mm, 5 µm) *n*-hexane/isopropanol 9:1 (v/v) 1.0 mL·min^{-1}, 25 °C, λ = 190 nm, t_R ((*S*)-**10a**) = 6.2 min, t_R ((*R*)-**10a**) = 10.8 min.

5.2.5 Preparation of Polymer Coated Electrodes

Preparation of Poly-L-Valine (19)

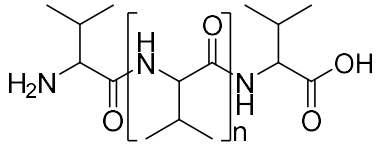

Poly-L-valine was produced by the NCA method: L-Valine (619 mg, 5.28 mmol,1 eq.) and triphosgene (524 mg, 1.77 mmol, 0.33 eq.) were added to a dry Schlenk-tube under nitrogen atmosphere. Dry THF (30 mL) was added and the reaction mixture was heated to 50 °C under nitrogen atmosphere until the monomer was completely dissolved (2.5 h). Then the THF was evaporated under reduced pressure to leave a white solid. Anhydrous dioxane (36 mL) and triethylamine (30 µL) were added and the reaction mixture was heated to 30 °C for 4 days. Subsequently, the precipitate was filtered off and washed with dioxane (30 mL), water (30 mL) and Et_2O. After drying in vacuo, the product was obtained as a white powder in 25% yield (152 mg, 1.29 mmol).

^{1}H-NMR (400 MHz, $CDCl_3$/trifluoroacetic acid): δ = 8.13 – 7.53 (m, 1 H), 4.50 – 4.13 (m 1 H), 2.19 – 1.95 (m, 1 H), 1.08 – 0.80 (m, 6 H).

$[\alpha]_D^{20}$= - 82° (c 1, trifluoroacetic acid).

IR-spectroscopy: 3264, 2962, 2359, 1628, 1541, 1506, 1456, 1387, 1225, 721 cm^{-1}.

MALDI

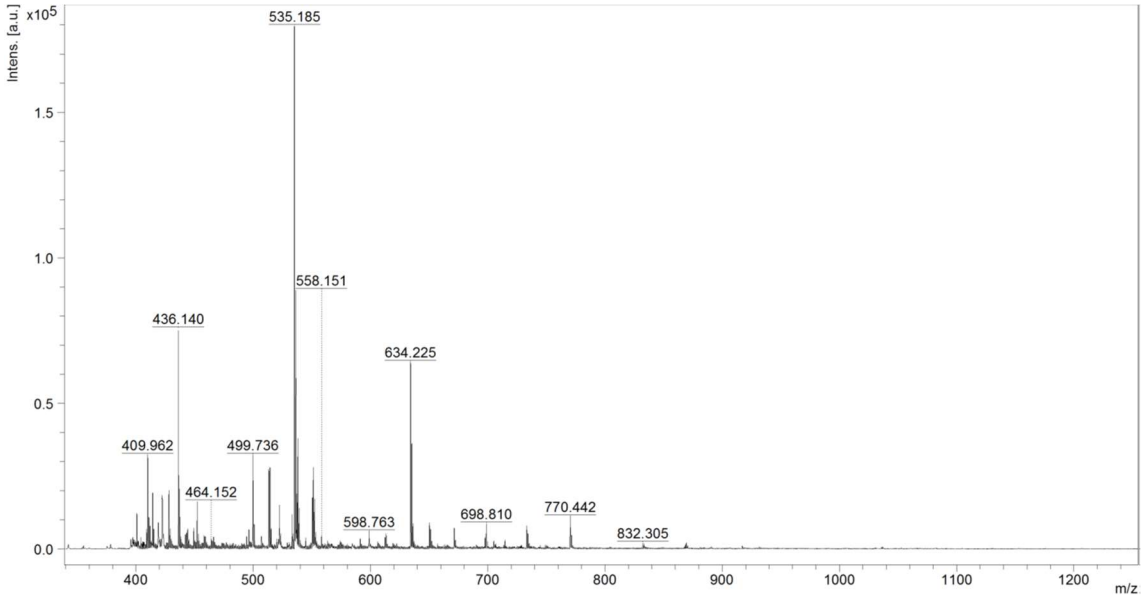

Preparation of Polypyrrole Films by Anodic Polymerisation

Method A1 (Potentiostatic electrolyis) A solution of pyrrole (3.5 µL, 0.05 mmol, 10 mM) and tetrabutylammonium tetrafluoroborate (164.6 mg, 0.5 mmol, 100 mM) in acetonitrile (5 mL) was filled into a 5 mL Electrasyn 2.0 vial. A graphite electrode (2.4 cm^2) was equipped as anode and a platinum electrode (1.5 cm^2) as cathode. A constant potential of 1.5 V (vs. Ag/AgCl) was applied for 2 minutes (passed charge:0.04 F mol^{-1}, 0.19 C).

Some parts of the electrode were not covered by the polypyrrole film.

Method B1 A solution of pyrrole (3.5 µL, 0.05 mmol, 10 mM) and tetrabutylammonium tetrafluoroborate (164.6 mg, 0.5 mmol, 100 mM) in acetonitrile (5 mL) was filled into a 5 mL Electrasyn 2.0 vial. A glassy carbon electrode (immersed surface area: 2.4 cm^2) was equipped as anode and a platinum electrode (immersed surface area: 1.5 cm^2) as cathode. A constant current of 1.2 mA (0.5 mA cm^{-2}) was applied for 8 minutes (0.12 F mol^{-1}, 0.58 C). During the electrolysis, the observed cell potential was between 2.3 V and 2.5 V.

Parts of the polypyrrole film peeled off when the electrode was dipped into a solution of poly-L-valine in TFA.

Method B2 A solution of pyrrole (3.5 µL, 0.05 mmol, 10 mM) and tetrabutylammonium tetrafluoroborate (164.6 mg, 0.5 mmol, 100 mM) in acetonitrile (5 mL) was filled into a 5 mL Electrasyn 2.0 vial. A glassy carbon electrode (2.4 cm^2) was equipped as anode and a platinum electrode (1.5 cm^2) as cathode. The solution was purged with N_2 before

the electrolysis. A constant current of 1.2 mA (0.5 mA cm^{-2}) was applied for 5 minutes (0.07 F mol^{-1}, 0.36 C). The initial cell potential was 2.6 V. During the electrolysis, a potential of 2.2 V was observed.

The polypyrrole film was stable when the electrode was dipped into a solution of poly-L-valine in TFA.

Preparation of Poly-L-Valine/ Polypyrrole Electrodes

The polypyrrole coated electrode (Method B2) was dipped into a 0.5 % solution of poly-L-valine (50 mg) in TFA (10 mL) for 15 minutes to give the modified electrode.

5.2.6 General Procedures - Electrochemical Sulfoxidation Reactions

General Procedure

Thioanisole (5.9 µL, 0.05 mmol, 10 mM) was added to a solution of tetrabutyl ammonium tetrafluoroborate (164.6 mg, 0.5 mmol, 100 mM) in acetonitrile-water (99:1, 5 mL). Platinum anode and cathode were used and a constant current of 4.8 mA (3.2 mA/cm^2) was applied for 33.5 minutes (2 F). After electrolysis the solvent was removed and the yield was determined by ^1H NMR (internal standard: 1,3,5-trimethoxybenzene).

5.2.7 Characterisation of Compounds from Chapter 2.2

***Tert*-butyl phenyl sulfide (29e)**

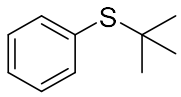

Tert-butyl phenyl sulfide was prepared according to a literature procedure. The spectral data are in agreement with the literature.[6]

^1H NMR (400 MHz, $CDCl_3$) δ = 7.61 – 7.48 (m, 2H), 7.44 – 7.27 (m, 3H), 1.29 (s, 9H).

Methyl phenyl sulfoxide (30a)

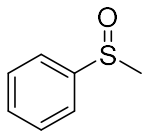

The spectral data are in agreement with the literature.[7]

^1H NMR (400 MHz, $CDCl_3$) δ = 7.67 – 7.64 (m, 2H), 7.55 – 7.51 (m, 3H), 2.73 (s, 3H).

HPLC analysis:

2D-HPLC (Agilent): ^{1}D Varian Si-5 μm (250 mm × 4.6 mm) *n*-hexane/isopropanol 9:1 (v/v) 1.0 mL·min^{-1}, 20 °C, λ = 254 nm, t_R(**25a**) = 13.7 min; ^{2}D CHIRALCEL® OD-H (250 mm × 4.6 mm, 5 μm) *n*-hexane/isopropanol 9:1 (v/v) 0.4 mL·min^{-1}, 20 °C, λ = 254 nm, t_R ((*R*)-**25a**) = 25.2 min, t_R ((*S*)-**25a**) = 27.9 min.

***Tert*-butyl phenyl sulfoxide (30e)**

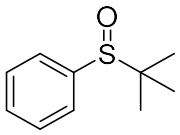

The spectral data are in agreement with the literature.[8]

^{1}H NMR (400 MHz, $CDCl_3$) δ = 7.63 – 7.55 (m, 2H), 7.53 – 7.47 (m, 3H), 1.17 (s, 9H).

5.3 Experimental Data for Chapter 3

5.3.1 General Procedures

General Procedure A – Oxychlorination with graphite electrodes

A 5 mL Electrasyn 2.0 vial was filled with $CoCl_2 \times 6\ H_2O$ (4 mg, 0.017 mmol, 3.3 mM, 10 mol%), $MgCl_2$ (48 mg, 0.5 mmol, 100 mM, 3 eq.) and $LiClO_4$ (53 mg, 0.5 mmol, 100 mM). The vial cap was equipped with both graphite anode and cathode (active surface area: 2.4 cm^2) and sealed with a rubber septum. The vial was flushed with oxygen *via* a balloon. A mixture of acetone (4.92 mL) and CH_2Cl_2 (0.08 mL), and styrene (19 µL, 0.165 mmol, 33 mM, 1eq.) were added *via* syringes. The solvent was purged with oxygen for 10 minutes. The reaction mixture was heated to 40 °C and the current was set to 24 mA (current density: 10 $mA \cdot cm^{-2}$). A charge of 4 $F \cdot mol^{-1}$ was passed (63.7 C, time: 44 min 13 s).

1H NMR yield: Subsequently, the solvent was removed and diethyl ether was added. The solution was then passed over a silica plug to remove the electrolyte and the catalyst. The diethyl ether was removed in vacuum and the yield was determined by ^1H NMR with 1,3,5-trimethoxybenzene as internal standard.

General Procedure B – Oxychlorination with RVC electrodes

A 10 mL Electrasyn 2.0 vial was filled with $CoCl_2 \times 6\ H_2O$ (8 mg, 0.033 mmol, 4 mM, 10 mol%), $MgCl_2$ (95 mg, 1.0 mmol, 100 mM, 3 eq.) and $LiClO_4$ (106 mg, 1.0 mmol, 100 mM). The vial cap was equipped with both RVC anode and cathode (dimensions of immersed electrode material: 30 mm × 0.8 mm × 0.2 mm) and sealed with a rubber septum. The vial was flushed with oxygen *via* a balloon. Acetonitrile (10 mL) and styrene (37.8 µL, 0.33 mmol, 33 mM, 1eq.) were added *via* syringes and the solvent was purged with oxygen for 10 minutes. The reaction mixture was heated to 40 °C and the current was set to 12 mA. A charge of 4 $F \cdot mol^{-1}$ was passed (127.4 C, time: 2 h 56 min 53 s).

Subsequently, the solvent was removed and diethyl ether was added. The solution was then passed over a silica plug to remove the electrolyte and the catalyst. After concentration of the solution in vacuo the crude product was obtained and purified *via* column chromatography.

General Procedure C – Dichlorination under N_2 atmosphere

A 10 mL Electrasyn 2.0 vial was filled with $CoCl_2 \times 6\ H_2O$ (10 mg, 0.04 mmol, 4 mM, 5 mol%), $MgCl_2$ (152 mg, 1.6 mmol, 160 mM, 2 eq.) and $LiClO_4$ (106 mg, 1.0 mmol, 100 mM). The vial cap was equipped with RVC anode (dimensions of immersed electrode material: 30 mm × 0.8 mm × 0.2 mm) and platinum foil cathode (active surface area: 1.5 cm^2) and sealed with a rubber septum. The vial was flushed with nitrogen *via* a balloon. Acetonitrile (8.34 mL), acetic acid (1.66 mL) and styrene (91.6 µL, 0.8 mmol, 80 mM, 1 eq.) were added *via* syringes and the solvent was purged with nitrogen for 10 minutes before the electrolysis. The reaction mixture was heated to 40 °C and the current was set to 24.5 mA. A charge of 2 $F \cdot mol^{-1}$ was passed (154.4 C, time: 1 h 45 min 01 s). The reaction mixture was quenched with saturated $NaHCO_3$ solution (50 mL) and the aqueous phase was extracted with CH_2Cl_2 (3 × 50 mL). The combined organic layers were washed with brine (100 mL), dried over $MgSO_4$ and concentrated *in vacuo* to give the crude product. The crude product was purified *via* column chromatography (Cyclohexane/Et_2O).

General Procedure D – Oxychlorination in MeCN/AcOH

A 10 mL Electrasyn 2.0 vial was filled with $MnCl_2 \times 4\ H_2O$ (8 mg, 0.04 mmol, 4 mM, 5 mol%), $MgCl_2$ (48 mg, 1.6 mmol, 160 mM, 2 eq.) and $LiClO_4$ (106 mg, 1.0 mmol, 100 mM). The vial cap was equipped with RVC anode (dimensions of immersed electrode material: 30 mm × 0.8 mm × 0.2 mm) and platinum foil cathode (active surface area: 1.5 cm^2) and sealed with a rubber septum. The vial was flushed with oxygen *via* a balloon. Acetonitrile (8.34 mL), acetic acid (1.66 mL) and styrene (91.6 µL, 0.8 mmol, 80 mM, 1 eq.) were added *via* syringes and the solvent was purged with oxygen for 10 minutes before the electrolysis. The reaction mixture was heated to 40 °C and the current was set to 24.5 mA. A charge of 2 $F \cdot mol^{-1}$ was passed (154.4 C, time: 1 h 45 min 01 s).

The reaction mixture was quenched with saturated Na_2CO_3 solution (10 mL) and the aqueous phase was extracted with CH_2Cl_2 (3 × 10 mL). The combined organic layers were dried over $MgSO_4$ and concentrated *in vacuo* to give the crude product. The crude product was purified *via* column chromatography (Cyclohexane/Et_2O).

General Method E – Oxybromination in MeCN

A 5 mL Electrasyn 2.0 vial was filled with $Mn(OAc)_2 \times 4\ H_2O$ (4 mg, 0.017 mmol, 3.3 mM, 10 mol%), KBr (99 mg, 0.83 mmol, 165 mM, 5 eq.) and $LiClO_4$ (53 mg, 0.5 mmol, 100 mM). The vial cap was equipped with both RVC anode and cathode (dimensions of

immersed electrode material: 25 mm × 0.8 mm × 0.2 mm) and sealed with a rubber septum. The vial was flushed with oxygen *via* a balloon. Acetonitrile (5 mL) and styrene (19 µL, 0.165 mmol, 33 mM, 1eq.) were added *via* syringes. The solvent was purged with oxygen for 10 minutes. The reaction mixture was heated to 40 °C and the current was set to 10 mA (current density: 10 $mA \cdot cm^{-2}$). A charge of 4 $F \cdot mol^{-1}$ was passed (63.7 C, time: 1 h 46 min 08 s).

Subsequently, the solvent was removed and a mixture of ethyl acetate and petroleum ether (1:9) was added. The solution was then passed over a silica plug to remove the electrolyte and the catalyst. The solvent was removed in vacuum and the yield was determined by ^1H NMR with 1,3,5-trimethoxybenzene as internal standard.

General Method F – Oxybromination in MeCN/AcOH

A 5 mL Electrasyn 2.0 vial was filled with $Mn(OAc)_2 \times 4\ H_2O$ (4 mg, 0.017 mmol, 3.3 mM, 10 mol%), KBr (126 mg, 1.06 mmol, 211 mM, 6.4 eq.) and Bu_4NClO_4 (86 mg, 0.25 mmol, 50 mM). The vial cap was equipped with both graphite anode and cathode (active surface area: 2.4 cm^2) and sealed with a rubber septum. The vial was flushed with oxygen *via* a balloon. Acetonitrile (4.2 mL), acetic acid (0.8 mL) and styrene (19 µL, 0.165 mmol, 33 mM, 1 eq.) were added *via* syringes. The solvent was purged with oxygen for 10 minutes. The reaction mixture was heated to 40 °C and the current was fixed to 10 mA (current density: 10 $mA \cdot cm^{-2}$). A charge of 4 $F \cdot mol^{-1}$ was passed (63.7 C, time: 1 h 46 min 08 s). The reaction mixture was concentrated *in vacuo*. The residues were quenched with saturated Na_2CO_3 solution (10 mL) and the aqueous phase was extracted with CH_2Cl_2 (3 × 10 mL). The combined organic layers were dried over $MgSO_4$ and concentrated *in vacuo* to give the crude product. The crude product was purified *via* column chromatography (Cyclohexane/EtOAc).

5.3.2 Characterisation of Compounds

2-Chloro-1-phenylethan-1-one (103a)

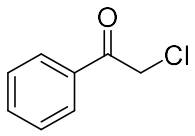

The pure compound was obtained from styrene (0.33 mmol) in 23 % yield (11 mg, 0.07 mmol) following general method B.

The pure compound was also obtained from styrene (0.8 mmol) in 25% yield (31 mg, 0.20 mmol) following general method D.

The spectral data are in agreement with the literature.[9]

^{1}H NMR (300 MHz, $CDCl_3$) δ 8.05 – 7.90 (m, 2H), 7.62 (t, *J* = 7.4 Hz, 1H), 7.50 (t, *J* = 7.5 Hz, 2H), 4.72 (s, 2H).

2-chloro-1-phenylethan-1-ol (104a)

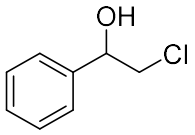

The pure compound was obtained from styrene (0.8 mmol) in 6% yield (7 mg, 0.05 mmol) by using general method D. The spectral data are in agreement with the literature.[10]

^{1}H NMR (300 MHz, $CDCl_3$) δ 7.41 – 7.34 (m, 5H), 4.91 (dd, *J* = 8.8, 3.5 Hz, 1H), 3.76 (dd, *J* = 11.2, 3.5 Hz, 1H), 3.65 (dd, *J* = 11.2, 8.8 Hz, 1H).

(1,2-Dichloroethyl)benzene (106a)

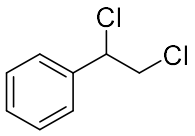

The pure compound was obtained from styrene (0.8 mmol) in 54% yield (75 mg, 0.43 mmol) by using method C. The spectral data are in agreement with the literature.[11]

^{1}H NMR (300 MHz, $CDCl_3$) δ 7.44 – 7.35 (m, 5H), 5.00 (dd, *J* = 7.9, 6.6 Hz, 1H), 4.00 (dd, *J* = 11.3, 6.6 Hz, 1H), 3.93 (dd, *J* = 11.3, 7.9 Hz, 1H).

2-Chloro-1-phenylethyl acetate (107a)

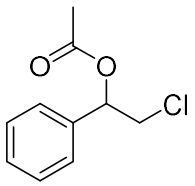

The pure compound was obtained as a side product from styrene (0.8 mmol) in 4% yield (5 mg, 0,03 mmol) by using method C. The spectral data are in agreement with the literature.[12]

^{1}H NMR (300 MHz, $CDCl_3$) δ 7.40 – 7.33 (m, 5H), 5.96 (dd, *J* = 7.9, 4.6 Hz, 1H), 3.80 (dd, *J* = 11.7, 7.9 Hz, 1H), 3.72 (dd, *J* = 11.6, 4.6 Hz, 1H), 2.14 (s, 3H).

2-Bromo-1-phenylethyl acetate (111a)

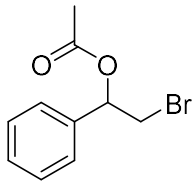

The pure compound was obtained from styrene (0.17 mmol) in 9% yield (4 mg, 0.016 mmol) by using method F. The spectral data are in agreement with the literature.[13]

^{1}H NMR (400 MHz, $CDCl_3$) δ 7.42 – 7.31 (m, 5H), 5.98 (dd, *J* = 8.0, 4.8 Hz, 1H), 3.72 – 3.63 (m, 1H), 3.59 (dd, *J* = 10.9, 4.7 Hz, 1H), 2.14 (s, 3H).

5.4 Experimental Data for Chapter 4

Bethan Winterson is gratefully acknowledge for providing 2-(pent-4-en-1-yl)isoindoline-1,3-dione, which was prepared according to literature.[14]

5.4.1 General Procedures

Method A (Bromohydroxylation): The electrolysis was performed in an undivided cell using a Vapourtec ion electrochemical flow reactor (500 µm FEP spacer, 600 µL reactor volume), a platinum on niobium plate electrode as the cathode and a graphite electrode as the anode (immersed surface area: 12 cm^2 each). A solution of styrene (1 eq., 100 mM, 1 mmol, 114.5 µL) and 48% hydrobromic acid (1.8 eq., 180 mM, 1.8 mmol, 205 µL) in 10 mL of a 7:3 mixture of acetonitrile and water was pumped with a syringe pump at a flow rate of 0.2 $mL \cdot min^{-1}$ into the ion electrochemical reactor. A constant current of 129 mA (4 $F \cdot mol^{-1}$) was applied. After reaching the steady state (2.5 reactor volumes, 1.5 mL, 7.5 min), the reaction mixture was collected for 35 min (7 mL). Subsequently, the reaction mixture was quenched with aqueous $Na_2S_2O_3$ solution and acetonitrile was removed *in vacuo*. The aqueous phase was extracted with Et_2O (3 × 25 mL). The combined organic layers were washed with brine (50 mL) dried over $MgSO_4$ and the solvent was removed *in vacuo*. The crude product was purified by flash column chromatography (EtOAc/Petroleum ether).

Method A was adapted in certain cases to overcome solubility issues by exchanging MeCN for THF.

Method B (Bromohydroxylation): The electrolysis was performed in an undivided cell using a Vapourtec ion electrochemical flow reactor (500 µm FEP spacer, 600 µL reactor volume), a platinum plate electrode as the cathode and a graphite electrode as the anode (immersed surface area: 12 cm^2 each). A solution of styrene (1 eq., 100 mM, 1 mmol, 114.5 µL) and 48% hydrobromic acid (1.8 eq., 180 mM, 1.8 mmol, 205 µL) in 10 mL of a 7:3 mixture of acetonitrile and water was pumped with a syringe pump at a flow rate of 0.4 $mL \cdot min^{-1}$ into the ion electrochemical reactor. A constant current of 193 mA (3 $F \cdot mol^{-1}$) was applied. After reaching the steady state (2.5 reactor volumes, 1.5 mL, 3.75 min), the reaction mixture was collected for 17.5 min (7 mL). Subsequently, the reaction mixture was quenched with aqueous $Na_2S_2O_3$ solution and acetonitrile was removed *in vacuo*. The aqueous phase was extracted with Et_2O (3 × 25 mL). The combined organic layers were washed with brine (50 mL), dried over $MgSO_4$ and the solvent was removed *in vacuo*. The crude product was purified by flash column chromatography (EtOAc/Petroleum ether).

Method B was adapted in as certain cases to overcome solubility issues by exchanging MeCN for THF.

Method C (Bromohydroxylation): The electrolysis was performed in an undivided cell using a Vapourtec ion electrochemical flow reactor (500 µm FEP spacer, 600 µL reactor volume), graphite electrodes for cathode and anode (immersed surface area: 12 cm^2 each). A solution of styrene (1 eq., 100 mM, 1 mmol, 114.5 µL) and 48% hydrobromic acid (1.8 eq., 180 mM, 1.8 mmol, 205 µL) in 10 mL of a 7:3 mixture of acetonitrile and water was pumped with a syringe pump at a flow rate of 0.2 $mL \cdot min^{-1}$ into the ion electrochemical reactor. A constant current of 129 mA (4 $F \cdot mol^{-1}$) was applied. After reaching the steady state (2.5 reactor volumes, 1.5 mL, 7.5 min), the reaction mixture was collected for 35 min (7 mL). Subsequently, the reaction mixture was quenched with aqueous $Na_2S_2O_3$ solution and acetonitrile was removed *in vacuo*. The aqueous phase was extracted with Et_2O (3 × 25 mL). The combined organic layers were washed with brine (50 mL) dried over $MgSO_4$ and the solvent was removed *in vacuo*. The crude product was purified by flash column chromatography (EtOAc/Petroleum ether).

Method D (Dibromination): The electrolysis was performed in an undivided cell using a Vapourtec ion electrochemical flow reactor (500 µm FEP spacer, 600 µLreactor volume), a platinum on titanium electrode (Vapourtec) as the cathode and a graphite electrode as the anode (immersed surface area: 12 cm^2 each). A solution of styrene (1 eq., 100 mM, 1 mmol, 114.5 µL) and 48% hydrobromic acid (6 eq., 600 mM, 6 mmol, 684 µL) in 10 mL of acetonitrile was pumped with a syringe pump at a flow rate of 0.4 $mL \cdot min^{-1}$ into the ion electrochemical reactor. A constant current of 257 mA (4 $F \cdot mol^{-1}$) was applied. After reaching the steady state (2.5 reactor volumes, 1.5 mL, 3.75 min), the reaction mixture was collected for 17.5 min (7 mL). Subsequently, the reaction mixture was quenched with aqueous $Na_2S_2O_3$ solution and acetonitrile was removed *in vacuo*. The aqueous phase was extracted with Et_2O (3 × 25 mL). The combined organic layers were washed with brine (50 mL) dried over $MgSO_4$ and the solvent was removed *in vacuo*. The crude product was purified by flash column chromatography (EtOAc/Petroleum ether).

Method E (Bromoalcoxylation): The electrolysis was performed in an undivided cell using a Vapourtec ion electrochemical flow reactor (500 µm FEP spacer, 600 µLreactor volume), a platinum plate electrode as the cathode and a graphite electrode as the anode (immersed surface area: 12 cm^2 each). A solution of styrene (1 eq., 100 mM, 1

mmol, 114.5 µL) and 48% hydrobromic acid (1.5 eq., 150 mM, 1.5 mmol, 171 µL) in 10 mL of a 7:3 mixture of acetonitrile and corresponding alcohol was pumped with a syringe pump at a flow rate of 0.4 mL·min^{-1} into the ion electrochemical reactor. A constant current of 257 mA (4 F·mol^{-1}) was applied. After reaching the steady state (2.5 reactor volumes, 1.5 mL, 3.75 min), the reaction mixture was collected for 17.5 min (7 mL). Subsequently, the reaction mixture was quenched with aqueous $Na_2S_2O_3$ solution and acetonitrile was removed *in vacuo*. The aqueous phase was extracted with Et_2O (3 × 25 mL). The combined organic layers were washed with brine (50 mL) dried over $MgSO_4$ and the solvent was removed *in vacuo*. The crude product was purified by flash column chromatography (EtOAc/Cyclohexane).

5.4.2 Characterization of Products

(1,2-Dibromoethyl)benzene (108a)

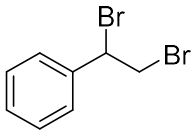

The product was obtained from styrene (0.66 mmol) as a colourless solid (86%, 150 mg, 0.57 mmol) by using method D. The spectral data are in agreement with the literature.[15]

^{1}H NMR (300 MHz, $CDCl_3$) δ = 7.51 – 7.29 (m, 5H), 5.15 (dd, *J* = 10.4, 5.6 Hz, 1H), 4.13 – 3.97 (m, 2H).

^{13}C NMR (75 MHz, $CDCl_3$) δ = 138.7, 129.3, 129.0, 127.8, 51.0, 35.1.

MP: 72-74 °C.

(2,3-Dibromopropyl)benzene (108b)

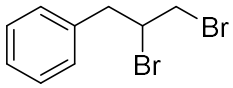

The product was obtained from allylbenzene (0.64 mmol) as a colourless solid (64%, 114 mg, 0.41 mmol) by using method D. The spectral data are in agreement with the literature.[15]

^{1}H NMR (300 MHz, $CDCl_3$) δ = 7.41 – 7.26 (m, 5H), 4.43 – 4.30 (m, 1H), 3.83 (dd, *J* = 10.5, 4.2 Hz, 1H), 3.63 (dd, *J* = 10.5, 9.0 Hz, 1H), 3.51 (dd, *J* = 14.5, 4.8 Hz, 1H), 3.13 (dd, *J* = 14.5, 7.8 Hz, 1H).

^{13}C NMR (75 MHz, $CDCl_3$) δ = 137.0, 129.7, 128.7, 127.4, 52.6, 42.1, 36.2.

2-(4,5-Dibromopentyl)isoindoline-1,3-dione (108c)

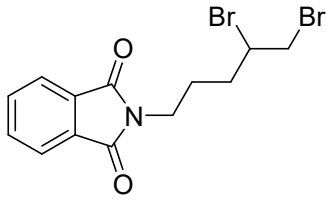

The product was obtained from 2-(pent-4-en-1-yl)isoindoline-1,3-dione (0.7 mmol) as a colourless viscous oil (84%, 221 mg, 0.59 mmol) by using method D.

^{1}H NMR (300 MHz, $CDCl_3$) δ = 7.84 (dd, *J* = 5.4, 3.1 Hz, 2H), 7.71 (dd, *J* = 5.4, 3.1 Hz, 2H), 4.20 (ddd, *J* = 12.9, 9.0, 4.2 Hz, 1H), 3.82 (dd, *J* = 10.3, 4.4 Hz, 1H), 3.73 (t, *J* = 6.7 Hz, 2H), 3.59 (t, *J* = 10.0 Hz, 1H), 2.29 – 2.09 (m, 1H), 2.09 – 1.91 (m, 1H), 1.91 – 1.74 (m, 2H).

^{13}C NMR (75 MHz, $CDCl_3$) δ = 168.4, 134.1, 132.1, 123.4, 51.9, 37.1, 36.1, 33.3, 26.2.

HRMS (EI+) *m/z*: calcd. for $[M]^+$ ($C_{13}H_{14}O_2N^{79}Br$): 373.93858; found: 373.9385.

IR ν_{max}/cm^{-1} (neat): 2936, 1771, 1701, 1614, 1466, 1435, 1395, 1364, 1188, 1020, 885, 716, 569, 529.

(1S,2S,4S,5S)-1,2,4,5-Tetrabromocyclohexane (108d)

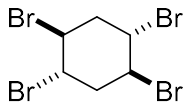

The product was obtained from 1,4-cyclohexadiene (0.7 mmol) as a colourless solid (34%, 95 mg, 0.24 mmol) by using method D. (4R,5R)-4,5-dibromocyclohex-1-ene was observed as minor product in the crude ^{1}H-NMR but could not be isolated in pure form.

The spectral data are in agreement with the literature.[16]

^{1}H NMR (300 MHz, $CDCl_3$) δ = 4.65 – 4.34 (m, 4H), 2.88 (bs, 4H).

^{13}C NMR (75 MHz, $CDCl_3$) δ = 50.8, 39.9.

MP: 190-192 °C.

2-Bromo-1-phenylethan-1-ol (109a)

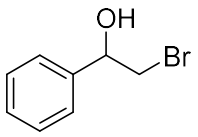

The product was obtained from styrene (0.68 mmol) as a colourless oil (81%, 111 mg, 0.55 mmol) by using method A with platinum foil instead of platinum on niobium as the cathode.

The product was obtained from styrene (0.7 mmol) as a colourless oil (77%, 108 mg, 0.54 mmol) by using method A.

The product was obtained from styrene (0.5 mmol) as a colourless oil (78%, 78 mg, 0.39 mmol) by using method C.

The spectral data are in agreement with the literature.[17]

^{1}H NMR (300 MHz, $CDCl_3$) δ = 7.43 – 7.29 (m, 5H), 4.93 (dd, *J* = 8.9, 3.4 Hz, 1H), 3.65 (dd, *J* = 10.5, 3.4 Hz, 1H), 3.55 (dd, *J* = 10.5, 9.0 Hz, 1H), 2.64 (s, 1H).

^{13}C NMR (75 MHz, $CDCl_3$) δ = 140.4, 128.8, 128.6, 126.1, 73.9, 40.3 ppm.

2-Bromo-1-(p-tolyl)ethan-1-ol (109b)

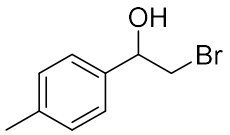

The product was obtained from 4-methylstyrene (0.66 mmol) as a yellow oil (76%, 108 mg, 0.50 mmol) by using method A. Platinum foil was used instead of platinum on niobium as the cathode.

The product was obtained from 4-methylstyrene (0.5 mmol) as a yellow oil (61%, 66 mg, 0.31 mmol) by using method C.

The spectral data are in agreement with the literature.[17]

^{1}H NMR (300 MHz, $CDCl_3$) δ = 7.32 – 7.23 (m, 2H), 7.19 (d, *J* = 8.0 Hz, 2H), 4.90 (d, *J* = 9.0 Hz, 1H), 3.63 (dd, *J* = 10.4, 3.5 Hz, 1H), 3.54 (dd, *J* = 10.4, 8.9 Hz, 1H), 2.57 (d, *J* = 2.6 Hz, 1H), 2.35 (s, 3H).

^{13}C NMR (75 MHz, $CDCl_3$) δ = 138.4, 137.4, 129.5, 126.0, 73.8, 40.4, 21.3.

2-Bromo-1-(4-fluorophenyl)ethan-1-ol (109c)

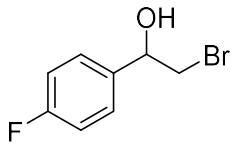

The product was obtained from 4-fluorostyrene (0.73 mmol) as a colourless oil (83%, 133 mg, 0.61 mmol) by using method A. The spectral data are in agreement with the literature.[18]

^{1}H NMR (300 MHz, $CDCl_3$) δ = 7.41 – 7.32 (m, 2H), 7.12 – 7.02 (m, 2H), 4.92 (dt, *J* = 8.8, 3.2 Hz, 1H), 3.62 (dd, *J* = 10.5, 3.4 Hz, 1H), 3.51 (dd, *J* = 10.5, 8.9 Hz, 1H), 2.63 (d, *J* = 3.1 Hz, 1H).

^{13}C NMR (75 MHz, $CDCl_3$) δ = 162.7 (d, *J* = 246.9 Hz), 136.2 (d, *J* = 3.0 Hz), 127.8 (d, *J* = 8.2 Hz), 115.7 (d, *J* = 21.6 Hz), 73.2, 40.2.

^{19}F NMR (376 MHz, $CDCl_3$) δ = -113.43 (tt, *J* = 8.9, 5.3 Hz).

2-Bromo-1-(4-chlorophenyl)ethan-1-ol (109d)

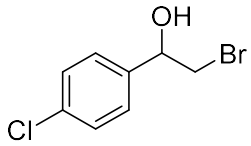

The product was obtained from 4-chlorostyrene (1.03 mmol) as a white solid (68%, 164 mg, 0.70 mmol) by using method B. Platinum on niobium was used instead of platinum foil. The spectral data are in agreement with the literature.[18]

^{1}H NMR (300 MHz, $CDCl_3$) δ = 7.39 – 7.30 (m, 4H), 4.91 (dt, *J* = 8.8, 3.3 Hz, 1H), 3.62 (dd, *J* = 10.5, 3.4 Hz, 1H), 3.50 (dd, *J* = 10.5, 8.8 Hz, 1H), 2.62 (d, *J* = 3.3 Hz, 1H).

^{13}C NMR (75 MHz, $CDCl_3$) δ = 138.8, 134.3, 128.9, 127.5, 73.1, 39.9.

MP: 59-61 °C.

2-Bromo-1-(4-bromophenyl)ethan-1-ol (109e)

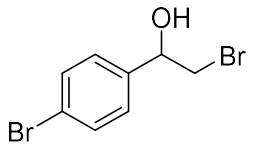

The product was obtained from 4-bromostyrene (0.72 mmol) as a white solid (71%, 144 mg, 0.51 mmol) by using method A. The spectral data are in agreement with the literature.[17]

^{1}H NMR (300 MHz, $CDCl_3$) δ = 7.54 – 7.48 (m, 2H), 7.31 – 7.24 (m, 2H), 4.90 (dt, *J* = 8.7, 3.3 Hz, 1H), 3.62 (dd, *J* = 10.5, 3.4 Hz, 1H), 3.50 (dd, *J* = 10.5, 8.8 Hz, 1H), 2.63 (d, *J* = 3.3 Hz, 1H).

^{13}C NMR (75 MHz, $CDCl_3$) δ = 139.3, 131.9, 127.8, 122.5, 73.2, 40.0.

MP: 69-72 °C.

2-Bromo-1-(4-methoxyphenyl)ethan-1-ol (109f)

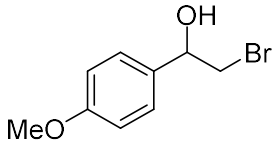

The product was obtained from 4-bromostyrene (0.72 mmol) as a white solid (66%, 109 mg, 0.47 mmol) by using method A. The spectral data are in agreement with the literature.[17]

^{1}H NMR (300 MHz, $CDCl_3$) δ = 7.33 – 7.27 (m, 2H), 6.93 – 6.86 (m, 2H), 4.87 (dd, *J* = 8.7, 3.7 Hz, 1H), 3.80 (s, 3H), 3.59 (dd, *J* = 10.4, 3.7 Hz, 1H), 3.52 (dd, *J* = 10.4, 8.8 Hz, 1H), 2.70 (s, 1H).

^{13}C NMR (75 MHz, $CDCl_3$) δ = 159.8, 132.5, 127.4, 114.2, 73.6, 55.4, 40.4 ppm.

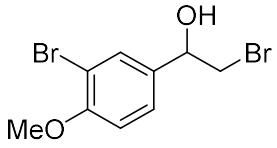

To a small extent, bromination of the aromatic ring was observed and **2-bromo-1-(3-bromo-4-methoxyphenyl)ethan-1-ol** was isolated as the side product (29 mg, 0.09mmol, 13 %).[17]

^{1}H NMR (300 MHz, $CDCl_3$) δ = 7.59 (d, *J* = 2.0 Hz, 1H), 7.29 (dd, *J* = 8.7, 2.0 Hz, 1H), 6.89 (d, *J* = 8.5 Hz, 1H), 4.86 (d, *J* = 8.9 Hz, 1H), 3.90 (s, 3H), 3.60 (dd, *J* = 10.5, 3.5 Hz, 1H), 3.50 (dd, *J* = 10.5, 8.8 Hz, 1H), 2.60 (d, *J* = 2.8 Hz, 1H).

1-([1,1'-Biphenyl]-4-yl)-2-bromoethan-1-ol (109g)

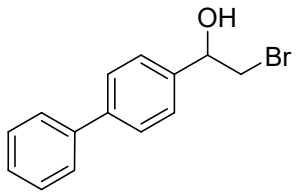

The product was obtained from 4-vinylbiphenyl (80 mM in a 3:3:4 mixture of H_2O/MeCN/THF, 0.752 mmol) as a white solid (65%, 135 mg, 0.49 mmol) by modifying method A. The spectral data are in agreement with the literature.[17]

^{1}H NMR (300 MHz, $CDCl_3$) δ = 7.60 (dd, *J* = 8.2, 6.5 Hz, 4H), 7.45 (t, *J* = 8.1 Hz, 4H), 7.36 (t, *J* = 7.3 Hz, 1H), 4.99 (dd, *J* = 8.9, 3.1 Hz, 1H), 3.69 (dd, *J* = 10.5, 3.4 Hz, 1H), 3.59 (dd, *J* = 10.4, 9.0 Hz, 1H), 2.66 (s, 1H).

^{13}C NMR (75 MHz, $CDCl_3$) δ = 141.6, 140.7, 139.3, 129.0, 127.6, 127.6, 127.3, 126.6, 73.7, 40.4.

MP: 80-83 °C.

2-Bromo-1-(naphthalen-2-yl)ethan-1-ol (109h)

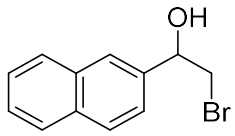

The product was obtained from 2-vinylnaphthalene (0.75 mmol) as a brown solid (54%, 101 mg, 0.40 mmol) by using method A. The spectral data are in agreement with the literature.[17]

^{1}H NMR (300 MHz, $CDCl_3$) δ = 7.90 – 7.79 (m, 4H), 7.54 – 7.45 (m, 3H), 5.10 (dd, *J* = 8.8, 3.4 Hz, 1H), 3.73 (dd, *J* = 10.5, 3.4 Hz, 1H), 3.63 (dd, *J* = 10.5, 8.9 Hz, 1H), 2.73 (s, 1H).

^{13}C NMR (75 MHz, $CDCl_3$) δ = 137.7, 133.4, 133.3, 128.7, 128.2, 127.9, 126.6, 126.4, 125.3, 123.7, 74.0, 40.3.

1-Bromo-2-phenylpropan-2-ol (109i)

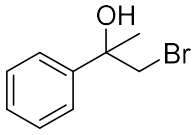

The product was obtained from α-methylstyene (0.7 mmol) as a yellow oil (48%, 73 mg, 0.34 mmol) by using method B. The spectral data are in agreement with the literature.[17]

^{1}H NMR (300 MHz, $CDCl_3$) δ = 7.51 – 7.43 (m, 2H), 7.42 – 7.34 (m, 2H), 7.34 – 7.26 (m, 1H), 3.77 (d, *J* = 10.4 Hz, 1H), 3.71 (d, *J* = 10.4 Hz, 1H), 2.55 (s, 1H), 1.69 (s, 3H).

^{13}C NMR (75 MHz, $CDCl_3$) δ = 144.3, 128.6, 127.7, 125.0, 73.3, 46.4, 28.2.

2-Bromo-1-phenylpropan-1-ol (109j)

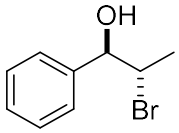

The product was obtained from trans-β-methylstyene (0.7 mmol) as a yellow oil (74%, 111 mg, 0.52 mmol, dr >20:1) by using method B.

The product was obtained from trans-β-methylstyene (0.5 mmol) as a yellow oil (45%, 48 mg, 0.22 mmol, dr >20:1) by using method C.

The spectral data are in agreement with the literature.[17]

^{1}H NMR (300 MHz, $CDCl_3$) δ = 7.42 – 7.28 (m, 5H), 5.02 (d, *J* = 3.1 Hz, 1H), 4.44 (qd, *J* = 6.8, 3.5 Hz, 1H), 2.47 (s, 1H), 1.55 (d, *J* = 6.8 Hz, 3H).

^{13}C NMR (75 MHz, $CDCl_3$) δ = 139.7, 128.5, 128.2, 126.5, 77.4, 56.3, 18.9.

2-Bromo-2,3-dihydro-1*H*-inden-1-ol (109k)

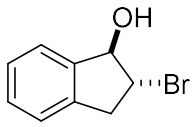

The product was obtained from indene (100 mM in a 3:7 mixture of H_2O/THF, 0.7 mmol) as a white solid (52%, 78 mg, 0.37 mmol, dr >20:1) by using a modified method B. The spectral data are in agreement with the literature.[17]

^{1}H NMR (300 MHz, $CDCl_3$) δ = 7.47 – 7.38 (m, 1H), 7.34 – 7.27 (m, 2H), 7.25 – 7.19 (m, 1H), 5.41 – 5.23 (m, 1H), 4.29 (dd, *J* = 13.9, 6.6 Hz, 1H), 3.58 (dd, *J* = 16.2, 7.2 Hz, 1H), 3.22 (dd, *J* = 16.2, 7.4 Hz, 1H), 2.38 (d, *J* = 4.1 Hz, 1H).

^{13}C NMR (75 MHz, $CDCl_3$) δ = 141.8, 139.9, 129.1, 127.8, 124.7, 124.2, 83.5, 54.6, 40.6.

MP: 128-130 °C.

Methyl 2-bromo-3-hydroxy-3-phenylpropanoate (109l)

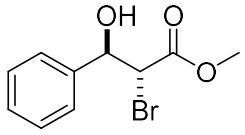

The product was obtained from methyl cinnamate (0.74 mmol) as a colourless oil (41%, 79 mg, 0.30 mmol, dr >20:1) by using method A. The spectral data are in agreement with the literature.[13]

^{1}H NMR (300 MHz, $CDCl_3$) δ = 7.42 – 7.34 (m, 5H), 5.09 (d, *J* = 8.1 Hz, 1H), 4.39 (d, *J* = 8.2 Hz, 1H), 3.81 (s, 3H), 3.11 (s, 1H).

^{13}C NMR (75 MHz, $CDCl_3$) δ = 170.0, 139.0, 129.0, 128.7, 127.1, 75.4, 53.3, 47.5.

MP: 58-60 °C.

3-Bromo-4-hydroxy-4-phenylbutan-2-one (109m)

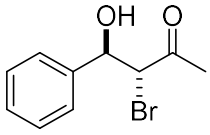

The product was obtained from trans-4-phenyl-3-buten-2-one (0.75 mmol) as a colourless oil (50%, 92 mg, 0.38 mmol, dr >20:1) by using method A. The spectral data are in agreement with the literature.[19]

^{1}H NMR (300 MHz, $CDCl_3$) δ = 7.42 – 7.33 (m, 5H), 5.06 (d, *J* = 8.6 Hz, 1H), 4.39 (d, *J* = 8.6 Hz, 1H), 3.21 (s, 1H), 2.40 (s, 3H).

^{13}C NMR (75 MHz, $CDCl_3$) δ = 202.9, 139.3, 128.9, 128.7, 127.2, 74.9, 54.5, 27.9.

2-Bromo-3-hydroxy-1,3-diphenylpropan-1-one (109n)

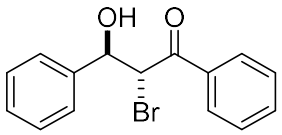

The product was obtained from trans-1,4-diphenyl-3-buten-2-one (0.74 mmol) as a yellow oil (39%, 88 mg, 0.29 mmol, dr >20:1) by using method A. The spectral data are in agreement with the literature.[20]

^{1}H NMR (300 MHz, $CDCl_3$) δ = 8.03 (d, *J* = 7.4 Hz, 2H), 7.62 (t, *J* = 7.4 Hz, 1H), 7.55 – 7.44 (m, 4H), 7.44 – 7.31 (m, 3H), 5.35 (d, *J* = 8.3 Hz, 1H), 5.24 (d, *J* = 8.3 Hz, 1H), 3.55 (s, 1H).

^{13}C NMR (75 MHz, $CDCl_3$) δ = 194.7, 139.5, 134.6, 134.3, 129.1, 129.0, 128.7, 128.6, 127.4, 74.9, 48.0.

2-Bromo-1-phenylpropane-1,3-diol (109o)

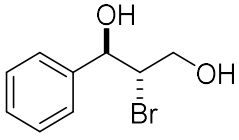

The product was obtained from cinnamyl alcohol (0.88 mmol) as a yellow oil (56%, 104 mg, 0.45 mmol, dr >20:1) by using method A. The spectral data are in agreement with the literature.[17]

^{1}H NMR (300 MHz, $CDCl_3$) δ = 7.44 – 7.28 (m, 5H), 5.02 (dd, *J* = 6.0, 3.3 Hz, 1H), 4.27 (dd, *J* = 10.9, 4.9 Hz, 1H), 4.06 – 3.94 (m, 1H), 3.92 – 3.80 (m, 1H), 3.37 (s, 1H), 2.81 (s, 1H).

^{13}C NMR (75 MHz, $CDCl_3$) δ = 140.4, 128.7, 128.6, 126.6, 76.9, 64.3, 59.4.

1-Bromo-3-phenylpropan-2-ol (109p) & 2-bromo-3-phenylpropan-1-ol (109p')

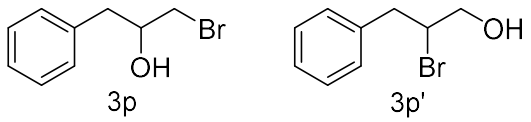

3p 3p'

The product was obtained from allyl benzene (0.7 mmol) as a 1.78:1.00 (**3p**/**3p'**) mixture of regioisomers (43%, 64 mg, 0.30 mmol) by using method A. Platinum foil was used instead of platinum on niobium. The separation of the regioisomers by column chromatography afforded 1-bromo-3-phenylpropan-2-ol (41 mg, 0.19 mmol, **3p**) and 2-bromo-3-phenylpropan-1-ol (23 mg, 0.11 mmol, **3p'**) as yellow oils.

The product was obtained from allyl benzene (1.48 mmol) as a 1.78:1.00 (**3p**/**3p'**) mixture of regioisomers (46%, 148 mg, 0.69 mmol) by using method B.

The spectral data are in agreement with the literature.[21,22]

1-Bromo-3-phenylpropan-2-ol (109p)

^{1}H NMR (300 MHz, $CDCl_3$) δ = 7.40 – 7.21 (m, 5H), 4.11 – 3.99 (m, 1H), 3.56 (dd, *J* = 10.4, 3.8 Hz, 1H), 3.42 (dd, *J* = 10.4, 6.3 Hz, 1H), 2.93 (d, *J* = 6.6 Hz, 2H), 2.20 (d, *J* = 4.3 Hz, 1H).

^{13}C NMR (75 MHz, $CDCl_3$) δ = 137.1, 129.5, 128.8, 127.0, 72.0, 41.5, 39.3.

2-Bromo-3-phenylpropan-1-ol (109p')

^{1}H NMR (300 MHz, $CDCl_3$) δ = 7.36 – 7.19 (m, 5H), 4.32 (tdd, *J* = 7.4, 6.1, 3.8 Hz, 1H), 3.83 (dd, *J* = 12.3, 3.7 Hz, 1H), 3.73 (dd, *J* = 12.4, 5.9 Hz, 1H), 3.27 (dd, *J* = 14.1, 7.3 Hz, 1H), 3.17 (dd, *J* = 14.2, 7.5 Hz, 1H), 2.10 (s, 1H).

1-Bromohexan-2-ol (109q) & 2-bromohexan-1-ol (109q')

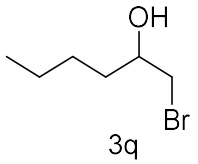

3q

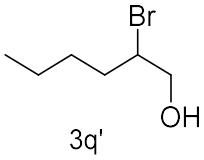

3q'

The product was obtained from 1-hexene (1.44 mmol) as a 79:21 (2q/3q) mixture of regioisomers (33%, 87 mg, 0.48 mmol) by using method B. The separation of the regioisomers by column chromatography afforded pure 1-bromohexan-2-ol (63 mg, **109q**) and a mixture of 1-bromohexan-2-ol and 2-bromohexan-1-ol (4 mg, **109q**/**109q'** 1.33:1.00 & 20 mg, **109q**/**109q'** 1.00:4.56) as yellow oils. The spectral data are in agreement with the literature.[23]

1-Bromohexan-2-ol (109q)

^{1}H NMR (300 MHz, $CDCl_3$) δ = 3.83-3.72 (m, 1H), 3.55 (dd, *J* = 10.3, 3.2 Hz, 1H), 3.39 (dd, *J* = 10.3, 7.1 Hz, 1H), 2.09 (s, 1H), 1.60 – 1.30 (m, 6H), 0.91 (t, *J* = 7.1 Hz, 3H).

^{13}C NMR (75 MHz, $CDCl_3$) δ = 71.2, 40.9, 34.9, 27.9, 22.7, 14.1.

2-bromohexan-1-ol (109q')

^{1}H NMR (300 MHz, $CDCl_3$) δ = 4.15 (ddd, *J* = 13.7, 6.9, 4.0 Hz, 1H), 3.78 (qd, *J* = 12.3, 5.3 Hz, 2H), 3.55 (dd, *J* = 10.3, 3.2 Hz, 0.22 x 1H, 3q), 3.39 (dd, *J* = 10.3, 7.1 Hz, 0.21 x 1H, 3q), 2.04 (s, 1H), 1.85 –1.81 (m, 2H), 1.64 – 1.24 (m, 4H), 0.92 (t, *J* = 7.2 Hz, 3H).

1-Bromodecan-2-ol (109r) & 2-bromodecan-1-ol (109r')

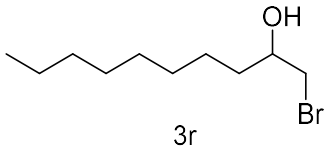

3r

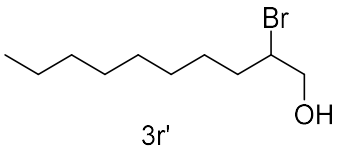

3r'

The product was obtained from 1-hexene (1.7 mmol) as a 1.00:1.04 (**109r/109r'**) mixture of regioisomers (59%, 239 mg, 1.01 mmol) by using method A. The separation of the regioisomers by column chromatography afforded pure 1-bromodecan-2-ol (87 mg, **109r**) and mixtures of 1-bromodecan-2-ol and 2-bromodecan-1-ol (24 mg, **109r**/**109r'** 1.13:1.00 & 128 mg, **109r**/**109r'** 1.00:6.69) as yellow oils. The spectral data are in agreement with the literature.[24]

1-Bromodecan-2-ol (109r)

^{1}H NMR (300 MHz, $CDCl_3$) δ = 3.84 – 3.71 (m, 1H), 3.55 (dd, *J* = 10.3, 3.2 Hz, 1H), 3.38 (dd, *J* = 10.3, 7.1 Hz, 1H), 2.08 (d, *J* = 5.0 Hz, 1H), 1.59 – 1.24 (m, 14H), 0.88 (t, *J* = 6.7 Hz, 3H).

^{13}C NMR (75 MHz, $CDCl_3$) δ = 71.1 (s), 40.8 (s), 35.2, 32.0, 29.6, 29.6, 29.3, 25.7, 22.8, 14.2.

2-Bromodecan-1-ol (109r')

^{1}H NMR (300 MHz, $CDCl_3$) δ = 4.16 (dtd, *J* = 10.0, 7.3, 4.2 Hz, 1H **3r'**), 3.94 – 3.58 (m, 2H **3r'** & 1H 3r), 3.55 (dd, *J* = 10.3, 3.2 Hz, 1H 3r), 3.38 (dd, *J* = 10.3, 7.1 Hz, 1H 3r), 2.24 – 1.21 (m, 15H **3r'** & 15H 3r), 0.88 (d, *J* = 13.0 Hz, 3H **3r'** & 3H 2r).

2-Bromocyclohexan-1-ol (109s)

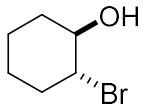

The product was obtained from cyclohexene (0.7 mmol) as a yellow oil (43%, 54 mg, 0.30 mmol, dr >20:1) by using method A.

The product was obtained from cyclohexene (1.18 mmol) as a colourless oil (37%, 78 mg, 0.44 mmol) by using method B.

The spectral data are in agreement with the literature.[19]

^{1}H NMR (300 MHz, $CDCl_3$) δ = 3.90 (ddd, *J* = 12.0, 9.4, 4.4 Hz, 1H), 3.60 (td, *J* = 9.8, 4.8 Hz, 1H), 2.55 (s, 1H), 2.42 – 2.25 (m, 1H), 2.21 – 2.05 (m, 1H), 1.91 – 1.63 (m, 3H), 1.45 – 1.20 (m, 3H).

^{13}C NMR (75 MHz, $CDCl_3$) δ = 75.4, 62.0, 36.3, 33.6, 26.8, 24.2.

(2-Bromo-1-methoxyethyl)benzene (116a)

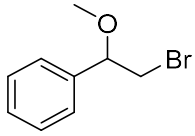

The product was obtained from styrene (100 mM MeOH/MeCN 3:7, 0.7 mmol) as a yellow oil (51%, 77 mg, 0.36 mmol) by using method D. The spectral data are in agreement with the literature.[25]

^{1}H NMR (300 MHz, $CDCl_3$) δ = 7.44 – 7.27 (m, 5H), 4.39 (dd, *J* = 8.1, 4.4 Hz, 1H), 3.54 (dd, *J* = 10.7, 8.1 Hz, 1H), 3.47 (dd, *J* = 10.7, 4.4 Hz, 1H), 3.32 (s, 3H).

^{13}C NMR (75 MHz, $CDCl_3$) δ = 139.1, 128.8, 128.7, 126.9, 83.5, 57.4, 36.5.

(2-Bromo-1-ethoxyethyl)benzene (116b)

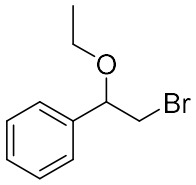

The product was obtained from styrene (100 mM MeOH/MeCN 3:7, 0.7 mmol) as a yellow oil (46%, 74 mg, 0.32 mmol) by using method D. The spectral data are in agreement with the literature.[25]

^{1}H NMR (300 MHz, $CDCl_3$) δ = 7.44 – 7.28 (m, 5H), 4.49 (dd, *J* = 8.1, 4.5 Hz, 1H), 3.58 – 3.41 (m, 4H), 1.23 (t, *J* = 7.0 Hz, 3H).

^{13}C NMR (75 MHz, $CDCl_3$) δ = 139.9, 128.7, 128.5, 126.8, 81.8, 65.1, 36.7, 15.3.

5-(Bromomethyl)dihydrofuran-2(3H)-one (111a)

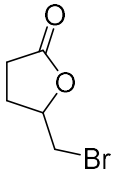

The product was obtained from 4-pentenoic acid (100mM in 100 % MeCN, 0.34 mmol) as a paleyellow oil (74%, 44 mg, 0.25 mmol) by using modified method A. The spectral data are in agreement with the literature.[26]

^{1}H NMR (300 MHz, $CDCl_3$) δ = 4.75 (dtd, *J* = 10.8, 6.2, 4.4 Hz, 1H), 3.61 – 3.48 (m, 2H), 2.73 – 2.52 (m, 2H), 2.51 – 2.38 (m, 1H), 2.19 – 2.06 (m, 1H).

^{13}C NMR (75 MHz, $CDCl_3$) δ = 176.3, 77.9, 34.2, 28.5, 26.3.

3-(Bromomethyl)isobenzofuran-1(3H)-one (4d) & 4-bromoisochroman-1-one (4d')

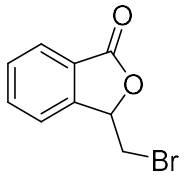

111c

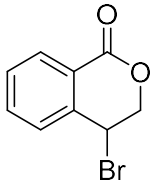

111c'

The product was obtained from 2-vinylbenzoic acid (0.7 mmol) as an off-white solid (57%, 90 mg, 0.40 mmol, mixture of regioisomers **111c**/**111c'** 9:1) by using method B. The spectral data are in agreement with the literature.[26,27]

^{1}H NMR (300 MHz, $CDCl_3$) δ = 8.12 (d, *J* = 7.2 Hz, 1H **111c'**), 7.92 (d, *J* = 7.6 Hz, 1H **111c**), 7.77 – 7.67 (m, 1H **111c**), 7.67 – 7.55 (m, 2H **111c** & 1H **111c'**), 7.52 (dd, *J* = 7.6, 1.1 Hz, 1H **111c'**), 7.47 (d, *J* = 7.7 Hz, 1H **c'**), 5.70 (t, *J* = 5.0 Hz, 1H **111c**), 5.34 (t, *J* = 2.9 Hz, 1H **111c'**), 4.78 (dd, *J* = 12.7, 2.8 Hz, 1H **111c'**), 4.71 (dd, *J* = 12.7, 3.1 Hz, 1H **111c'**), 3.77 (d, *J* = 5.0 Hz, 2H **111c**).

^{13}C NMR (75 MHz, $CDCl_3$) δ = 169.5 (**111c**), 147.2 (**111c**), 139.5 (**111c'**), 134.5 (**111c'**), 134.4 (**111c**), 130.8 (**111c'**), 130.1 (**111c** & **111c'**), 127.4 (**111c'**), 126.4 (**111c**), 125.9 (**111c**), 123.9 (**111c'**), 122.5 (**111c**), 78.7 (**111c**), 72.1 (**111c'**), 41.3 (**111c'**), 32.4 (**111c**).

2-(Bromomethyl)-1-tosylindoline (132a) & 5-bromo-2-(bromomethyl)-1-tosylindoline (132b)

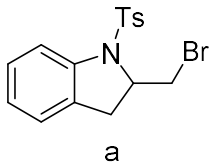

a

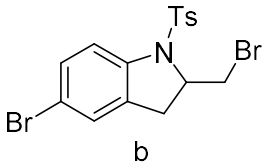

b

The products were obtained from N-(2-allylphenyl)-4-methylbenzenesulfonamide (100 mM in H_2O/MeCN 5:95, 0.76 mmol) as white solids (22%, 62 mg, 0.17 mmol, **132a** & 21%, 70 mg, 0.16 mmol,**132b**) by using a modified method A. The separation of mono and dibrominated products by column chromatography afforded pure 2-(bromomethyl)-1-tosylindoline (30 mg, **132a**), a mixture of 2-(bromomethyl)-1-tosylindoline and 5-bromo-2-(bromomethyl)-1-tosylindoline (72 mg, **132a**/**b** 1.00:1.04) and pure 5-bromo-2-(bromomethyl)-1-tosylindoline (30 mg, **132b**). The spectral data are in agreement with the literature.[28]

2-(Bromomethyl)-1-tosylindoline (132a)

^{1}H NMR (300 MHz, $CDCl_3$) δ = 7.65 (d, *J* = 8.1 Hz, 1H), 7.56 (d, *J* = 8.3 Hz, 2H), 7.26 – 7.21 (m, 1H), 7.19 (d, *J* = 8.0 Hz, 2H), 7.10 – 6.99 (m, 2H), 4.43 (dddd, *J* = 9.9, 7.4, 5.2, 3.8 Hz, 1H), 3.82 (dd, *J* = 9.9, 3.7 Hz, 1H), 3.41 (t, *J* = 9.9 Hz, 1H), 2.98 – 2.83 (m, 2H), 2.36 (s, 3H).

^{13}C NMR (75 MHz, $CDCl_3$) δ = 144.4, 141.2, 134.5, 130.7, 129.9, 128.1, 127.2, 125.4, 125.1, 117.0, 62.3, 36.1, 33.3, 21.7.

HRMS (EI+) *m/z*: calcd. for $[M]^+$ ($C_{16}H_{16}O_2N^{79}Br^{32}S$): 365.00796; found: 365.0076.

MP: 154-156 °C.

5-Bromo-2-(bromomethyl)-1-tosylindoline (132b)

^{1}H NMR (300 MHz, $CDCl_3$) δ = 7.56 (d, *J* = 8.3 Hz, 2H), 7.53 (d, *J* = 8.7 Hz, 1H), 7.34 (dd, *J* = 8.6, 2.0 Hz, 1H), 7.22 (d, *J* = 8.1 Hz, 2H), 7.19 (d, *J* = 1.6 Hz, 1H), 4.42 (dddd, *J* = 9.3, 7.4, 5.4, 3.7 Hz, 1H), 3.79 (dd, *J* = 10.0, 3.7 Hz, 1H), 3.42 (t, *J* = 9.8 Hz, 1H), 2.91 (d, *J* = 6.1 Hz, 2H), 2.38 (s, 3H).

^{13}C NMR (75 MHz, $CDCl_3$) δ = 144.8, 140.6, 134.2, 133.0, 131.1, 130.1, 128.5, 127.2, 118.2, 117.9, 62.4, 36.0, 33.1, 21.7.

HRMS (EI+) *m/z*: calcd. for $[M]^+$ ($C_{16}H_{16}O_2N^{79}Br^{81}Br\,^{32}S$): 444.91643; found: 444.9161.

MP: 120-122 °C.

5-Bromo-2-(bromomethyl)-7-methyl-2,3-dihydrobenzofuran (133a) & 3,6-dibromo-8-methylchromane (133b)

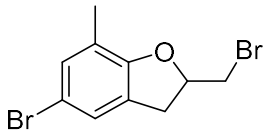

4f

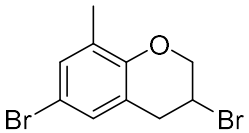

4f'

The product was obtained from 2-allyl-6-methylphenol (100 mM in 100% MeCN, 0.74 mmol) as a colourless oil (22%, 50 mg, 0.40 mmol, mixture of regioisomers **133a/133b** 2.33:1.00) by using a modified method A. The ratio of regioisomers in the isolated product mixture does not reflect selectivity. The spectral data are in agreement with the literature.[29]

^{1}H NMR (300 MHz, $CDCl_3$) δ = 7.16 (s, 1H **b**), 7.14 (s, 1H **b**), 7.10 (s, 1H **a**), 7.07 (s, 1H **a**), 5.05 – 4.94 (m, 1H **a**), 4.66 (t, *J* = 9.1 Hz, 1H **b**), 4.47 (dd, *J* = 9.5, 5.4 Hz, 1H **b**), 3.91 – 3.80 (m, 1H, **b**), 3.63 – 3.55 (m, 1H **a** & 1H **b**), 3.49 (dd, *J* = 10.4, 7.1 Hz, 1H **a**), 3.43 – 3.32 (m, 1H **a** & 1H **b**), 3.12 (dd, *J* = 16.1, 6.5 Hz, 1H **a**), 2.17 & 2.18 (s, 3H **a** & s 3H **b**).

^{13}C NMR (75 MHz, $CDCl_3$) δ = 158.0 (**b**), 156.9 (**a**), 133.3 (**b**), 132.1 (**a**), 129.0 (**b**), 127.2 (**a**), 125.3 (**a**), 125.0 (**b**), 122.5 (**b**), 121.8 (**a**), 112.5 (**a**), 112.2 (**b**), 81.3 (**a**), 76.2 (**b**), 45.0 (**b**), 34.7 (**a**), 34.7 (**b**), 34.5 (**a**), 15.2 (**a**), 15.1 (**b**).

HRMS (CI+) *m/z*: calcd. $[M]^+$ ($C_{10}H_{10}O^{79}Br_2$): 303.90929; found: 303.9097.

The reaction of 4-pentenol and 5-hexenol under modified conditions A without cosolvent did not lead to the formation of cyclised products.

5.5 References

(1) Vapourtec Ltd. *Ion electrochemical reactor*. https://www.vapourtec.com/products/flow-reactors/ion-electrochemical-reactor-features, (accessed September 2022).

(2) Yang, H.-P.; Fen, Q.; Wang, H.; Lu, J.-X. Copper Encapsulated Alkaloids Composite: An Effective Heterogeneous Catalyst for Electrocatalytic Asymmetric Hydrogenation. *Electrochem. Commun.* **2016**, *71*, 38–42. https://doi.org/10.1016/j.elecom.2016.08.004.

(3) Durán Pachón, L.; Yosef, I.; Markus, T. Z.; Naaman, R.; Avnir, D.; Rothenberg, G. Chiral Imprinting of Palladium with Cinchona Alkaloids. *Nat. Chem.* **2009**, *1*, 160–164. https://doi.org/10.1038/nchem.180.

(4) Nakajima, M.; Fava, E.; Loescher, S.; Jiang, Z.; Rueping, M. Photoredox-Catalyzed Reductive Coupling of Aldehydes, Ketones, and Imines with Visible Light. *Angew. Chem. Int. Ed.* **2015**, *54*, 8828–8832. https://doi.org/10.1002/anie.201501556.

(5) Marques, C. S.; Burke, A. J. Enantioselective Catalytic Synthesis of Ethyl Mandelate Derivatives Using Rh(I)-NHC Catalysts and Organoboron Reagents. *Tetrahedron Asymmetry* **2013**, *24*, 628–632. https://doi.org/10.1016/j.tetasy.2013.04.011.

(6) Munbunjong, W.; Lee, E. H.; Ngernmaneerat, P.; Kim, S. J.; Singh, G.; Chavasiri, W.; Jang, D. O. Indium-Mediated Cleavage of Diphenyl Diselenide and Diphenyl Disulfide: Efficient One-Pot Synthesis of Unsymmetrical Diorganyl Selenides, Sulfides, and Selenoesters. *Tetrahedron* **2009**, *65*, 2467–2471. https://doi.org/10.1016/j.tet.2009.01.072.

(7) Wang, X.; Wang, X.; Guo, H.; Wang, Z.; Ding, K. Self-Supported Heterogeneous Titanium Catalysts for Enantioselective Carbonyl-Ene and Sulfoxidation Reactions. *Chem. Eur. J.* **2005**, *11*, 4078–4088. https://doi.org/10.1002/chem.200500239.

(8) le Fur, N.; Mojovic, L.; Plé, N.; Turck, A.; Queguiner, G.; Reboul, V.; Metzner, P. Ortho-Metalation of Enantiopure Aromatic Sulfoxides and Stereocontrolled Addition to Imines. *J. Org. Chem.* **2006**, *71*, 2609–2616. https://doi.org/10.1021/jo052358p.

(9) Tian, S.; Lv, S.; Jia, X.; Ma, L.; Li, B.; Zhang, G.; Gao, W.; Wei, Y.; Chen, J.; Gmbh, C. W. V.; Kgaa, C.; Tian, S.; Lv, S.; Jia, X.; Ma, L.; Li, B.; Zhang, G.; Gao, W.; Wei, Y. CV-Driven Optimization: Cobalt-Catalyzed Electrochemical Expedient Oxychlorination of Alkenes via ORR. *Adv. Synth. Catal.* **2019**, *361*, 5626–5633. https://doi.org/10.1002/adsc.201901260.

(10) Haak, R. M.; Berthiol, F.; Jerphagnon, T.; Gayet, A. J. A.; Tarabiono, C.; Postema, C. P.; Ritleng, V.; Pfeffer, M.; Janssen, D. B.; Minnaard, A. J.; Feringa, B. L.; de Vries, J. G. Dynamic Kinetic Resolution of Racemic β -Haloalcohols: Direct Access to Enantioenriched Epoxides. *J. Am. Chem. Soc.* **2008**, *130*, 13508–13509. https://doi.org/10.1021/ja805128x.

(11) Fu, N.; Sauer, G. S.; Lin, S. Electrocatalytic Radical Dichlorination of Alkenes with Nucleophilic Chlorine Sources. *J. Am. Chem. Soc.* **2017**, *139*, 15548–15553. https://doi.org/10.1021/jacs.7b09388.

(12) Mendonça, G. F.; Sanseverino, A. M.; de Mattos, M. C. S. Trichloroisocyanuric Acid as a Cohalogenating Reagent: An Efficient Transformation of Alkenes into

Chlorohydrins, β-Chloroethers and β-Chloroacetates. *Synthesis (Stuttg)* **2003**, *1*, 45–48. https://doi.org/10.1055/s-2003-36250.

(13) Agrawal, M. K.; Adimurthy, S.; Ganguly, B.; Ghosh, P. K. Comparative Study of the Vicinal Functionalization of Olefins with 2:1 Bromide/Bromate and Iodide/Iodate Reagents. *Tetrahedron* **2009**, *65*, 2791–2797. https://doi.org/10.1016/j.tet.2009.01.095.

(14) Winterson, B.; Rennigholtz, T.; Wirth, T.; Flow Electrochemistry: A Safe Tool for Fluorine Chemistry. *Chem. Sci.* **2021**, *12*, 9053–9059. https://doi.org/10.1039/d1sc02123k.

(15) Yuan, Y.; Yao, A.; Zheng, Y.; Gao, M.; Zhou, Z.; Qiao, J.; Hu, J.; Ye, B.; Zhao, J.; Wen, H.; Lei, A. Electrochemical Oxidative Clean Halogenation Using HX/NaX with Hydrogen Evolution. *iScience* **2019**, *12*, 293–303. https://doi.org/10.1016/j.isci.2019.01.017.

(16) Christl, M.; Groetsch, S. Cyclohexa-1,2,4-Triene from 1-Bromocyclohexa-1,4-Diene. *Eur. J. Org. Chem.* **2000**, *10*, 1871–1874. https://doi.org/10.1002/(SICI)1099-0690(200005)2000:10<1871::AID-EJOC1871>3.0.CO;2-3.

(17) Song, S.; Huang, X.; Liang, Y. F.; Tang, C.; Li, X.; Jiao, N. From Simple Organobromides or Olefins to Highly Value-Added Bromohydrins: A Versatile Performance of Dimethyl Sulfoxide. *Green Chem.* **2015**, *17*, 2727–2731. https://doi.org/10.1039/c5gc00184f.

(18) Cui, H. B.; Xie, L. Z.; Wan, N. W.; He, Q.; Li, Z.; Chen, Y. Z. Cascade Bio-Hydroxylation and Dehalogenation for One-Pot Enantioselective Synthesis of Optically Active β-Halohydrins from Halohydrocarbons. *Green Chem.* **2019**, *21*, 4324–4328. https://doi.org/10.1039/c9gc01802f.

(19) Masuda, H.; Takase, K.; Nishio, M.; Hasegawa, A.; Nishiyama, Y.; Ishii, Y. A New Synthetic Method of Preparing Iodohydrin and Bromohydrin Derivatives through in Situ Generation of Hypohalous Acids from H_5IO_6 and $NaBrO_3$ in the Presence of $NaHSO_3$. *J. Org. Chem.* **1994**, *59*, 5550–5555. https://doi.org/10.1021/jo00098a012.

(20) Imamoto, T.; Kusumoto, T.; Yokoyama, M. A New Aldol Reaction via Cerium Enolates. *Tetrahedron Lett.* **1983**, *24*, 5233–5236. https://doi.org/10.1016/S0040-4039(00)88405-1.

(21) Roy, C. D.; Brown, H. C. A Highly Regio- and Chemoselective Synthesis of Vicinal Bromohydrins by Ring Opening of Terminal Epoxides with Dibromoborane-Dimethyl Sulfide. *J. Organomet. Chem.* **2007**, *692*, 1608–1613. https://doi.org/10.1016/j.jorganchem.2006.11.032.

(22) D'Arrigo, P.; Fuganti, C.; Fantoni, G. P.; Servi, S. Extractive Biocatalysis: A Powerful Tool in Selectivity Control in Yeast Biotransformations. *Tetrahedron* **1998**, *54*, 15017–15026. https://doi.org/10.1016/S0040-4020(98)00941-7.

(23) Stalpaert, M.; Cirujano, F. G.; de Vos, D. E. Tetrabutylphosphonium Bromide Catalyzed Dehydration of Diols to Dienes and Its Application in the Biobased Production of Butadiene. *ACS Catal* **2017**, *7*, 5802–5809. https://doi.org/10.1021/acscatal.7b01765.

(24) Chini, M.; Crotti, P.; Gardelli, C.; Macchia, F. Regio- and Stereoselective Synthesis of β-Halohydrins from 1,2-Epoxides with Ammonium Halides in the Presence of Metal Salts. *Tetrahedron* **1992**, *48*, 3805–3812. https://doi.org/10.1016/S0040-4020(01)92271-9.

(25) Élinson, M. N.; Makhova, I. v.; Nikishin, G. I. Selective Electrochemical Bromoalkoxylation of Aryl Olefins. *Bull. Acad. Sci. USSR, Div. Chem. Sci.* **1988**, *37*, 1636–1641. https://doi.org/10.1007/BF00961113.

(26) Armstrong, A.; Braddock, D. C.; Jones, A. X.; Clark, S. Catalytic Asymmetric Bromolactonization Reactions Using (DHQD) 2PHAL-Benzoic Acid Combinations. *Tetrahedron Lett.* **2013**, *54*, 7004–7008. https://doi.org/10.1016/j.tetlet.2013.10.043.

(27) Hanusek, J. J.; Váňa, J.; Sedlák, M.; Kammel, R.; Roithová, J.; Škríba, A.; Jašík, J.; Hanusek, J. J. Inverse Neighboring Group Participation: Explanation of an Unusual S→N Alkyl Migration of Isothiuronium Salts Containing a Lactone Group. *J. Org. Chem.* **2013**, *78*, 4456–4462. https://doi.org/10.1021/jo400460x.

(28) Yu, S. N.; Li, Y. L.; Deng, J. Enantioselective Synthesis of 2-Bromomethyl Indolines via BINAP(S)-Catalyzed Bromoaminocyclization of Allyl Aniline. *Adv. Synth. Catal.* **2017**, *359*, 2499–2508. https://doi.org/10.1002/adsc.201700106.

(29) Furst, C. G.; Cota, P. H. P.; dos Santos Wanderley, T. A.; Alberto, E. E. Synthesis of 2-Bromomethyl-2,3-Dihydrobenzofurans from 2-Allylphenols Enabled by Organocatalytic Activation of: N -Bromosuccinimide. *New J. Chem.* **2020**, *44*, 15677–15684. https://doi.org/10.1039/d0nj03432k.